1. Introduction

1.1 Background

The serum and glucocorticoid inducible kinase (SGK) family consists of three distinct but highly homologous isoforms, all of which are activated in a phosphoinositide 3-kinase (PI3-K) dependent manner in response to extracellular stimuli. To date the PI3-K/SGK signalling pathway has been implicated in several core cell processes including cell proliferation, ion channel regulation and cell survival. In addition, all three SGK isoforms share substantial homology with the v-akt murine thymoma viral oncogene homolog/protein kinase B (AKT/PKB) family in the catalytic domain and hence the SGK family has been implicated in the regulation of the broad range of cellular process associated with AKT function.

The substantial homology shared between the SGK and AKT families is reflected in their many shared downstream targets, along with emerging reports of oncogenic potential, however to date AKT remains far better characterised in both normal cell physiology and tumourigenesis, with research into the SGK family comparatively still very much in its infancy. Most studies characterising the SGK family have focused on SGK1, thus the regulation and targets of SGK2 and SGK3 remain far less defined. Recent studies have indicated a potential role for SGK3 in tumourigenesis and the observation that SGK3 transcript levels are increased in a panel of ovarian tumour cells (Sheppard and Pearson, unpublished data) **(Figure 1.1)** makes this a potentially novel kinase involved in tumourigenesis. This chapter will provide an introduction to the SGK family, covering protein structure, expression, regulation, and cellular localisation. Additionally, this chapter will also discuss SGK regulated processes, associated physiology and pathophysiology, with a particular focus on the involvement of this kinase family in tumourigenesis.

1.2 Identification and characterisation of the three *sgk* genes

1.2.1 Discovery and cloning of the sgk genes

Sgk1 was the first SGK gene to be discovered, and was originally identified as a novel member of the serine/threonine protein kinase family that is transcriptionally regulated by glucocorticoids and serum in a rat mammary tumour cell line; hence the name serum and glucocorticoid inducible kinase. Subsequently, human *sgk1* was detected in a differential screen for cell volume sensitive transcripts in a human hepatoma cell line (Waldegger et al. 1997). Human *sgk1* is localised to a single locus on human chromosome 6 at position 6q23 (Waldegger et al. 1998), encodes a protein of 49kDa, and shares significant sequence homology with many members of the AGC (Cyclic AMP-dependent protein kinase, cyclic GMP-dependent protein kinase and protein kinase C family) kinase family, which includes protein kinase A (PKA), protein kinase C (PKC), S6 Kinase (S6K) and AKT (Webster et al. 1993b).

Two additional genes of the SGK family were subsequently discovered through identification of human ESTs, which exhibited considerable similarity to the original *sgk1* gene (Kobayashi et al. 1999), which were termed *sgk2* and *sgk3*. Simultaneously, studies using murine IL-3 dependent 32D cells identified the mouse homolog of human SGK3, known as cytokine independent survival kinase (CISK) in a genetic screen to identify factors that mediate IL-3 dependent survival of hematopoietic cells (Liu et al. 2000). Several splice variants for both *sgk2* and *sgk3* have also been identified. The human gene encoding *sgk2* is localised to chromosome 20q12 (Lang and Cohen 2001), while the gene encoding *sgk3* (also referred to as *sgk-l* (serum/ glucocorticoid regulated kinase-like)) is localised to chromosome 8q12.2 (Dai et al. 1999) in humans. Tissue distribution studies have demonstrated that all *sgk* genes are quite ubiquitously expressed at the mRNA level although their mRNA abundance can vary considerably form tissue to tissue (www.genecards.org).

1.2.2 SGK isoform protein domain structure

Each isoform of the SGK family shares a similar basic structure, consisting of an amino-terminal domain (N-terminal), which often contains a signal peptide sequence, which is able to direct the localisation or delivery of a protein to the appropriate organelle. In addition a central catalytic (kinase) domain containing the catalytic function of the kinase, and a carboxyl-terminal (C-terminal) regulatory domain, often involved in protein sorting. **Figure 1.2** shows a schematic of SGK isoform variant domain structure. Despite protein domain similarity, levels of sequence similarity vary quite substantially between the SGK isoforms in particular regions. The catalytic domain of each SGK isoform shares approximately 80% identity, while the C-terminal regulatory domain of each isoform share between 48-68% identity. SGK1 and SGK3 share 25% identity in the N-terminal region, while SGK2 has no sequence identity with the other isoforms in this region (Kobayashi et al. 1999).

1.2.2.1 N-terminal domain

Each of the *sgk* genes has been identified to have at least two splice variants **(Figure 1.2)**. *Sgk1* has 4 splice variants, each encoding proteins with different N-terminal domain lengths. The longest two splice variants of *sgk1* encode proteins with a six amino acid hydrophobic motif in the N-terminal domain that allows localisation to the endoplasmic reticulum (ER) through an amphipathic α-helix. Association with the ER induces rapid turnover of these SGK1 variants through polyubiquitin modification and ultimate degradation via the 26S proteasome-dependant pathway (Arteaga et al. 2006; Bogusz et al. 2006). The shorter two splice variants of SGK1 exhibit a lower basal level of expression and low protein turnover, and do not have signals to direct them to membrane-formed compartments, so remain in the cytoplasm or shuttle to the nucleus using the nuclear localisation signal (NLS) in the catalytic domain (Maiyar et al. 2003; Arteaga et al. 2007; Simon et al. 2007; Raikwar et al. 2008). Localisation of SGK1 to the mitochondria has also been demonstrated (Engelsberg et al. 2006; Cordas et al. 2007). A recent report has also demonstrated that the aldosterone-induced

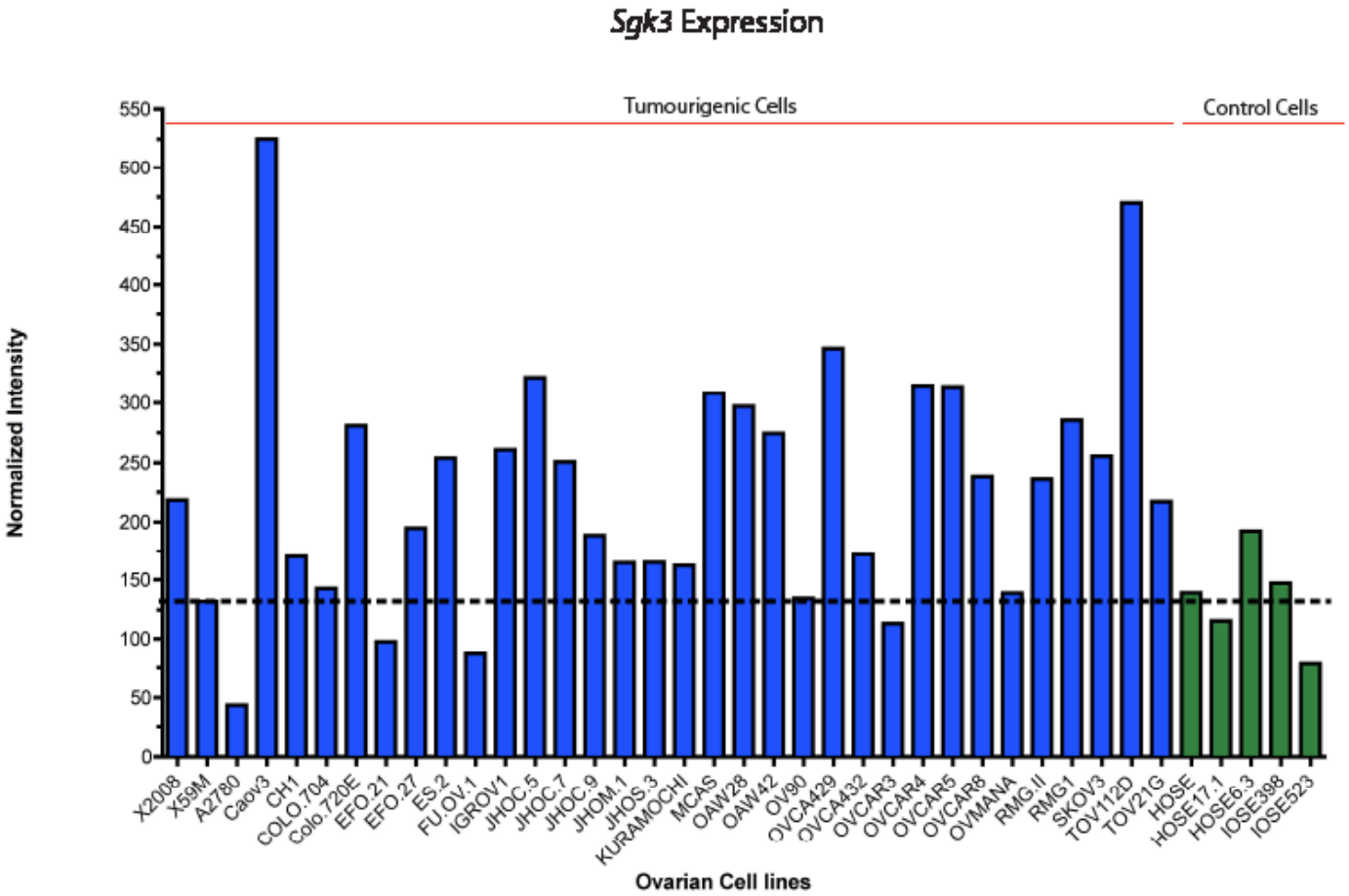

Figure 1.1: *Sgk3* gene expression in a panel of ovarian non-tumourigenic control cells and tumourigenic epithelial cells

Gene expression analysis of *Sgk3* in a panel of ovarian epithelial tumour cells compared with control ovarian epithelial non-tumourigenic cells. Black dotted line represents average normalized intensity (Sheppard and Pearson, unpublished data).

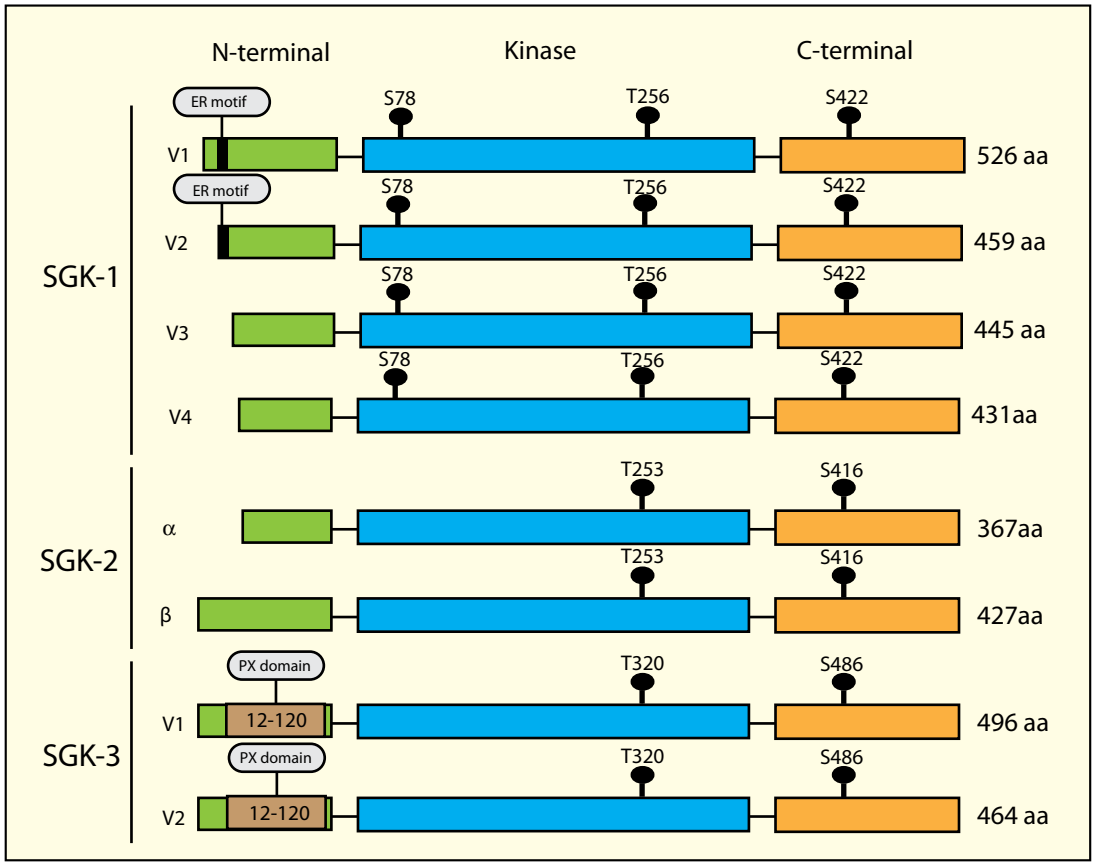

Figure 1.2: SGK isoform protein structure

The SGK family consists of three distinct protein isoforms, all of which are products of distinct genes. All SGK isoforms have at least two key regulatory sites, consisting of a Ser site in the C-terminal hydrophobic motif, and a Thr site in the activation loop of the catalytic domain, both of which require phosphorylation for complete activation. Each SGK isoform is able to produce multiple splice variants. SGK1 has four splice variants, all of which differ in the N-terminal region, and two of which contain an ER motif, enabling rapid degradation via the 26S proteasome. Both SGK2 and SGK3 have two variants, with all SGK3 variants containing a PX domain in the N-terminal region allowing SGK3 to bind to PtdIns(3)P, and localise to the early endosomes.

chaperone glucocorticoid-induced leucine zipper protein-1 (GILZ1) is able to decrease SGK1 localisation to the ER thereby inhibiting SGK1 ubiquitinylation and subsequent proteasome-mediated degradation, and prolonging its half-life and increasing steady-state expression levels (Soundararajan et al. 2010). To date there have been no type of protein import signals identified in the N-terminal domain of proteins encoded by the SGK2 splice variants, remaining predominantly cytoplasmic.

SGK3 is unique within the SGK family, as it contains an N-terminal Phox-homology (PX) domain, initially shown to be important for targeting SGK3 to vesicle-like structures (Liu et al. 2000). The PX domain in many proteins acts as a specific phosphoinositide-binding module, which has varying lipid binding specificities. The most common binding specificity for the PX domain appears to be for phosphatidylinositol 3-phosphate (PtdIns(3)P), hence several PX domain containing proteins localize to PtdIns(3) P-rich endosomal and vacuolar structures through this domain (Ellson et al. 2002). Further characterisation has demonstrated that SGK3 binds strongly and selectively to PtdIns(3)P through its PX domain, which is required for targeting SGK3 to the endosomal compartment (Virbasius et al. 2001). Mutation of the CISK PX domain at the phospholipid binding pocket abolishes phospholipid binding, endosomal localisation and SGK3 activity (Xu et al. 2001).

Taken together these studies suggest that the N-terminal domain exhibits the greatest differences and least amount of sequence identity between the SGK kinases, with a much higher level of sequence identity existing between the isoforms in the catalytic and C-terminal domains. The AKT kinases also share the greatest levels of sequence identity with the SGK family in the catalytic domain, but differ substantially in the N-terminal domain, with the AKT family sharing a Pleckstrin Homology (PH) domain in the N-terminal region, thereby targeting the AKT kinases to the plasma membrane (Haslam et al. 1993). The inherent substrate specificity of both the SGK and AKT kinase families is very similar, and it is likely that the differences in cellular localisation, as dictated by the N-terminal domain, reduce the level of *in vivo* functional redundancy existing between these kinases.

1.2.2.2 Catalytic and regulatory domains

The catalytic domain of SGK1 shares 54% amino acid identity with AKT1 (Kobayashi et al. 1999), and importantly contains a functional serine/threonine protein kinase domain, which includes Lys-127 in the adenosine triphosphate ATP binding site and Thr-256 in the activation loop. Both of these sites require phosphorylation for full catalytic activity (Firestone et al. 2003). The equivalent residues for SGK2 and SGK3 are Lys-124, Thr-253 and Lys-191, Thr-320 respectively. In addition, the central catalytic domain of SGK1 also contains a NLS between amino acids 131 and 141, which has shown to be required for *in vitro* interaction with importin-α, required for the serum-induced nuclear import of SGK1 (Maiyar et al. 2003). Alignment of the SGK isoform sequences also show NLS-like sequences in SGK2 and SGK3, however only the sequence detected in SGK1 has been functionally tested (Maiyar et al. 2003).

The C-terminal hydrophobic domain of SGK1 contains a second phosphorylation site, Ser-422, which is required for complete kinase activation (Kobayashi et al. 1999). The equivalent residues for SGK2 and SGK3 are Ser-416 and Ser-486 respectively.

1.3 Regulation of SGK isoforms

Despite displaying similar domain structures, the SGK isoforms have demonstrated unique cellular localisation and regulation. Most protein kinases are regulated predominately at the level of post-translational modification. SGK1 is an unusual kinase in that active levels are tightly regulated via multiple mechanisms, including rapid transcriptional expression (Webster et al. 1993a), post-translational modification (Park et al. 1999), constitutive ubiquitin-mediated degradation (Brickley et al. 2002) and nuclear-cytoplasmic shuttling (Buse et al. 2007). **Figure 1.3** shows a schematic demonstrating differences between SGK isoform regulation**.** It is likely that such tight regulation allows SGK1 to be rapidly available to the cell at the appropriate time and for sufficient duration when the cell requires rapid/temporal responses to extracellular cues. Regulation of SGK2 and SGK3 activity is far less complex with the major regulatory mechanism being post-translational modification, i.e. phosphorylation.

1.3.1 Transcriptional Regulation

Sgk1 was initially discovered as an immediate early gene that is transcriptionally responsive to glucocorticoids and serum in epithelial cells (Webster et al. 1993b). Indeed *sgk1* gene transcription is stimulated by a multitude of stimuli in addition to serum and glucocorticoids (Firestone et al. 2003; Kim et al. 2007) including mineralocorticoids (Naray-Fejes-Toth et al. 1999; Fakitsas et al. 2007; Bertog et al. 2008), the p53 tumour suppressor protein (Maiyar et al. 1996), follicle stimulating hormone (FSH) (Richards et al. 1995; Alliston et al. 1997), progestin (Feroze-Zaidi et al. 2007), thrombin (BelAiba et al. 2006), endothelin (Wolf et al. 2006), granulocyte/macrophage colony stimulating factor (GM-CSF) (Cowling and Birnboim 2000), transforming growth factor beta (TGF-β) (Waldegger et al. 1999), and growth factors such as fibroblast growth factor (FGF) and platelet derived growth factor (PDGF) (Lang et al. 2006a). Further activators include ischemic injury of the brain (Imaizumi et al. 1994), oxidative stress (Kim et al. 2007; Shibata et al. 2007) chronic viral hepatitis (Fillon et al. 2002), hyperosmotic stress (Waldegger et al. 1997; Bell et al. 2000), heatshock (Leong et al. 2003), excessive glucose concentrations (Lang et al. 2006a), chelation of Ca^{2+} (Pfau et al. 2007), metabolic acidosis (Faroqui et al. 2006), electroconvulsive therapy, sleep deprivation and fluoxetine (Conti et al. 2007). Conversely, *sgk1* transcription is down-regulated by cyclic adenosine monophosphate (cAMP) in pancreatic tumour cells (Klingel et al. 2000), heparin, dietary iron and nucleotides (Lang et al. 2006a; Li et al. 2007).

Through cloning and subsequent analysis of 4kb of the rat *sgk1* promoter, potential regulatory sites on the *sgk1* promoter responsible for stimulus specific induction of

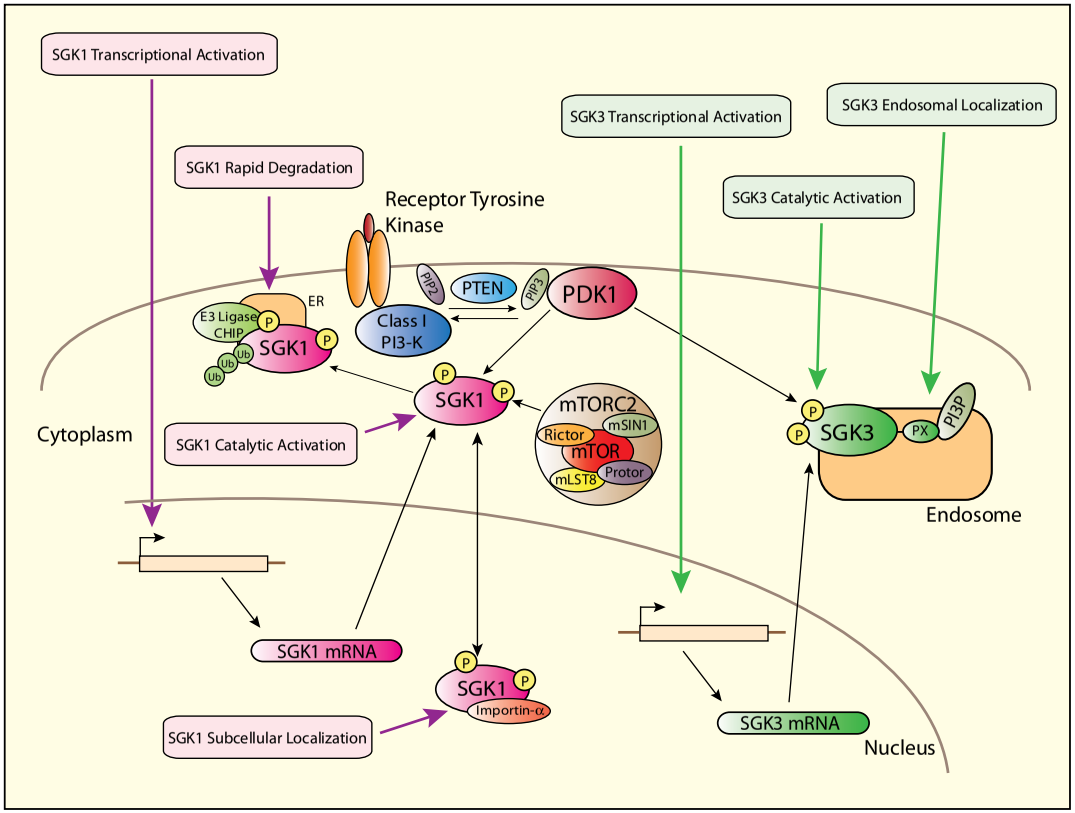

Figure 1.3: Levels of SGK1 and SGK3 regulation

SGK1 is acutely regulated at several levels, including gene transcription, post-translational modification, rapid degradation and subcellular localisation. Multiple types of stimuli are able to induce *sgk1* gene transcription and subsequent activation via phosphorylations, allowing an immediate response to various types of cell stress. SGK1 is also able to shuttle between the cytoplasm and nucleus in order to elicit cell-specific responses. A final level of SGK1 regulation involves polyubiquitination via the 26S proteasome at the ER. SGK3 has shown to be transcriptionally regulated by estrogen. Through binding of PtdIns(3)P to its PX domain, SGK3 is able to localise to the early endosomes where it is fully activated through phosphorylation at two key residues.

sgk1 have been identified (Firestone et al. 2003). A functional glucocorticoid response element (GRE) is present within the promoter, which is thought to be responsible for rapid induction of *sgk1* by glucocorticoids (Maiyar et al. 1996; Maiyar et al. 1997), and aldosterone (Chen et al. 1999). Multiple Sp-1 DNA binding sites are present which mediate FSH and hyperosmotic stress (via the p38/MAPK pathway) induced *sgk1* gene transcription. Given that the *sgk1* promoter contains multiple Sp-1 DNA binding sites, it is probable that they are responsible for the regulation of *sgk1* by many other types of stimuli (Firestone et al. 2003). Other binding sites identified in the promoter include sites for vitamin D receptor (VDR), retinoids (RXR), farnesoids (FXR), sterol regulatory element binding protein (SREBP), peroxysome proliferator activator receptor gamma (PPARγ), camp response element binding protein (CREB), activating transcription factor 6 (ATF6), heat shock factor (HSF), reticuloendotheliosis viral oncogene homolog (c-Rel), nuclear factor κB (NFκB), signal transducers and activators of transcription (STAT), TGF-β dependent transcription factors mothers against decapentaplegic homolog 4 (SMAD) -3 and SMAD4 and forkhead activin signal transducer (FAST) (Firestone et al. 2003; Lang et al. 2009).

Growth factors have been shown to stimulate *sgk1* gene transcription through the extracellular signal regulated kinases 1/2/Mitogen-activated protein kinase (ERK1/2/MAPK) pathway (Mizuno and Nishida 2001). Following phosphorylation, ERK1/2 is able to translocate into the nucleus and induce transcription of several genes through phosphorylation of an array of targets. *Sgk1* has also been identified as an ERK-inducible gene, as the induction of *sgk1* in murine fibroblast NIH-3T3 cells correlates with the extent to which ERK is activated by a variety of growth factors (Mizuno and Nishida 2001).

Mapping of the promoters of *sgk2* and *sgk3* demonstrates a multitude of predicted binding sites for transcription factors for both these kinases (www.genecard.org). Despite their name, *sgk2 and sgk3 are* not transcriptionally regulated by serum or glucocorticoids and are thought to be constitutive expressed (Kobayashi et al. 1999; Tessier and Woodgett 2006b). However, recent studies have demonstrated that *sgk3* has estrogen receptor binding regions and that the promoter can be transcriptionally induced with estrogen (Wang et al. 2011).

1.3.2 SGK isoform activation

Phosphoinositide 3-kinase (PI3-K) has been implicated in many fundamental cell processes including cell growth, proliferation and survival (Krasil'nikov et al. 1999), and is considered a key mediator of intracellular signalling through its ability to induce phosphorylation and subsequent activation of AGC kinase family members (Biondi et al. 2001). All SGK isoforms are enzymatically activated via phosphorylation in a PI3-K-dependent manner (Park et al. 1999; Tessier and Woodgett 2006a). SGK1 activity has shown to be stimulated in a PI3-K-dependent manner by many different activators, including insulin (Kobayashi and Cohen 1999; Perrotti et al. 2001), insulin-like growth factor (IGF-I) (Kobayashi and Cohen 1999; Hayashi et al. 2001), FSH

(Richards et al. 2002), sorbitol (Bell et al. 2000), hydrogen peroxide (Kobayashi and Cohen 1999), hepatic growth factor (HGF) (Shelly and Herrera 2002) and serum (Buse et al. 1999).

Furthermore, studies have also demonstrated that SGK1 can be activated by an increase in intracellular calcium, mediated through a calmodulin-dependent protein kinase kinase (CaMKK) but PI3-K-independent pathway in CHO cells (Imai et al. 2003), and Ras-related C3 botulinum toxin substrate 1 (Rac1), the small G protein is able to activate SGK1 also via a PI3-K-independent pathway (Shelly and Herrera 2002). Several other activators of SGK1 have been identified, including adhesion to fibronectin (Shelly and Herrera 2002), oxidation (Kobayashi and Cohen 1999), neuronal depolarisation (Kumari et al. 2001), lithium (Kumari et al. 2001) and cAMP (Perrotti et al. 2001). Both SGK2 and SGK3 phosphorylation and activation has shown to be stimulated by oxidation, insulin and IGF-I (Kobayashi and Cohen 1999; Virbasius et al. 2001), and SGK3 specifically by IL-3 (Liu et al. 2000) and estrogen (Wang et al. 2011).

1.3.2.1 Class IA and class III PI3K

The PI3-K family is integral in a variety of cellular processes as they function to coordinate the localisation and activity of a multitude of important downstream effector proteins, including both the SGK and AKT isoforms. Both the SGK and AKT families are phosphorylated and activated in a class I PI3-K dependent manner via phosphoinositide-dependent kinase-1 (PDK1), and thus class I PI3-K regulation is central to both SGK and AKT isoform activity and function. While the class III PI3-K human vacuolar sorting protein 34 (hVps34) has not been directly linked with the SGK family, it is possible that it may be involved in SGK3 function given its endosomal localisation and ability to recruit proteins with PtdIns3P binding domains. This section will discuss the PI3-K classes, where only class I and III PI3-Ks will be discussed here, as these are the most relevant to SGK isoform activation, followed by how these kinases activate SGK isoforms and their physiological relevance.

PI3-K lipid products are generated through the phosphorylation of the 3 hydroxyl group of the inositol ring of the three species of phosphatidylinositol (PtdIns) lipid substrates, which include PtdIns, PtdIns-4-phosphate (PtdIns(4)P), and PtdIns-4,5-bisphosphate (PtdIns(4,5)P_2) (Vanhaesebroeck and Waterfield 1999). The PI3-K family is made up of three distinct classes, all of which are grouped according to structure, function and lipid substrate preference. The class I PI3-K family is activated by growth factor stimulation, generates the lipid product PtdIns(3,4,5)P_3, and induces subsequent membrane localisation and activation of downstream kinases including PDK1, of which can then induce phosphorylation of SGK and AKT isoforms. The class I PI3-K family can be further divided into class IA and IB, both of which are heterodimers made up of a catalytic subunit and a regulatory subunit. Class 1A PI3-K are made up of one of the three different p110 catalytic subunits, (p110α, p110β and p110δ),

all products of separate genes (*PIK3CA, PIK3CB,* and *PIK3CD* respectively), and one of the five p85 regulatory subunits including p85α, p55α and p50α, all of which are splice variants of a single gene (*PIK3R1)*, with the remaining two p85 variants p85β and p55γ both products of separate genes (*PIK3R2* and *PIK3R3)* respectively (Vanhaesebroeck et al. 2010).

The class IB PI3-K family can be distinguished from IA, as the catalytic subunit p110γ, encoded by gene *PIK3CG* does not bind p85 regulatory subunit, but instead binds regulatory subunits p101 or p87, encoded by genes *PIK3R5* and *PIK3R6* respectively. The inability to bind the p85 regulatory subunit has upstream signalling consequences in that p85 regulatory subunit contains Src Homology 2 Domains (SH2), which are able to bind phosphorylated Tyrosine correlating with its ability to be activated through receptor tyrosine kinases (RTK), therefore enabling class IA to be activated by RTKs, and class 1B to be activated by G protein coupled receptors (GPCR), and both class IA and 1B being able to be activated indirectly by v-Ha-ras Harvey rat sarcoma viral oncogene homolog (H-Ras) (Fruman 2010).

The class III PI3-K family consists of only one catalytic subunit, hVps34, which was originally identified in a screen for genes involved in endosomal sorting in *Saccharomyces cerevisiae* (Backer 2008). HVps34 forms a constitutive heterodimer with Vps15, and has shown a limited substrate specificity for only PtdIns, thereby producing a single lipid product PtdIns3P, allowing it to function in the recruitment of proteins containing PtdIns3P binding domains to intracellular membranes (Yan and Backer 2007; Backer 2008; Yan et al. 2009). Many studies have demonstrated an important role for hVps34 in vesicular trafficking in the mammalian endosomal system (Thoresen et al. 2010), with stable hVps34 knockdown blocking the formation of multivesicular body formation, and slowing receptor degradation. However, more recent studies in mammalian systems have also recognised that hVps34 is involved in autophagy through association with Beclin-1, and nutrient sensing through signalling to mammalian target of rapamycin (mTOR) (Byfield et al. 2005; Nobukuni et al. 2005; Gulati et al. 2008).

While a number of studies have demonstrated that the SGK isoforms are activated in a class I PI3-K dependent manner via PDK1, to date there has not been any studies to conclusively link hVps34 direct or indirect interaction with the SGK isoforms. HVps34 has shown involvement in the regulation of the mTOR pathway through studies involving hVps34 knockdown, which demonstrated a block in insulin-stimulated phosphorylation of both S6 kinase 1 (S6K1) and eukaryotic initiating factor 4E (eiF4E) binding protein 1 (4EBP1), both key downstream effectors in the mTOR complex 1 (mTORC1) growth signalling pathway and readouts of mTORC1 activity (Backer 2008). Furthermore, over-expression of hVps34 activates S6K1 in the absence of insulin stimulation, and conversely hVps34 knockdown blocks amino acid stimulation of S6K1. Inhibition of mTORC1 with rapamycin does not affect hVps34, activity indicating that it is upstream of mTORC1 (Backer 2008). The Class III PI3-K family have not yet been shown to be

directly involved in the activation of the SGK isoforms, however given their endosomal localisation and demonstrated signalling through mTORC1, it is possible that this lipid kinase family may signal to mTOR through SGK3.

1.3.2.2 Cellular localisation and activation

The SGK family are quite distinct from the AKT family in that all AKT isoforms require the PH domain for phosphorylation by PDK1 and thus activation. Recently it has been demonstrated that SGK3 endosomal localisation is a prerequisite for full kinase activity. Mutation of the SGK3 PX domain combined with the addition of a myristolation signal, which localises SGK3 predominantly to the plasma membrane, interferes with PDK1 dependent Thr-320 phosphorylation of SGK3. However, if the hydrophobic motif of SGK3 is constitutively active by mimicking phosphorylation of the Ser residue, mutation of the PX domain does not affect full SGK3 activation. Hence, it has been suggested that endosomal localisation is essential for SGK3 to co-localize with a PI3-K dependent kinase responsible for phosphorylating Ser residue in the hydrophobic domain, and thus allowing PDK1 phosphorylation at Thr-320 for complete activation of SGK3 (Tessier and Woodgett 2006a).

The N-terminus of SGK1 is involved in phosphoinositide binding, despite the lack of an obvious domain structure. Protein lipid overlay assays demonstrate that an N-terminal region of SGK1 exhibiting high homology to that of the SGK3 PX domain, interacts specifically with PI(3)P, PI(4)P, and PI(5)P. Further characterisation of the role of the SGK1 N-terminal has shown that unlike the SGK3 PX domain, it is not required for SGK1 catalytic activity, however the phosphoinositide binding is important for multiple SGK1 functions, including stimulation of the ENaC (epithelial sodium channel) and inhibition of the pro-apoptotic Forkhead transcription factor 3a (FOXO3a) (Pao et al. 2007).

1.3.2.3 Phosphorylation at Serine and Threonine sites for kinase activation

SGK1 contains a Thr-256 site in its activation loop and a Ser-422 site in its hydrophobic motif that both require phosphorylation for maximal kinase activation (Kobayashi and Cohen 1999). Phosphorylation at the hydrophobic motif site of SGK1 is the initial step in full activation of SGK1, as it is able to convert SGK1 into a PDK1 substrate, and thus promotes the interaction between the PDK1 interacting fragment (PIF) binding pocket of PDK1 and the activation loop of SGK1 (Biondi et al. 2001), allowing phosphorylation at the Thr site in the activation loop to occur for full activation of the SGK isoform (Frodin et al. 2002; Collins et al. 2005). It has also been reported that PI3-K dependent phosphorylation of SGK1 requires formation of a complex between heat shock protein 90 (Hsp90) and SGK1, as inhibition of Hsp90 results in a complete loss of SGK1 activity (Belova et al. 2008). Studies also show that an alternate mechanism of SGK1 activation by PDK1 involves the scaffold protein Na^+/H^+ exchanger regulating factor 2

(NHERF2), where NHERF2 is able to mediate the assembly of SGK1 and PDK1 via its PDZ domains and PIF consensus sequence (Chun et al. 2002).

The WNK (With No Lysine K) family of serine-threonine kinases, activated by both hyper- and hypo- osmotic stresses (Lenertz et al. 2005) and associated with hypertension (Wilson et al. 2001) and regulation of blood pressure (Zambrowicz et al. 2003), are implicated in the activation of SGK1 by PDK1 (Xu et al. 2005a). Studies demonstrate that IGF-I is able to induce activation of SGK1 by stimulating WNK1 phosphorylation at Thr-58, a site phosphorylated by AKT (Xu et al. 2005b). Moreover, knockdown of WNK1 also results in substantial loss of SGK1 activity (Heise et al. 2010). Interestingly, kinase activity of WNK1 is not required for SGK1 activation, however it has been demonstrated that the N-terminal 220 residues of WNK1 are required for activation of SGK1 (Xu et al. 2005b). Given that WNK1 binds SGK1 but does not directly phosphorylate it, it is possible that WNK is involved as a scaffold protein to facilitate maximal SGK1 activation (Lang et al. 2006a), however further investigation is required to delineate the mechanism involved in WNK1 control of SGK1 activation. Both SGK2 and SGK3 activation have also shown to be regulated by WNK1, albeit to a lesser extent (Xu et al. 2005b).

Studies attempting to elucidate the kinase responsible for phosphorylating SGK1 at the hydrophobic motif have yielded conflicting results. Initially it was demonstrated that mTORC1 is able to phosphorylate SGK1 at the Ser-422 site, leading to p27 phosphorylation and G1 progression, deregulating the cell cycle in cancers (Hong et al. 2008). However, more recently it has been suggested that mTOR complex 2 (mTORC2) and not mTORC1 controls hydrophobic motif phosphorylation and thus activation of SGK1 (Garcia-Martinez and Alessi 2008; Lu et al. 2010; Lyo et al. 2010). Further studies have also determined that mammalian stress-activated protein kinase-interacting protein (mSIN1) is the specific component in mTORC2 that interacts and recruits SGK1 into mTORC2 to undergo phosphorylation at Ser-422 in the hydrophobic motif (Lu et al. 2011).. These studies also demonstrated that while mSIN1 is able to bind SGK1, it was unable to bind AKT, a well-characterised mTORC2 substrate, suggesting that mTORC2 uses specific mechanisms to recruit different substrates. The kinase responsible for phosphorylation of SGK2 and SGK3 at their respective Ser sites still remains undefined.

Both big MAP kinase (BMK-1 (ERK5)) and ERK have been shown to phosphorylate SGK1 at Ser-78 in the N-terminal domain. BMK-1, a member of the MAPK family directly phosphorylates Ser-78 during growth factor induced cell proliferation, and this is shown to be PDK1-independent (Hayashi et al. 2001). Furthermore, ERK phosphorylation of SGK1 at Ser-78 was demonstrated to indirectly activate SGK1 at both Thr-256 and Ser-422, activating spatial memory formation in rats (Lee et al. 2006). SGK1 has also been shown to be both a downstream kinase substrate as well as a transcriptionally regulated gene target of the stress and cytokine responsive p38 MAPK pathway in response to interleukin-6 (IL-6), involving SGK1 in survival

signalling by IL-6 in human cancers (Meng et al. 2005). Taken together these studies suggest that SGK1 Ser-78 may be a common target of the MAPK family.

1.3.3 Negative regulation of SGK isoform activity

Another important level of SGK1 regulation involves rapid turnover via ubiquitin modification and degradation. It has been demonstrated that SGK1 is a direct target of polyubiquitin modification, and ultimate degradation by a 26S proteasome-dependent pathway. The 60 amino acid N-terminal of SGK1 has shown to be essential for rapid degradation, as upon deletion of this domain the normal ~30 minute half life of SGK1 is increased more than three fold (Brickley et al. 2002). More specifically, a six amino acid hydrophobic motif (GMVAIL, amino acids 19-24) in the N-terminal domain of SGK1 is required for ubiquitin modification and degradation (Bogusz et al. 2006). This region is also required for association of SGK1 with the ER (Bogusz et al. 2006). As described in section 1.2.2.1 the *sgk1* gene has four splice variants, with reports suggesting that only two of these splice variants result in proteins with the N-terminal six amino acid sequence required for ER localisation and rapid degradation of SGK1 (Arteaga et al. 2007). It is thought that SGK1 co-localizes with the stress-associated E3 ligase CHIP (C-terminus of Hsc (heat shock cognate protein) 70-interacting protein) at the ER, and forms a complex, which is essential for the ubiquitin modification and rapid proteasomal degradation of SGK1 (Belova et al. 2006). Moreover, it has also been suggested that SGK1 degradation may be mediated by the E3 ubiquitin-protein ligase Nedd4-2. Nedd4-2 is a direct substrate of SGK1, perhaps indicating that through feedback inhibition, SGK1 is able to induce its own degradation (Zhou and Snyder 2005).

More recent reports suggest an alternative mechanism of SGK1 ubiquitination involving an E3 ubiquitin ligase complex formed between Rictor, Cullin-1 and Rbx1, promoting the ubiquitination of SGK1(Gao et al. 2010a), despite the involvement of Rictor in phosphorylating and activating SGK1 as part of the mTORC2 pathway (Garcia-Martinez and Alessi 2008). The complex formation is likely to be an mTOR independent function of Rictor. Interestingly, these studies demonstrate that SGK1 and other AGC kinases including AKT are also able to phosphorylate Rictor at Thr-1135, not affecting the kinase activity of Rictor but promoting Rictor dissociation from Cullin-1 and impairing SGK1 ubiquitination, suggesting a possible feedback mechanism that may contribute to SGK1 over-expression due to aberrant signalling(Gao et al. 2010a; Gao et al. 2010b). Protein phosphatase 2A (PP2A), which dephosphorylates the Thr residue in the catalytic domain, has also been shown to be a negative regulator of SGK1 activity *in vitro*, (Park et al. 1999).

1.3.4 SGK localisation

A further level of regulation involves the subcellular localisation of SGK1 between the nucleus and the cytoplasm, which is controlled in a stimulus-dependent manner in certain cell types, and which correlates to the proliferative state of the cell (Buse et

al. 1999). The serum-induced nuclear import of SGK1 requires the NLS-dependent recognition of SGK1 by importin-α, in addition to PI3-K dependent activation (Maiyar et al. 2003). More recently it has also been reported that SGK1 and ERK co-localize together in the nucleus in an importin-α dependent manner and that ERK activation is required (Buse et al. 2007). Suggesting that activation of the RAS/ERK pathway is necessary for nuclear SGK1 mediated effects.

1.4 Biological processes regulated by SGK isoforms

Following activation, SGK has been shown to both positively and negatively regulate a number of targets through phosphorylation. A detailed list of both activators and targets of the SGK isoforms can be found in **Figure 1.4 and Table 1.1.** These targets then go on to effect a variety of core cell processes including cell proliferation, growth, survival, migration and ion channel regulation. To date most studies investigating the role of the SGK family in regulating cellular processes have been carried out using the SGK1 isoform, therefore most of what will be discussed in the following sections is based on SGK1, with data on the other SGK isoforms included where available.

1.4.1 SGK substrate specificity

The substrate specificities for the SGK family have been determined through a panel of synthetic peptides, and demonstrate that they preferentially phosphorylate Ser and Thr residues within the Arg-Xaa-Arg-Xaa-Xaa-Ser/Thr-φ motifs, (where Xaa stands for any amino acid) (Park et al. 1999; Biondi et al. 2001; Frodin et al. 2002; Collins et al. 2003), similar to the substrate specificity of the AKT family (Kobayashi et al. 1999). Characterisation of SGK3 substrate specificity has shown that it tolerates the presence of Lys instead of Arg at position *n*-3 (where *n* is the site of phosphorylation) (Kobayashi et al. 1999). This difference is consistent with the ability of SGK3 to target substrates such as atrophin-1 interacting protein 4 (AIP4) (Slagsvold et al. 2006) and flightless-I (FLI-I) (Xu et al. 2009), which are not SGK1, or SGK2 substrates. It is important to note that many substrates recognised as targets of the SGK family are *in vitro* targets only, and have yet to be demonstrated as bona fide *in vivo* targets.

1.4.2 SGK knockout mice

A more comprehensive investigation into possible functional redundancies existing between the SGK isoforms has been achieved through the generation of various *sgk* gene knockout mice. The *sgk1*$^{-/-}$ mouse was first generated in 2002 (Wulff et al. 2002), displaying a phenotype showing no differences on a standard diet with normal NaCl levels. However, under conditions of NaCl deprivation, *sgk1*$^{-/-}$ mice are unable to adequately up-regulate Na^+ reabsorption, eventually leading to substantial decreases in mean arterial blood pressure (Wulff et al. 2002). Moreover, these mice also demonstrate an inability to sufficiently regulate K^+ elimination after an acute and chronic K^+ load (Huang et al. 2004). Recent studies using the *sgk1*$^{-/-}$ mouse have also demonstrated an inhibition of cell proliferation and $p27^{kip1}$ cytosol translocation in vein

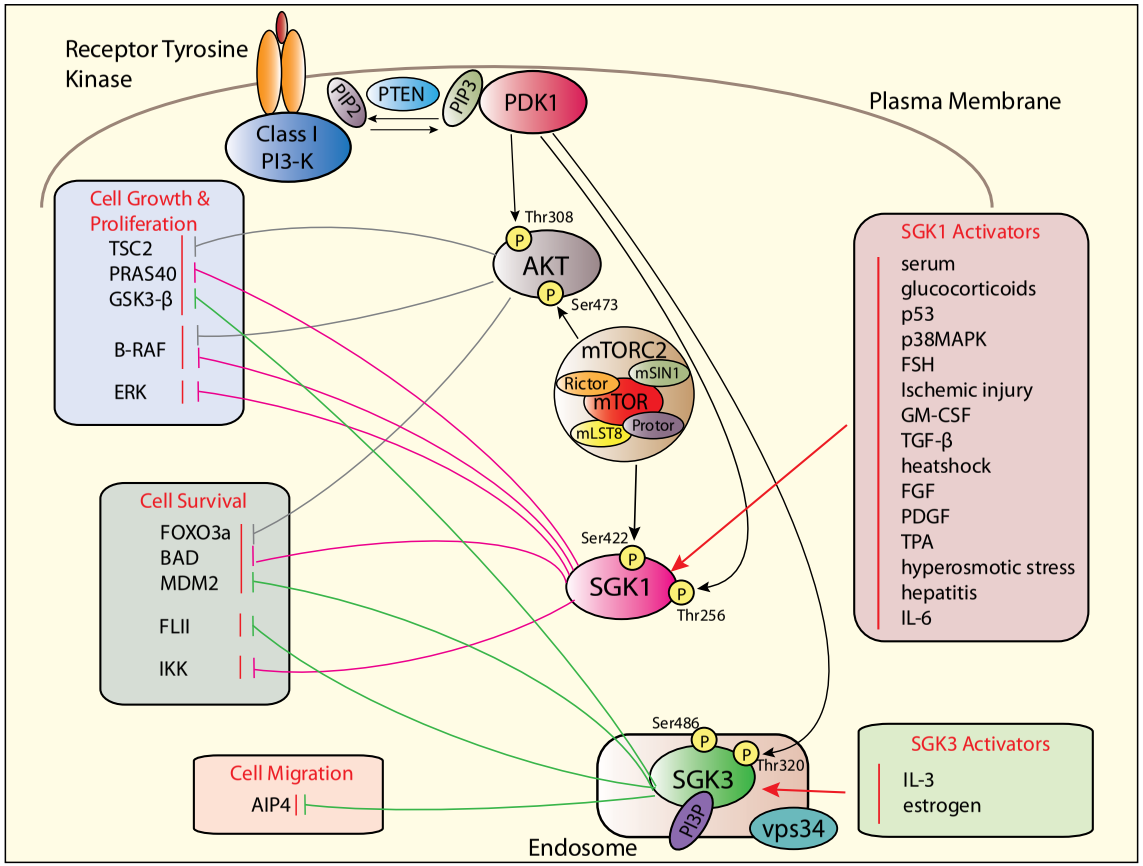

Figure 1.4: Activators and substrates of SGK1 and SGK3

Multiple cytokines, growth factors and cell stressors are able to activate either SGK1 and/or SGK3. The activation of SGK1 requires direct phosphorylation by PDK1 and mTORC2, and SGK3 localises to the endosome where it is phosphorylated by PDK1 and likely mTORC2 for full activation. SGK1 has also shown to be phosphorylated by BMK-1 and p38 MAPK at Ser-78. Following complete activation, multiple proteins involved in cell growth, proliferation, survival and migration are targeted by both SGK1 and SGK3. Arrows represent positive regulation, and lines represent negative regulation.

Table 1.1: SGK isoform regulation and activation summary

Table showing important regulators and effectors of the SGK isoforms.

ISOFORM	ACTIVATORS & INHIBITORS				EFFECTORS		
	FUNCTION	TYPE	NAME	REFERENCE	FUNTION	NAME	REFERENCE
SGK1	TRANSCRIPTIONAL REGULATION	CYTOKINES	IL-6 GM-CSF	Meng (2005) Cowling (2000)	CELL GROWTH & PROLIFERATION	ERK2 TSC2 GSK3 B-Raf MEKK3 P27	Won (2009) Aoyama (2005) Kobayashi (1999) Zhang (2001)
		GROWTH FACTORS	Glucocorticoid Serum TGF-β FGF PDGF FSH	Webster (1993) Webster (1993) Waldegger (1999) Mizuno (2001) Mizuno (2001) Alliston (1997)			
		CELL STRESS	Heatshock UV Hyperosmotic Ischemic injury Hepatitis	Leong (2003) Leong (2003) Waldegger (1997) Imaizumi (1994) Fillon (2002	CELL SURVIVAL	Foxo3a NF-κB	Brunet (2001) Zhang (2005)
	REGULATION OF ACTIVATION	GROWTH FACTORS	Serum Insulin IGF1 FSH HGF	Buse et al. (1999) Perrotti (2001) Hayashi (2001) Richards (2002) Shelly (2002)	ION CHANNEL REGULATION	SCN5A ROMK1 Nedd4-2 KCNQ1/KCNE KV1.3 ClC-2 Channels	Boehmer (2003) Palmada (2003) Snyder (2004) Embark (2003) Gamper (2002) Palmada (2004)
		CELL STRESS	Sorbitol Hydrogen peroxide	Bell (2000) Kobayashi (1999)			
		PHOSPHORYLATION	mTORC2 PDK1 P38 MAPK BMK-1	Garcia-Martinez (2008) Kobayashi (1999) Meng (2005) Hayashi (2001)	NEUROCHEMISTRY	NDRG1 NDRG2 Huntingtin Tau	Murray (2004) Rangone (2004) Chun (2004) Chun (2004)
	INHIBITION	PHOSPHATASE	PP2A	Park (1999)			
SGK2	REGULATION OF ACTIVATION	PHOSPHORYLATION	PDK1	Kobayashi (1999)	ION CHANNEL REGULATION	KCNQ1/KCNE	Ebark (2003)
SGK3	TRANSCRIPTIONAL REGULATION	HORMONE	Estrogen	Wang (2011)	CELL MIGRATION	AIP4	Slagsvold (2006)
					CELL SURVIVAL	BAD Foxo3a FLII	Liu (2000) Liu (2000) Xu (2009)
	REGULATION OF ACTIVATION	CYTOKINES	IL-3	Liu (2000)	CELL GROWTH & PROLIFERATION	GSK3 PRAS40 TSC2	Liu (2000) Bruhn (unpublished) Bruhn (unpublished)
		PHOSPHORYLATION	PDK1	Kobayashi (1999)	ION CHANNEL REGULATION	KCNQ1/KCNE HERG GluR1	Embark (2003) Maier (2006) Strutz-Seebohm (2006)

grafts (Cheng et al. 2010). Characterisation of *sgk3*$^{-/-}$ mice demonstrated a distinct defect in hair follicle morphogenesis, producing a wavy hair phenotype. Further analysis revealed a defect in proliferation and nuclear accumulation of β-catenin in hair-bulb keratinocytes, however these mice exhibited normal sodium and glucose handling (McCormick et al. 2004; Alonso et al. 2005). More recent studies using *sgk3*$^{-/-}$ mice also reveal involvement of SGK3 in the regulation of calcitriol plasma concentration, renal phosphate excretion and mineralization of bone(Bhandaru et al. 2011). To date characterisation of an *sgk2*$^{-/-}$ mouse has not been reported.

A double *sgk1*$^{-/-}$/*sgk3*$^{-/-}$ mouse has also been generated, and exhibited the combined phenotype of *sgk1*$^{-/-}$ and *sgk3*$^{-/-}$ mice, displaying a wavy hair phenotype and impairment of renal Na^+ retention on a low salt diet (Grahammer et al. 2006). These studies using both single and double knockout animals have assisted in determining possible functional redundancies within the SGK family, with both *sgk1*$^{-/-}$ and *sgk3*$^{-/-}$ single knockout mice exhibiting quite different phenotypes. Furthermore, the combined knockout of both *sgk1* and *sgk3* did not produce a more severe phenotype, suggesting that these two isoforms most likely do not compensate for each other. However, it is possible that the phenotype of *sgk1*$^{-/-}$/*sgk3*$^{-/-}$ mouse is not more severe as SGK2 may be able to compensate and maintain some level of homeostasis, despite no detectable increase of SGK2 transcript levels in these mice (Grahammer et al. 2006).

Recent studies characterizing an *akt2*$^{-/-}$/*sgk3*$^{-/-}$ mouse found that the defect in hair growth is markedly worse in the double knockout mice than in *sgk3*$^{-/-}$ mice only (Mauro et al. 2009). *Akt2*$^{-/-}$ mice display insulin resistance, hyperinsulinemia and increased β-cell proliferation and mass (Cho et al. 2001a), however further characterisation of the *akt2*$^{-/-}$/*sgk3*$^{-/-}$ mice also revealed these animals have a markedly greater impairment of glucose homeostasis than AKT2 knockout only (Yao et al. 2011).

1.4.3 Cell proliferation

Cell proliferation is regulated through the coordinated modulation of cell cycle machinery, which consists of the cyclins, cyclin-dependent kinases (CDK) and CDK inhibitors (Nam and Kim 2008; Malumbres and Barbacid 2009). CDK activity requires the binding of the regulatory subunits cyclins, which are synthesized and destroyed at specific times of the cell cycle. Protein modification such as phosphorylation (by kinases) and dephosphorylation (by phosphatases) of the cyclins and CDKs are also critical regulatory mechanisms that dictate entry into, and progression through, the cell cycle (Ivanchuk and Rutka 2004). The CDK inhibitors are another fundamental level of cell cycle regulation, which include CDK inhibitor protein (CIP) and CDK inhibitor kinase (KIP), and are capable of abrogating catalytic kinase activity throughout the cell cycle (Ivanchuk and Rutka 2004). SGK1 is involved in cell proliferation through both the direct and indirect modulation of cell cycle machinery.

1.4.3.1 Regulation of cell proliferation

Studies have demonstrated that SGK1 is involved in cell cycle regulation through the direct phosphorylation and inhibition of $p27^{Kip1}$, a member of the KIP family of CDK inhibitors (Hong et al. 2008; Cheng et al. 2010). $p27^{Kip1}$ is involved in inhibiting G0 and early G1 cell cycle progression by inhibiting cyclin E-CDK2 and Cyclin D-CDK4 complexes. It also is required for the activation and assembly of cyclin D-CDKs in early G1 (Chun et al. 2003). Loss of $p27^{Kip1}$ inhibitory function can confer an advantage in tumourigenesis by promoting cell cycle progression.

Phosphorylation of $p27^{Kip1}$ at Thr-157 reduces $p27^{Kip1}$ nuclear import through the disruption of a NLS and thus decreases its ability to inhibit cyclin E-CDK2 and cyclin D-CDK4 (Viglietto et al. 2002). SGK1 is able to phosphorylate Thr-157 of $p27^{Kip1}$, reducing its nuclear and increasing its cytoplasmic localisation (Hong et al. 2008). In addition, SGK1 and SGK3 are able to indirectly regulate $p27^{Kip1}$ through regulation of forkhead transcription factors, which are involved in the induction of $p27^{Kip1}$ transcription. The regulation of FOXO3a by SGK occurs via phosphorylation at multiple sites, and ultimately prevents FOXO3a from localizing to the nucleus to affect its targets. In addition to transcriptional regulation of $p27^{Kip1}$, the FOXO proteins are also involved in the regulation of other cell cycle machinery, including CDK4, cyclin D1 and retinoblastoma (pRB) members p107 and p130 (Ho et al. 2008), thus SGK regulation of FOXO3a is likely to impact cell cycle regulation at many levels.

Glycogen synthase kinase 3-β (GSK-3β) is involved in the regulation of numerous physiological processes, including the phosphorylation of cyclin D1, important in cell cycle transition. Following phosphorylation by GSK-3β, cyclin D1 is marked for degradation by the proteasome (Vivanco and Sawyers 2002), and similar to AKT, both SGK1 and SGK3 can phosphorylate and inactivate GSK-3β allowing cyclin D1 to continue its role in the cell cycle (Kobayashi and Cohen 1999; Dai et al. 2002). Inactivation of GSK-3β by SGK1 and SGK3 has also been associated with the stimulation of cardiac fibrosis caused by mineralcorticoid excess (Wyatt et al. 2006), and the alteration of β-catenin dynamics, leading to the formation of adherens junctions and tight junction sealing in mammary epithelial tumour cells (Failor et al. 2007).

B-Raf (v-raf murine sarcoma viral oncogene homolog B1) is a member of the MAPK/ERK cascade, which is important in the regulation of cell proliferation, differentiation and apoptosis (Chong et al. 2003), and uncontrolled activation of the RAS/RAF/MAPK/ERK pathway is prevalent in many human cancers (Guan et al. 2000). SGK1 has been implicated in the regulation of B-Raf, as active SGK1 is able to phosphorylate B-Raf at Ser-364 *in vitro* and inactivate it (Zhang et al. 2001). Given that SGK1 gene transcription and activation is stimulated by growth factors through the ERK/MAPK pathway (Mizuno and Nishida 2001; Firestone et al. 2003), it is feasible that SGK1 may be involved in a negative feedback loop, intended to repress activity of the MAP kinase cascade (Zhang et al. 2001). However, more recent reports investigating the influence of SGK1 on hepatocyte proliferation have demonstrated that SGK1 is able

to enhance ERK phosphorylation and the association between ERK1/2 and mitogen-activated protein kinase kinase (MEK)1/2 (Won et al. 2009). Moreover SGK1 and ERK are able to co-localize to either the nucleus or the cytoplasm during growth factor signalling (Buse et al. 2007). Taken together these data suggest functional cross talk between SGK1 and the ERK/MAPK pathways, however further investigation is necessary to more specifically determine the influence of SGK1 on ERK signalling.

SGK1 has also shown to regulate another member of the MAPK pathway, mitogen-activated protein kinase kinase kinase 3 (MEKK3) (Ho et al. 2008). Unlike other components of the MAPK signalling cascade, MEKK3 is associated with blocking signalling to cell proliferation and cell cycle progression. Studies have demonstrated that SGK1 can phosphorylate and inactivate MEKK3, thereby preventing it from phosphorylating its downstream effectors mitogen-activated protein kinase kinase 3 (MKK3) and stress-activated protein kinase (SAPK) (Chun et al. 2003).

Further evidence supporting a specific role for SGK3 in the regulation of cell proliferation comes from multiple studies implicating SGK3 in epidermal growth factor (EGF) receptor signalling. SGK3 can activate gene expression through β-catenin/ Lef-1 in cultured keratinocytes, but represses FOXO3a mediated gene transcription. Conversely, ectopic expression of dominant negative (DN) SGK3 inhibited EGF activated Lef-1 reporter activity, suggesting that EGF activation of β-catenin/Lef-1 dependent transcription could potentially be mediated by SGK3 (McCormick et al. 2004). SGK3 has also shown to be activated by EGF (Virbasius et al. 2001) and co-localize with the EGF receptor at the early endosome (Xing et al. 2004). Importantly, EGF signalling from the endosome is sufficient to activate both proliferation and survival pathways (Wang et al. 2002). In addition, the *egfr*$^{-/-}$ mouse also displays similarities to the *sgk3*$^{-/-}$ mouse, as both display a wavy hair phenotype (McCormick et al. 2004; Alonso et al. 2005; Okada et al. 2006), further suggesting that SGK3 acts as a mediator of EGF receptor signalling. Many groups have demonstrated a clear role for the SGK family in cell cycle progression and cell proliferation through the direct and indirect modulation of multiple components of the cell cycle machinery. Whilst many targets have been identified for SGK1, SGK3 is also becoming recognised as playing a role in growth factor induced cell proliferation.

1.4.4 Cell growth

Cell growth is defined as an increase in cell mass and cell size through macromolecular biosynthesis (Fingar et al. 2004), and is a carefully orchestrated process in that it occurs very specifically and requires a coordinated increase in cell growth and cell proliferation to maintain cell size and contribute to the overall growth of an organ or whole organism (Fingar et al. 2002); a number of studies have demonstrated that cell proliferation and cell growth are distinct yet coordinated processes. While in most cases proliferation and growth are coordinated processes, these processes can also become uncoupled. To date a well-established role in regulating cell growth at multiple levels has been described for the AKT kinases, and as such it is possible that the

SGK isoforms may also be involved in regulating growth in a similar manner. **Figure 1.5** shows a schematic detailing signalling through the growth pathway. This section describes important regulators of cell growth, along with the potential relevance of SGK signalling.

Early studies using *S. cerevisiae* demonstrated that inhibiting cell division does not inhibit cell growth, however in the same system nutrient deprivation induces a coordinated block of yeast cell division and cell growth, suggesting that cell growth is required for cell cycle progression (Johnston et al. 1977; Fingar et al. 2002). Similar studies using *D. melangaster* have also shown that under certain conditions growth and proliferation can act as separate processes (Weigmann et al. 1997; Fingar et al. 2002). Importantly, these studies have also extended to mammalian systems, where it has been demonstrated that growth and proliferation are indeed distinct processes, with cell growth reliant on mTORC1 and PI3-K dependent signalling (Fingar et al. 2002).

mTOR is a phosphoinositide 3-kinase-related kinase (PIKK), that integrates nutrient and growth signals and thus acts as a central controller of cellular and organism growth, mainly through the regulation of ribosome biogenesis and protein translation. Homozygous deletion of the mTOR kinase domain results in embryonic lethality shortly after implantation in mice, (Gangloff et al. 2004; Murakami et al. 2004), and a conditional deletion of a region essential for mTOR kinase activity reveals a decreased cell size and blocked proliferation in embryonic stem (ES) cells (Murakami et al. 2004). The importance of mTOR in growth and proliferation has also been well established in *S. cerevisiae* (Barbet et al. 1996) and *D. melangaster* (Montagne et al. 1999; Zhang et al. 2000) in addition to mammals (Wullschleger et al. 2006). Further characterisation of mTOR has also defined its involvement in a number of other important processes including gene transcription, autophagy and metabolism (Wullschleger et al. 2006; Jung et al. 2010).

mTOR forms two distinct complexes termed mTORC1 and mTORC2, with both complexes comprising of mTOR and mammalian lethal with sec thirteen (mLST8), while only mTORC1 contains raptor, a protein involved in recruiting substrates for mTOR. mTORC2 contains many other proteins not present in mTORC1, including rictor, Sin1, and protor (Wang and Proud 2011). Further characterization of these two mTOR complexes has revealed that mTORC1 plays a critical role in the phosphorylation and activation of key regulators of cell growth machinery which include S6 Kinase and 4EBP1 (Corradetti and Guan 2006), while mTORC2 plays an essential role in actin polymerisation and cytoskeleton reorganization (Jacinto et al. 2004). More recently, mTORC2 has also been identified as the kinase responsible for phosphorylating the Ser residue located in the hydrophobic motif of both AKT (Sarbassov et al. 2005) and SGK1 (Garcia-Martinez and Alessi 2008) allowing full activation of these kinases, thus also placing it up-stream of mTORC1 and therefore important in mTORC1 signalling.

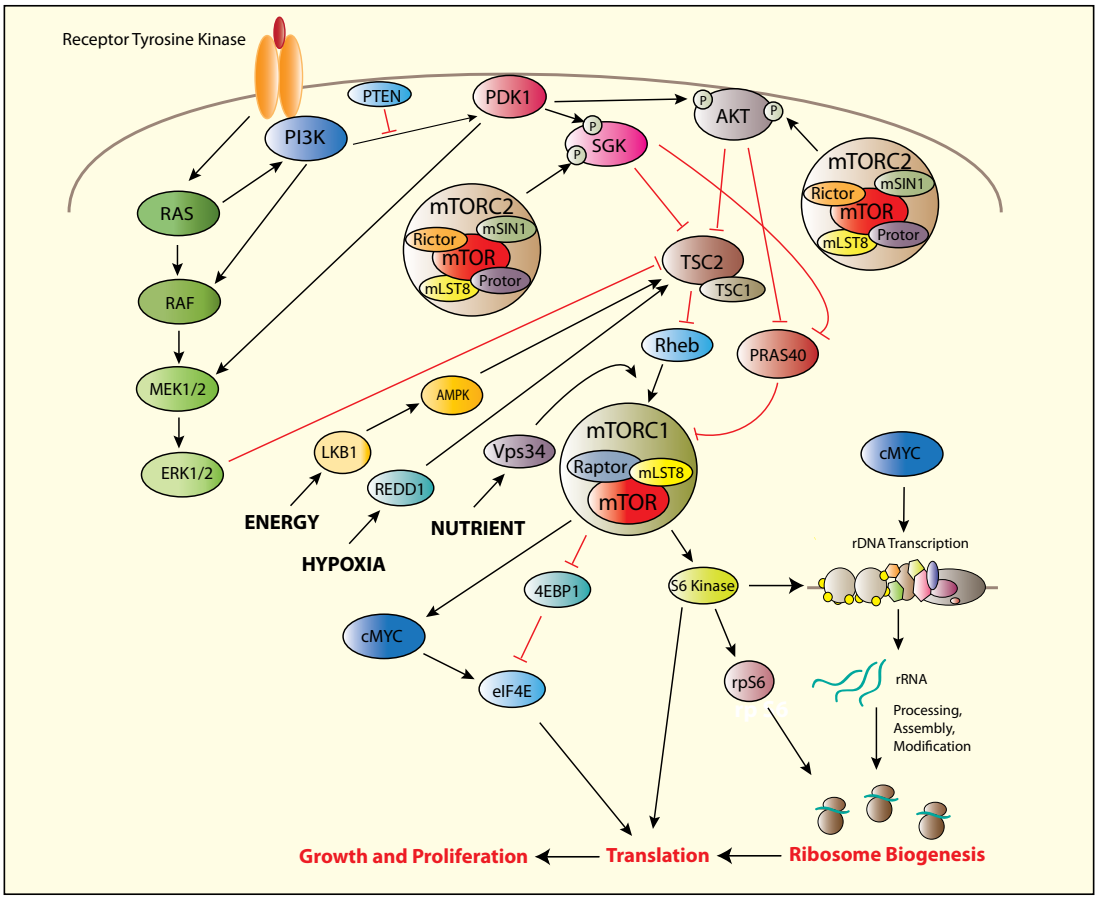

Figure 1.5: The PI3-K/mTORC1 signalling network in cell growth and proliferation

Activation of PI3-K by RTKs leads to phosphorylation of PDK1, subsequently leading to phosphorylation and activation of both AKT and SGK. Following activation these kinases can inhibit TSC2 and PRAS40, leading to activation of mTORC1, an important node in signalling to protein synthesis and cell growth. The RAS and PI3-K pathways are able to interact at many levels, including RAS activation of PI3-K, PI3-K activation of B-Raf. SGK is also able to promote ERK1/2 activity, which can then go on to inhibit TSC1/2 complex. Inhibitory feedbacks also exist between these pathways (red lines) with both AKT and SGK able to phosphorylate and inhibit B-Raf activity. Feeding into the core of PI3-K/mTORC1 signalling are pathways modulated by energy, oxygen and nutrient status. Black arrows depict activating events and red lines indicate inhibitory action.

1.4.4.1 mTORC1 regulation of cell growth

Following activation via both amino acids and growth factors, mTORC1 acts as a key modulator of cell growth, through the regulation of its two main substrates, S6K and 4EBP1, both of which are crucial players in regulating the translational machinery (Fingar et al. 2002). The direct phosphorylation of S6K by mTORC1 is able to increase the translational capacity of the cell as it promotes protein synthesis through the phosphorylation of the 40S ribosomal protein S6 (rpS6) by activated S6K, which subsequently increases the translation of 5' polypyrimidine tract (5'TOP) containing mRNAs, which encode many of the protein synthesis machinery, including ribosomal proteins and elongation factors along with other components required for translation (Jefferies et al. 1997; Meyuhas 2000). Moreover, in *s6k*$^{-/-}$ mice 5' TOP mRNA translation is not reduced, suggesting that other pathways may be involved in regulating this process also (Pende et al. 2004).

The direct phosphorylation of 4EBP1 by mTORC1 increases translational efficiency as it allows the dissociation of eukaryotic initiation factor 4E (eiF4E) from 4EBP1, so that it is then able to form a functional initiation complex with eukaryotic initiation factor 4G (eiF4G), often referred to as eiF4F. This initiation complex is then able to increase translation initiation of mRNA through binding to the 5'-cap structure of eukaryotic mRNAs, thereby facilitating ribosome recruitment and initiating translation (Wang and Proud 2009).

1.4.4.2 Ribosome biogenesis

The central role of mTORC1 in modulating translational machinery via multiple mechanisms is much like a nutritional checkpoint, where mTORC1 will adjust protein biosynthetic activity depending on the availability of nutrients. To meet the increased demand for proteins during cellular adaptation to changing environments the cell must increase translational capacity by up-regulating ribosome biogenesis (Sulic et al. 2005). Ribosome biogenesis is a complex process that consumes a great amount of energy, and as such is tightly regulated to nutrient availability (Mayer and Grummt 2006).

The mammalian ribosome is made up of two-thirds RNA and one-third protein, and assembled into two subunits referred to as 60S and 40S. The larger 60S subunit contains three different RNA species, 28S, 5.8S and 5S ribosomal RNAs (rRNA), along with approximately 49 ribosomal proteins (r-proteins) (Moss et al. 2007). The smaller 40S subunit contains only a single RNA, which is the 18S RNA and approximately 33 r-proteins (Moss et al. 2007). The three rRNA species 18S, 5.8S and 28S are synthesized, processed and assembled into ribosomes in the nucleolus, and are transcribed by RNA Polymerase I (Pol I) from the ribosomal DNA (rDNA) as a single precursor referred to as the 45S rDNA repeat (**Figure 1.6)**. The remaining rRNA species 5S is independently transcribed by RNA Polymerase III (Pol III) in the nucleus, and then subsequently exported to the nucleolus for ribosome assembly (Sulic et al. 2005).

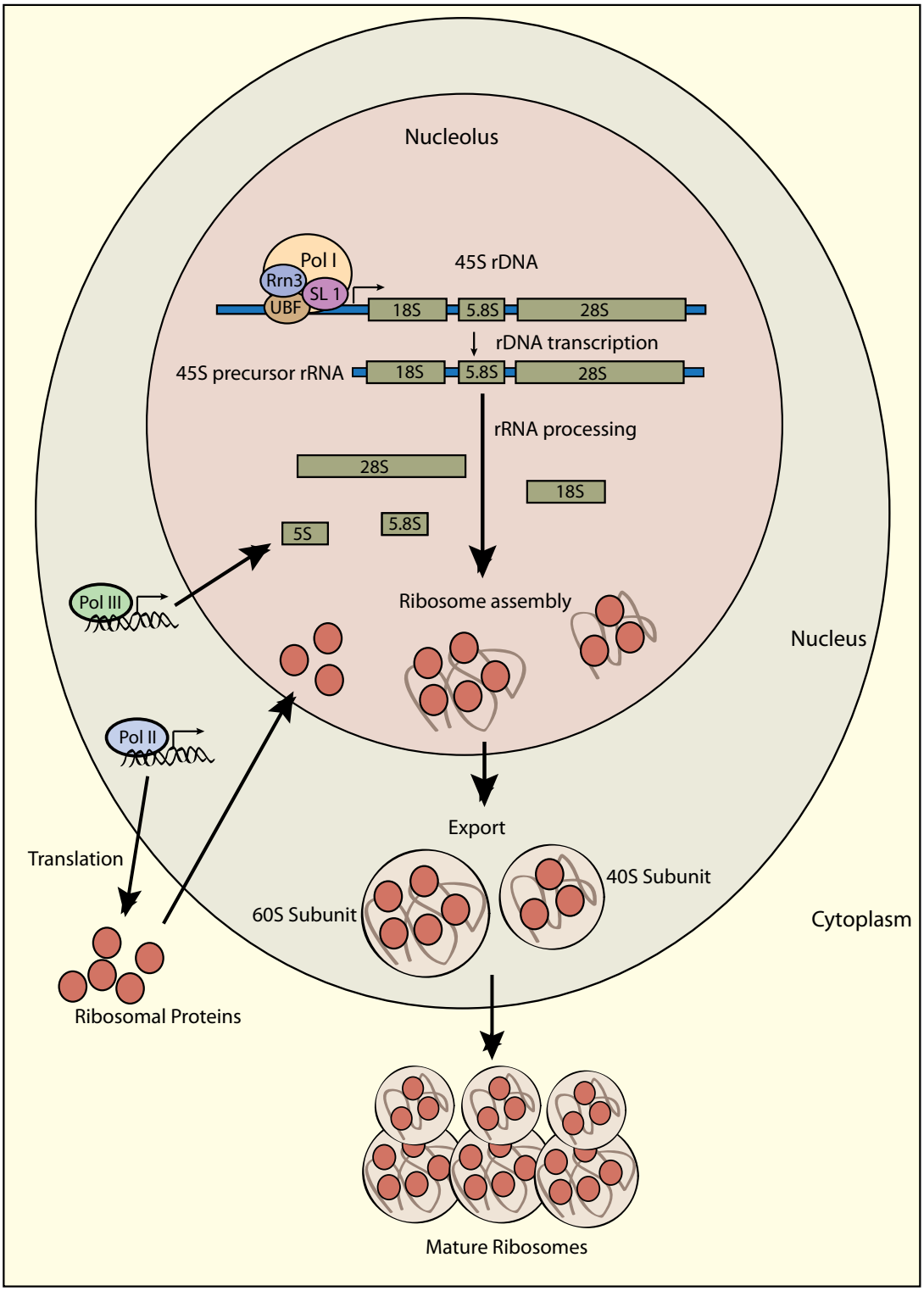

Figure 1.6: Schematic representation of ribosome biogenesis

Ribosome biogenesis involves the coordinated regulation of all three RNA polymerases, allowing generation of both ribosomal RNA (rRNA) and ribosomal protein, which can then go on to form functional ribosomes. The 45S precursor rRNA is generated by RNA Pol I transcription (rDNA transcription). RNA Pol III generates 5S rRNA, and RNA Pol II transcribes ribosomal protein genes. The 45S precursor is processed to produce 18S, 28S and 5.8S rRNA. The rRNA along with ribosomal proteins are then assembled in the nucleolus, and are exported to the nucleus as the 60S and 40S ribosomal subunits. The ribosomal subunits are then transported into the cytoplasm as a functional ribosome (Sulic et al. 2005).

All ribosomal proteins required for ribosomal assembly are transcribed by RNA Polymerase II (Pol II), exported to the cytoplasm for translation into protein and then imported into the nucleolus for ribosome assembly. Following assembly, mature ribosomes are then translocated to the cytoplasm (Sulic et al. 2005). Given the complexity of this process, and the required coordination of all three RNA polymerases, it is clear how this process can be one of the largest metabolic tasks that a proliferating cell can undergo (Moss et al. 2007).

In mammalian cells the direct correlation between cell growth and rRNA synthesis has been well established, in that rRNA synthesis is high in proliferating cells (Raska et al. 2004). The production of rRNA has been considered a rate-limiting step in ribosome biogenesis, and as such metabolically active cells must have high rates of Pol I transcription to maintain this process (Mayer and Grummt 2006). Studies demonstrating that rapamycin is able to inhibit ribosome biogenesis have confirmed that mTORC1 is critical for this process, and further investigation has revealed that mTORC1 is involved in regulating Pol I transcription initiation activity via the transcription factor upstream binding factor (UBF) (Mayer and Grummt 2006). Recent evidence from our laboratory demonstrating that AKT is able to directly regulate rDNA transcription via both mTORC1 dependent and independent mechanisms (Chan et al. 2011) suggest that SGK3 may also be involved in the regulation of rDNA transcription, which is a specific aim addressed in this thesis.

1.4.4.3 Upstream Regulation of mTORC1

Signalling to cell growth machinery through mTORC1 is controlled by amino acids and growth factor signalling, where amino acid signalling is necessary for complete mTORC1 activation. The main pathway leading to regulation of mTORC1 by growth factors is via PI3K activation of PDK1 and subsequent activation of AKT and inhibition of tuberous sclerosis complex (TSC) 1/2 (Schmelzle and Hall 2000; Gingras et al. 2001). mTORC1 activation by amino acids remains somewhat ill-defined. Early studies have demonstrated that the endosomally localized Class III PI3-K hVps34 is involved in mTORC1 regulation, as refeeding amino acids or glucose back into starved cells increased the activity of hVps34, and knockdown of hVps34 expression reduced the ability of insulin to induce S6K1 phosphorylation in amino acid-fed cells, but did not affect the ability of insulin to activate AKT (Byfield et al. 2005; Nobukuni et al. 2005)

The growth factor signalling regulation of mTORC1 via PI3-K/AKT signalling is a well characterised signalling node (Kozma and Thomas 2002; Engelman et al. 2006) (**Figure 1.5)**, with activated AKT phosphorylating and inactivating the tuberous sclerosis protein 2 (TSC2), which when complexed with TSC1 acts as a negative regulator of mTOR via the inhibition of the GTPase, Ras homolog enriched in brain (Rheb) (Manning et al. 2002; Potter et al. 2002). More recently another regulator of mTORC1 activity has been identified as the proline rich AKT substrate of 40kDa (PRAS40), and as the name suggests is a substrate of AKT. PRAS40 acts as an inhibitor of mTORC1, with AKT abolishing this negative inhibition through phosphorylation of PRAS40, allowing

mTORC1 to signal to growth machinery (Sancak et al. 2007).

Many studies have demonstrated a clear involvement of AKT in growth regulation, with perhaps the most compelling evidence originating from the AKT knockout mice. The *akt1*$^{-/-}$ mice have approximately a 20% reduction in body weight due to a global decrease in cell size (Cho et al. 2001b), and the brains of *akt3*$^{-/-}$ mice are approximately 20% smaller when compared with wildtype, due to a reduction in cell size and cell number (Easton et al. 2005). To date, few studies have demonstrated a clear role for the SGK family in cell growth signalling, however an earlier investigation into SGK1 signalling using cardiomyocytes demonstrated that SGK1 may be involved in signalling through the mTOR growth pathway. Studies using an adenovirus construct to express constitutively active SGK1 in cardiomyocytes were able to identify SGK1 induced phosphorylation of several downstream effectors of growth signalling, including TSC2, p70S6K and GSK3β. Furthermore, activated SGK1 also contributed to a hypertrophic phenotype (Aoyama et al. 2005). Given the structural and function similarities existing between the SGK and AKT families, it is likely that SGK3 also regulates cell growth processes, and one of the aims of this thesis is to investigate this role.

A recent study using *C.elegans* revealed that rictor loss of function causes developmental delays, reduced body size and reproduction and excess fat accumulation. These phenotypes were also recapitulated through knockdown of other members of the mTORC2 complex (Jones et al. 2009). Interestingly, these studies also found that phenotypes caused by rictor inactivation were independent of AKT, but were mimicked by loss of *sgk1* function, and suppressed by gain of function *sgk1* mutant (Jones et al. 2009). Similar studies in *C.elegans* have also demonstrated a specific role for SGK1 in mediating metabolic and growth processes (Soukas et al. 2009). Furthermore, in *S. cerevisiae* mTORC2 has shown to regulate ceramide synthesis through the activation of *YPK2* (an SGK homologue), which is required for membrane synthesis and active cell growth (Aronova et al. 2008). Taken together these studies demonstrate that SGK1 does play an important role in signalling upstream of mTORC1 and influencing growth in a variety of systems, further suggesting the possibility that other members of the SGK family such as SGK3 may also play fundamental roles in regulating cell growth processes.

1.4.5 Cell survival

To date there have been many studies that have established the SGK family as a family of cell survival kinases, with each isoform demonstrating the ability to promote resistance to cell death via a number of different mechanisms. The induction of SGK1 transcription as an early response to a variety of stress cues, combined with its rapid protein turn-over makes it a likely stress response gene, allowing it to act quickly during unfavourable cellular conditions (Brickley et al. 2002). While SGK3 is not transcriptionally regulated, it can promote cell survival during unfavourable cellular conditions also (Liu et al. 2000). Moreover, both SGK1 and SGK3 regulate via phosphorylation a number of well established cell survival effectors, many of which

are also targets of the AKT kinase family (Liu et al. 2000; Brunet et al. 2001).

SGK1 has been shown to protect cells from growth factor withdrawal-induced apoptosis in many cell types (Mikosz et al. 2001; Leong et al. 2003). In mammary epithelial cells, ectopic SGK1 expression was shown to protect the cells from growth factor withdrawal-induced apoptosis, which was further confirmed using a kinase-dead dominant negative SGK1 mutant, which inhibited protection from apoptosis. These studies led to the discovery of a novel glucocorticoid receptor (GR)-initiated anti-apoptotic pathway mediated by the transcriptional induction of SGK1 (Mikosz et al. 2001). SGK1 has also been implicated in glucocorticoid-mediated inhibition of chemotherapy induced cell death in tumourigenic mammary epithelial cells (Wu et al. 2004) and human ovarian tumours (Melhem et al. 2009). Further reports have also suggested that SGK1 is able to negatively regulate the c-Jun N-terminal kinase (JNK)/SAPK signalling pathway through direct phosphorylation of SEK1 at Ser-78 following treatment with the chemotherapeutic drug paclitaxel in human breast cancer cells, indicating a possible mechanism contributing to the cytoprotective effect of glucocorticoids in breast cancer cells treated with chemotherapeutic drugs (Kim et al. 2007).

SGK1 modulates the transcriptional activity of NF-κB, through phosphorylation of I kappa B kinase beta (IKKβ). This enhances IKK activity, and thereby increases the phosphorylation of I-κB, and promotes its degradation via the 26S proteasome. This results in translocation of the NF-κB complex to the nucleus (Zhang et al. 2005; Tai et al. 2009), and thus promotes transcription of cell survival proteins. A recent report has also demonstrated that SGK1 acts through NF-κB in Xenopus embryos to stimulate production of bone morphogenetic protein (BMP7) to promote ectodermal survival by decreasing death-inducing signalling complex (DISC) (Endo et al. 2011).

Both SGK1 and AKT play a role in negatively regulating the pro-apoptotic FOXO transcription factor family. FOXO3a is a member of the Forkhead transcription factor family that is involved in the induction of cell cycle arrest and apoptosis by transcription of the death cytokine Fas Ligand (FasL), and pro-apoptotic Bim molecule (Kops et al. 1999; Tran et al. 2003). When FOXO3a is phosphorylated, it becomes inactivated and translocates to the cytoplasm, and is therefore unable to activate its pro-apoptotic gene targets (Vivanco and Sawyers 2002). SGK1 acts synergistically with AKT to regulate the function of FOXO3a through phosphorylation at three distinct sites, demonstrating that SGK1 and AKT may have complementary rather than redundant properties as cell survival regulators (Brunet et al. 2001). It has also been demonstrated that SGK1 plays an important role in glucocorticoid receptor mediated FOXO3a inactivation and subsequent mammary epithelial cell survival, independently of AKT activation (Wu et al. 2006). A more recent report demonstrates that SGK1 is able to regulate Notch1, another transcription factor implicated in cell survival, by increasing Notch1 protein degradation and ubiquitination through phosphorylation of F-box/WD repeat containing protein 7 (Fbw7) (Mo et al. 2011).

A further cell survival pathway that SGK1 is implicated in regulating is murine double minute 2 (MDM2) mediated inactivation of p53 via ubiquitination (Amato et al. 2009). p53 is a crucial modulator of many core cell processes including both intrinsic/ mitochondrial and extrinsic apoptosis pathways (Soengas et al. 1999), cell cycle arrest and cellular senescence. SGK1-dependent regulation of p53 abundance via MDM2 reportedly stimulates cell proliferation and transition of epithelial cells towards mesenchymal differentiation (Amato et al. 2009). A similar role for AKT in MDM2 mediated inactivation of p53 has also been demonstrated (Mayo and Donner 2001), and it is likely that both SGK1 and AKT are able to increase cell survival through ultimately preventing the p53-mediated transcription of pro-apoptotic proteins bcl-2-binding component 3 (BBC3) and phorbol-12-myristate-13-acetate-induced protein 1 (PMAIP1) (Villunger et al. 2003).

There have been a number of studies highlighting the role of SGK3 in cell survival. SGK3 was initially identified in a genetic screen using enhanced retroviral mutagen vectors, as a novel factor involved in mediating IL-3 dependent survival of 32D and BAF3 hematopoietic cells (Liu et al. 2000). Further analysis demonstrated that SGK3 activity is regulated by IL-3 in a PI3-K dependent manner, supporting the possibility that SGK3 is involved in IL-3 mediated survival downstream of PI3-K. To further define the mechanism by which SGK3 regulates cell survival, a number of well established AKT cell survival targets were analysed to determine if they are were also SGK3 targets. Interestingly, this study found that SGK3 can negatively regulate activity of the pro-apoptotic FOXO transcription factor FOXO3a, in addition to increasing the level of phosphorylated Bcl-2 homology domain 3 (BH3)-only Bcl-2 associated death promoter (BAD) and thereby attenuating cell death via B-cell CLL/lymphoma 2 (BCL-2) (Liu et al. 2000). One of the most compelling studies demonstrating SGK3's ability to regulate cell survival independently of AKT was a study in which there was a clear dependence on SGK3 for cell viability in *PI3KCA* mutant cancer cell lines and breast tumours that had minimal AKT activation, but robust PDK1 activity (Vasudevan et al. 2009). This study highlighted the ability of SGK3 to act as an alternate, AKT-independent signalling pathway capable of transducing critical cell survival signals.

SGK3 has also been reported to be involved in cell survival signalling in estrogen receptor-positive breast cancer cells, with initial microarray studies revealing a 5.7 fold increase of SGK3 expression in estrogen receptor-positive tumours when compared with estrogen receptor -negative tumours (Wang et al. 2011). As an extension of these studies, SGK3 was shown to be transcriptionally regulated by estrogen/ estrogen receptor, and a critical mediator of estrogen-mediated survival of estrogen receptor -positive breast cancer cells (Wang et al. 2011). Another group has also identified FLI-I to be a novel downstream target of SGK3 (Xu et al. 2009). FLII acts as a co-activator for nuclear hormone receptors such as the estrogen receptor, acting to enhance estrogen receptor activity, and promote proliferation and survival. Taken together these studies suggest that there may be a positive feedback loop existing between SGK3 and estrogen receptor, which may play an important role in estrogen

signalling in estrogen receptor -positive breast cancer and highlight a crucial role for SGK3 in cell survival signalling (Wang et al. 2011).

1.4.6 Cell migration

To date there have been few studies addressing the role of the SGK family in migration. The phosphorylation and subsequent inactivation of GSK-3β by both SGK1, SGK3 and the AKT family has been implicated with alteration of β-catenin dynamics, leading to the formation of adherens junctions and tight junction sealing in mammary epithelial cells (Failor et al. 2007), raising the possibility that SGK family may be involved in cell polarity and migration. Characterisation of the *sgk3*$^{-/-}$ mouse exhibited a wavy hair phenotype, with further analysis revealing disorganization of hair follicles and cells in the outer root sheath, suggesting dysregulation of cell polarity (McCormick et al. 2004; Alonso et al. 2005).

SGK3 also negatively regulates the lysosomal degradation of the chemokine (C-X-C motif) receptor 4 (CXCR4), whose signalling is strongly associated with the promotion of cell invasion, migration and adhesion during metastasis in breast cancers (Muller et al. 2001; Gassmann et al. 2009). SGK3 was shown to be able to co-localize, interact and phosphorylate the E3 ubiquitin ligase AIP4 in the early endosomes, thereby specifically attenuating the ubiquitin-dependent degradation of CXCR4 (Slagsvold et al. 2006). Importantly, despite the homology and similar substrate specificity existing between SGK1 and SGK3, SGK1 was not able to mimic this phosphorylation, even though SGK1 regulates ubiquitin ligase hNedd4-2 at the plasma membrane (Snyder et al. 2002), thus providing evidence for isoform specific roles.

1.4.7 Regulation of ion channels and transporters

SGK1 involvement in ion channel regulation has been demonstrated clearly through characterisation of the *sgk1*$^{-/-}$ animals, which revealed a defect in sodium homeostasis**.** When placed on a standard NaCl diet *sgk1*$^{-/-}$ animals were indistinguishable from their wildtype littermates. However when placed on a low salt diet they were unable to adequately up-regulate Na^+ reabsorption (Wulff et al. 2002), a process that occurs in the distal nephron of the kidney through the ENaC (Tessier and Woodgett 2006b). A screen to identify novel regulators of the ENaC in A6 cells of renal distal nephron origin identified SGK1 as a candidate (Chen et al. 1999), and further studies demonstrated that SGK1 is able to stimulate Na^+ transport by increasing the amount of the ENaC at the cell surface (Alvarez de la Rosa et al. 1999). Further studies revealed that SGK1 is able to physically interact with the ENaC subunits (Wang et al. 2001), and regulate ENaC activity via direct phosphorylation (Diakov and Korbmacher 2004).

Expression of the ENaC has shown to be regulated by the ubiquitin ligase neural precursor cell-expressed developmentally down-regulated protein 4-2 (Nedd4-2) (Flores et al. 2003), and studies have demonstrated that SGK1 is also able to indirectly

regulate the ENaC via phosphorylation of Nedd4-2 (Debonneville et al. 2001; Snyder et al. 2002; Asher et al. 2003; Snyder et al. 2004), thereby reducing the interaction between Nedd4-2 and ENaC, which reduces ENaC ubiquitination and increases the cell-surface expression of the ENaC (Alvarez de la Rosa et al. 1999; Kamynina and Staub 2002). Further studies have demonstrated that all three SGK isoforms are able to phosphorylate Nedd4-2 with varying efficiencies (Palmada et al. 2004b), and the relatively mild *sgk1*$^{-/-}$ mice phenotype also suggests that SGK2 and SGK3 may be able to compensate. Regulation of the ENaC implicates the SGK family in the control of blood pressure and hypertension, where accumulation of active ENaC at the cell surface and increased Na^+ absorption in the distal nephron can result in elevated blood pressure (Rotin and Schild 2008).

In addition to regulation of the ENaC, the SGK family are involved in mediating several other channels, mainly via phosphorylation of Nedd4-2, and in some cases requiring the scaffold protein NHERF2. These channels include renal outer medullary K^+ channel (ROMK1) (Yoo et al. 2003), cardiac and epithelial K^+ channels (KCNQ1/KCNE) (Embark et al. 2003), inner ear K^+ channels (KCNQ4), (Embark et al. 2004a; Seebohm et al. 2005), voltage-gated K^+ channels (KV1.3, KV1.5 and Kv4.3) (Gamper et al. 2002a; Gamper et al. 2002b; Warntges et al. 2002; Henke et al. 2004; Baltaev et al. 2005; Ullrich et al. 2005), renal and inner ear Cl^- channel (ClC-Ka), (Embark et al. 2004a), ubiquitous Cl^- channel (ClC2) (Palmada et al. 2004a), renal epithelial Ca^{2+} channel (TRPV5) (Embark et al. 2004b; Lang et al. 2006a), cardiac voltage gated Na^+ channel (SCN5A) (Boehmer et al. 2003c), the cystic fibrosis transmembrane conductance regulator Cl^- channel (CFTR) (Embark et al. 2004a), Orai1 the pore-forming unit of Ca^{2+} -release-activated- Ca^2 (CRAC) channel (Eylenstein et al. 2011; Borst et al. 2012), and the cation channels created by 4F2/LAT (Wagner et al. 2000).

SGK isoforms are also implicated in the regulation of a number of transporters and pumps including the amino acid transporters ASCT2 (Palmada et al. 2005), glutamine transporter SN1 (Boehmer et al. 2003b), glutamate transporters EAAT1 (Boehmer et al. 2003a), EAAT2 (Boehmer et al. 2006), EAAT3 (Schniepp et al. 2004), EAAT4 (Bohmer et al. 2004) and EAAT5 (Boehmer et al. 2005), Na^+-glucose cotransporter (SGLT1) (Dieter et al. 2004), facilitative glucose transporter (GLUT1) and GLUT4 (Palmada et al. 2006; Jeyaraj et al. 2007), Na^+-dicarboxylate cotransporter (NaDC-1) (Boehmer et al. 2004), intestinal phosphate cotransporter (NaPiIIb) (Palmada et al. 2004b), creatine transporter (SLC6A8) (Strutz-Seebohm et al. 2007), myo-inositol transporter SMIT (Klaus et al. 2008), Na^+/ H^+ exchanger (NHE3) (Yun et al. 2002; He et al. 2011) and the Na^+- K^+-ATPase (Setiawan et al. 2002). In most cases both SGK1 and SGK3 are able to regulate the same channels and transporters, with SGK2 demonstrating involvement in far fewer. Some channels including Human ether-a-go-go (HERG) (Maier et al. 2006) and GluR1 (Strutz-Seebohm et al. 2006) have also shown to be regulated by SGK3 only.

In addition to being associated with the regulation of a number of ion channels and

transporters, SGK1 is significantly up-regulated following exposure to a hypertonic environment and significantly down-regulated following exposure to a hypotonic environment (Waldegger et al. 1997). Alterations of cell volume are crucial events during many core cell processes including cell proliferation and apoptosis, migration, hormone release, metabolism and epithelial transport, and in order for cells to survive, excessive alterations of cell volume are avoided via cell volume regulatory mechanisms able to control osmotic activity between the internal and external cellular environments (Lang et al. 1998). Mechanisms involved in regulating cell volume including ion transport across the cell membrane, act accordingly during instances of cell shrinkage or cell swelling (Fillon et al. 2001). It is likely that the SGK isoforms are able to provide a mechanism by which they are able to adjust cell volume accordingly via their downstream regulation of ion channels and transporters.

1.5 SGK associated pathophysiology

To date the SGK family have been implicated in many disease states, including hypertension (BelAiba et al. 2006), obesity (Dieter et al. 2004), diabetes (Schwab et al. 2008), fibrosis (Waerntges et al. 2002) and several neurological disorders in addition to cancer. Furthermore, recent evidence has also emerged that SGK1 is involved in coeliac disease (Szebeni et al. 2010) and reproductive failure (Feroze-Zaidi et al. 2007; Salker et al. 2011). This section will briefly review some of the pathophysiology associated with the SGK family.

1.5.1 Hypertension and diabetes

In addition to studies demonstrating a role for SGK1 in modulation of salt balance through characterisation of *sgk1*$^{-/-}$ mice, a variant of the SGK1 gene [the combined presence of distinct polymorphisms in intron 6 (I6CC) and in exon 8 (E8CC/CT)] has demonstrated involvement with increased blood pressure (Busjahn et al. 2002; Busjahn and Luft 2003), likely involving up-regulation of sodium channels. This gene affects 3-5% of the Caucasian population and 10% of an African population (Schwab et al. 2008). Also, given that the SGK family modulates many different ion channels and transporters, it is likely that up-regulation of the SGKs contributes to deranged electrolyte concentrations and possible hypertension (Tessier and Woodgett 2006b). Moreover, SGK1 activation via WNK1, a kinase up-regulated in hypertensive patients is involved in increased sodium transport, impacting on modulation of blood pressure (Xu et al. 2005b).

Further studies have also linked the same *sgk1* gene variant with increased body weight, and demonstrated a higher prevalence in patients with type 2 diabetes (Schwab et al. 2008). It is likely that enhanced stimulation of the Na^+ coupled glucose transporter SGLT1 by SGK1 and SGK3 may be involved with accelerating intestinal glucose absorption, possibly leading to excessive insulin release resulting in increased body weight (Dieter et al. 2004; Lang et al. 2006a; Lang et al. 2009).

Moreover, SGK1 has also been implicated in diabetes through increased extracellular glucose concentrations shown to induce SGK1 transcription, along with increased SGK1 expression detected in renal tissue of diabetic patients (Wang et al. 2008). A recent report has demonstrated that a novel SGK inhibitor with anti-hypertensive potency was able to significantly decrease blood pressure and decrease body weight, suggesting that SGK1 is a useful target in counteracting hypertension and type II diabetes (Ackermann et al. 2011).

1.5.2 Neurodegenerative disease

Much evidence suggests that the SGK family has an important role in neuronal signalling and associated neurodegenerative disease states. Initial studies revealed SGK1 transcript expression in all cerebral structures of the human brain, and demonstrated a role for SGK1 in regulating neuronal excitability through modulation of neuronal potassium channels (Warntges et al. 2002). SGK1 has shown to be 4-fold higher in the hippocampus of fast learners than slow learners in a water maze learning task to assess memory consolidation and spatial learning in rats (Tsai et al. 2002), and enrichment training also increased both mRNA and protein levels in the hippocampus mediated through the α-amino-3-hydroxy-5-methyl-4-isoxazolepropionic acid (AMPA) receptor (Lee et al. 2003). Furthermore, *sgk3*$^{-/-}$ mice show a deficit in precision and goal-directed navigation in space, reduced exploratory activity and locomotion, potentially due to deranged neuronal regulation of transporters and ion channels (Lang et al. 2006b; Tessier and Woodgett 2006b), with reports showing that AMPA subunit GluR1 is significantly lower in *sgk3*$^{-/-}$ mice than their wildtype littermates (Strutz-Seebohm et al. 2005).

Gene expression studies have shown up-regulation of sgk1 in several neurochemical lesion models of Parkinson's disease and in a transgenic model of Amyotrophic Lateral Sclerosis (Schoenebeck et al. 2005; Stichel et al. 2005), with up-regulation correlating mainly with the incidence of cell death, in addition to increased FOXO3a phosphorylation (Schoenebeck et al. 2005). Interestingly, pre-treatment with glucocorticoids to further induce sgk1 expression prior to neurochemical treatment significantly decreased cell death, providing evidence that SGK1 has a neuroprotective role (Schoenebeck et al. 2005). Earlier studies also detected increased expression of sgk1 in the rat brain following dehydration (Warntges et al. 2002) and ischemic brain injury (Nishida et al. 2004), consistent with a neuroprotective role.

A further neuroprotective role in Huntington's disease (HD) has also been demonstrated for SGK1, shown by increased expression in the brain of patients with HD, and direct phosphorylation of huntingtin protein at Ser-421, which can protect striatal neurons against polyQ-huntingtin-induced toxicity (Rangone et al. 2004). The polyQ expansion in HD leads to the dysfunction and death of specific neurons including striatal and cortical neurons in the brain of HD patients (Gusella and MacDonald 2000; Rangone et al. 2004). Earlier studies also determined that AKT was also able to abrogate polyQ-

huntingtin toxicity through phosphorylation of Ser-421 (Humbert et al. 2002). Reports also demonstrate that SGK1 is able to phosphorylate Tau at Ser-214, a microtubule-associated protein involved in several neuronal processes and Alzheimer's disease (Chun et al. 2004). Furthermore, transgenic mice over-expressing TGF-β, also a stimulator of SGK1 expression (Waldegger et al. 1999), develop Alzheimer's disease-like vascular and meningeal alterations (Gaertner et al. 2005). Gene expression studies have also shown an up-regulation of *sgk1* in a murine model of Rett syndrome, a severe form of mental retardation (Nuber et al. 2005), and up-regulated in the brain tissue of epileptic patients (Wang et al. 2010b).

1.6 SGK and cancer

The importance of the PI3-K pathway in a number of cancer types has been well established (Mills et al. 2001; Vivanco and Sawyers 2002; Lu et al. 2003), with genetic defects leading to the hyperactivation of the PI3-K cascade and/or the RAS/MAPK pathway occurring in 45% of ovarian cancers (2011). There is clear evidence to suggest that the PI3-K pathway leads to activation of the SGK isoforms, in addition to the RAS/MAPK pathway, promoting SGK isoform expression and activity (Mizuno and Nishida 2001). Within the PI3-K pathway, AKT plays a key role in mediating the tumorigenic signal (Vivanco and Sawyers 2002), but given the structural and functional similarities existing between both the AKT and SGK isoforms, in addition to SGK signalling downstream of two well-characterised oncogenic pathways, it is likely that SGK3 is also involved in oncogenic signalling. Moreover, recent studies support a specific role for SGK3 in tumourigenesis (Vasudevan et al. 2009), including reports demonstrating that the knock in oncogenic *akt1* mutations found in ovarian cancer are not sufficient to recapitulate *PIK3CA* mutant phenotypes. Together, these results suggest that the PI3-K pathway requires effectors other than AKT to drive oncogenic signalling (Lauring et al. 2010). Thus, these studies suggest that the SGK family, with particular focus on SGK3, likely performs a crucial function in oncogenic signalling downstream of PI3-K. This section will firstly describe class I PI3-K and phosphatase and tensin homolog (PTEN) in the context of cancer, given that these factors are crucial regulators of SGK isoform activity, and have both demonstrated frequent mutation in many cancer types. This will then be followed by discussion of the function of both AKT and SGK in relation to cancer.

1.6.1 Class I PI3-K and cancer

The class IA PI3-K signalling cascade is a crucial modulator linking oncogenes such as the SGK and AKT isoforms, and multiple receptor classes to many core cell processes, including cell cycle, cell survival, protein synthesis, growth, metabolism, motility and angiogenesis. Numerous reports have demonstrated an active role for this pathway in many types of human cancers, with one or more of its signalling components exhibiting constitutive activation due to a genetic aberration, which ultimately leads to a malignant phenotype. Deregulation of several components of the PI3-K pathway,

including PTEN and AKT have been demonstrated in human cancer, with probably the most prevalent affecting the *PIK3CA* gene and tumour suppressor PTEN (Markman et al. 2010b). Furthermore, receptor tyrosine kinases such as EGFR, human epidermal growth factor receptor 2 (HER2) and platelet-derived growth factor receptor (PDGFR) are often up-regulated in human cancer and engage the PI3-K pathway via interaction with the p85 regulatory subunit (Hu et al. 1992; McGlade et al. 1992; Zhu et al. 1992). The PI3-K subunit p110 can also bind RAS directly (Peyssonnaux et al. 2000), thereby providing a link between RAS and PI3-K signalling. Furthermore, *PIK3CA* activating mutations are often present with other concurrent genetic alterations that activate the PI3-K pathway (Yuan and Cantley 2008; Wong et al. 2010).

The *PIK3CA* gene located on chromosome 3, encodes for the p110α subunit of class IA PI3-K, and is either mutated or amplified in a number of different cancer types (Samuels and Velculescu 2004; Samuels et al. 2004; Markman et al. 2010a). *PIK3CA* knockout mouse embryonic fibroblasts are deficient in cellular signalling in response to various growth factors, and resistant to oncogenic transformation induced by RTKs (Zhao et al. 2006), together suggesting that PI3K is involved in growth factor signalling and fundamental to tumourigenesis. The somatic missense mutations affecting the *PIK3CA* gene have been mapped to hotspot regions, exon 9, which codes the helical domain of p110α, and exon 20, which encodes the catalytic domain of p110α. These mutations constitutively activate AKT through increased production of $PI(3,4,5)P_3$ and induce oncogenic transformation both *in vitro* and *in vivo* (Bader et al. 2005; Isakoff et al. 2005; Samuels et al. 2005; Zhao et al. 2005; Samuels and Ericson 2006; Markman et al. 2010b). In addition to the frequent hot spot mutations, almost 100 rare mutations have also been identified in *PIK3CA* (Gymnopoulos et al. 2007; Vogt et al. 2009). The *PIK3R1,* which encodes for the p85 subunit of PI3-K also exhibits mutations in colorectal and ovarian cancers, which result in overactivity of PI3-K signalling through loss of p85 subunit inhibition of the p110 catalytic subunit of PI3-K (Philp et al. 2001; Shekar et al. 2005).

PTEN, is a phosphoinositide 3-phosphatase that metabolises phosphatidylinositol 3,4,5-trisphosphate (PtdIns(3,4,5)P(3)), and thus acts to inhibit PI3-K signalling. *PTEN* is frequently lost in many cancers (Li et al. 1997; Myers et al. 1998). Mice with *PTEN* deletion and mutation are highly susceptible to tumour induction and conditional knockout of *PTEN* leads to neoplasia in multiple organs including mammary gland, skin, prostate (Suzuki et al. 1998; Li et al. 2002; Backman et al. 2004). The somatic aberrations that affect PTEN can occur through allelic losses leading to either complete deletion of the *PTEN* locus, or either point or truncating *PTEN* mutations, which result in functional inactivation (Markman et al. 2010b).

1.6.2 AKT isoforms and cancer

Much of the aberrant regulation through the PI3-K pathway detected in tumourigenesis is upstream of AKT, therefore causing hyperactivation of AKT. Although dysregulation of upstream signalling stimulates AKT activity, the *akt1* gene has also found to be

amplified, with an elevated level of AKT1 phosphorylation in a proportion of head and neck, gastric, pancreatic and ovarian tumours (Staal 1987; Bellacosa et al. 1995; Hennessy et al. 2005). Furthermore, a missense mutation identified in the pleckstrin homology domain of *akt1* has recently been described at low frequency in breast, colorectal and ovarian cancers (Carpten et al. 2007), which leads to targeting of AKT1 to the plasma membrane, constitutive activation of the kinase and enhanced downstream signalling. Genetic aberrations associated with *akt2* and *akt3* have also been reported, with *akt2* frequently amplified in ovarian and breast cancer (Bellacosa et al. 1995), along with an activation of AKT2 kinase activity in approximately 36% of ovarian tumours (Yuan et al. 2000). An increase in *akt3* copy number has also been observed in approximately 70% of sporadic melanomas (Stahl et al. 2004).

1.6.3 SGK isoforms and cancer

To date there have been few reports of *sgk* mutations in cancer (http://www.sanger.ac.uk/generics/CGP/cosmic), and only a small gain (20-30%) in copy number of *sgk2* and *sgk3* in many cancer types (http://www.progenetix.net). *Sgk1* does not show a gain or loss of copy number. Gene expression profiles generated in our laboratory using Affymetrix GeneChip technology of 37 human ovarian tumour cell lines and four cell lines derived from non-tumourigenic epithelial tissue demonstrated an increase in *sgk3* gene expression in 80% of the tumour cell lines, while *sgk2* is up-regulated in only 50% of cell lines. *Sgk1* gene expression was down-regulated in 90% of tumour cell lines (Sheppard and Pearson, unpublished).

Several reports have commented on *sgk1* gene expression levels in various tumours and tumour cell lines, with reports of *sgk1* down-regulation in ovarian tumour (Chu et al. 2002), prostate tumours (Rauhala et al. 2005), hepatocellular carcinoma (Chung et al. 2002), and colorectal tumours (Segditsas et al. 2008), with further studies in colorectal tumours indicating that down-regulation of *sgk1* is largely independent of promoter hypermethylation (Lessi et al. 2010). There have also been several reports of *sgk1* up-regulation in breast cancer (Adeyinka et al. 2002; Sahoo et al. 2005; Zhang et al. 2005), suggesting that SGK isoform signalling is likely to be tumour specific. Moreover, a recent report has demonstrated that while SGK1 protein expression is high in most untreated prostate cancers relatively low expression of SGK1 is associated with higher tumour grade and increased cancer recurrence, and is a potential indicator of aberrant androgen receptor (AR) signalling (Szmulewitz et al. 2012). Preliminary studies using the SGK1 antagonist GSK650394 in androgen-sensitive human prostate adenocarcinoma cells have determined that small molecule inhibitors of SGK1 may be an effective approach for the treatment of AR-driven prostate cancer (Sherk et al. 2008).

Further *in-vivo* evidence suggesting a role for SGK1 in tumourigenesis comes from studies using *sgk1*$^{-/-}$ mice subjected to chemical carcinogenesis. *sgk1*$^{-/-}$ mice developed significantly less colonic tumours than *sgk1*$^{+/+}$ mice, with *sgk1* deficiency increasing expression of FOXO3a and bcl-2-like protein 11 (BIM) (Nasir et al. 2009).

Furthermore, studies investigating the role of SGK1 in colorectal tumourigenesis using mice carrying a defective adenomatous polyposis coli (APC) gene (APC is commonly inactivated in familial adenomatous polyposis and sporadic colorectal cancer), crossed with *sgk1*$^{-/-}$ mice demonstrated that SGK1 expression increases the development of intestinal tumours in APC-defective mice. An increase in β-catenin protein levels in colon tissue from *sgk1*$^{+/+}$ mice was detected in these studies (Wang et al. 2010a). This work is consistent with other reports demonstrating an increase in SGK1 expression via increased β-catenin stabilization, suggesting that SGK1 is a direct β-catenin target gene (Naishiro et al. 2005; Dehner et al. 2008). Taken together these studies suggest a role for SGK1 in regulation of colonic tumour growth, where it is likely that SGK1 is able to affect WNT signalling on multiple levels, including through increasing the abundance of β-catenin via phosphorylation of GSK3β, resulting in the impairment of oncogenic β-catenin degradation. SGK3 is also able to phosphorylate GSK3β (Dai et al. 2002), and activated SGK3 increases the activity of a β-catenin/Lef-1 driven reporter in keratinocytes (McCormick et al. 2004), further suggesting that SGK3 is involved in the regulation of WNT/β-catenin signalling.

In addition to mediating a number of other cell survival pathways, the SGK family is also involved in mediating IL-6-dependent survival of cholangiocarcinoma cells (Meng et al. 2005), along with IL-2-dependent survival in kidney cancer cells (Amato et al. 2007). It is also important to consider the role that the SGK family play in regulating a vast number of ion and solute channels, with SGK over-expression often resulting in up-regulation of these channels, all of which are involved in meeting the excessive demands of a tumourigenic environment.

Surprisingly, in both breast and ovarian cancers, AKT activity has been shown to correlate poorly with *PIK3CA* mutations (Stemke-Hale et al. 2008), indicating the existence of alternative PI3-K-dependent mediators of tumourigenesis. The most obvious candidate for PI3-K signalling to tumourigenesis, independent of AKT, would be the SGK protein isoforms. Given that they play roles in cell survival, proliferation and growth, and share many of the same substrates with AKT. However, the most convincing data to support this view was recently reported, where in *PIK3CA* mutant tumour cells with minimal AKT activation, SGK3 was identified as a PDK1 substrate that conferred increased cell viability, and these cells also demonstrated a functional dependency on SGK3 (Vasudevan et al. 2009). These observations suggest that SGK3 may be an important downstream effector for many breast and ovarian cancers harbouring *PIK3CA* mutations, and an alternative therapeutic drug target for treatment of malignancies demonstrating this genetic aberration.

The PI3-K pathway is speculated to be one of the most crucial for cancer development and maintenance, with the ubiquitous nature of PI3-K pathway activation making both upstream and downstream components of the PI3-K signalling pathway attractive therapeutic targets. Currently in clinical trials there are around 30 small molecule and other inhibitors that target this pathway. The recent discovery of functional dependency

of PI3-K signalling on SGK3 in cancer indicates that SGK3 may offer another avenue for targeted therapy. It also places SGK3 as a potential oncogene, thus understanding how this kinase may contribute to the cancer phenotype is of great importance.

1.7 Hypothesis and Aims

The importance of the PI3-K pathway to signal through to a number of different processes is fundamental to maintain cellular homeostasis. Over the last decade it has become increasingly evident that the AKT kinase family is not the only set of kinases that act as mediators of PI3-K signalling, as the SGK family of kinases have begun to emerge as crucial components of this signalling pathway in both physiology and pathophysiology. Much of the knowledge we have on the SGK family, and in particular SGK3 has emerged since the commencement of studies reported in this thesis. The studies outlined in this thesis aim to firstly determine if many of the well-established roles of the AKT family, such as the regulation of growth and proliferation are also mediated by SGK3 under normal physiological conditions. In particular during the course of this thesis our laboratory established a central role for AKT in the regulation of growth through modulation of RNA Polymerase I transcription and ribosome biogenesis (Chan et al. 2011). In light of this a further aim was to determine the potential role of SGK3 in modulation of ribosome biogenesis. Finally, these studies also aim to further define the role of SGK3 in modulating hallmarks of tumourigenesis and malignant transformation using human ovarian epithelial and foreskin fibroblasts cells.

Hypothesis

- SGK3 regulates cell growth and proliferation
- SGK3 is involved in oncogenic cell transformation of human ovarian surface epithelial cells and human foreskin fibroblasts cells

Specific Aims

- To investigate the role of SGK3 in the regulation of ribosome biogenesis, growth and proliferation in human ovarian surface epithelial cells and human foreskin fibroblasts cells
- To investigate the role of SGK3 in oncogenic cell transformation of human ovarian surface epithelial cells and human foreskin fibroblasts cells

2. Materials and Methods

2.1 Cell line maintenance

Human ovarian surface epithelial cell lines HOSE and IOSE523 used in these studies were immortalised using HPV-E6E7 (Tsao et al. 1995) and Simian virus 40 (SV40) large T and small t antigen (kindly provided by Canadian Ovarian Tissue Bank; Vancouver, Canada), respectively. IOSE523 were only partially immortalised, which allowed the cells to be passaged for up to 20 times before cells would begin to senesce. These cells were cultured in media consisting of 1:1 MCDB-105 (Sigma) and Medium M199 (Sigma), and supplemented with 10% (v/v) foetal bovine serum (FBS) (JRH Biosciences). The media for HOSE and IOSE523 cells were further supplemented with 1% (v/v) antibiotic-antimycotic (Gibco) and 1% (v/v) gentamycin (Gibco), respectively.

Both human foreskin fibroblast cell lines used in these studies; BJ-hTERT and BJ-LST cells (Hahn et al. 1999) were cultured in media consisting of 1:4 Dulbecco's Modified Eagle Medium (DMEM) (Sigma) and Medium 199 (Sigma), and supplemented with 15% (v/v) FBS and 3.75mM L-glutamine. Human embryonic kidney cells expressing (SV40) T antigen (HEK293T) were cultured in DMEM (Sigma) supplemented with 10% (v/v) FBS and 1% (v/v) antibiotic-antimycotic (Gibco). Cell lines were passaged by washing once with phosphate buffered saline (PBS) and detached from tissue culture plastic using 0.25% (v/v) trypsin-EDTA (Gibco); with the exception of IOSE523 cells that required 0.12% (v/v) trypsin-EDTA (Gibco). All cells were incubated at 37°C with 5% CO_2. All tissue culture plasticware was manufactured by Falcon, Greiner, Sarstedt or Techno Plastic Products, unless otherwise stated.

2.2 Generation of plasmid constructs

2.2.1 Generation of myc-tagged wildtype SGK3 expression construct

Wildtype SGK3 was initially cloned by Julia Zebol (Growth Control Lab, Peter MacCallum Cancer Centre) from human SKOV3 cell line cDNA using forward primer 5'-CGCGGATCCACATCAACCTGGGACCGTC-3' and reverse primer 5'-CGCGA ATTCGGAGGCAATCCATACAGCA-3' in a polymerase chain reaction (PCR). This generated a 1526 nucleotide (nt) fragment encoding full length human SGK3 protein (nt 197 – 1723). This fragment also included restriction sites *XbaI* and *SmaI,* which were used for ligation into the expression vector pCIneo (promega). The correct sequence was confirmed by sending samples off-site for sequencing at Baker IDI Heart and Diabetes Institute.

A myc-tag was then added to the fragment encoding full length human SGK3 via PCR amplification from pCIneo-hSGK3 using forward primer 5'-CTCGCTAGCCTC GAGGCCACCATGGAGCAGAAGCTTATCTCCGAGGAGGACCTGCAAAGAGAT CACACCATGGAC-3' and reverse primer 5'-CGCGCGGCCGCCTCGAGTCACA

AAAATAAGTCTTCTGA-3'. This generated a fragment encoding full length human SGK3 with an N-terminal myc-tag, along with restriction sites *NheI* and *NotI* which were used for ligation into expression vector pcDNA3.1(-) (Invitrogen). The fragment encoding myc-tagged full length human SGK3 was then subcloned from pCDNA3.1(-)-myc.hSGK3 into the MSCV-IRES-GFP (pMIG) retroviral expression vector (Growth Control Laboratory, Peter MacCallum Cancer Centre) via existing *XhoI* restriction sites, generating pMIG-SGK3 WT retroviral expression vector. The correct sequence was confirmed by sequencing.

2.2.2 Site directed mutagenesis to generate SGK3 mutant constructs

Multiple SGK3 mutant constructs were generated to conduct experiments detailed in this thesis. These include SGK3 constitutively active (CA) (generated by Julia Zebol, Peter MacCallum Cancer Centre), SGK3 constitutively active and Phox homology domain (CA PX) (generated by Maressa Bruhn during the course of this project) and SGK3 kinase dead (KD) mutant constructs (generated by Maressa Bruhn during the course of this project). The SGK3 CA mutant was generated through substitution of Serine (Ser) 486 in the C-terminal hydrophobic motif for an Aspartic acid (Asp) residue, which mimics phosphorylation at this residue, thereby resembling the original residue, but appearing as a phosphorylated form. The SGK3 CA PX mutant contains a CA Ser-486 substitution for an Asp, as well as an Arginine (Arg) 90 substitution for an Alanine (Ala) in the N-terminal PI(3)P binding pocket. This mutant therefore mimics phosphorylation in the hydrophobic domain, and abolishes PI(3)P binding at the PX domain. The SGK3 KD mutant was generated through substitution of Lysine (Lys) 191 in the ATP binding site for a Methionine (Met), rendering this kinase catalytically inactive.

2.2.2.1 Primer Design and PCR Reaction

In order to generate SGK3 CA and SGK3 KD mutants, primers were designed for site directed mutagenesis using pMIG-SGK WT as an initial template (**Table 2.1** for site directed mutagenesis primer sequences). Following this, the pMIG-SGK3 CA PX mutant was then generated using pMIG-SGK3 CA as a template for site directed mutagenesis. The forward primer was initially phosphorylated in a reaction containing 17μM forward primer, 20U T4 Polynuclear kinase (Promega), 1 x T4 Polynuclear kinase buffer (Promega), 1mM ATP, 20μg/ml BSA stock (Promega), followed by incubation at 37°C for 1 hour (hr). The enzyme was then heat inactivated at 68°C for 10 mins (min).

PCR was performed using appropriate templates. Reactions contained 50ng DNA template, 200nM dNTPs, 334nM phosphorylated reverse primer, 200nM forward primer, 1 x Pfu buffer, 3U Pfu polymerase (Promega). Reactions were incubated using the following PCR conditions; 1 cycle of 94°C 4 min, 5 cycles of 94°C 1 min, x°C 2 min, 72°C 14min, 25 cycles of 94°C 30 sec, x°C 2 min, 72°C 14 min, 1 cycle of 72°C 1 min and then 10°C affinity (∞). Annealing temperatures (x) were specific for each

Table 2.1: Mutations and primer sequences used for site directed mutagenesis

Construct	Nucleotide Mutation	Forward Primer	Reverse Primer	Annealing Temperatures
pMIG-SGK3 CA	1670 T to G 1671 C to A	5'-GAT TAT GCA CCT CCT TCA GAA GAC TTA-3'	5'-GAA ACC AAC GAA TGC ATC ATC TGC CTC-3'	57°C
pMIG-SGK3 CA PX	485 C to G 486 G to C	5'-ATT CAG AAC CTA GTT AGG TAT CCA GAA C-3'	5'-GAA TTC GTT TAG TCC TGC TGC TCT TTG-3'	57°C
pMIG-SGK3 KD	786 A to T 787 A to G	5'-CTG TCA TGG TGT TAC AGA AAA AAA TAG TTC-3'	5'-CAT AAA ATT TTC CAT CCA GTT TCC GTT TTG-3'	58°C

different primer set and are listed in **Table 2.1**. Correct product size was verified by agarose gel electrophoresis. The PCR product was isopropanol precipitated at -20°C for 1 hr with by adding 10μl millique (MQ) water, 10μl 3M sodium acetate, 200μl isopropanol. MQ water generated from Millipore MQ filtration system. Samples were then centrifuged at 16,000 x g for 20 min, washed with 70% (v/v) ethanol and air dried prior to being resuspended in 30μl MQ water. Samples were then *DpnI* treated to digest methylated DNA with the addition of 5μl restriction enzyme buffer B (Promega), 2μl *DpnI* (Promega) and 13μl MQ water. Samples were incubated at 37°C overnight, followed by heat inactivation of the enzyme at 68°C for 10 min. *DpnI* digested samples were separated by agarose gel electrophoresis and the correct sized bands excised and purified using QIAquick Gel Extraction Kit (QIAGEN) according to manufacturer's instructions, and eluted in 50μl MQ water. Samples were then isopropanol precipitated and resuspended in 20μl of MQ water.

A blunt end ligation was performed by adding 10μl sample, 1.5μl 10mM ATP (Promega), 1.5μl 10x ligase buffer (Promega), 1μl MQ water and 1μl T4 DNA ligase (Promega). Reactions were incubated overnight at 16°C. Ligated DNA was then isopropanol precipitated and transformed by adding 5μl of sample to 45μl of Bioline ElectroSHOX (Bioline) competent cells using an electroporator (Biorad) (2.5kV, 25μF, 200Ω). Cells were allowed to recover in 1ml super optimal broth with catabolite repression (SOC) media (Bioline) with shaking at 37°C for 1 hr prior to spreading onto agar plates containing ampicillin (50μg/ml) for selection at 37°C overnight. Colonies were then picked and incubated with shaking at 37°C in 5ml Luria Broth (LB) containing ampicillin (50μg/ml) overnight. Plasmid DNA was extracted using a plasmid DNA miniprep kit (QIAGEN), and sequenced to determine if correct mutations had been inserted

2.2.3 Constructs

All AKT expression constructs were in both the pMIG and MSCV-IRES-cherry (pMIC) vector backbone, and both contain an N-terminal myristoylation sequence and N-terminal HA-tag attached to full length AKT1, AKT2 and AKT3. The myristolation sequence allows direct targeting of these proteins to the plasma membrane. These myristoylated gain of function AKT constructs were generated by Joanna Chan (Chan et al. 2011) and Megan Astle (Astle et al. 2011) (Peter MacCallum Cancer Centre). The

H-Ras^{v12} expression constructs are in both pMIG and pMIC vector backbones, where full length H-Ras contains a substitution (valine substitution at residue 12) conferring constitutive activity. These constructs were generated by Luke Dow (Dow et al. 2008) (Peter MacCallum Cancer Centre).

2.3 Generation of stable cell lines

2.3.1 Retrovirus production

All stable cell lines were generated using retroviral transduction. HEK293T cells were plated at a density of 2 x 10^6 cells per 94mm plate and incubated overnight. 20μg of amphotrophic envelope helper plasmid DNA (Muller et al. 1991) and 10μg of plasmid DNA containing a long terminal repeat and gene of interest were combined with 0.5M calcium chloride ($CaCl_2$) and 2x HEBS [0.28M sodium chloride (NaCl), 0.05M 4-(2-hydroxyethyl)-1-piperazineethanesulfonic acid (HEPES), 1.5mM disodium hydrogen phosphate (Na_2HPO_4)]. This transfection mix was incubated at room temperature for 20 min and then added dropwise to the HEK293T cells. Transfection media was replaced 16-18 hr later with media required by the target cell line. Retroviral supernatant was harvested from HEK293T cells 48 hr later by filtering through a 0.45μM pore filter (Sartorius) and stored at -80°C.

2.3.2 Retroviral transduction

Parental cells were plated approximately 16-18 hr prior to transduction. In 94mm plates, BJ cells were plated at a density of 3 x 10^5 cells and IOSE523 and HOSE cells were plated at density of 2 x 10^5 cells. Parental cells were transduced with a 3ml aliquot of retroviral supernatant (generated as described in 2.3.1), made to a final volume of 7ml with cell line specific media, and containing 4μg/ml Polybrene (Sigma). Transduction of parental cells was repeated a total of three times during a 48 hr period to generate stable cells. Approximately 8 hr after the final retroviral transduction, the retroviral supernatant was changed to cell line specific media and cells were left to recover for two passages prior to selection.

2.3.3 Stable cell line selection

Selection for cells stably expressing green fluorescent protein (GFP) or cherry fluorescent protein (RFP) was performed by fluorescence activated cell sorting (FACS). To FACS sort, cells were detached according to Chapter 2.1, and put through a 35μM cell strainer cap (BD Falcon) to ensure single cell suspension. Cells were immediately taken to the Peter MacCallum Cancer Centre FACS core facility for sorting. All cells retrovirally transduced (Chapter 2.3.2) were FACS sorted for cells expressing the gene of interest prior to experimental work. When FACS sorting the BJ and IOSE523 cells, only the top 20% of GFP or RFP expressing cells were collected. When FACS sorting the HOSE cells the top 50% GFP expressing populations were collected due to the poor transduction efficiency of HOSE cells.

2.4 Cell treatments

All cells were serum starved prior to treatment with inhibitors. Serum starvation involved 2 x wash with PBS and then a overlay with media containing no serum for 48 hr. Serum starved cells were then pre-treated with 20 nM rapamycin (Calbiochem) or 5μM AKT isozyme-selective inhibitor AKTi 1/2 (Calbiochem) for 30 min **(Table 2.2)**, followed by serum stimulation with 15% (v/v) FBS if required. Cells were then harvested for RNA, protein and cell number.

Table 2.2: Inhibitor concentrations

Name	Concentration	Vehicle	Company
Akt inhibitor isozyme-selective Akti 1/2	5 μM	DMSO	Merck
Rapamycin	20 nM	Ethanol	Merck

2.5 Harvesting for protein and preparation of extracts

To harvest for protein, cells were firstly washed twice with phosphate buffered saline (PBS). Cells were then scraped in western solubilisation buffer (WSB) [0.5M EDTA, 20mM HEPES pH 7.9, 2% SDS], transferred to a 1.5ml microfuge tube and boiled for 10 minutes at 95°C. Samples were sheared by sonication at 30 sec intervals for 15 min using the Bioruptor (Diagenode, Liege, Belgium) and stored at -20°C. Alternatively, for cytosolic fractions proteins were extracted placing plated cells on ice, washing once with ice-cold PBS, and scrapped cells on plates in Rac Lysis Buffer (RLB) [50mM Tris-HCl pH 7.5, 120mM NaCl, 1% (v/v) nonyl phenoxypolyethoxylethanol (NP-40), 1mM EDTA, 50mM NaF, 40mM β-glyerolphosphate, 1mM benzamidine and 0.5mM phenylmethylsulfonyl fluoride (PMSF)]. Lysed cells were scraped and transferred into 1.5 ml microcentrifuge tubes and cleared by centrifugation at 16,000x g for 10 min at 4°C. Supernatant was collected, snap frozen and stored at -80°C. Protein concentration was determined by DC™ Protein assay (Biorad) (based on Lowry protein determination assay) as per manufacturers' instructions.

2.6 Harvesting for RNA

To harvest for RNA, plated cells were placed on ice and washed twice with ice-cold PBS. Cells were scrapped in 500μl of guanidine thiocyanate (GTC) Solution D [4M GTC, 25mM sodium citrate pH 7, 0.5% (w/v) sarcosyl, 0.1M β-mercaptoethanol] and transferred to a 1.5ml microfuge tube. All samples were then stored at -20°C prior to RNA isolation (Chapter 2.10). Cell number was also determine from a separate dedicated plate each time an RNA harvest was performed in order to accurately load for rDNA transcription assays (Chapter 2.8) or measuring RNA content per cell (Chapter 2.7). Cell number was determined by lifting cells from plastic with trypsin (Chapter 2.1), resuspending in cell line specific media and counting using the Coulter Counter Z Series (Beckman Coulter).

2.7 Measuring protein and RNA content per cell

Cells were plated at a density of 1.5 x 10^5 cells per 60 mm plate, and allowed to adhere overnight, with cells plated in triplicate for both protein and RNA. Cells were then serum starved by washing twice with PBS and overlaying with media containing no serum for 48 hr. Cells were then harvested for protein using WSB (Chapter 2.5) and RNA (Chapter 2.6). Furthermore, from the three plates to be harvested for protein, one plate was used to determine cell number by taking a small sample before harvesting with WSB for protein. Cell number was determined by lifting cells from plastic with trypsin (Chapter 2.1), resuspending in cell line specific media and counting 50μl using the Coulter Counter Z Series (Beckman Coulter). Protein concentration was determined using the DC™ Protein Assay (Biorad), and protein per cell determined by normalizing back to cell number. RNA was isolated, corrected for % recovery and normalised back to cell number to determine RNA per cell (Chapter 2.10).

2.8 Measuring rDNA transcription

To perform rDNA transcription assays, cells were plated in 10% serum at low density (60% confluency) in 100 mm plates and left to recover overnight. Cells were then serum starved for 36 hr followed by a pre-treatments with either vehicle or 20nM rapamycin treatment before being supplemented with 15% serum, for 12 hr in the presence or absence of rapamycin. Prior to harvesting, cells were washed 2 x PBS and harvested for RNA (Chapter 2.6). RNA from equal cell numbers was analysed using the RPA (Chapter 2.11) to measure differences in rDNA transcription rates, and cell size was determined by using cell volume measurement from the Coulter Counter Z Series (Beckman Coulter) for each cell.

2.9 Synthesis of 5' externally transcribed spacer (5' ETS) ^{32}P-labelled antisense riboprobe

The riboprobe plasmid construct corresponding to the (5' ETS) region of the ribosomal RNA (rRNA) gene was synthesised from an 80 bp fragment corresponding to nucleotides 1-80 and subcloned by PCR into pGEM-3Z vector with the addition of a *HindIII* restriction site at the 5' end and an *EcoRI* at the 3' end. The 5' ETS riboprobe construct was generated by Kerith Sharkey (Chan et al. 2011) (Growth Regulation Laboratory, Peter MacCallum Cancer Centre).

^{32}P-labelled antisense riboprobe was generated using the above linearised plasmid construct as template. T7 RNA polymerase (20U) (Promega) was used to transcribe 1 μg of linearised DNA template in transcription buffer [10 mM DTT, 500 μM ATP, 500 μM CTP, 500μM GTP, 11.25 μM UTP, 0.835μM ^{32}P-UTP (Perkin Elmer), RNasin (40 U, Promega)] in a final volume of 20 μl for 30 min at 37°C. Diethylpyrocarbonate (DEPC)-treated water (30μl) was then added to the riboprobe mix and 1μl was spotted onto DE-81 paper (Whatman) to count total radioactivity. Incorporated radioactivity was determined by spotting 1μl of riboprobe mix onto DE-81 paper, and washed twice

for 5 min in 0.5M sodium phosphate buffer (pH 7). 5μl 1 M Tris-HCl (pH 8), 1μl 1M $MgCl_2$, 10μg yeast tRNA, RNasin (40 U) and Dnase (20 U) was then added to the riboprobe mix and incubated at 37°C for 15 min. 60μl of a 1:1 TE-saturated phenol and chloroform:isoamyl alcohol (24:1) was added to precipitate the labelled riboprobe. The riboprobe mix was vortexed and the aqueous layer isolated by centrifugation at 13000x g. The aqueous layer was extracted, and the riboprobe was then purified using a G25 Sephadex column (GE Healthcare). The final probe was made up to 200μl using hybridisation buffer [80% deionised formamide, 40mM PIPES pH 6.7, 0.4M NaCl, 1mM EDTA]. 1 μl of the final riboprobe mix was spotted onto DE-81 paper to count recovered radioactivity. All spotted DE-81 paper was placed in 5ml of scintillant and counted using the Tri-Carb 2100TR liquid scinitillation analyser (Perkin-Elmer) to calculate riboprobe specific activity.

2.10 RNA Isolation

Based on the (Chomczynski and Sacchi 1987) method. On ice, cells were washed twice with cold PBS, lysed into 500μl of GTC Solution D and scraped from the plate and transferred into a 1.5 ml microcentrifuge tube. To calculate RNA recovery, prior to RNA isolation, the GTC Solution D lysate was spiked with a ^{32}P-labelled riboprobe (Chapter 2.9) at ~50,000 counts per min (CPM). RNA was extracted with addition of 1/10th volume of 2M NaAc pH 4, 1 volume water saturated phenol (Sigma) and 1/5th volume chloroform:isoamyl alcohol (Sigma) 49:1. The aqueous phase was isolated by centrifugation at 13000x g for 20 min at 4°C, and transferred into a 1.5ml microcentrifuge tube, and RNA isolated with 1 volume of cold isopropanol for 2 hr at -20°C. RNA was pelleted at 10,000x g for 15 min at 4°C and resuspended into 300μl of GTC Solution D. RNA was precipitated again with 1 volume of cold isopropanol for 1 hr at -20°C. RNA was pelleted at 10000x g for 15 min at 4°C, washed twice with 800μl of cold 70% ethanol in DEPC-treated water, air-dried and resuspended in 20μl of DEPC-treated water. RNA recovery was quantitated by counting the recovered ^{32}P-labelled riboprobe from 2μl of isolated RNA, using the Tri-Carb 2100TR Liquid Scintillation Analyser (Perkin-Elmer). RNA concentration was determined using the NanoDrop ND-1000 Spectrophotometer (Thermo Fisher).

2.11 Ribonuclease protection assay

The ribonuclease protection assay (RPA) is used to directly detect and quantitate mRNA levels through hybridisation of a specific ^{32}P-labelled antisense riboprobe to isolated sample RNA, where transcripts of interest are visualised on a phosphorimage following RNase digestion of single stranded non-hybridised RNA (Prediger 2001). To measure RNA transcript levels, isolated RNA (described in Chapter 2.10) was added to hybridisation buffer to a volume of 25μl. 5μl of a ^{32}P-labelled antisense riboprobe (described in Chapter 2.9) was then added to make a final sample volume of 30μl. Samples were heated to 85°C for 5 min to denature RNA and immediately incubated at 45°C to hybridise overnight. Following hybridisation, 300μl of RNase digestion buffer was added [10μg RNase A (Roche), 250U RNase T1 (Roche), 10mM Tris-HCl

pH 7.5, 5mM EDTA, 300mM NaCl] and samples incubated at 37°C for 1 hr. The reaction was terminated upon addition of 50μg of proteinase K and 1% (w/v) SDS and incubated at 37°C for 15 min to terminate the reaction. RNA was then precipitated using 500μl of cold isopropanol and 5μg yeast total RNA at -20°C for 1 hr. RNA was pelleted at 10,000x g for 10 min and then washed with 800μl of cold 70% (v/v) ethanol in DEPC-treated water. Samples were dried using the RVC 2-25 Speedivac (Christ) and reconstituted in 9μl of RNA loading dye [15% (w/v) Ficoll-400, 0.25% (w/v) bromophenol blue, 0.25% (w/v) xylene cyanol]. Samples were then loaded onto a 5% (w/v) non-denaturing acrylamide gel and run at 200 volts for 1 hr in TBE buffer [90 mM Tris-HCl pH 7.4, 90 mM boric acid, 200 μM EDTA]. The gel was then dried at 80°C for 30 min using the Model 583 Gel Drier (Biorad) and exposed to a phosphorimager screen (Molecular Dynamics) overnight. The phosphorimage was developed using the Storm 820 Phosphorimager (GE Healthcare) and band intensities quantitated using ImageQuant Software (GE Healthcare).

2.12 Cell signalling experiments

Cells were plated at 2 x 10^6 in 150mm plates and left to recover to achieve approximately 70% confluency. Cells were serum starved for 48 hours followed by pre-treatment with 20nM rapamycin or vehicle for 30 minutes followed by the addition of plus or minus 15% serum for a further 30 minutes (Chapter 2.4). Cells were harvested for protein using either RLB or western solubilisation buffer (WSB) and protein concentrations determined using a DC™ Protein Assay (Chapter 2.5). Western blot analysis was then conducted using a panel of phospho and total antibodies (Chapter 2.13, **Table 2.3**).

2.13 Immunoblotting

Protein extracts were separated by SDS-polyacrylamide gel electrophoresis (SDS-PAGE) using either 6% (w/v), 10% (w/v) or 15% (w/v) gels with a 5% (w/v) stacker and transferred onto Immobilon-P polyvinylidene fluoride (PVDF) membranes (Millipore) using the Trans-Blot Electrophoretic Transfer Cell or the Trans-Blot SD Semi Dry Transfer Cell (Bio-Rad). Membranes were blocked for 1 hr at room temperature in Tris Buffered Saline (TBS) containing 5% (w/v) skim milk powder (Diploma) and 0.05% (v/v) Tween-20 (MP Biomedicals) (TBS-TM), followed by overnight incubation with primary antibodies at 4°C in TBS-TM (See **Table 2.3** for details on all antibodies used). Membranes were then washed 3 x 10 min in TBS-TM, followed by a 1 hr room temperature incubation with an appropriate secondary horseradish peroxidase (HRP)-conjugated antibody **(Table 2.3)** in TBS-TM. Membranes were then washed 5 x 10 min with TBS-T and visualised by Western Lightening Chemiluminescence Plus (Perkin Elmer). Signals were detected by exposure to film (Hyperfilm™, GE Healthcare). Protein size was estimated by comparison to a Benchmark pre-stained protein ladder (Invitrogen, product code 10748-010).

Table 2.3: Antibodies used for immunoblotting

Antibody	Source	Size (kDa)	Dilution	Buffer Used	% Gel	Company	Product-Code
Myc-tag 4A6	Mouse	-	1:2000	WSB	10	Millipore	05-724
HA Tag (12CA5)	Mouse	-	1:2000	WSB	10	In-house (Pearson Laboratory, Peter MacCallum Cancer Centre (PMCC))	N/A
SGK3	Rabbit	57	1:1000	WSB	10	ProteinTech Group	12699-1-AP
SGK3	Rabbit	57	1:1000	WSB/RLB	10	Abgent	AP7949a
SGK3	Rabbit	57	1:1000	WSB/RLB	10	Novus Biologicals	NLS7240
SGK3	Goat	57	1:1000	WSB/RLB	10	Santa-Cruz	SC-47394
SGK3	Goat	57	1:1000	WSB/RLB	10	Santa-Cruz	SC-47396
Phospho-AKT (Ser473)	Rabbit	60	1:2000	WSB	10	Cell Signalling Technology (CST)	4058
AKT (pan)	Sheep	60	20:3000	WSB	10	In-house (Pearson Laboratory, PMCC)	N/A
Phospho-PRAS40 (Thr246)	Rabbit	40	1:1000	WSB	10	(CST)	2297
PRAS40	Rabbit	40	1:1000	WSB	10	(CST)	2610
Phospho-RP S6 (Ser240/244)	Rabbit	32	1:1000	RLB	15	(CST)	2215
RP S6	Rabbit	32	1:1000	RLB	15	(CST)	2217
Phospho-4EBP1 (Thr37/46)	Rabbit	15-20	1:1000	RLB	15	(CST)	2855
Phospho-TSC2 (Thr1462)	Rabbit	200	1:1000	WSB	6	(CST)	3611
TSC2	Rabbit	200	1:1000	WSB	6	Santa Cruz	SC-893
Phospho-GSK3β (Ser9)	Rabbit	46	1:1000	WSB	10	(CST)	9336
GSK3β	Rabbit	46	1:1000	WSB	10	(CST)	9315
SV40 Large T/ small t	Mouse	94/21	1:1000	WSB	15	Santa Cruz	sc-58665
H-Ras	Rabbit	20	1:1000	WSB	15	Santa Cruz	sc-520
Tubulin	Mouse	50	1:10000	RLB/WSB	10/15	Sigma	T5168
Adaptin	Mouse	112	1:2000	WSB	6	BD Transduction Laboratories	A43920
Actin	Mouse	42	1:20000	RLB/WSB	10/15	MP Biomedicals	691002
HRP-mouse	Goat	-	1:2000	-	-	Biorad	170-6516
HRP-rabbit	Goat	-	1:2000	-	-	Biorad	170-6515
HRP-sheep	Goat	-	1:2000	-	-	DAKO	P0163
HRP-goat	Rabbit	-	1:5000	-	-	DAKO	P0160

2.14 Cell proliferation assay

Cells were plated at a density of 2 x 10^4 in 6 well plates and allowed to adhere for 4 hr prior to the 0 hr time point harvest. Cells were harvested by washing once with PBS, lifted off the plastic by addition of 500μl 0.25% trypsin-EDTA (Gibco) and neutralised with 1ml DMEM (Sigma) supplemented with 10% (v/v) FBS. Analysis of cell number (cells/ml) and cell size (fL) was performed using the Coulter Counter Z Series (Beckman Coulter). Cell harvests were repeated at time points 24, 48, 72, 96, 120 and 144 hr. Cell numbers at each time point was used to determine proliferation rates and cell doubling times using GraphPad Prism Software (GraphPad Software).

2.15 Scratch migration assay

Cells were plated at a density of 4 x 10^4 in 24 well plates and incubated for 48 hr. Cells were then serum starved overnight by washing twice with PBS and overlaying with serum free media. Media was aspirated from the well and replaced with PBS prior to making a single scratch in the centre of the well using a 24 well IncuCyte cell scratching apparatus (Essen). PBS was then replaced with media containing serum and 1μg/ml Mitomycin C (Kyowa). An image of the scratch was taken at 0 hr and then every 2 or 4 hr, for the period indicated in figure legends, using the IncuCyte and IncuCyte software (Essen). Wound confluence (%) and wound width (μm) were calculated using the associated IncuCyte software (Essen).

2.16 Colony formation assay

Cells were seeded into semi-solid media at a concentration of 10,000 cells per well to assess their ability to grow in an anchorage independent manner. Sterile 0.8% molten agarose (Biorad) equilibrated in a water bath to 42°C was mixed at a 1:1 ratio with 2 x cell line specific culture media equilibrated at 37°C to give a final concentration of 0.4% agarose. 2ml of molten 0.4% (w/v) agarose/culture media solution was pipetted into a 35 mm non-tissue culture, plate and allowed to polymerise. This polymerised solution constituted the bottom semi-solid layer and inhibited cell outgrowth to the bottom of the dish. Cells were then trypsinised (Chapter 2.1), counted for cell number using the Coulter Counter Z Series (Beckman Coulter), and resuspend into a solution consisting of a 1:1 ratio of culture media and 0.5% (w/v) agarose (to give a final agarose concentration of 0.25%). The cell suspension/agarose/culture media solution was pipetted on top of the polymerised 0.4% bottom semi-solid layer and allowed to set to constitute the anchorage independent growth layer. 1ml of cell type specific culture media, acting as a nutrient provision overlayer, was pipetted on top of the semi-solid agarose complexes. Cells were cultured at 37°C with 5% CO_2 and the media was changed 1-2 times per week. After 2-3 weeks of continuous culture, the media was removed and the cultures stained with 500μl of 2 mg/ml thiazolyl blue tetrazolium bromide (MTT) (Sigma). Photographs of colonies were obtained via placement of the cultures on a light box, and photographed with a digital camera (Nikon). Colony size and number were assessed using Metamorph imaging software (Molecular Devices).

2.17 SGK3 localisation

Cells were plated at a density of 1 x 10^4 cells per well of a 24 well plate onto glass coverslips. 48 hr later, cells were washed twice with PBS, and fixed with 4% Paraformaldehyde (PFA; Sigma) in PBS at room temperature for 10 min. Cells were then washed three times with PBS, permeabalised with 0.1% Triton X-100 (Sigma) in PBS for two min at room temperature and washed three times with PBS. Coverslips were then incubated in blocking buffer (3% Bovine Serum Albumin (BSA) in PBS) at room temperature for 30 min. The relevant primary antibodies **(Table 2.4)** were then added (diluted in 3% BSA/PBS) and incubated for one hr at room temperature. Coverslips were washed three times with PBS and incubated for one hr at room temperature in secondary antibody (**Table 2.4**) (diluted in 3% BSA/PBS). Coverslips were washed three times with PBS and mounted using VectaShield+DAPI (Vector Labs). Localisation was visualised using a Leica SP5 Confocal Microscope (Leica Microsystems).

Table 2.4: Antibodies used for SGK3 localisation

Antibody	Source	Dilution	Company
EEA1	Mouse	1:500	BD Biosciences
Myc-Tag (71D10)	Rabbit	1:500	Cell Signaling Technology
Alexa fluor 594	Rabbit	1:700	Molecular Probes
Alexa fluor 647	Mouse	1:700	Molecular Probes

2.18 Cell cycle analysis

Cells were collected by trypsinisation (Chapter 2.1), washed once in PBS and cell pellets resuspended in 300μl cold PBS. Cells were fixed by the dropwise addition of 700μl of 95% (v/v) ice-cold ethanol while gently vortexing. Fixed cells were washed twice with PBS containing 2% FBS (PBS-F) and resuspended at a concentration of 1 x 10^6 cells per ml in propidium iodide (PI) stain (PBS-F supplemented with 20μg/ml propidium iodide and 200μg/ml RNase A (Roche)). Cells were incubated in the dark at 37°C for 30 min and then analysed using the FACS Canto Flowcytometer (BD Biosciences) interfaced with ModFit software (Verity Software House) to determine the percentage of cells in each phase of the cell cycle.

2.19 Cell death assay

Cells were seeded at a density of 1 x 10^5 cells per well of a six well plate and allowed to adhere overnight. Cytotoxic drugs **(Table 2.5)** were then added at appropriate doses (as described in figure legends) and harvested 24, 48 and 72 hr later. Cells were harvested by transferring the media to a 10ml tube into which subsequent washes and trypsinised cells were combined into. Adherent cells were washed with 500μl PBS and removed from culture dishes with 500μl of trypsin-EDTA. The wells were

rinsed for remaining cells with a further 500μl. Collected cells were pelleted at 200x g for 4 min, washed twice with PBS and resuspended in 100μl of Annexin V binding buffer (140mM NaCl, 10mM HEPES pH 7.4, 5mM $CaCl_2$) and 2μl of PI citrate solution (38mM tri-sodium citrate, 68.8μM propidium Iodide). Cell viability was then analysed using the FACS Canto Flowcytometer (BD Biosciences).

Table 2.5: Cytotoxic agents used for cell death assays

Name	Source	Vehicle	Mechanism
Cisplatin	Sigma-aldrich	MQ Water	Forms cytotoxic adducts with the DNA dinucleotide d(pGpG), inducing intrastrand cross-links.
Taxol	Sigma-aldrich	MQ Water	Binds to the N-terminus of β-tubulin and and stabilizes microtubules arresting the cell cycle at the G2/M phase.
Vincristine	Sigma-aldrich	Ethanol	Inhibits microtubule assembly by binding tubulin and inducing coiled spiral aggregate formation. Arrests cell cycle in G2/M-phase by blocking mitotic spindle formation

2.20 Microarray Experiments

2.20.1 Microarray sample preparation

Cells were seeded at a density of 1 x 10^6 cells per 94mm plate and incubated until approximately 70% confluent. Cells were the harvested by washing twice with PBS and lysed into 600μl of RLT buffer from the RNeasy Kit (QIAGEN), by scraping into a 1.5ml microcentrifuge tube. Cells were then sheared five times by passing through a 21” gauge needle and RNA isolated using the RNeasy Kit according to manufacturer’s instructions. RNA concentration was determined using the NanoDrop ND-1000 Spectrophotometer (Thermo Fisher), and 500ng of RNA analysed on the Bioanalyzer (Agilent) to confirm RNA purity and integrity. All samples were sent to The Ramaccotti Centre (Sydney) to be run on human Affymetrix 1.0 ST expression arrays.

2.20.2 Microarray data analysis

Gene expression data was analysed using software packages from Bioconductor (Gentleman et al. 2004), with data from each experiment loaded into the statistical program R (Team 2011). Chips were assessed for overall quality using the package affyPLM (Bolstad 2004; Bolstad et al. 2005; Brettschneider et al. 2007). All data was normalised and background corrected using the robust multi-array average (RMA) expression (Irizarry et al. 2003). The Affy (Gautier et al. 2004) and Limma (Smyth 2005) software packages were used to model the data, adjusting for any batch effects and then to assess differential expression. For each probeset the average log2- expression for each treatment was calculated. Then for each contrast of interest log fold changes and standard errors were estimated. Any probesets that had False Discovery Rate (FDR) adjusted p-Value less than 0.05 were considered differentially expressed, and a fold change threshold of 2 was also applied to the data to increase stringency during expression analysis.

Analysis of differential gene expression was conducted using the MetaCore™ platform by GeneGo (http://www.genego.com/metacore.php), which allowed assessment of functional ontology categories and analysis of pathways enriched in gene expression data. Analysis of differential gene expression was also conducted using Gene Set Enrichment Analysis (GSEA) (Broad Institute http://www.broadinstitute.org/gsea) (Mootha et al. 2003; Subramanian et al. 2005). Gene sets from the C2 (curated) set were used to test if the phenotypes where enriched in a particular pathway. To determine the null distribution gene permutation, rather than sample permutation, was used due to the small number of samples. All primary bioinformatics analysis of raw data was conducted with the aid of Peter MacCallum Cancer Centre Bioinformatics core (Jason Ellul).

2.21 Statistical Analysis

Statistical analysis was performed using One-way ANOVA with Newman-Keuls comparison test using Graphpad Prism Software (GrapahPad Software). All graphs were plotted using Graphpad Prism Software.

3. SGK3 regulation of cell growth and proliferation

3.1 Introduction

Cell growth and proliferation are distinct yet highly coordinated and stringently regulated processes that are critical for cell development and survival (Neufeld and Edgar 1998). Cell growth can be defined as an increase in cell mass through the synthesis of macromolecules such as protein and RNA, and it is a requirement for cells to reach a critical cell mass in order to transit through the cell cycle and divide (Schmelzle and Hall 2000; Montanaro et al. 2007). Aberrant regulation of cell growth and proliferation machinery is associated with a wide variety of disease states, and is a well-characterised hallmark of cell transformation and tumourigenesis (Neshat et al. 2001; Guertin and Sabatini 2005; Shaw and Cantley 2006).

Sustained protein synthesis is required for cells to reach a critical mass and maintain normal cellular processes (Montanaro et al. 2007), and it is modulated through either an increase in the synthesis of ribosomes, which elevates the translational capacity of a cell, or by increasing the translational efficiency of existing ribosomes (Morgan and Beinlich 1997). However, of these processes it is thought that the cells ability to efficiently respond to environmental cues to modulate ribosome biogenesis is the major determinant in modulating the overall cellular protein biosynthetic capacity (Mayer and Grummt 2006).

The PI3K/mTORC1 pathway has been identified as a crucial regulator of growth and proliferation, through the ability of mTORC1 to exquisitely coordinate growth factor and nutrient signalling. mTORC1 through convergence on downstream targets ribosomal S6 kinase (S6K) and the translation initiation factor 4E-binding proteins (4E-BPs) regulates core growth processes, including ribosome biogenesis, transcription, translation initiation and protein degradation (James and Zomerdijk 2004; Wang and Proud 2006; Yang et al. 2008). Many studies have identified AKT as an important modulator of mTORC1 and thus cell growth, and proliferation. AKT phosphorylates the tumour suppressor tuberous sclerosis factor 2 (TSC2), a crucial negative regulator of mTORC1, at two distinct sites (Ser939 and Thr1462), thereby inhibiting TSC2 function and promoting mTORC1 activation (Corradetti and Guan 2006). Furthermore AKT has also been shown to phosphorylate a proline-rich AKT substrate of 40kDa (PRAS40), a protein associated with mTORC1. Phosphorylation of PRAS40 at Thr246 by AKT prompts its dissociation from mTORC1 and subsequently indirectly activates mTORC1 signalling (Sancak et al. 2007; Vander Haar et al. 2007).

As previously described there is high homology between the AKT and SGK kinase families, which is highlighted by the similarity in their substrate targets. Although there is no current evidence to suggest that SGK3 plays a direct role in mediating growth signalling through mTORC1, it has been shown that SGK1 is able to negatively

regulate TSC2 through phosphorylation at Thr1462 in cardiac myocytes (Aoyama et al. 2005), thus promoting increased growth signalling through mTORC1 activation. Moreover, recent studies in *C.elegans* have implicated SGK1 as an essential mediator of TORC2 signalling in the regulation of lipid accumulation, life span and growth, highlighting that in addition to AKT, the SGK family is an important mediator of the PI3-K/mTOR pathway (Jones et al. 2009; Soukas et al. 2009).

In a similar manner to AKT, both SGK1 and SGK3 have also been implicated in regulating cell proliferation by inhibiting GSK3 through direct phosphorylation of Ser9 (Liu et al. 2000; Dai et al. 2002; Sakoda et al. 2003). GSK3 is a crucial modulator of the cell cycle, and inhibition of GSK3 prevents it from negatively regulating its targets, which include Cyclin D1, c-myc and Cyclin E, thereby allowing Cyclin D1 to continue its role in the cell cycle. Moreover, SGK3 knockout mice exhibit a notable defect in keratinocyte proliferation (McCormick et al. 2004; Alonso et al. 2005), further implicating SGK3 in the regulation of cell proliferation.

To date much evidence has been accumulated to suggest that the SGK family plays an important role in regulating cell growth and proliferation processes, however this evidence is based on studies characterising the role of SGK1, with no direct association with involvement in ribosome biogenesis. The purpose of these studies was to elucidate a possible role specifically for SGK3 in the regulation of cell growth and proliferation. In addition to modifying the amount and activity of SGK3, the studies presented in this chapter have employed mutants that allowed the unique endosomal subcellular localisation of SGK3 to be explored as a possible level of regulation that defines the functional ability of SGK3 to mediate these core cell processes.

3.2 Results

3.2.1 Characterisation of HOSE SGK3 stable cell lines

To carry out SGK3 gain of function studies we firstly utilised a non-tumourigenic human ovarian surface epithelial (HOSE) cell that was immortalized through transfection with the human papilloma virus (HPV) E6/E7 oncogenes (Tsao et al. 1995). Studies in our laboratory have identified SGK3 as being expressed at low levels in HOSE cells, in addition SGK3 messenger RNA (mRNA) levels were increased in 80% (27/34) (as described in Chapter 1.1) of ovarian tumour cell lines when compared to the HOSE cells, suggesting a possible role for SGK3 in ovarian tumourigenesis, and making the HOSE cells an interesting candidate cell line to further characterise SGK3 functionality using gain of function mutants. The SGK3 mutants stably introduced into the HOSE cells to carry out studies presented in this chapter include a wild type SGK3 (SGK3 WT) construct, and a constitutively active SGK3 (SGK3 CA) construct, where the Ser residue (Ser 486) has been substituted for an Asp residue in the hydrophobic motif, creating a phospho-mimetic mutant **(Figure 3.1)**. All SGK3 constructs were generated with a myc-tag, allowing exogenous protein expression to be detected using a myc-tag antibody and are described more extensively in Chapter 2.2)

Following the generation of these two stable cell models through retroviral transduction (as described in Chapter 2.3), the cell lines were analysed to validate appropriate protein expression through western blot analysis (methods described in Chapter 2.13) along with localisation studies using immunofluorescence to determine if the mutant constructs were localising to the appropriate cellular compartments (as described in Chapter 2.17). Several commercially available SGK antibodies were tested during the course of these studies. These antibodies included total anti-SGK3 antibodies from Abgent, ProteinTech Group, Novus Biologicals and Santa Cruz (See Table 2.3 for further detail). All antibodies were tested on a variety of cell lines, lysed in multiple buffers including RLB and WSB (data not shown), however under experimental conditions none of these antibodies were able to reliably identify endogenous SGK3. Only one of the tested anti-SGK3 antibodies generated by ProteinTech Group was able to detect over-expression of myc-tagged SGK3 as a single band at the correct size of 60kDa **(see Figure 3.2)**. This suggests that levels of endogenous SGK3 protein expression are likely to be quite low. Endogenous SGK3 protein expression was barely detectable in the vector only (pMIG) samples, as a band of 60kDa mobility **(Figure 3.2, Lane 1)**, but anti-SGK3 detected a band at the correct mobility (60kDa) in cells over-expressing SGK3 WT **(Figure 3.2, Lane 2)** and SGK3 CA **(Figure 3.2, Lane 3)** as did the anti-myc-tag antibody. Myc-tagged SGK3 constructs were expected to be slightly larger (60kDa) than endogenous SGK3 (57kDa). In all samples the expression levels of the housekeeping protein β-Actin were similar.

SGK3 is the only SGK family member that contains a Phox Homology domain in its N-terminal region, which is responsible for the binding of phosphoinositides, particularly PtdIns(3)P, and subsequently localises SGK3 mainly to the early endosomal compartment, where it is activated. To determine if the two stably expressed myc-tagged-SGK3 constructs reflect the correct cellular localisation in HOSE cells, we conducted immunofluorescence studies. The Early Endosomal Antigen 1 (EEA1) antibody was used as a marker for the early endosomes, and a myc-tag antibody was used to detect localisation of exogenous myc-tagged SGK3. In addition, DAPI, a DNA stain was used to detect cell nuclei. A complete panel of SGK3 mutant immunofluorescence staining is shown in **Figure 3.3 A**, and myc-tag, EEA1 and merged images of each mutant from this panel have been enlarged in order to view localisation more easily **(Figure 3.3 B-C)**. As expected immunofluorescence analysis of empty vector control pMIG cells detected no myc-tag expression, however robust EEA1 expression was evident **(Figure 3.3 B)**. Analysis of SGK3 WT cells showed predominant co-localisation with EEA1 and some diffuse cytoplasmic localisation **(Figure 3.3 B)**, whereas SGK3 CA cells exhibited both nuclear and early endosomal localisation of SGK3 **(Figure 3.3 C)**. These studies confirm the predominant early endosomal localisation of both SGK3 constructs.

Figure 3.1: SGK3 mutant constructs

Schematic of SGK3 mutant constructs used for functional studies. SGK3 wildtype (SGK3 WT) construct, SGK3 constitutively active (SGK3 CA), where Ser 486 in the C-terminal domain has been substituted for an Asp residue, mimicking phosphorylation at this residue. The SGK3 constitutively active phox homology domain (SGK3 CA PX) mutant also has Ser 486 in the C-terminal domain substituted for an Asp residue to mimic phosphorylation, in addition to a substitution at Arg 90 for Ala in the N-terminal PI(3)P binding pocket, thereby abolishing PI(3)P binding at the phox homology domain. Lastly, the SGK3 kinase dead (SGK3 KD) mutant was generated through substitution of Lys191 in the ATP binding site for a Met, rendering this kinase catalytically inactive. All constructs contain an N-terminal Myc-tag.

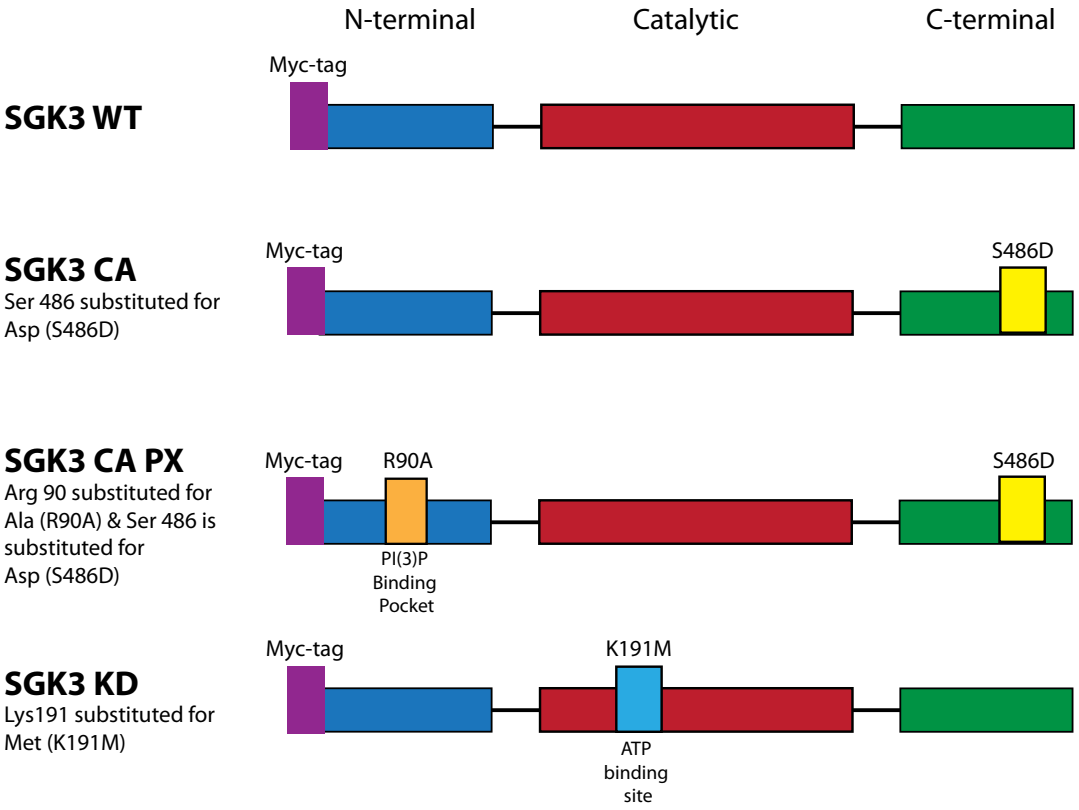
N-terminal
Catalytic
C-terminal
Myc-tag
SGK3 WT
Myc-tag
S486D
SGK3 CA
Ser 486 substituted for
Asp (S486D)
SGK3 CA PX
Arg 90 substituted for
Ala (R90A) & Ser 486 is
substituted for
Asp (S486D)
Myc-tag
R90A
S486D
PI(3)P
Binding
Pocket
Myc-tag
K191M
SGK3 KD
Lys191 substituted for
Met (K191M)
ATP
binding
site

Figure 3.2: Protein expression in stable SGK3 mutant HOSE cells

Exponentially growing HOSE cells stably transduced with empty vector pMIG, SGK3 WT and SGK3 CA were harvested for protein, and 20μg of protein was separated using 10% SDS-PAGE gels. Expression of proteins was determined by western blot analysis using total anti-SGK3 antibody (60kDa) (ProteinTech Group) and anti-Myc-tag antibody (60kDa). Membranes were stripped and reprobed using the anti-β-actin housekeeping antibody.

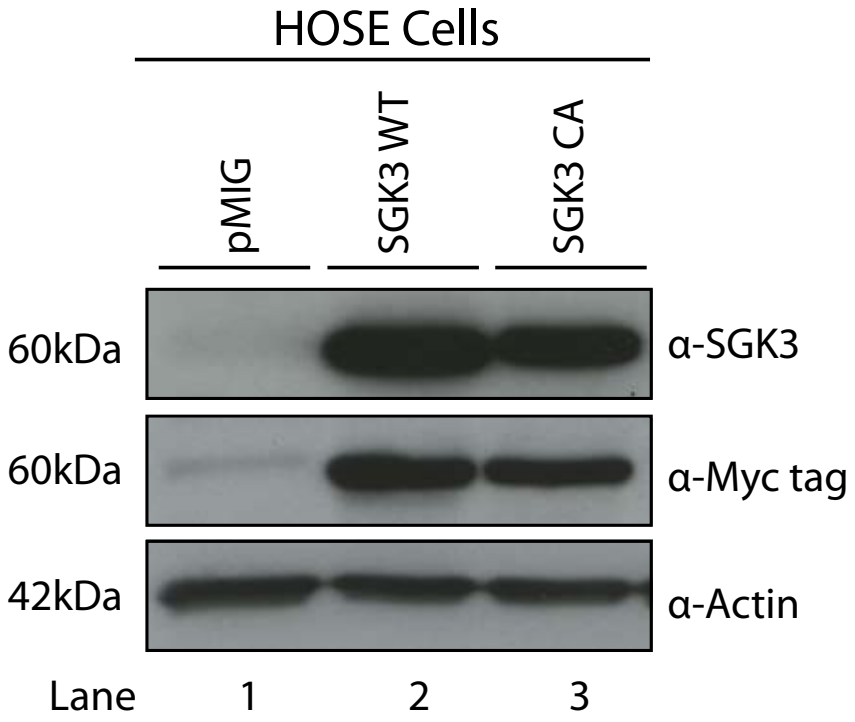
HOSE Cells
pMIG
SGK3 WT
SGK3 CA
60kDa
α-SGK3
60kDa
α-Myc tag
42kDa
α-Actin
Lane
1
2
3

Figure 3.3: SGK3 mutant localisation in HOSE cells

HOSE cells exhibiting stable protein expression of pMIG empty vector, SGK3 WT and SGK3 CA were plated at 0.1 x 10^4 in a 12 well plate onto glass coverslips, and were fixed and permeabilised for immunofluorescence staining following 48 hr incubation. **(A)** Fixed and permeabilised cells were incubated with primary antibody against the myc-tag epitope and secondary antibody conjugated to Alexa fluor 594. Early Endosomes were detected using a primary antibody directed against EEA1 and a secondary antibody coupled to Alexa fluor 647. Cell nuclei were stained with DAPI. **(B) and (C)** Particular sections of Figure 3.3 (A) enlarged in order to more easily view co-localisation of SGK3 WT and mutants with EEA1.

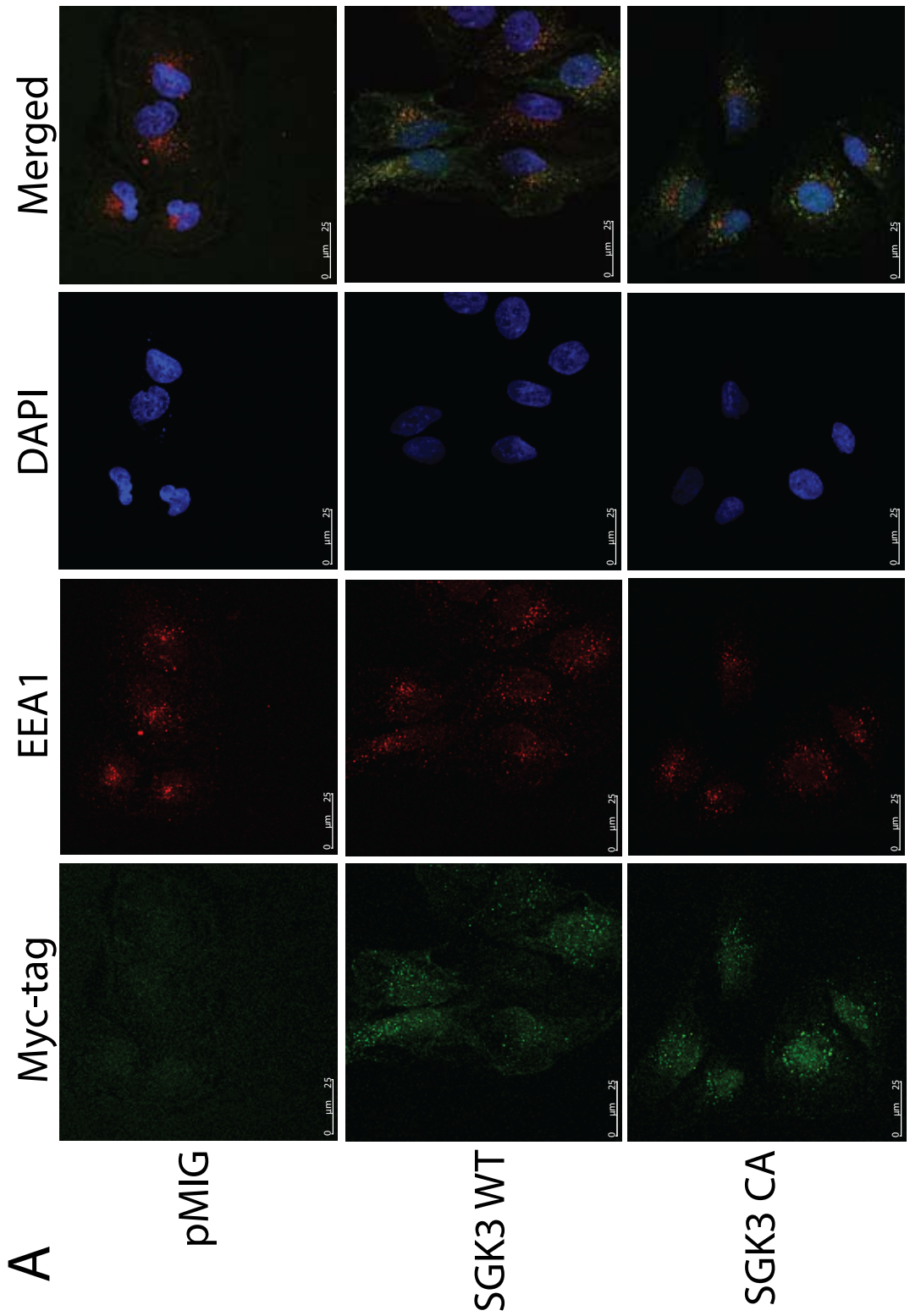
A
pMIG
SGK3 WT
SGK3 CA
Myc-tag
EEA1
DAPI
Merged

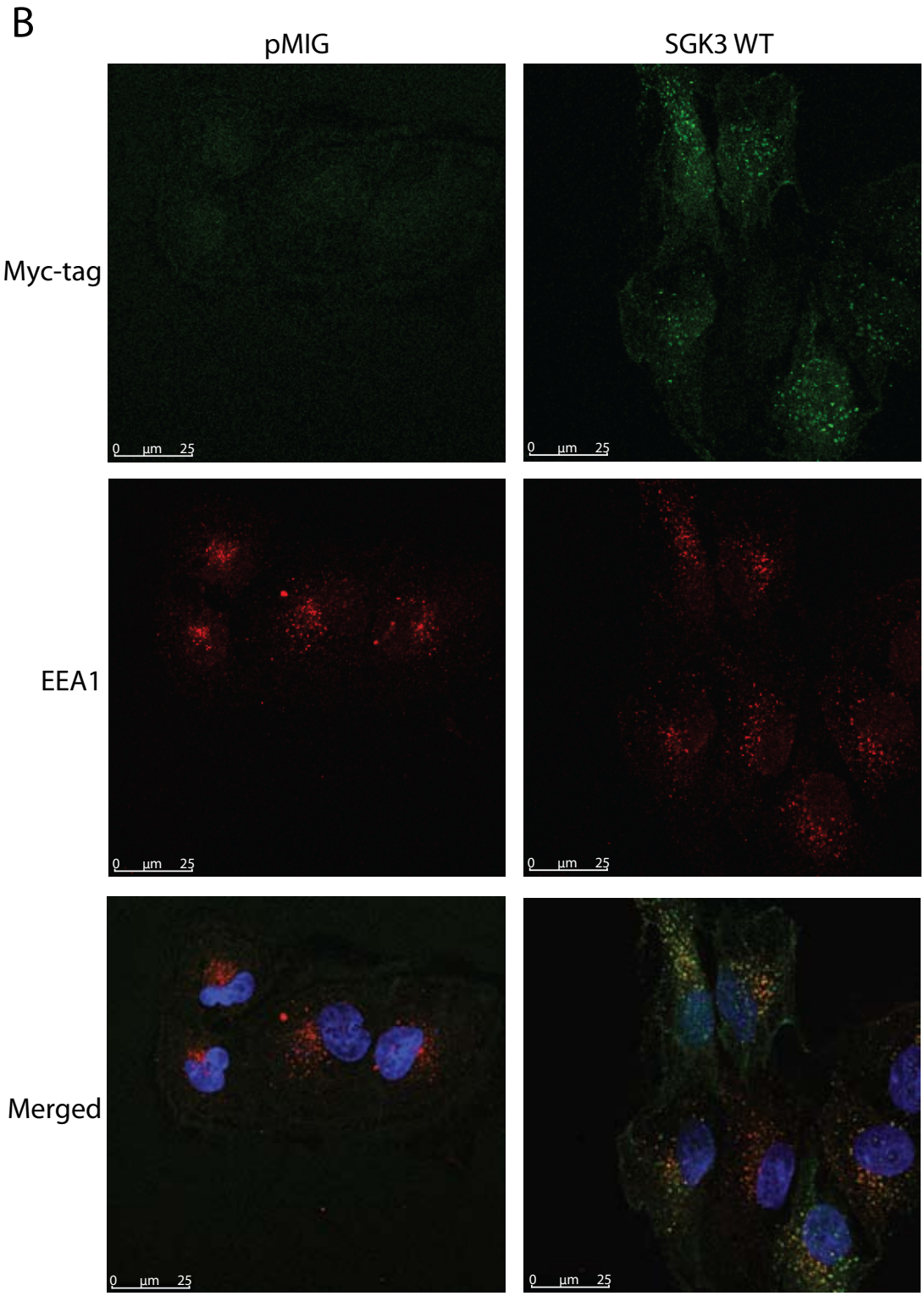
B
pMIG
SGK3 WT
Myc-tag
EEA1
Merged
0 µm 25

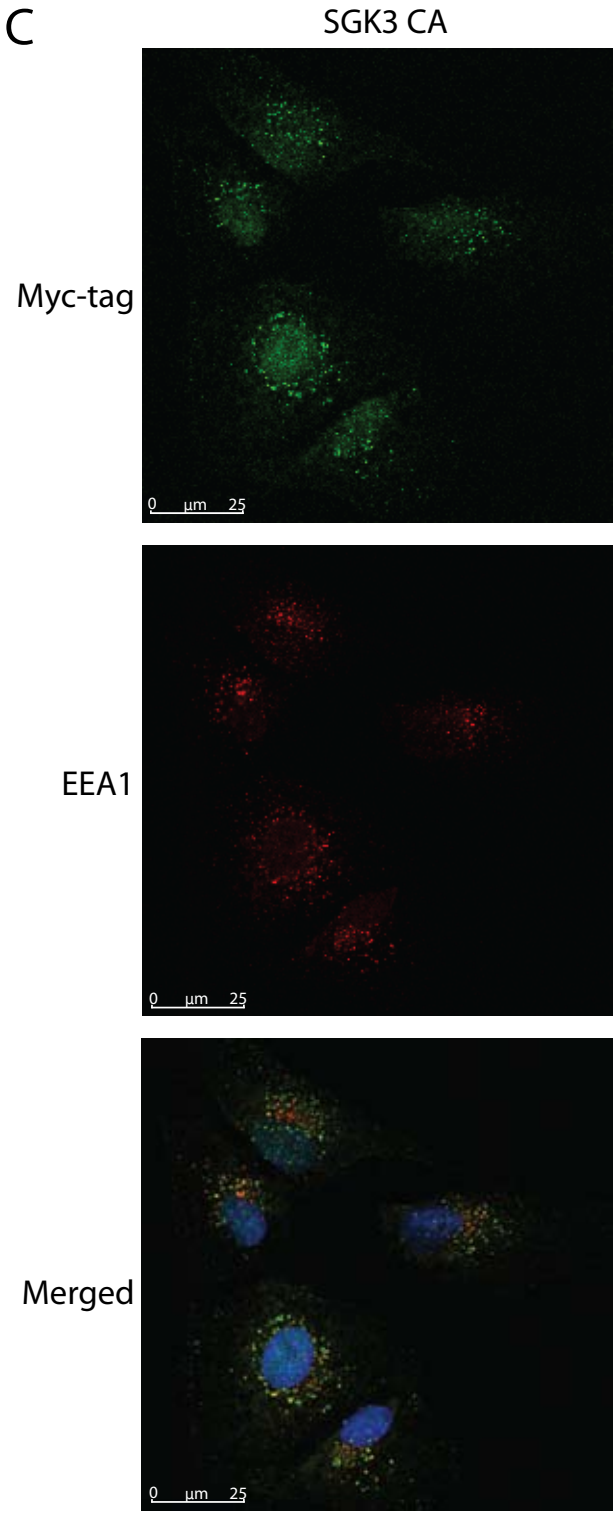
C
SGK3 CA
Myc-tag
EEA1
Merged
0 µm 25
0 µm 25
0 µm 25

3.2.2 Characterisation of BJ-hTERT SGK3 stable cell lines

In addition to the HOSE model, a genetically defined system of foreskin fibroblast cells termed 'BJ' where the cells have been transduced with hTERT, the catalytic subunit of telomerase (BJ-hTERT) rendering them immortal (Hahn et al. 1999), was used to validate key observations from our initial HOSE model. The SGK3 gain of function mutants stably introduced into the BJ-hTERT cells included both the SGK3 WT construct and the SGK3 CA construct as described in Chapter 3.2.1 **(Figure 3.1)**, along with two further mutant constructs not previously described. The two further mutant constructs included a constitutively active SGK3 with a second mutation in the N-terminal Phox Homology domain, where the Arg in the phosphoinositol binding pocket (Arg 90) is substituted for an Ala which abolishes the phosphoinositide binding site, thereby diminishing SGK3's ability to localise to the early endosomes (Tessier and Woodgett 2006a), termed 'SGK3 CA PX' **(Figure 3.1)**. The final mutant introduced into the BJ-hTERT cells was a kinase dead SGK3 mutant (SGK3 KD), which was generated through substitution of a Lysine (Lys 191) in the ATP binding site for a Met, rendering the construct catalytically inactive **(Figure 3.1)**. Both the SGK3 CA PX and the SGK3 KD mutants were not used in SGK3 studies using the HOSE cells (described above in Chapter 3.2.1) as they were unable to be stably introduced successfully into the HOSE cells. Several attempts were made to retrovirally transduce the HOSE cells with these constructs and establish stable cell lines, however all attempts were unsuccessful as enforced expression of these constructs produced a senescent phenotype. All SGK3 constructs introduced into the BJ-hTERT cells also contained a myc-tag, allowing exogenous protein expression to be detected using a myc-tag antibody. Using the BJ-hTERT cells allowed validation of HOSE-SGK3 studies, in addition to allowing more extensive investigations incorporating additional SGK3 mutants, and enabled a more comprehensive assessment of the level of regulation imposed by SGK3 on cell growth and proliferation.

Following the generation of BJ-hTERT stable cell lines using retroviral transduction (as described in Chapter 2.3), all cell lines were analysed via western blot analysis (as described in Chapter 2.13) and immunofluorescence (as described in Chapter 2.17). Consistent with the HOSE cells, in the BJ-hTERT cells levels of endogenous SGK3 were undetectable and as expected the myc-tag antibody did not identify any protein expression in the pMIG vector control cells **(Figure 3.4, Lane 1)**. However both the SGK3 and myc-tag antibody detected robust expression levels in SGK3 WT **(Figure 3.4, Lane 2)**, SGK3 CA **(Figure 3.4, Lane 3)**, SGK3 CA PX **(Figure 3.4, Lane 4)** and SGK3 KD **(Figure 3.4, Lane 5)** cell lines. Expression levels of the loading control tubulin remained similar between all samples.

Immunofluorescence analysis conducted on the BJ-hTERT cells was consistent with the HOSE data demonstrating that SGK3 WT, SGK3 CA and SGK3 KD all localise predominantly to the endosomal compartment, while the PX domain mutant exhibits a more cytoplasmic localisation (**Figure 3.5 A**, and enlarged images **Figure 3.5 B-D)**. Immunofluorescence staining with myc-tag exhibits some non-specific nuclear

staining in pMIG cells, but consistent with the western analysis, myc-tag SGK3 is detectable in the cytoplasm and early endosome of all SGK3 mutants (first panel of each row). Unfortunately non-specific binding of the myc-tag antibody in the nucleus did not allow us to confirm the observation from the HOSE studies (Chapter 3.2.1) that activated SGK3 is located in the nucleus. Notably, the majority of SGK3 staining in SGK3 CA PX cells was cytoplasmic and diffuse **(Figure 3.5 A**) confirming that the PX mutation was inhibiting localisation of this construct to the endosome as observed in previous studies utilizing this mutant (Virbasius et al. 2001; Tessier and Woodgett 2006a). The merged images in the fifth panel show that WT, CA and KD SGK3 mutants are localised mainly in the endosomal compartment with minimal cytoplasmic staining. SGK3 CA also appear to localise to other discrete structures other than early endosomes which is consistent with PtdIns(3)P being found in structures identified as multivesicular endosomes which lack EEA1 (Gillooly et al. 2003).

3.2.3 Activated SGK3 increases signalling to cell growth

After confirming stable over-expression of all SGK3 mutants in both HOSE and BJ-hTERT cell lines, the next step was to determine the effect of enforced SGK3 expression on key components of the PI3-K/mTORC1 growth signalling pathway using our validated epithelial and fibroblast cell lines **(Figure 3.6)**. In addition, to further investigate the extent to which SGK3 growth signalling is affected following the inhibition of mTOR, rapamycin, a well-characterised mTORC1 inhibitor was used, in order to provide a more thorough understanding of the mechanism behind any potential signalling to growth via SGK3.

3.2.3.1 SGK3 signalling in HOSE cells

HOSE cells exhibiting stable expression of SGK3 WT and SGK3 CA were treated according to Chapter 2.12, and harvested for western blot analysis according to Chapter 2.5. Signalling analysis was conducted using phospho and total antibodies against several key components of the PI3-K/mTORC1 cell growth pathway, including AKT, TSC2, PRAS40, ribosomal protein S6 and 4EBP1. A schematic demonstrating the established PI3-K/AKT/mTORC1 growth signalling pathway is shown in **Figure 3.6**, where the antibodies used for analysis are coloured in solid green.

AKT- Changes in activated AKT were analysed using an antibody directed towards Ser 473, a crucial AKT activation site regulated via growth factor induced phosphorylation. As expected activated AKT was expressed in all cells treated with serum, and inhibition of mTORC1 with rapamycin treatment did not affect this activation. There were no observable differences in phospho Ser 473 or total AKT protein levels HOSE cells over-expressing SGK3 CA and SGK WT **(Figure 3.7, Lane 11 and 12)** when compared to pMIG control cells (**Figure 3.7, Lane 3 and 4)**. These data suggest that any downstream changes seen in growth signalling in the SGK3 mutant cell lines are unlikely to be due to SGK3 mediated changes in AKT levels or activation.

Figure 3.4: Protein expression in SGK3 mutant stable BJ-hTERT cells

Exponentially growing BJ-hTERT cells stably transduced with empty vector pMIG, SGK3 WT and SGK3 CA, SGK3 CA PX and SGK3 KD were harvested for protein, and 20μg of protein was separated using 10% SDS-PAGE gels. Expression of proteins was determined by western blot analysis using total anti-SGK3 antibody (60kDa) (ProteinTech Group) and anti-Myc-tag antibody (60kDa). Membranes were stripped and reprobed with the house keeping protein anti-tubulin antibody.

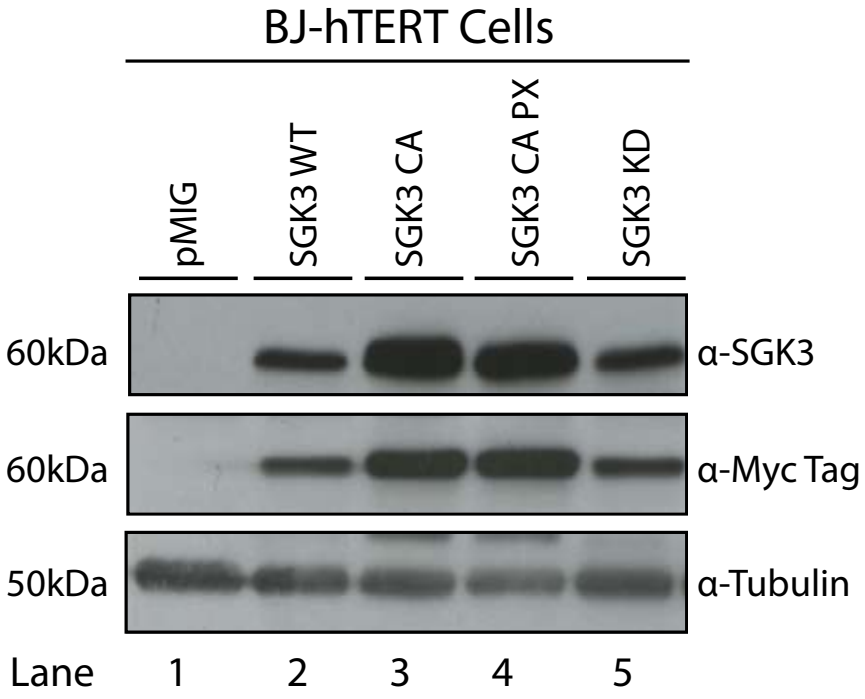
BJ-hTERT Cells
pMIG
SGK3 WT
SGK3 CA
SGK3 CA PX
SGK3 KD
60kDa
α-SGK3
60kDa
α-Myc Tag
50kDa
α-Tubulin
Lane
1
2
3
4
5

Figure 3.5: SGK3 mutant localisation in BJ-hTERT cells

BJ-hTERT cells exhibiting stable protein expression of pMIG empty vector, SGK3 WT, SGK3 CA, SGK3 CA PX and SGK3 KD were plated at 0.1 x 10^4 in a 12 well plate onto glass coverslips, then fixed and permeabilised for immunofluorescence staining following 48 hr incubation. **(A)** Fixed and permeabilised cells were incubated with primary antibody against the myc-tag epitope and secondary antibody conjugated to Alexa fluor 594. Early endosomes were detected using a primary antibody directed against EEA1 and a secondary antibody coupled to Alexa fluor 647. GFP expression was detected as all vectors contain GFP cassette. Cell nuclei were stained with DAPI. **(B), (C) and (D)** Particular sections of Figure 3.5 (A) enlarged in order to more easily view co-localisation of SGK3 WT and mutants with EEA1.

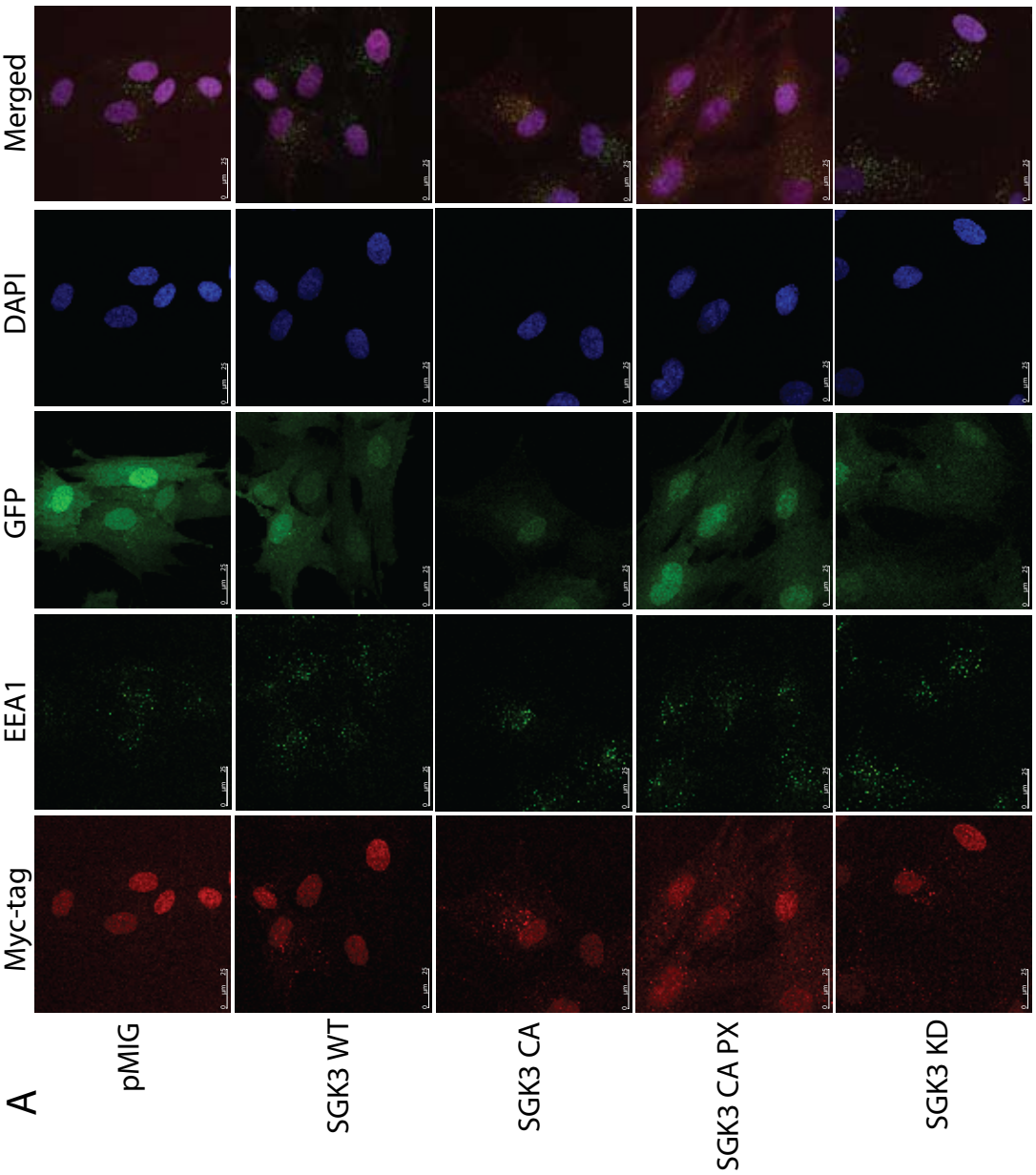
A
pMIG
SGK3 WT
SGK3 CA
SGK3 CA PX
SGK3 KD
Myc-tag
EEA1
GFP
DAPI
Merged

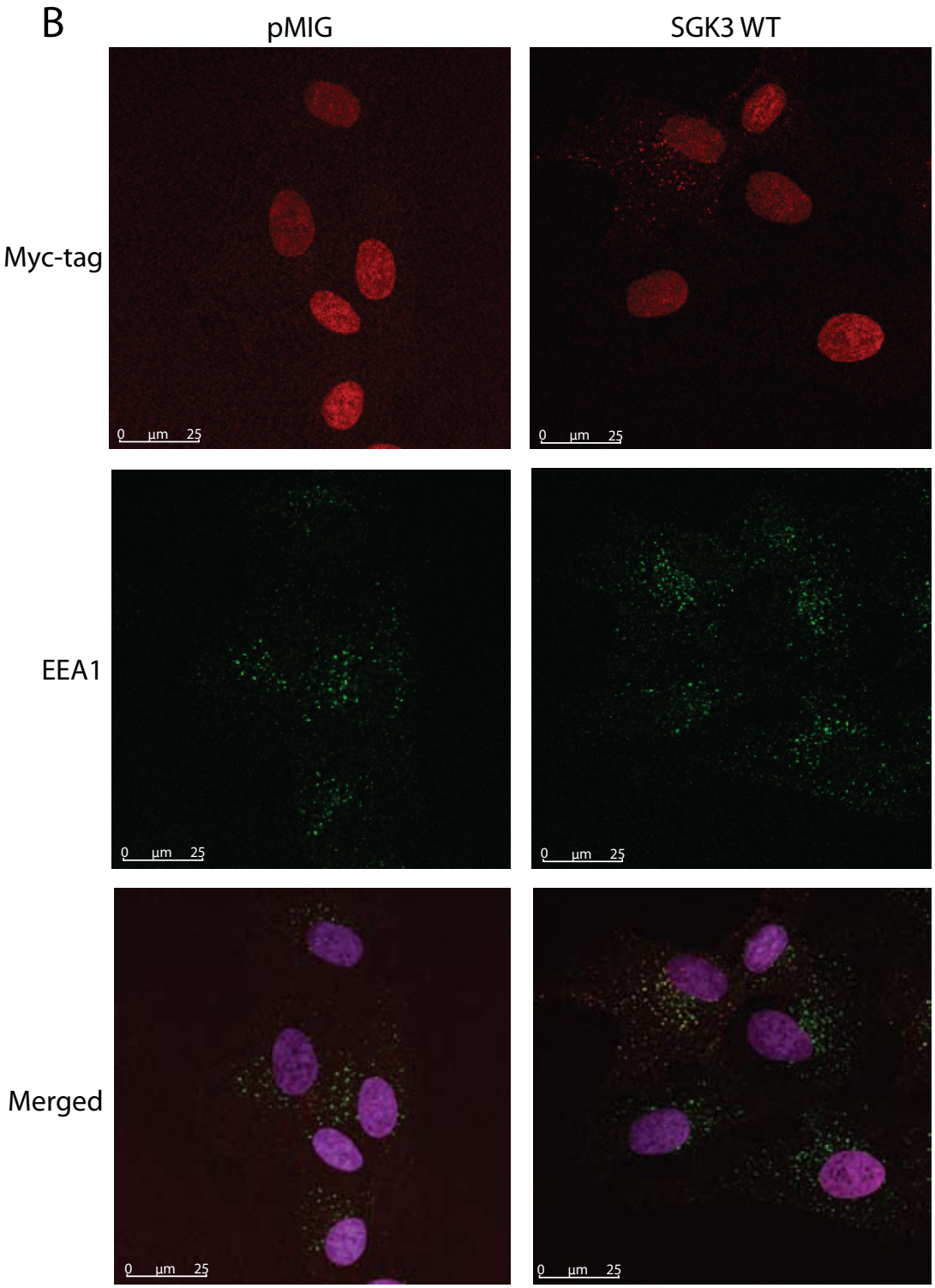
B
pMIG
SGK3 WT
Myc-tag
EEA1
Merged
0 µm 25
0 µm 25
0 µm 25
0 µm 25
0 µm 25
0 µm 25

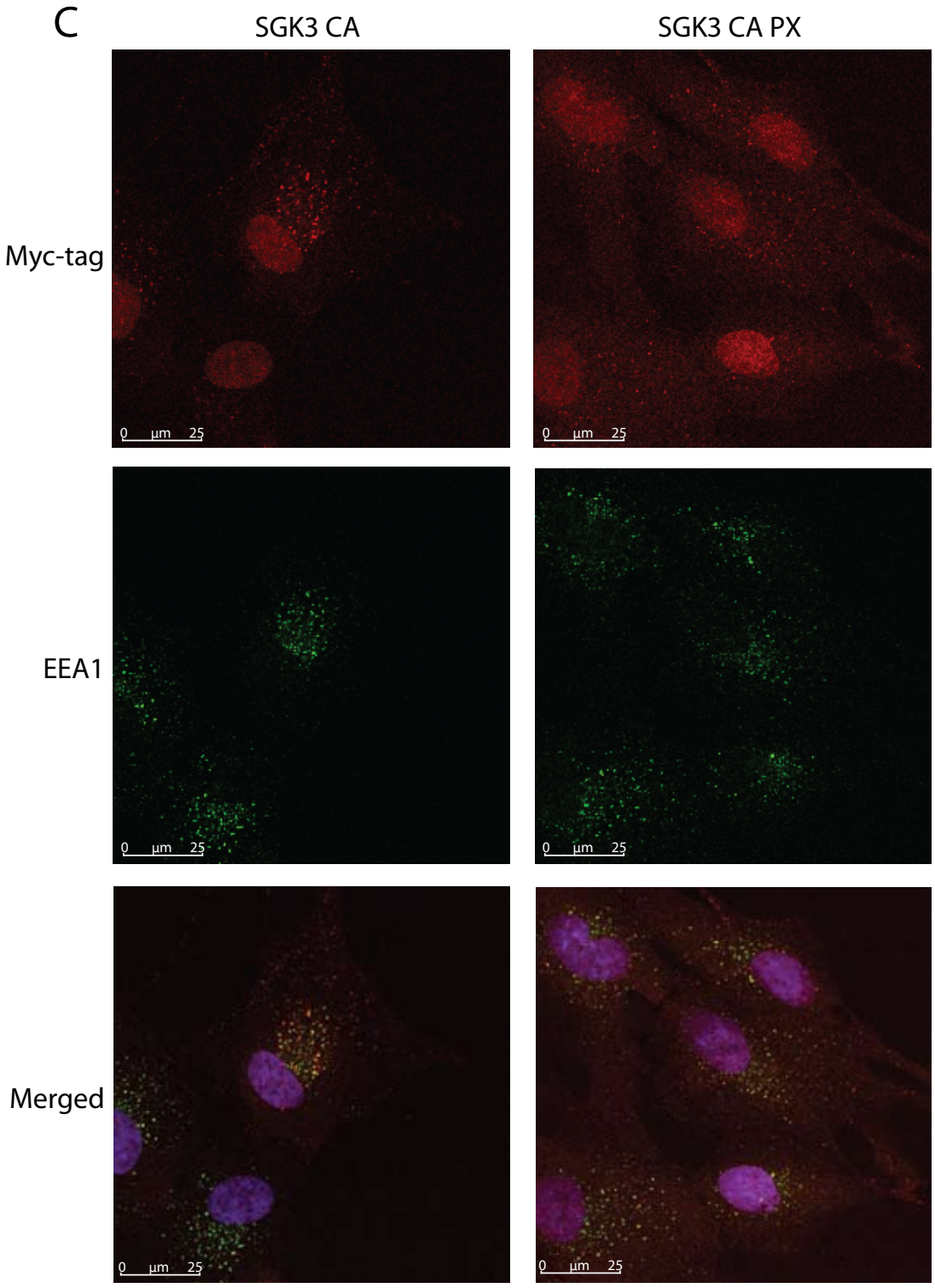
C
SGK3 CA
SGK3 CA PX
Myc-tag
EEA1
Merged
0 µm 25

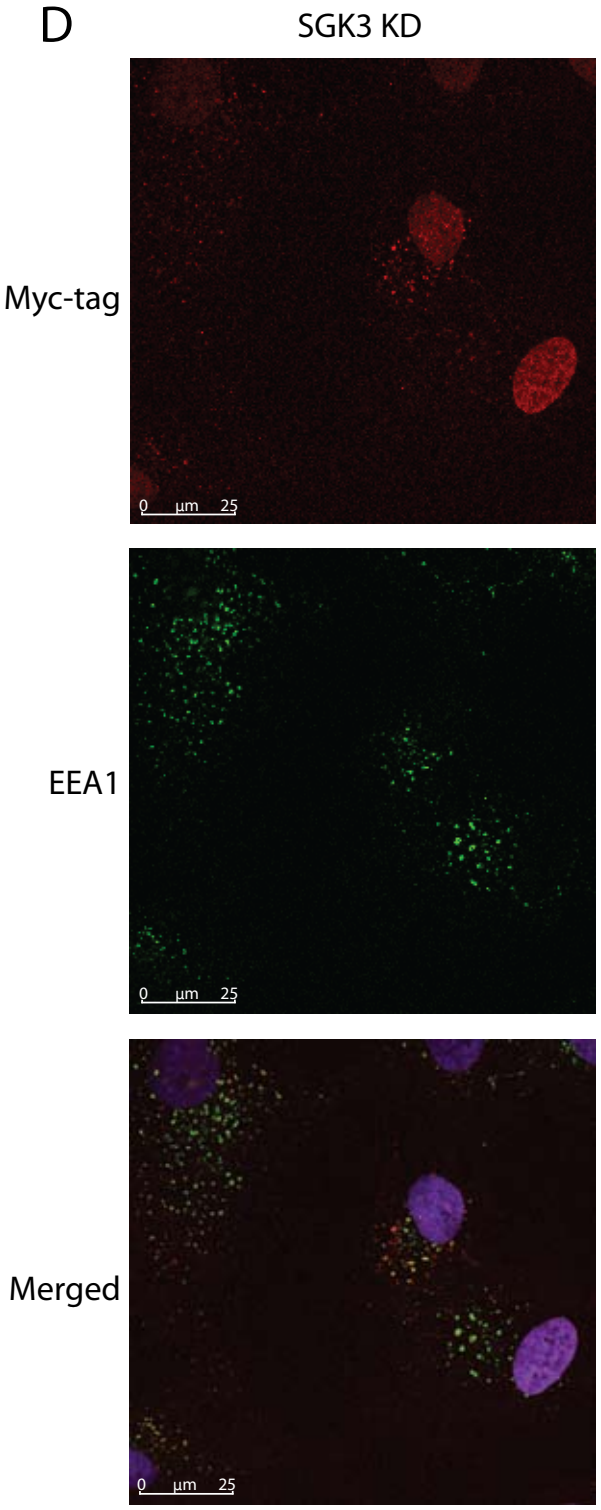
D
SGK3 KD
Myc-tag
EEA1
Merged
0 µm 25
0 µm 25
0 µm 25

TSC2- We next investigated SGK3-mediated TSC2 signalling. TSC2 is a critical modulator of mTORC1, via its ability to form a complex with TSC1 and inhibit mTORC1 activity. Growth factor signalling stimulates the phosphorylation of TSC2 by both AKT and ERK at multiple residues, leading to the dissociation of TSC2 from TSC1, thereby allowing the activation of mTORC1 through Rheb. Our studies demonstrate that over-expression of SGK3 WT and SGK3 CA in serum starved HOSE cells stimulated levels of phosphorylated TSC2 to a similar extent as control serum treated cells **(Figure 3.7)**. As expected the inhibition of mTORC1 by rapamycin had no effect on phospho-TSC2 levels. Furthermore, total levels of expression for TSC2 show no changes between cell lines and treatments. Taken together, these results suggest that TSC2 is either directly or indirectly modulated by SGK3 signalling.

PRAS40- PRAS40 is also able to negatively regulate mTORC1 activity through phosphorylation. Similar to TSC2, SGK3 WT and SGK3 CA robustly activated pPRAS40 (Thr 246) in the HOSE cells, and the level of activation was greater than vector cells with serum **(Figure 3.7)**. Inhibition of mTORC1 with rapamycin increased levels of phosphorylated PRAS40 in both control, SGK WT and SGK3 CA HOSE cells under serum free conditions. These data indicate that inhibition of mTORC1 results in an increase in signalling to PRAS-40, perhaps due to inhibition of a negative feedback mechanism that is known to exist in this pathway (Haruta et al. 2000). Total levels of expression for PRAS40 show no obvious changes between cell lines and treatments.

RPS6- A key readout of mTORC1 activity and an integral member of the growth pathway is ribosomal protein S6 (RPS6). RPS6 is activated by S6K1 mediated phosphorylation and results in increased translation of 5' oligopyrimidine tract (5'TOP) mRNAs consisting mainly of ribosomal proteins and other elements required for translation. RPS6 activity is downstream of mTORC1 and is potently inhibited in most cell systems by treatment with rapamycin. As such then activation status of phospho RPS6 may possibly distinguish between the ability of SGK3 to regulate growth in an mTORC1 independent or dependent manner. Under serum free conditions, HOSE cells stably over-expressing either SGK3 WT or SGK3 CA displayed increased phosphorylation of RPS6 at residues Ser240 and Ser244, and when treated with rapamycin these levels were robustly decreased, indicating that SGK3 likely signals to S6K via mTORC1 **(Figure 3.7)**. There are no changes evident in total RPS6 levels between any of the HOSE cell lines.

4EBP1- Phosphorylation of 4EBP1 by mTORC1 results in the release of eukaryotic initiation factor 4E (eIF4E), allowing the formation of a functional initiation complex with eukaryotic initiation factor 4G (eIF4G). This complex increases the translation initiation of mRNAs with highly structured 5' untranslated regions (UTR), which, include several proteins required for cell cycle progression and ribosome biogenesis. There are four sites within 4EBP1 that all require phosphorylation for complete activation and complex formation. All sites are phosphorylated in a hierarchical manner, with priming site Thr

Figure 3.6: PI3-K/AKT/mTORC1 growth signalling pathway

Schematic showing signalling via PI3-K/AKT/mTORC1 pathway, where proteins coloured in solid green are the SGK3-mediated growth signalling proteins examined by western blotting. Note that arrows denote positive regulation, while lines with dashes denote negative regulation. Briefly, activation of Class I PI3-K by receptor tyrosine kinases (RTK) leads to phosphorylation of PDK1 and in turn phosphorylation and activation of AKT. Additionally, AKT is also phosphorylated by mTORC2 for full activation. AKT through phosphorylation and thus inhibition of TSC2 and PRAS40 leads to activation of mTORC1, an important convergence point for nutrient and growth factor signalling. mTORC1 complex regulates cell growth by increasing the activity of S6K1 via direct phosphorylation, and eIF4e via phosphorylation and inhibition of 4EBP1, leading to increased rates of rDNA transcription, ribosome biogenesis, protein synthesis and cell growth.

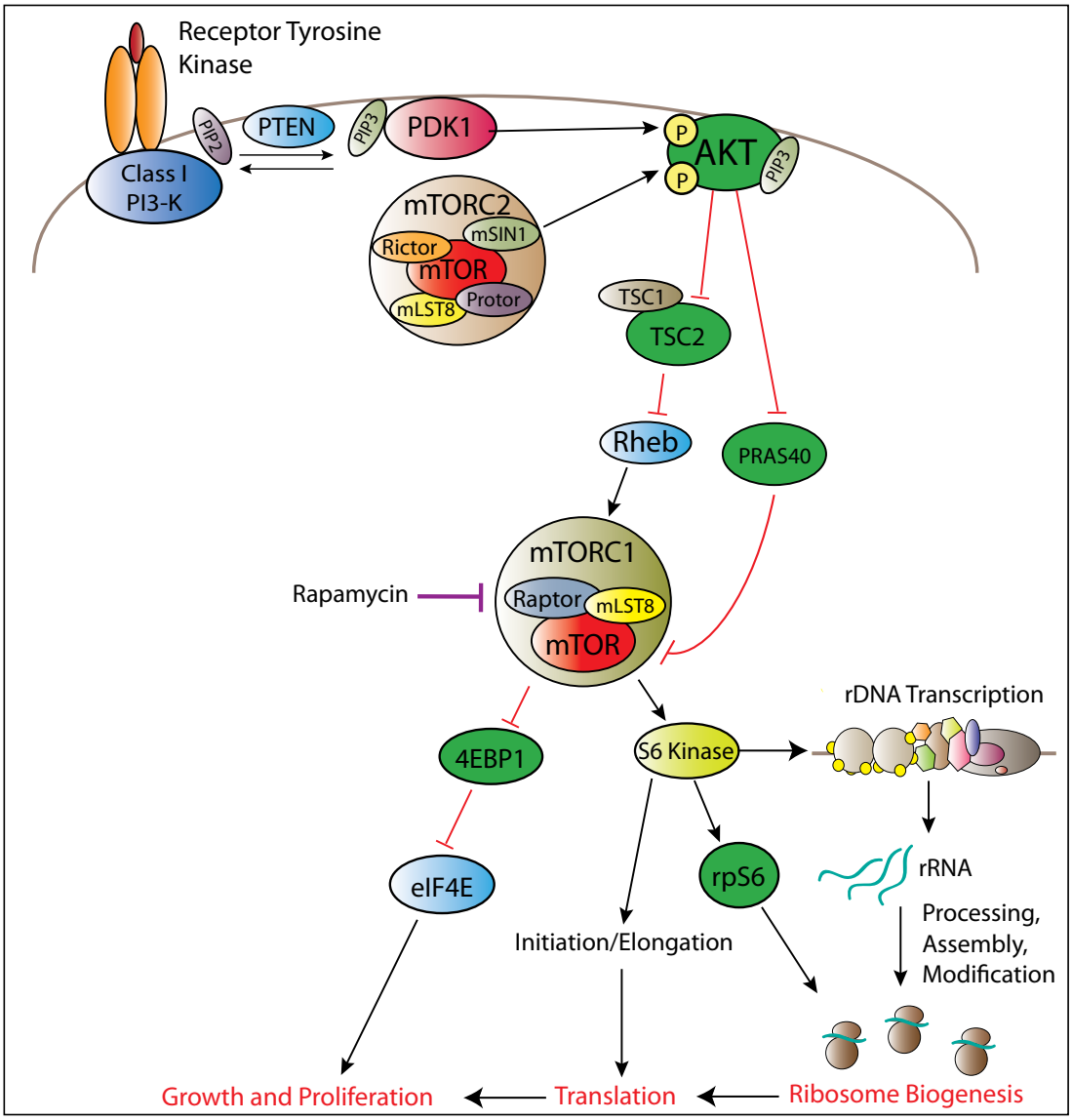
Receptor Tyrosine Kinase
Class I PI3-K
PIP2
PTEN
PIP3
PDK1
P
AKT
P
PIP3
mTORC2
Rictor
mSIN1
mTOR
mLST8
Protor
TSC1
TSC2
Rheb
PRAS40
mTORC1
Rapamycin
Raptor
mLST8
mTOR
rDNA Transcription
4EBP1
S6 Kinase
eIF4E
rpS6
rRNA
Processing, Assembly, Modification
Initiation/Elongation
Growth and Proliferation
Translation
Ribosome Biogenesis

Figure 3.7: SGK3 increases signalling to cell growth in HOSE cells

HOSE cells exhibiting stable expression of pMIG empty vector, SGK3 WT and SGK3 CA were plated at 1 x 10^6 in 150mm plates and at approximately 70% confluency were serum starved for 48 hr. Cells were then treated with either ± 20nM rapamycin or ± 15% FBS, or both for 30 min and then harvested for protein extracts. 50μg of protein was separated by either 6%, 10% or 15% SDS-PAGE gels depending on protein size (see Table 2.3) and expression of proteins determined by western analysis using indicated antibodies. All blots were not probed more than twice. Western blots representative of n=1-2.

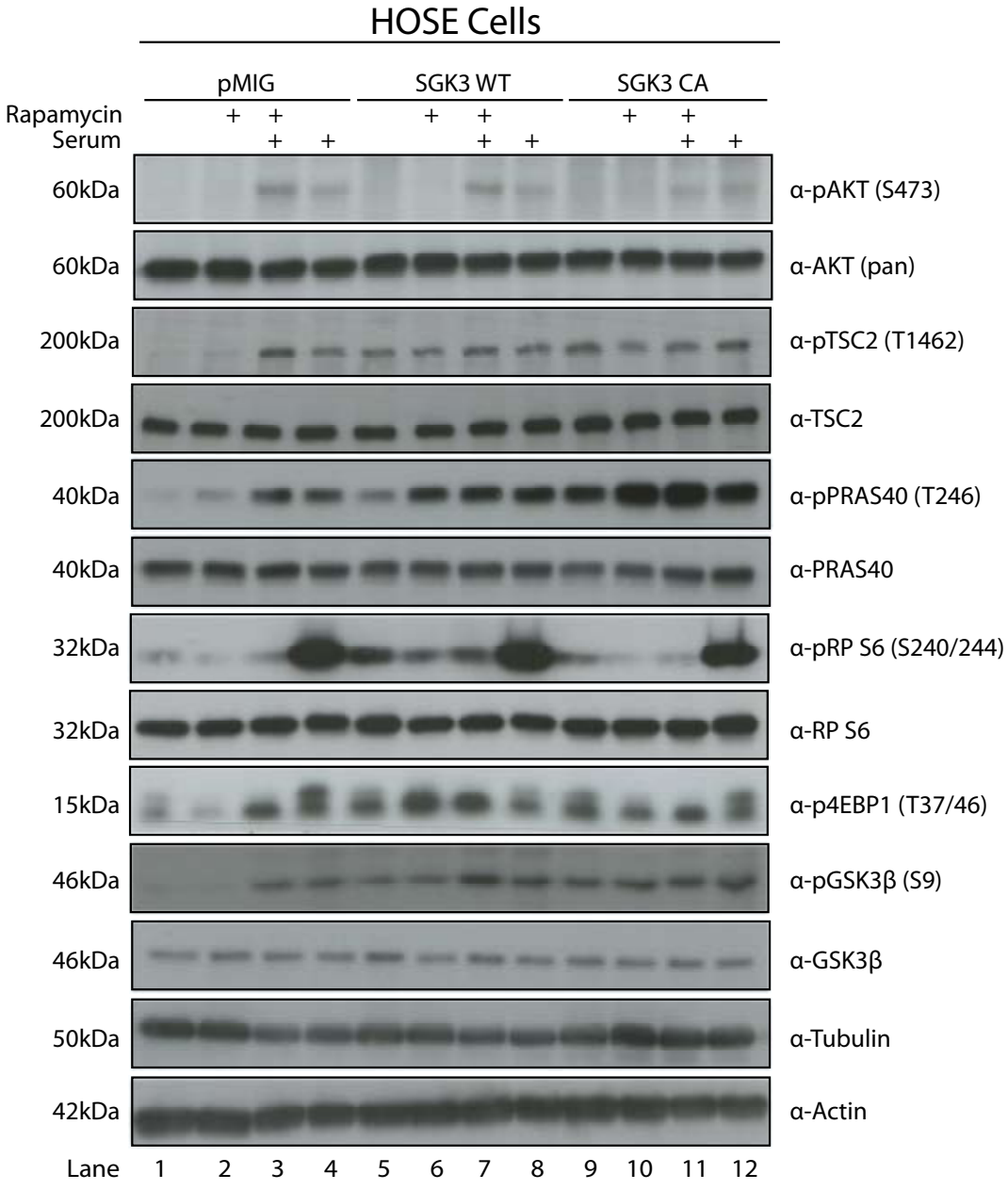
HOSE Cells
pMIG
SGK3 WT
SGK3 CA
Rapamycin
Serum
60kDa
α-pAKT (S473)
60kDa
α-AKT (pan)
200kDa
α-pTSC2 (T1462)
200kDa
α-TSC2
40kDa
α-pPRAS40 (T246)
40kDa
α-PRAS40
32kDa
α-pRP S6 (S240/244)
32kDa
α-RP S6
15kDa
α-p4EBP1 (T37/46)
46kDa
α-pGSK3β (S9)
46kDa
α-GSK3β
50kDa
α-Tubulin
42kDa
α-Actin
Lane 1 2 3 4 5 6 7 8 9 10 11 12

37/Thr 46 phosphorylated initially, followed by phosphorylation of Thr 70/Ser 65. To assess if SGK3 plays a role in modulating important mediators of cell growth, 4EBP1 signalling, a key readout of mTORC1 activity was investigated using the HOSE stable cell lines. To determine 4EBP1 activity a phospho-specific antibody directed against the 4EBP1 Thr 37/46 site, which is thought to be the priming site for subsequent phosphorylation at Thr 70 and Ser 65 was used. Multiple phosphorylation states of 4EBP1 are detected using this particular antibody through the identification of different electrophoretic motilities at 15-20 kDa, with the slower migrating band representing maximal activation of 4EBP1. Both SGK3 WT and SGK3 CA cells displayed a marked increase in 4EBP1 activity compared with pMIG control cells under serum starved conditions, and treatment with rapamycin reduced phosphorylation of Thr 70 and Ser 65 (upper band) **(Figure 3.7)**. Together, these data demonstrate that SGK3 signalling to mTORC1 also can regulate cell growth via 4EBP1.

GSK3β- SGK3 has demonstrated involvement in GSK3β signalling through phosphorylating and negatively regulating GSK3β, thereby preventing it from inhibiting its cell cycle target cyclin D1 (Kobayashi and Cohen 1999; Dai et al. 2002). GSK3β is involved in formation of adherens junctions and tight junction sealing in mammary epithelial tumour cells following inactivation by SGK3 (Failor et al. 2007). In HOSE cells SGK3 WT and SGK3 CA, increased levels of activated GSK3β compared with control vector pMIG cells **(Figure 3.7)**. The increase in phosphorylated GSK3β induced by SGK3 CA was similar to that induced by serum. Inhibition of mTOR did not affect GSK3β activity, demonstrating that activation of GSK3β by SGK3 is not downstream of mTORC1. Levels of total GSK3β do not differ between cell lines or treatment conditions. Importantly, total levels of the housekeeping proteins tubulin and β-actin do not change between cell lines or treatment conditions. Taken together these results suggest that consistent with previous reports, SGK3 is able to increase GSK3β phosphorylation, independently of mTOR.

3.2.3.2 SGK3 signalling in BJ-hTERT cells

A similar pattern of signalling through critical members of the growth pathway was also observed in BJ-hTERT cells **(Figure 3.8)**, however the additional mutants introduced into this cell line allowed further characterisation of SGK3 signalling in growth, with a particular focus on SGK3 localisation as a requirement for optimal functionality. BJ-hTERT cells exhibiting stable expression of SGK3 WT, SGK3 CA, SGK3 CA PX and SGK3 KD were treated according to Chapter 2.12, and harvested for western blot analysis according to Chapter 2.5. Signalling analysis was conducted using phospho and total antibodies as described in Chapter 3.2.3.1.

In BJ-hTERT pMIG vector control cells and all BJ-hTERT SGK3 mutant cell lines, activated AKT (S473) was only detected in the presence of serum, and levels of total AKT did not change between any of the cell lines **(Figure 3.8)**. Furthermore, under serum-starved conditions, levels of activated TSC2 (Thr 1462 phosphorylation)

and PRAS40 activity (Thr 246 phosphorylation) were increased by SGK3 CA and SGK3 CA PX but not SGK3 KD cells when compared to pMIG vector control cells. Moreover, consistent with HOSE studies, and as expected, treatment with rapamycin had no effect on the phosphorylation levels of either TSC2 or PRAS40. Levels of total TSC2 remained similar between all cell lines and treatment conditions. Under serum starvation RPS6 phosphorylation was still detectable, and this was increased in all SGK3 transduced cells, particularly SGK3 CA**.** Treatment with rapamycin reduced SGK3 dependent activation of phospho-RPS6 back to that of control levels, demonstrating that the effect of SGK3 was likely via mTORC1. Levels of total RPS6 remained similar between all cell lines and treatment conditions.

All SGK3 mutant lines, with the exception of SGK3 KD, increased the levels of activated 4EBP1 (Thr 37/46) under serum-starved conditions, when compared with pMIG vector control cells. Furthermore, treatment with rapamycin did not reduce levels of activated 4EBP1 in SGK3 CA and SGK3 CA PX cells. SGK3 WT modestly increased, while SGK3 CA and SGK3 CA PX robustly activated GSK3β (Ser 9) in serum starved cells. Total levels of GSK3β did not change between cell lines and treatment conditions. In addition total levels of housekeeping proteins adaptin, actin and tubulin also exhibited no change between cell lines and treatment conditions, indicating consistency in protein loading. (Due to the different mobilities of signalling molecules studied, three different housekeeping proteins of different mobilities were used). These results demonstrate that activated SGK3 is able to activate signalling through the growth pathway in both epithelial and fibroblast cell lines. SGK3 increased phosphorylation of both TSC2 and PRAS40 upstream of mTOR, leading to the rapamycin sensitive activation of key mTORC1 effectors rpS6 and 4EBP1. These data also demonstrate that SGK3 is also able to increase phosphorylation of GSK3β in a rapamycin insensitive manner.

3.2.4 Activated SGK3 increases cell proliferation in non-tumourigenic ovarian epithelial cells

Following analysis of SGK3 growth signalling, the effects of SGK3 on cell proliferation were examined. Cells were plated at low density and harvested at multiple time points to determine the influence that each SGK3 mutant has on cell proliferation rates (Chapter 2.14). Introduction of both SGK3 WT and SGK3 CA into the HOSE cells resulted in a significant increase in proliferation rates compared with pMIG vector control cells. Cell doubling times for SGK3 WT and SGK3 CA were 37 hr and 34 hr respectively, compared with 51 hr for pMIG vector control cells **(Figure 3.9 A)**. The difference in proliferation rates of the HOSE SGK3 cell lines was further investigated through collection, fixing and propidium iodide staining of exponentially growing cells, followed by flow cytometer analysis to determine percentage of cells in each phase of the cell cycle phase. An increase in the population of cells in S phase in both the SGK3 WT (49%) and SGK3 CA (46%) cell lines compared with pMIG vector control cells (27%), along with a decrease of SGK3 WT (23%) and SGK3 CA (36%) cells in G1 compared with pMIG control cells (54%) **(Figure 3.9 B)** was observed. These data suggest that over-expression of SGK3 is able to drive cells through the G1/S transition point of the cell cycle.

Figure 3.8: Activated SGK3 increases signalling to cell growth in BJ-hTERT cells

BJ-hTERT cells exhibiting stable expression of pMIG empty vector, SGK3 WT, SGK3 CA, SGK3 CA PX and SGK3 KD were plated at 1 x 10^6 in 150mm plates and at approximately 70% confluency were serum starved for 48 hr. Cells were treated with either ± 20nM rapamycin or ± 15% FBS or both for 30 min and then harvested for protein extracts. 50μg of protein was separated by either 6%, 10% or 15% SDS-PAGE gels depending on protein size (see Table 2.3) and expression of proteins determined by western analysis using indicated antibodies. Different gels are separated using a black line. Each separate gel has been run with a densitometry control (20μg of HOSE-SGK3 CA lysate) to allow comparisons to be made between gels. All blots were not probed more than twice. Western blots representative of n=1-2.

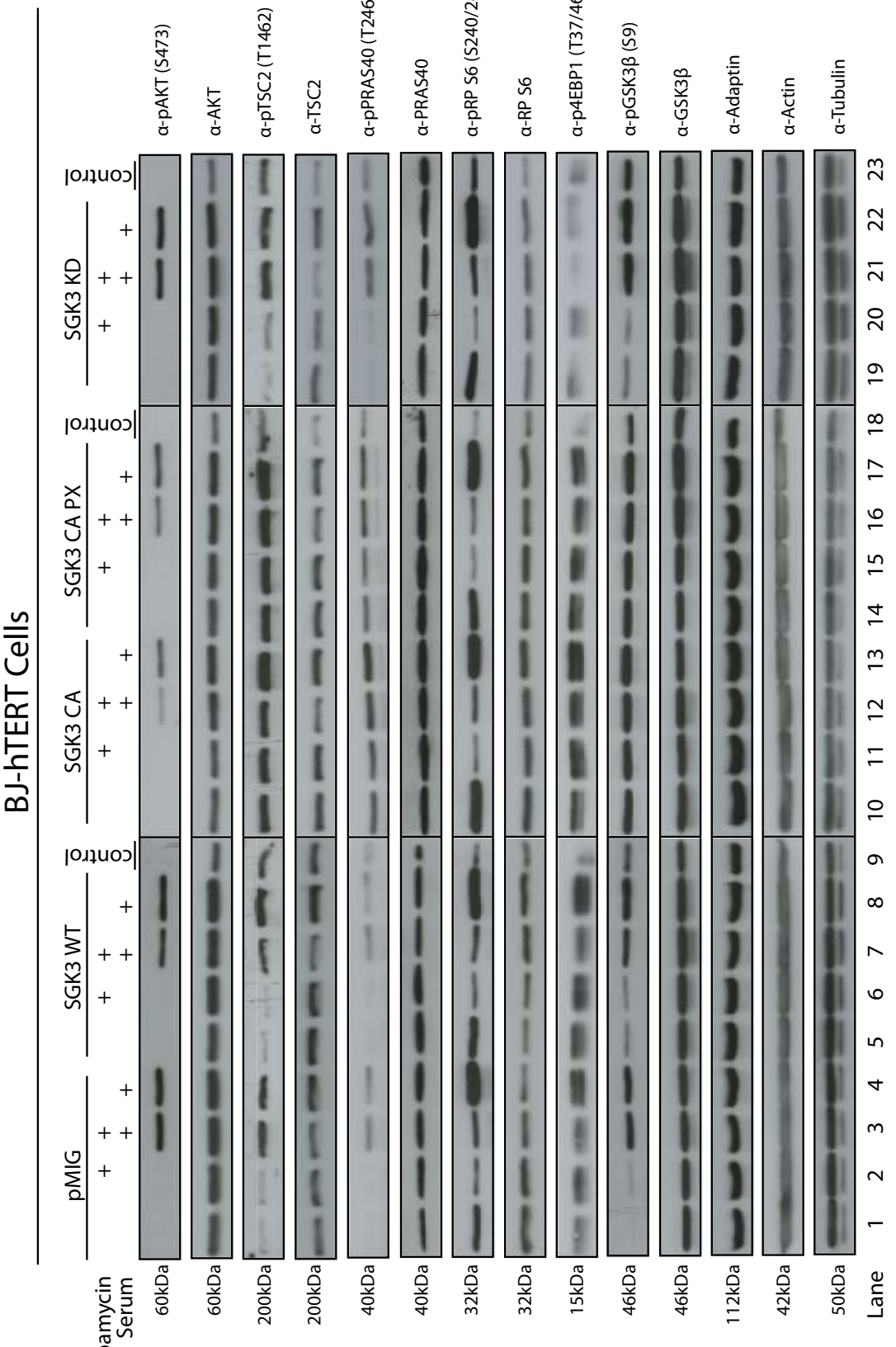
BJ-hTERT Cells
pMIG
SGK3 WT
SGK3 CA
SGK3 CA PX
SGK3 KD
Control
Rapamycin
Serum
α-pAKT (S473)
α-AKT
α-pTSC2 (T1462)
α-TSC2
α-pPRAS40 (T246)
α-PRAS40
α-pRP S6 (S240/244)
α-RP S6
α-p4EBP1 (T37/46)
α-pGSK3β (S9)
α-GSK3β
α-Adaptin
α-Actin
α-Tubulin
60kDa
60kDa
200kDa
200kDa
40kDa
40kDa
32kDa
32kDa
15kDa
46kDa
46kDa
112kDa
42kDa
50kDa
Lane
1 2 3 4 5 6 7 8 9 10 11 12 13 14 15 16 17 18 19 20 21 22 23

3.2.5 Activated SGK3 does not increase cell proliferation in non-tumourigenic foreskin fibroblast cells

In contrast to HOSE cells, BJ-hTERT cell lines expressing SGK3 CA, SGK3 CA PX and SGK3 KD did not show any marked differences in proliferation rates between the SGK3 mutants and pMIG vector control cells, with doubling times remaining similar between all BJ-hTERT cell lines, with pMIG at 34.7 hr, SGK3 CA at 36.2 hr, SGK3 CA PX at 32.4 hr and SGK3 KD at 35.9 hr **(Figure 3.10 A)**. Cell cycle phase distribution analysis of exponentially growing BJ-hTERT cells also determined that the majority of cells from pMIG (66.9%), SGK3 CA (68.9%), SGK3 CA PX (70%) and SGK3 KD (72.6%) were in G1 phase, with fewer cells from pMIG (25.9%), SGK3 CA (24.7%), SGK3 CA PX (25.9%) and SGK3 KD (20.5%) in S phase **(Figure 3.10 B)**, demonstrating that in the BJ-hTERT cell lines over-expression expression of SGK3 is unable to increase cell proliferation rates.

3.2.6 Activated SGK3 increases cell size and key parameters of cell growth

During proliferation analysis of both HOSE and BJ-hTERT cell lines, data on cell volume was collected and used as an initial read out for cell size. The 48 hr harvest point was chosen to investigate possible differences in steady state cell size as all cell lines maintained an exponential phase of growth at this time point, removing the possible complicating effects of confluency on cell size. In the HOSE cell lines, SGK3 CA cells exhibited a significantly larger cell size when compared to both pMIG vector control cells and SGK3 WT cells **(Figure 3.11 A)**, despite the fact that SGK3 WT cells and SGK3 CA cells have a similar doubling time and cell cycle profile. These data suggest that SGK3 WT is able to increase both cell growth and proliferation to an equal extent, whereas SGK3 CA is able to disproportionately increase cell growth when compared with proliferation. The latter likely suggests that growth and proliferation has become uncoupled in the HOSE SGK3 CA cells. Furthermore, in the BJ-hTERT cells, exponentially growing SGK3 CA cells, but not the SGK3 CA PX or SGK3 KD mutant cell lines displayed a larger cell size when compared to the pMIG control cells, but this did not reach statistical significance **(Figure 3.11 B)**. Taken together studies using both HOSE and BJ-hTERT cells suggest that activated SGK3 is able to preferentially increase cell size, and can trigger cell growth and proliferation to become uncoupled. Furthermore, studies using the SGK3 CA PX mutant in the BJ-hTERT cells demonstrate that SGK3 endosomal localisation is likely required for optimal SGK3 activity on cell growth.

To further investigate the mechanism by which SGK3 is able to regulate cell growth processes, we next examined if other key functional readouts of cell growth were also altered in the HOSE and BJ-hTERT cell lines. As previously described, cell growth is defined as an increase in macromolecules, which include RNA, protein and lipids which together lead to an increase in cell mass. However, cell size can also be influenced osmotically through the regulation of ion channels. Therefore, to distinguish

between these two possibilities we examined the ability of SGK3 to modulate the cellular abundance of total RNA (protein translation capacity) and protein per cell (translation activity). Furthermore, all experiments carried out on HOSE and BJ-hTERT cells to determine changes in both RNA and protein per cell were performed using cells deprived of growth factors in order to further understand if SGK3 is sufficient to drive these processes in the absence of growth factors. All cells were plated at low density and serum starved for 48 hr prior to harvesting for total RNA and protein. In addition, while collecting samples to determine total RNA and protein levels, cell size was analysed again to determine if SGK3 was able to increase cell size even in the absence of growth factors.

In HOSE cells with enforced expression of SGK3 CA, the abundance of total RNA per cell was significantly greater than in the pMIG vector control cells **(Figure 3.12 A)**. Consistent with this, HOSE cells stably expressing SGK3 CA also displayed a significantly increased amount of protein per cell compared with both pMIG control cells **(Figure 3.12 B)**. Similarly, SGK3 CA cells also displayed a significantly larger cell size under growth factor deprived conditions compared with pMIG control cells and SGK3 WT cells **(Figure 3.12 C)**. In the BJ-hTERT cells, total cellular RNA content in SGK3 CA cells was significantly increased compared to pMIG control cells. Neither the SGK3 CA PX nor the SGK3 KD exhibited significant differences in RNA content, although there was a trend towards an increase for the SGK3 CA PX **(Figure 3.13 A)**. Consistent with these data, cellular protein content was also significantly higher in the SGK3 CA and SGK3 CA PX cells compared with pMIG control **(Figure 3.13 B)**. Analysis of cell size demonstrated that even under serum starved conditions both SGK3 CA and SGK3 CA PX are able to significantly increase basal cell size compared to pMIG control cells and SGK3 KD cells **(Figure 3.13 C)**. Taken together, studies in both the HOSE and BJ-hTERT cells demonstrate that increase in cell size conferred by the enforced expression of activated SGK3 is due to an increase in macromolecular content, and is likely dependent on endosomal localisation.

3.2.7 Activated SGK3 increases rDNA transcription in epithelial and fibroblast cell lines

Having observed a marked increase in the activity of key components of PI3-K/mTORC1 growth signalling (Chapter 3.2.3), in addition to an increase in parameters of cell growth/size in cells stably expressing activated SGK3 (Chapter 3.2.6), the effect of enforced expression of SGK3 on ribosome biogenesis was investigated next. As described in Chapter 1, a major rate-limiting step for ribosome biogenesis is rDNA transcription, and thus measuring the levels of rDNA transcription can be used as a robust readout for activation of the ribosome biogenesis pathway. To determine the effects of SGK3 on rDNA transcription, we measured the abundance of the 5' external transcribed spacer (5'ETS) pre-rRNA. rRNA is transcribed by Pol I as 45S precursor, termed pre-rRNA, which is rapidly processed at externally transcribed spacer (ETS) and internally transcribed spacer (ITS) regions to give rise to the mature ribosomal RNAs. Whereas the mature rRNAs have half lives of hr to days, the processed ETS

Figure 3.9: SGK3 increases cell proliferation in HOSE cells

(A) HOSE cells exhibiting stable expression of pMIG empty vector, SGK3 WT and SGK3 CA were plated at 0.2 x 10^5 in 6 well plates using media containing 10% FBS and harvested by trypsinisation approximately 4 hr after plating. Cell number was determined using the Coulter Counter (Beckman Coulter). Cells were then harvested every 24 hr for the next 7 days and cell number analysed. Doubling time of cells was determined using non-linear regression analysis, n=7, ± SEM, * $p < 0.05$. **(B)** HOSE cells exhibiting stable expression of pMIG empty vector, SGK3 WT and SGK3 CA were plated at low density in 6 well plates and harvested by trypsinisation after 48 hr and fixed in 95% ethanol. Cells were prepared for cell cycle analysis using the FACS Canto Flow cytometer (BD Biosciences). Cell cycle phase distribution was analysed using Modfit Software (Verity Software House). n=1.

HOSE Cells

A.

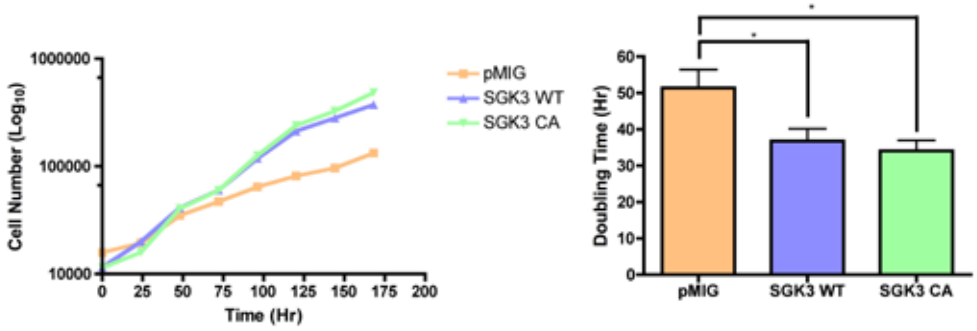

B.

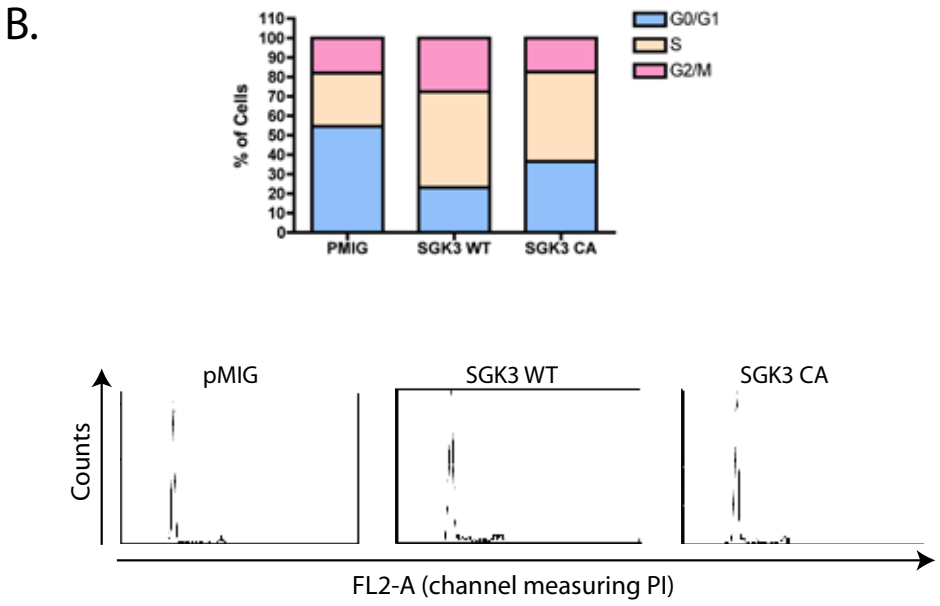

Figure 3.10: SGK3 does not increase cell proliferation in BJ-hTERT cells

(A) BJ-hTERT cells exhibiting stable expression of pMIG empty vector, SGK3 WT, SGK3 CA, SGK3 CA PX and SGK3 KD were plated at 0.2 x 10^5 in 6 well plates using media containing 10% FBS and harvested by trypsinisation approximately 4 hr after plating. Cell number was determined using the Coulter Counter (Beckman Coulter). Cells were then harvested every 24 hr for the next 7 days and cell number analysed. Doubling time of cells was determined using non-linear regression analysis. n=1. **(B)** BJ-hTERT cells exhibiting stable expression of pMIG empty vector, SGK3 WT, SGK3 CA, SGK3 CA PX and SGK3 KD were plated at low density in 6 well plates and harvested by trypsinisation after 48 hr and fixed in 95% ethanol. Cells were prepared for cell cycle analysis using the FACS Canto Flowcytometer (BD Biosciences). Cell cycle phase distribution was analysed using Modfit Software (Verity Software House). n=1.

BJ-hTERT Cells

A.

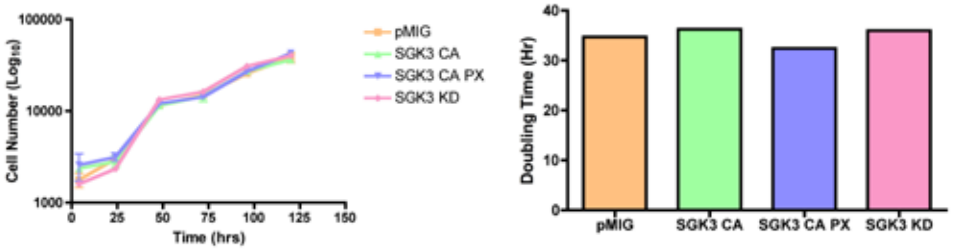

B.

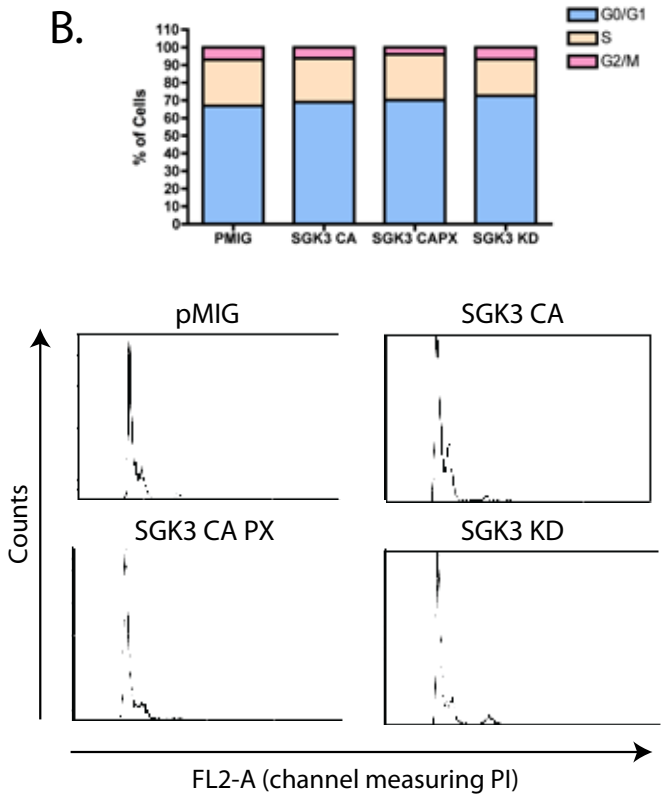

Figure 3.11: Exponentially growing cell size is increased by activated SGK3 in both HOSE and BJ-hTERT cells

(A) HOSE cells exhibiting stable expression of pMIG empty vector, SGK3 WT and SGK3 CA were plated at 0.2 x 10^5 in 6 well plates using media containing 10% FBS and harvested by trypsinisation approximately 4 hr after plating. Cell size was determined by using the Coulter Counter (Beckman Coulter). Cells were then harvested every 24 hr for the next 7 days and cell size analysed. 48 hr time point was chosen for exponential growth cell size analysis n=7, ± SEM. ** $p < 0.01$ * $p < 0.05$. **(B)** BJ-hTERT cells exhibiting stable expression of pMIG empty vector, SGK3 CA, SGK3 CA PX and SGK3 KD were plated at 0.2 x 10^5 in 6 well plates using media containing 10% FBS and harvested by trypsinisation approximately 4 hr after plating. Cell number was determined using the Coulter Counter (Beckman Coulter). Cells were then harvested every 24 hr for the next 7 days and cell size analysed. 48 hr time point was chosen for exponential growth cell size analysis n=1, ± SEM.

HOSE Cells

A.

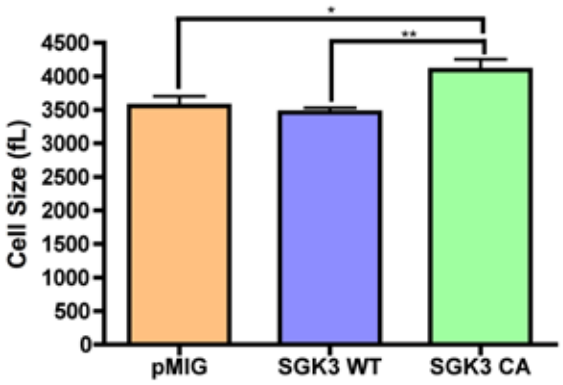

BJ-hTERT Cells

B.

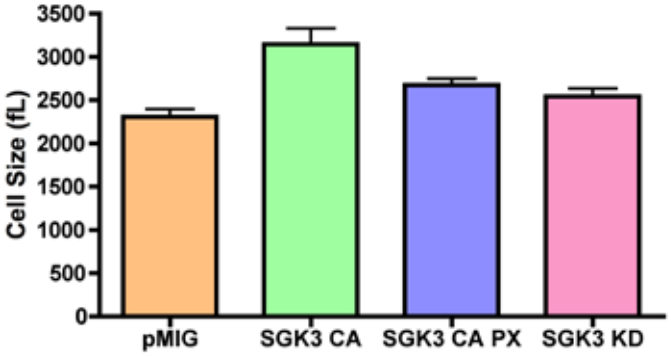

Figure 3.12: Activated SGK3 increases macromolecular content and cell size in HOSE cells

HOSE cells exhibiting stable expression of pMIG empty vector, SGK3 WT and SGK3 CA were plated to analyse various critical parameters of cell growth. **(A)** To determine levels of RNA per cell, cells were plated at low density in 6 well plates and following overnight recovery were serum starved for 48 hr. Cells were then harvested for RNA, and a separate plate was harvested to determine cell number only using the Coulter Counter (Beckman Coulter). RNA concentration was determined using the NanoDrop ND-1000 Spectrophotometer (Thermo Fisher). n=4. ± SEM. * $p < 0.05$. To determine levels of protein per cell and growth factor deprived cell size, cells were plated at low density in 6 well plates and following overnight recovery were serum starved for 48 hr. Cells were then harvested for **(B)** protein. Protein concentration was determined using the DC Assay (Biorad). n=6. ± SEM. ** $p < 0.01$. **(C)** for cell size using trypsinisation. Cell size was determined using the Coulter Counter (Beckman Coulter). n=5. ± SEM. *** $p < 0.001$.

HOSE Cells

A.

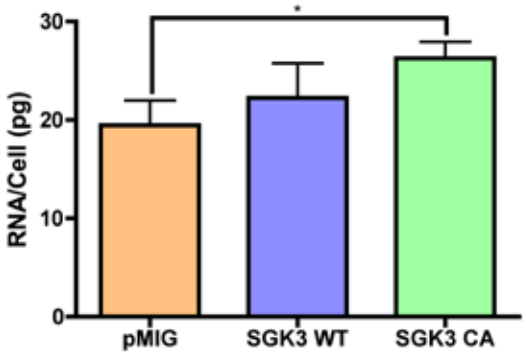

B.

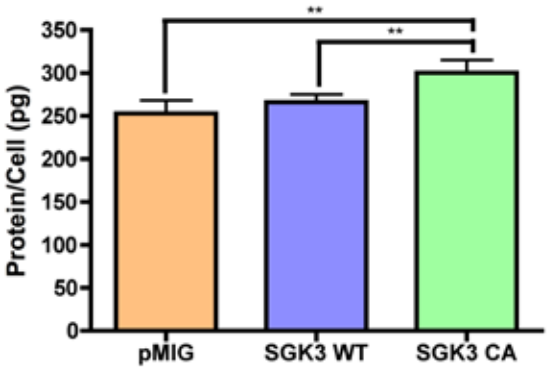

C.

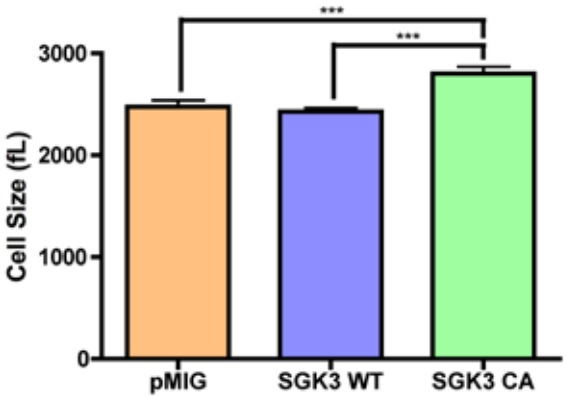

Figure 3.13: Activated SGK3 increases macromolecular content and cell size in BJ-hTERT cells

BJ-hTERT cells exhibiting stable expression of pMIG empty vector, SGK3 CA, SGK3 CA PX and SGK3 KD were plated to analyse various critical parameters of cell growth. **(A)** To determine levels of RNA per cell, cells were plated at 0.15 x 10^6 in 60mm plates and following overnight recovery were serum starved for 48 hr. Cells were then harvested for RNA, and a separate plate was harvested for cell number only using the Coulter Counter (Beckman Coulter). RNA concentration was determined using the NanoDrop ND-1000 Spectrophotometer (Thermo Fisher). To determine levels of protein per cell and growth factor deprived cell size, cells were plated at 0.15 x 10^6 in 60mm plates and following overnight recovery were serum starved for 48 hr. Cells were then harvested **(B)** for protein and protein concentration was determined using the DC Assay (Biorad). **(C)** for cell size using trypsinisation. Cell size was determined using the Coulter Counter (Beckman Coulter). n=4. ± SEM. ** $p < 0.01$, * $p < 0.05$.

BJ-hTERT Cells

A.

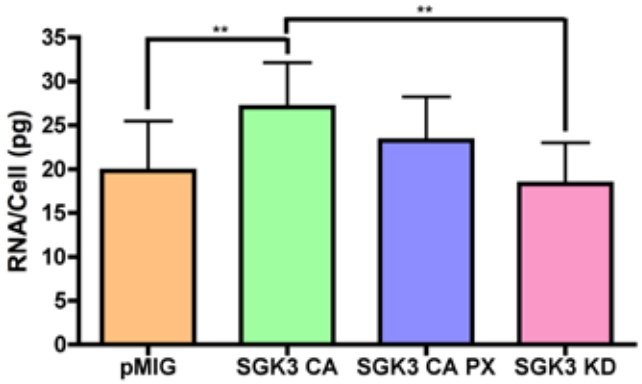

B.

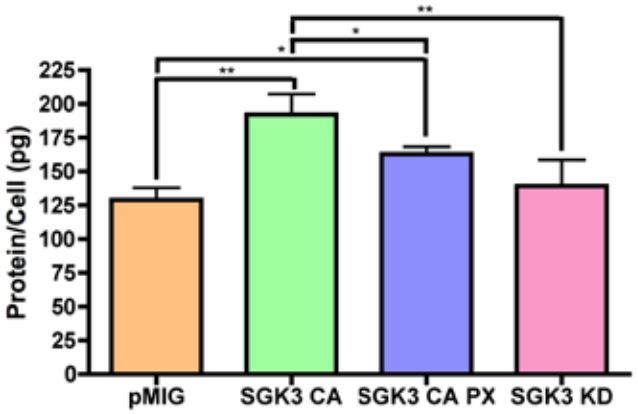

C.

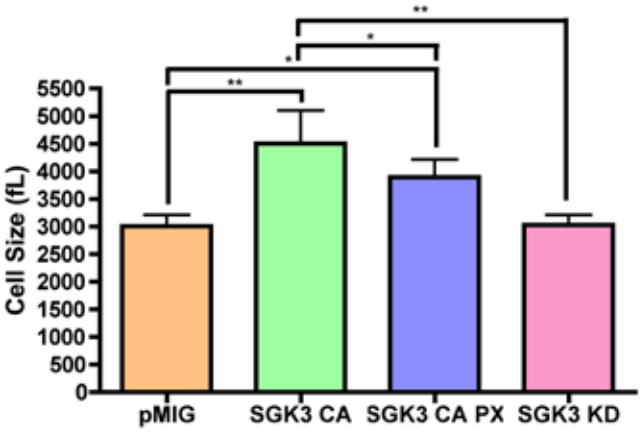

and ITS have half lives of min, and thus their abundance can be used as a measure of rDNA transcription rates (Hannan et al. 2003; Poortinga et al. 2004). The abundance of 5' ETS rRNA was determined using ribonucleic acid protection assay (RPA) with a 32-P labelled antisense riboprobe targeting the 5'ETS of the ribosomal 45S precursor (as described in Chapter 2.8 – 2.11). Furthermore, rapamycin treatment was also used in these experiments to determine the contribution of mTORC1 in SGK3 mediated rDNA transcription (as described in Chapter 2.4).

rDNA transcription experiments were performed on HOSE cells stably expressing SGK3 WT and SGK3 CA according to Chapter 2.8. In the HOSE cells SGK3 CA but not SGK3 WT significantly increased cell size in serum starved and serum refed cells **(Figure 3.14 A).** The increase in cell size was in part dependent on mTORC1 signalling as it was blocked completely by rapamycin in serum-starved cells, and partially repressed in serum refed cells. Strikingly, HOSE SGK3 WT cells were consistently smaller than pMIG control cells, which is consistent with the observation that SGK3 WT was able to decrease the doubling time (i.e. increase the proliferation rate) of HOSE cells, despite having no significant effect on total RNA levels and protein content. Thus, if cells are doubling faster without increased macromolecular synthesis their average population cell size would decrease over time. In contrast, SGK3 CA is able to increase both cell size and doubling rate. These data suggest that growth and proliferation can be uncoupled in these cells. Furthermore, consistent with this, SGK3 CA but not SGK3 WT significantly increased rDNA transcription rates under both serum starved conditions and serum refed conditions compared with pMIG control cells, which was completely inhibited by rapamycin **(Figure 3.14 B).** Together with cell size experiments, these studies demonstrate that SGK3 CA is sufficient to robustly increase ribosome biogenesis and growth in an mTORC1-dependent manner. Furthermore, the ability of SGK3 CA to further increase these parameters in serum refed cells suggests that even under accelerated growth conditions SGK3 activity is limiting for ribosome biogenesis and cell growth.

Similar cell size and rDNA transcription experiments were also carried out on BJ-hTERT cells stably expressing SGK3 WT, SGK3 CA, SGK3 CA PX and SGK3 KD mutant constructs according to Chapter 2.8. Additionally, in order to determine the dependence, if any, of SGK3 signalling on AKT, to modulate rDNA transcription, an AKT inhibitor (AKTi) was utilized in the BJ-hTERT cell lines. The AKT inhibitor targets the PH linker region of the AKT isoforms, and therefore does not affect SGK3 activity. The AKT inhibitor has been previously optimised in our laboratory and used at 5nM which is an IC90 of inhibition of activity, and was used accordingly on serum starved cells at 5nM for 30 min followed by a 12 hr refeed with 15% serum. Following treatments, cells were harvested for RNA and cell size. RNA from equal cell numbers was analysed using the RPA to measure differences in rDNA transcription rates as described above.

The BJ-hTERT cell model displayed similar trends in cell size between SGK3 mutants under all treatment conditions. Strikingly, SGK3 CA and SGK3 CA PX cells displayed a

significantly larger size than pMIG control cells and SGK3 KD cells under all conditions **(Figure 3.15 A)**. Furthermore, this increase in cell size was not affected by rapamycin treatment in both the presence and absence of serum. Given that only slight differences were observed between proliferation rates and cell cycle profiles of the BJ-hTERT SGK3 CA and SGK3 CA PX cells, it is likely that enforced SGK3 expression is sufficient to uncouple growth and proliferation irrespective of cellular localisation in BJ-hTERT cells. SGK3 CA, but not SGK3 CA PX, SGK3 WT or SGK3 KD significantly increased rDNA transcription in serum starved BJ-hTERT cells **(Figure 3.15 B)**. Rapamycin attenuated SGK3 CA induced activation of rDNA transcription rates almost back to serum starved control levels (although this did not reach significance) suggesting mTOR signalling is required for activation of rDNA transcription by SGK3. SGK3 CA also further increased rDNA transcription rates in serum refed cells, which was repressed by rapamycin and to a lesser extent by AKTi, although neither activation by SGK3 or repression by rapamycin or AKTi reached significance. Taken together in both the HOSE and BJ-hTERT cell lines, these data demonstrate that activated SGK3 is able to increase rDNA transcription rates in an mTORC1 dependent manner. Furthermore, studies using SGK3 CA PX also demonstrate that the ability of SGK3 to increase rDNA transcription rates is dependent on endosomal localisation.

3.3 Discussion

3.3.1 Overview of results

The results in this chapter demonstrate a role for SGK3 in the regulation of cell growth and proliferation. Studies in HOSE cell lines revealed that enforced expression of activated SGK3 was able to increase cell proliferation, and in both HOSE and BJ-hTERT SGK3 was also able to significantly increase cell size and macromolecular content (RNA and protein). Furthermore, our results suggest that increases in these important growth parameters are most likely through increased rates of rDNA transcription, the rate-limiting step in ribosome biogenesis, and cellular growth. Moreover, studies presented in this chapter also demonstrate that the regulation of cell proliferation and growth processes is not always coupled, with experiment in both epithelial and fibroblast cell lines demonstrating that SGK3 is able to regulate these processes differentially to predominantly drive growth.

Further investigation of rDNA transcription rates and growth signalling using the mTORC1 inhibitor rapamycin, revealed that SGK3 regulation of growth is likely in to be predominantly mTORC1-dependent. However, as rapamycin also inhibited basal rDNA transcription rates its was not possible to conclude if mTOR is necessary for growth per se or whether it specifically mediates SGK3's activation of rDNA transcription. Furthermore, inhibition of AKT demonstrated a much less pronounced inhibitory effect on SGK3 driven rDNA transcription than rapamycin, perhaps suggesting that SGK3 can rescue rDNA transcription in the absence of AKT signalling. However further studies are required to more specifically investigate both the requirement of mTORC1 for SGK3-mediated rDNA transcription, and the ability of SGK3 to drive

Figure 3.14: Activated SGK3 increases rDNA transcription in HOSE cells

HOSE cells exhibiting stable expression of pMIG empty vector, SGK3 WT and SGK3 CA were plated at 0.10 x 10^6 cells in 6 well plates and left to recover overnight. Cells were serum starved for 36 hr and then pre-treated for 30 min with ± 20nM rapamycin followed by a 12 hr refeed with ±15% FBS. Cells were harvested for RNA with GTC and cell number using trypsinisation. Cell number and size was determined using the Coulter Counter (Beckman Coulter). RNA was isolated, and RNA from all cells was analysed for expression of 5'ETS using the RPA. **(A)** The cell size of each cell line and treatment was determined using the Coulter Counter (Beckman Coulter). **(B)** The phosphorimages show 5'ETS expression. Different gels are separated with black lines. Bands were quantified using ImageQuant Software (GE Healthcare) and values were plotted on the graph below. Phosphorimage is representative only. n=2-7, ± SEM, *** $p < 0.001$, ** $p < 0.01$, * $p < 0.05$.

HOSE Cells

A.

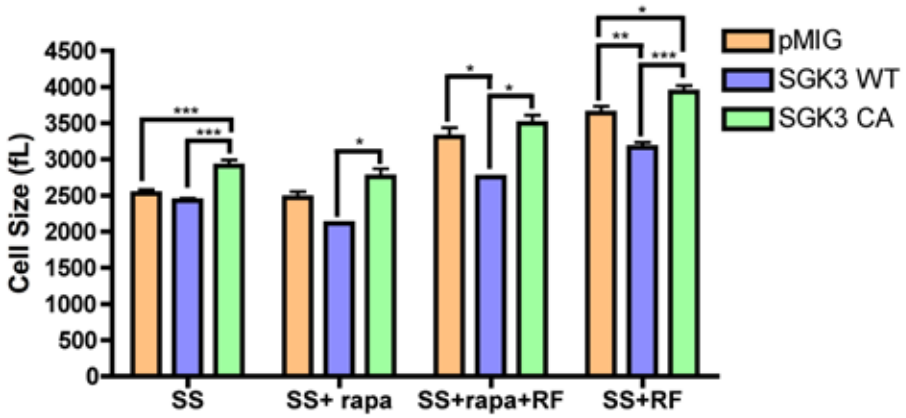

B.

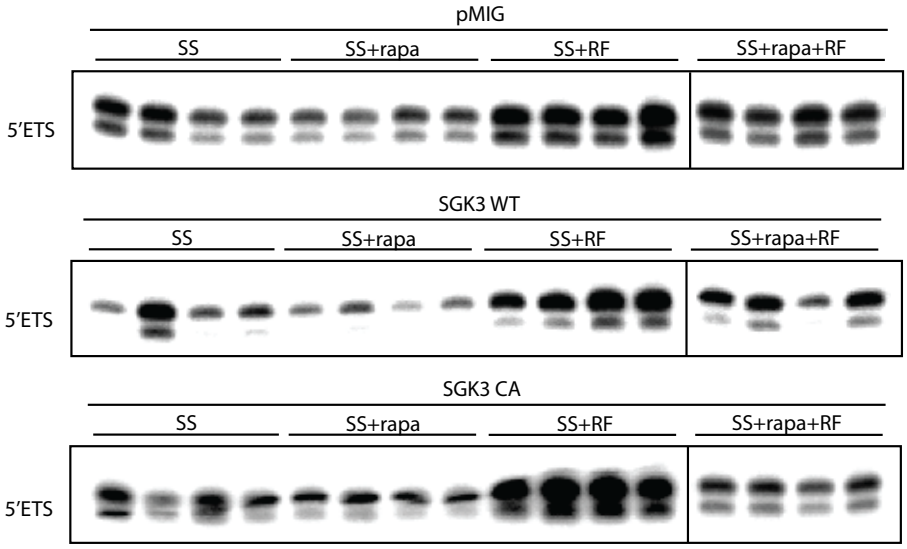

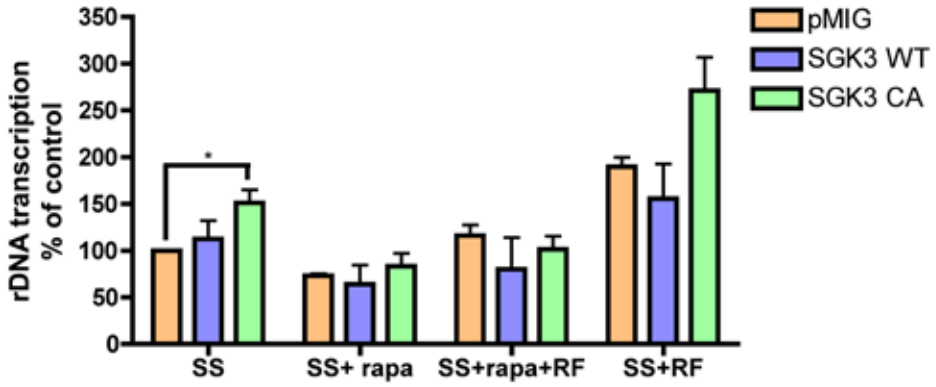

Figure 3.15: Activated SGK3 increases rDNA transcription in BJ-hTERT cells

BJ-hTERT cells exhibiting stable expression of pMIG empty vector, SGK3 WT, SGK3 CA, SGK3 CA PX and SGK3 KD were plated at 0.2 x 10^6 cells in 100mm plates and left to recover overnight. Cells were serum starved for 36 hr and then pre-treated for 30 min with ± 20nM rapamycin or ± 5μM AKTi1/2, followed by a 12 hr refeed with ±15% FBS. Cells were harvested for RNA with GTC and cell number using trypsinisation. Cell number and size was determined using the Coulter Counter (Beckman Coulter). RNA was isolated, and RNA from 30,000 cells was analysed for expression of 5'ETS using the RPA. **(A)** The cell size of each cell line and treatment was determined using the coulter counter. n=1-4, ± SEM, *** $p < 0.001$, ** $p < 0.01$, * $p < 0.05$. **(B)** The phosphorimages show 5'ETS expression. Different gels are separated with black lines. Bands were quantified using ImageQuant Software (GE Healthcare) and values were plotted on the graph below. Phosphorimage is representative only. n=1-3. ± SEM. * $p < 0.05$.

BJ-hTERT Cells

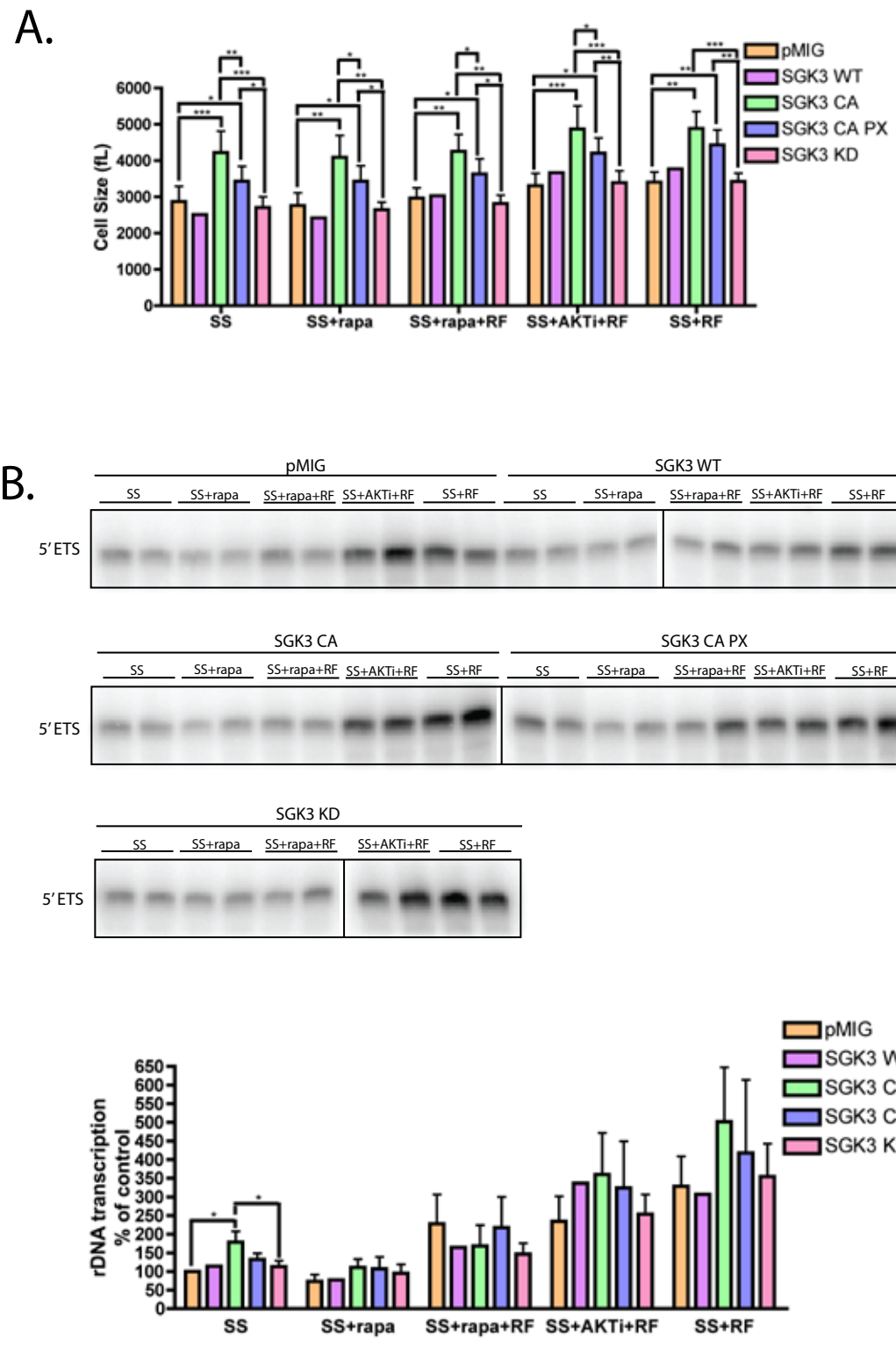

rDNA transcription in the absence of AKT, as although the effects of rapamycin and AKTi show strong trends they were not statistically significant. Finally, the results from these studies also suggest that endosomal localisation of SGK3 is important for optimal potency of this kinase to drive core cell growth processes.

3.3.2 SGK3 influence on cell growth signalling

To further investigate potential mechanisms by which SGK3 may modulate cell growth and proliferation, constructs expressing SGK3 mutants were stably introduced into HOSE and BJ-hTERT cells, and levels of both phospho-activity and total protein of a panel of well known proteins associated with the PI3-K/mTORC1 signalling were investigated. Studies presented in this chapter demonstrate for the first time that enforced expression of both wildtype and activated SGK3 produced an increase in the phosphorylation and inhibition of upstream repressors of mTOR, TSC2 and PRAS40, while concomitantly increasing the activity of downstream readouts of mTORC1 activity, rpS6 and 4EBP1. Importantly, SGK3 was able to drive changes in activity of these components of PI3-K/mTORC1 growth signalling in the absence of growth factors. The ability of SGK3 to signal to key mediators of cell growth in an mTORC1-dependent manner was further confirmed using the mTOR inhibitor, rapamycin, with results showing a reduction in rpS6 and 4EBP1 phosphorylation following treatment of HOSE SGK3 cell lines. However, given that not all signalling downstream of mTORC1 was abolished in response to rapamycin, it is probable that there is also a component of SGK3 signalling to cell growth that is mTORC1-independent. Recent studies demonstrating a role for AKT in modulating cell growth in an mTORC1-independent manner also further suggests that SGK3 may also modulate cell growth via similar mTORC1-independent mechanisms (Chan et al. 2011).

In addition to HOSE cells, SGK3 was also shown to be an important regulator of cell growth via TORC1 signalling in the BJ-hTERT fibroblast thus, demonstrating that the ability SGK3 to regulate growth signalling is not cell type specific. However, a notable difference in SGK3 WT signalling between BJ-hTERT and HOSE cells was in the BJ-hTERT cells, enforced expression of SGK3 WT was unable to increase the phosphorylation of upstream regulators of mTOR, TSC2 and PRAS40. The differences identified in signalling between HOSE SGK3 WT and BJ-hTERT SGK3 WT cells may be due to a number of factors, possibly including more robust protein expression of SGK3 WT in HOSE cells than in BJ-hTERT cells, or higher basal level of PI3-K signalling in growth factor deprived HOSE cells, increasing the basal activity of all components of this pathway. However, it does demonstrate that increases in signalling down the PI3-K/mTORC1 pathway are not always indicative of robust functional changes, given that while HOSE SGK WT cells show an increase in phosphorylation of critical members of the PI3-K/mTORC1 pathway, these cells are still significantly smaller than SGK3 CA under both steady state and serum starved conditions, suggesting that while detectable, SGK3 WT signalling to growth is not robust or sustained enough to elicit the same functional changes as SGK3 CA.

To date the main downstream effector of PI3-K signalling to mTORC1 has been considered to be the AKT family, with AKT playing a key role in the regulation of mTOR via phosphorylation of upstream regulators TSC2 and PRAS40 (Memmott and Dennis 2009). Studies in this chapter have demonstrated for the first time that SGK3 is also able to directly increase phosphorylation of these factors. It is possible that despite differences in localisation, with SGK3 shown to localise at the endosomal compartment (Xu et al. 2001; Tessier and Woodgett 2006a; He et al. 2011), and AKT at the plasma membrane (Gao et al. 2011), these two kinases are able to regulate growth processes via the same pathway, likely sharing some level of redundancy, however this will require further investigation. Furthermore, given that PI3-K/AKT/mTORC1 signalling has demonstrated an essential role in malignant transformation (Aoki et al. 2001; Chang et al. 2003; Cheng et al. 2005; Guertin and Sabatini 2005; Hay 2005), it is also likely that SGK3 also plays a key role in this network. Taken together, these results suggest that like AKT, SGK3 is sufficient to regulate key components of the PI3-K/mTORC1 signalling pathway, and through regulation of this pathway can likely act as a potent mediator of cell growth. Based on these growth signalling studies, our proposed model of SGK3 signalling to cell growth is shown in **Figure 3.16,** where like AKT, SGK3 is likely able to directly regulate TSC2 and PRAS40 via phosphorylation, which are then able to induce activation of mTORC1 and cell growth.

In addition to identifying SGK3 as a novel growth regulator, studies presented in this chapter also specifically engineered an SGK3 mutant construct that allowed further investigation into the importance and requirement of SGK3 endosomal localisation in the context of cell growth. Analysis of signalling in the BJ-hTERT SGK3 CA PX cells suggested that signalling through the growth pathway is weaker than in SGK3 CA cells, however both SGK3 CA cells and SGK3 CA PX cells still increased phosphorylation of the same components of the growth pathway. Together, these data suggest that SGK3 CA is still able to signal through mTORC1 even when not localised to the endosome.

3.3.3 Activated SGK3 increases proliferation and key parameters of cell growth

After elucidating a novel role for SGK3 in mediating signalling to cell growth via mTORC1, both epithelial and fibroblast cell lines were used to further investigate functional changes elicited by enforced expression of SGK3 on key parameters of cell proliferation and growth. Studies in the HOSE cells demonstrated that enforced expression of both wildtype and activated SGK3 increased cell proliferation, significantly reducing doubling time, and increasing cells in S phase of the cell cycle in both cell lines. Additionally, more recently the ability of SGK3 to increase cell cycle progression through G1 has also been shown in hepatocellular carcinoma (Liu et al. 2012). Using measurements of cell volume, total RNA and protein content per cell, it was demonstrated that neither SGK3 WT nor SGK3 CA cells exhibited smaller size despite faster doubling times demonstrating that growth rates were increased to match the accelerated proliferation thus preventing the cells from dividing at a smaller size. In fact the HOSE SGK CA cells exhibited increased size and macromolecular content

Figure 3.16: Proposed model of SGK3 signalling to cell growth and proliferation

Proposed model of SGK3 signalling to cell growth includes activation in PI3-K dependent manner via PDK1, in addition to phosphorylation by an as yet unidentified second kinase, which may be mTORC2 given that this kinase is responsible for phosphorylation of all AKT isoforms and SGK1 at the C-terminal Ser site. Activated SGK3 is then able to activate mTORC1 signalling via phosphorylation and inhibition of TSC2 and PRAS40. mTORC1 is then able to signal to downstream regulators of cell growth, including 4EBP1 and RPS6. Furthermore, activated SGK3 is also able to phosphorylate and negatively regulate an important cell cycle regulator GSK3β.

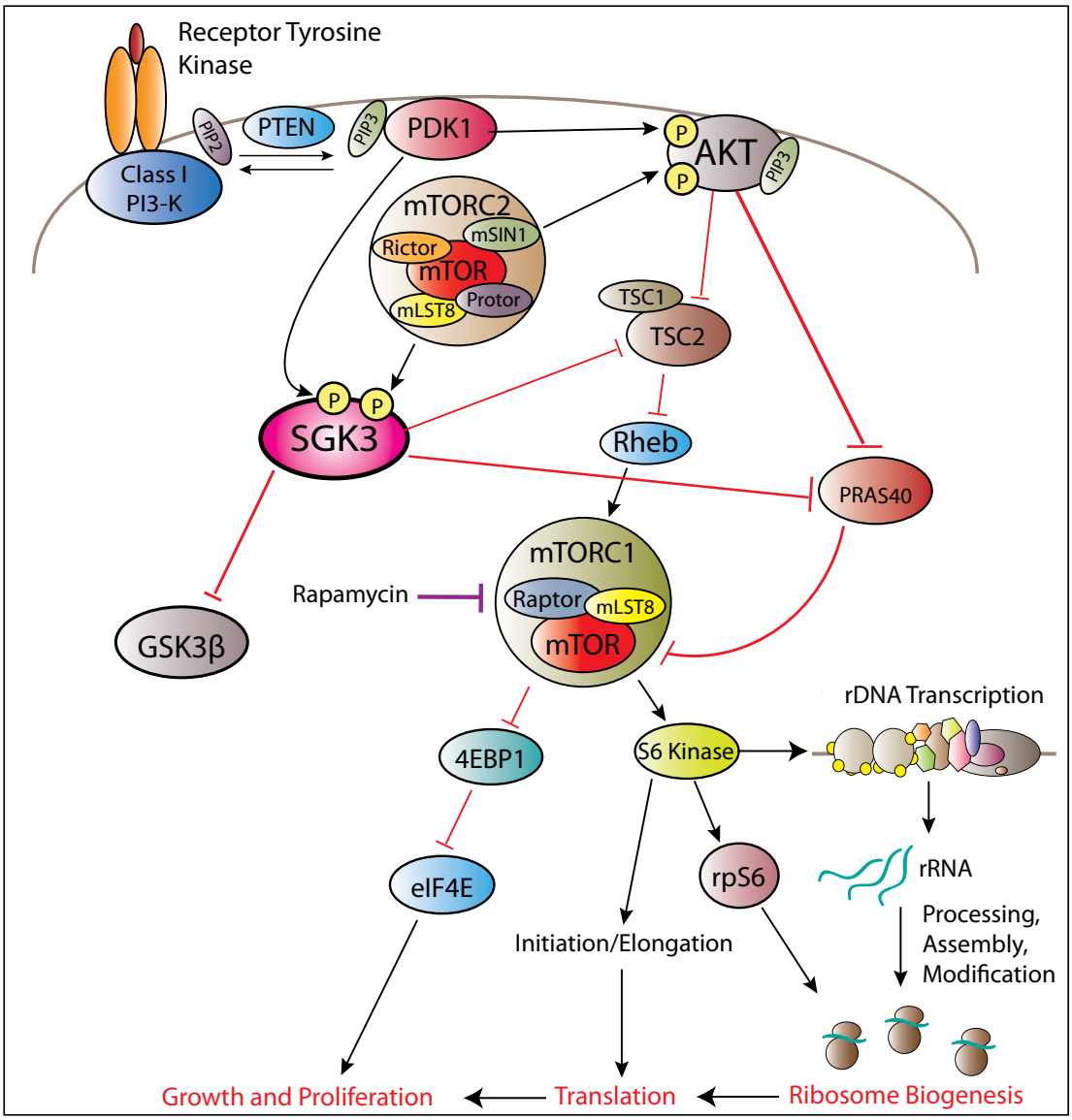
Receptor Tyrosine Kinase
Class I PI3-K
PIP2
PTEN
PIP3
PDK1
AKT
P
P
PIP3
mTORC2
mSIN1
Rictor
mTOR
mLST8
Protor
TSC1
TSC2
SGK3
P
P
Rheb
PRAS40
mTORC1
Raptor
mLST8
mTOR
Rapamycin
GSK3β
rDNA Transcription
4EBP1
S6 Kinase
eIF4E
rpS6
rRNA
Processing, Assembly, Modification
Initiation/Elongation
Growth and Proliferation
Translation
Ribosome Biogenesis

suggesting that SGK CA was able increase growth proportionately more than doubling time. Thus in the HOSE cells hyperactivated SGK3 signalling is able to uncouple growth and proliferation processes which have traditionally thought to be coupled in an obligatory manner. Similar results were observed in BJ-hTERT fibroblasts cells confirming a more general role for SGK3 in the regulation of growth and proliferation of mammalian cells.

The ability of activated SGK3 to drive growth and cell doubling time in a disproportionate manner in comparison to wildtype SGK3 in the HOSE cells is likely due to its ability to drive more robust and sustained signalling through the PI3-K/mTORC1 pathway. This may be because of a reduced requirement of upstream signalling factors for SGK CA activity, which would otherwise be limiting for wildtype SGK3 activity. Moreover, constitutive activation of SGK3 likely results in stronger and more sustained signalling to downstream growth targets, allowing SGK3 CA to elicit a more significant impact of cell growth. It is also possible that constitutive SGK3 signalling may engage additional downstream targets, which the wildtype SGK3 may not activate.

3.3.4 Activated SGK3 increases rDNA transcription

Studies in mammalian cells have demonstrated a strong correlation between cell growth and rDNA transcription (Murano et al. 2008), a process thought to be the major rate-limiting step in ribosome biogenesis (Hannan et al. 2003). Ribosome biogenesis is regulated in response to nutrient availability and growth factor signalling in order to adjust the translational capacity of the cell to match new growth requirements (Powers and Walter 1999; Mayer and Grummt 2006). mTORC1 is considered to be an important nutrient checkpoint (Foster and Fingar 2010), and studies using rapamycin have demonstrated that mTORC1 is a critical regulator of ribosome biogenesis (Iadevaia et al. 2012). Given that SGK3 has shown to lie upstream of mTORC1 it is also possible that SGK3 is able to regulate rDNA transcription via mTORC1. Furthermore, earlier studies presented in this chapter show enforced expression of SGK3 CA in both HOSE and BJ-hTERT cell lines increases key parameters of cell growth, including cell size, and both total RNA and protein per cell. Given that rRNA makes up 85% of total RNA per cell (McDermott et al. 1989), these studies together led us to predict that SGK3 signalling might be a physiologically important mechanism to regulate rDNA transcription. In mammalian cells. given the robust nature of AKT signalling through mTOR to rDNA transcription (Chan et al. 2011), an equally important question was if SGK3 could regulate rDNA transcription, how important was its contribution to this process compared to AKT; and further, was enforced expression of SGK3 sufficient to modulate rDNA transcription independent of other growth factors.

We found that enforced expression of SGK3 CA in HOSE cells resulted in a significant increase in rates of rDNA transcription in the absence of growth factors, which was reduced with rapamycin treatment. These results demonstrated that activated SGK3 signalling was sufficient to stimulate an increase in macromolecular content (RNA and protein per cell) and rDNA transcription in an mTORC1-dependent manner.

Interestingly, despite inducing robust signalling through the PI3-K/mTORC1 pathway, enforced expression of SGK3 WT did not significantly increase rDNA transcription rates, nor did it increase total RNA and protein per cell or cell size. Similarly in BJ-hTERT cells, enforced expression of SGK3 CA but not SGK3 WT or significantly increased rates of rDNA transcription in the absence of growth factors, or SGK3 CA PX. Furthermore, treatment with rapamycin only partially reduced rDNA transcription in the BJ-hTERT SGK3 CA cells, suggesting that SGK3 is able to activate rDNA transcription independent of mTOR. Taken together these data suggest that SGK3 CA signalling to rDNA transcription may be partially mTORC1-independent. Studies to confirm this could involve the use of raptor knockout (KO) murine embryonic fibroblasts (MEFs). Raptor is a required component for a functional mTORC1 complex, and thus enforced expression of SGK3 in a mTORC1 null cell line would directly test its requirement for SGK3 to promote rDNA transcription. Our laboratory has obtained the transgenic knock in mice from Professor Mike Hall (University of Basel, Switzerland), where the raptor gene is floxed by CRE recombinase allowing inducible knockout of raptor *in vivo and in vitro*.

To date AKT has been reported to be a core mediator of PI3-K signalling to growth and rDNA transcription (Hay and Sonenberg 2004). To test the degree of redundancy between AKT and SGK3 signalling to drive rDNA transcription we tested whether enforced expression of SGK3 could rescue repression of rDNA transcription following treatment of the cells with the AKT inhibitor. It was shown that SGK3 CA is able to rescue repression of rDNA transcription by AKTi back to levels exhibited by control cells treated with serum. This finding provides further evidence to suggest that the SGK and AKT families share a certain degree of signalling redundancy to ribosome biogenesis. The degree of redundancy could in future experiments be tested by co-enforced expression of AKT and SGK isoforms to determine if the responses on rDNA transcription were additive. Finally, the results above specifically demonstrate the ability of SGK3, despite endosomal localisation, to drive rDNA transcription in a similar manner to AKT.

3.3.5 The influence of SGK3 localisation on cell growth and proliferation

Cell localisation studies in both HOSE and BJ-hTERT cells were performed in order to confirm the localisation of the SGK3 mutant constructs. As expected the enforced expression of SGK3 CA in both cell lines demonstrated a predominantly endosomal localisation, compared with the subcellular localisation of SGK3 CA PX in the BJ-hTERT cells which demonstrated a diffuse pattern of staining with predominantly cytoplasmic localisation. Studies in the BJ-hTERT cells were able to compare the ability of SGK3 to regulate proliferation and parameters of cell growth both based on its subcellular localisation.

In BJ-hTERT cells, it was clear that SGK3 CA not only induced a larger cell size, but also increased rates of rDNA transcription in the absence of growth factors compared with not only the control pMIG cells, but relative to SGK3 CA PX cells, suggesting that

SGK3 requires endosomal localisation not only for full activation but also to be able to influence core growth processes such as RNA and protein synthesis. These studies indicate that using a phospho-mimetic hydrophobic motif mutant to confer constitutive activity without a functional PX domain is not sufficient to replicate the level of activity achieved with the same mutant containing a functional PX domain. Previous studies in HEK293 cells have demonstrated that SGK3 requires endosomal localisation for phosphorylation of Ser 486 of the hydrophobic motif (HM), which then allows PDK1 to bind to the HM and phosphorylate Thre 320 in the activation loop, generating a fully activated kinase. Furthermore, if the HM is already phosphorylated (which is what our SGK3 CA mutant mimics) then endosomal localisation is not required to yield fully activated SGK3 (Tessier and Woodgett 2006a).

In agreement with Tessier et al (Tessier and Woodgett 2006a), in our hands the SGK3 CA PX mutant was able to maintain some level of activity, however our functional readouts suggest that SGK3 CA localised to the endosome and was able to more robustly increase multiple key readouts of cell growth. It is probable that decreased functionality in SGK3CA PX cells is due to limited availability of PDK1, the specific upstream signalling factor required to phosphorylate the Thr site in the catalytic domain of SGK3. This may be because PDK1 is typically recruited to the plasma membrane following PI3-K activation (Mora et al. 2004), and non-endosomal SGK3 has shown to be largely cytoplasmic (Virbasius et al. 2001; Tessier and Woodgett 2006a).

It is not clear how PDK1 localises to the endosomal compartment, however a previous study has reported that SGK3 is able to facilitate the recruitment of PDK1 to the endosomes only after phosphorylation at S486 in HM by a PI3-K dependent kinase (Slagsvold et al. 2006). More recently it has also been shown that in vascular smooth muscle cells PDK1 is recruited to the endosomes by Angiotensin-II to facilitate AKT1 activation and subsequent mTOR/S6K signalling (Nazarewicz et al. 2011). Thus whilst there are studies identifying PDK1 localisation at the endosome, further analysis is required to determine the mechanism behind PDK1 recruitment to the endosomes and activation of SGK3.

3.3.6 Possible model of SGK3 signalling to cell growth

The increased potency of SGK3 CA mutant compared to SGK3 CA PX mutant on cell growth parameters highlight the potential importance of endosomal localisation for robust SGK3 function. The mechanism of how endosomal SGK3 can signal to cell growth is unknown, however the endosomally localised class III PI3-K hVps34, may possibly play an important role in SGK3 activation at the endosome. hVps34 is recruited to the endosome in a complex with hVps15 via Rab5 where it has shown to play a key role in endocytic sorting via myotubularin 1 (MTM1) and Rab5/7, in addition to autophagy via Beclin-1 (Backer 2008). More recently hVps34 has also exhibited an important role in the regulation of protein synthesis via nutrient signalling through mTOR/S6K1, however the mechanism behind this signalling has not yet been determined (Nobukuni et al. 2005).

At the endosome, hVps34 is able to produce PtdIns(3)P, thereby recruiting proteins containing PtdIns(3)P binding domains, such as Fab1/YOTB/2K632.12/Vac1/EEA1 (FYVE) and PX domains, many of which are involved in vesicular trafficking and receptor sorting. While SGK3 has shown to be involved in receptor sorting at the endosome through regulating the degradation of the E3 ligase AIP4, important for degradation of the chemokine receptor CXCR4 (Slagsvold et al. 2006), it is plausible that SGK3 may also play a role in mediating hVps34-dependent regulation of protein synthesis via mTOR/S6K1 In this model hVps34 would recruit SGK3 to the endosome via PtdIns(3)P binding, thereby allowing Class I PI3-K dependent phosphorylation of it's HM at S486 and subsequent phosphorylation by PDK1 at T320. Fully activated SGK3 may then be able to act as a novel convergence point between growth factor and nutrient signalling potentially through TSC2 and mTORC1/S6K to drive protein synthesis and growth, in addition to performing established receptor sorting roles.

Furthermore, studies presented in this chapter also raise interesting questions as to how SGK3 signalling in the endosomal compartment, and AKT signalling localised to other cellular compartments may essentially modulate equivalent pathways to control cell growth. It is likely that differential upstream regulation of these kinases, in addition to localisation and availability of downstream growth targets will distinguish the requirement of SGK3 and AKT to signal to cell growth from their respective cellular compartments. Studies have demonstrated that mTORC1 localisation is predominantly cytoplasmic (Rosner and Hengstschlager 2012), however studies also show that mTORC1 can be recruited to the endosomal compartment (Real et al. 2011). For example, recently it has been demonstrated that the E2F1 transcription factor, shown to play important roles in the regulation of apoptosis and proliferation, also has an important role in growth via inducing mTORC1 translocation to the endosomal compartment in an amino acid sensitive manner, which also correlates with an increase in S6K (Real et al. 2011). Furthermore, E2F1 regulation of growth has shown to be AKT-independent. It is possible that E2F1 is capable of inducing a gene expression program that could determine cellular growth, and as such may potentially be involved in SGK3 regulation, thereby modulating SGK3-mediated growth factor and nutrient signalling to cell growth at the endosome. However, further investigation is required to delineate signalling pathways to cell growth based on cellular compartment, and determine the conditions that trigger both SGK3 and AKT to signal to growth.

In summary, these studies demonstrate for the first time that SGK3 plays an important role in regulating both proliferation and cell growth processes, largely via signalling through the PI3-K/mTORC1 growth pathway to effect core protein synthesis machinery, resulting in increased levels of rDNA transcription leading to significant increases in functional readouts of cell growth. Despite AKT being a well established modulator of the PI3-K/mTORC1 pathway, studies presented in this chapter demonstrate many similarities between SGK3 and AKT in the regulation of growth processes, suggesting that despite SGK3's endosomal localisation, and in addition to a level of redundancy shown between SGK3 and the AKT family, it is possible that these kinases may also

cooperate in some instances to further promote signalling to growth, however further investigation is required. Finally, given the role of SGK3 in signalling through the PI3-K/mTORC1 pathway, it is likely that SGK3 is also involved in malignant transformation through increased activation of cell growth machinery.

4. The influence of SGK3 compared with AKT on crucial hallmarks of cell transformation and tumourigenesis

4.1 Introduction

The PI3-K pathway is one of the most commonly altered pathways in human cancers, with accumulating genetic and cancer biology studies indicating a prominent role for this pathway in cell transformation and tumourigenesis. The ability of the PI3-K pathway to integrate signals from growth factors, insulin, nutrients and oxygen to initiate a plethora of downstream responses, including cell growth, proliferation, metabolism, migration and survival makes it a pivotal target for cancer therapy. To date, much of the evidence gathered supporting PI3-K as a critical modulator of tumourigenic activity has revealed the main downstream effector to be the AKT family of kinases, with all three AKT isoforms playing both overlapping and distinct roles in cell transformation and tumourigenesis (Manning and Cantley 2007). However, despite this paradigm for PI3-K-dependent transformation via AKT, there are multiple alternative oncogenic pathways such as RAS/RAF/ERK, liver kinase B1 (LKB1) and Myc that interact with the core PI3-K signalling module both upstream and downstream of AKT (Shaw et al. 2004; Wandzioch et al. 2004; Ma et al. 2005; Solomon and Pearson 2009).

Interestingly, even though AKT is considered to be the main downstream effector of PI3-K, many AKT targets are also shared by the SGK family. These shared targets include the forkhead transcription factors, BAD (Liu et al. 2000), MDM2 (Amato et al. 2009) and the NF-κB pathway (BelAiba et al. 2006). Furthermore, even though in many instances both SGK and AKT protein isoforms have shown to target the same residues on their shared downstream substrate, it has been observed that SGK and AKT target different residues for phosphorylation on FOXO3a, a member of the forkhead transcription factor family involved in the induction of cell cycle arrest and apoptosis (Liu et al. 2000; Brunet et al. 2001; McCormick et al. 2004). This example, in addition to the evidence demonstrating clear differences in cellular localisation between these kinase families indicates the potential for SGK and AKT to have complementary rather than redundant function as downstream effectors of PI3-K.

Given the accumulating evidence suggesting SGK3 is an important effector of PI3-K and modulator of several processes associated with tumourigenesis, studies outlined in this chapter sought to further investigate the influence that SGK3 has on these cellular functions associated with malignant cell transformation, in addition to growth and proliferation as described in Chapter 3. In addition, throughout these studies comparisons have been made to the AKT family, an established and well-studied family of potent oncogenes that share a similar domain structure and high amino acid sequence identity to the SGK family. These comparative studies will aid in uncovering potential similarities and differences between these kinase families.

4.2 Results

To further elucidate a possible role for SGK-3 in cell transformation and tumourigenesis, in addition to delineating possible differences between the role that SGK-3 and the AKT kinase family play in influencing markers of cell transformation, studies presented in this chapter utilized two distinct genetically defined gain-of-function cell lines. Genetically defined models of cell transformation are useful tools to investigate the possibility of alternative genetic elements substituting for established drivers of cell transformation. Genetically defined models have been generated using a range of different cell types, and it has become widely accepted that expression of four specific genetic components is required for the transformation of human cells (Hahn et al. 1999; Elenbaas et al. 2001; Zhao et al. 2003) **(Figure 4.1 A)**.

These four genetic components include hTERT, the catalytic subunit of human telomerase, which induces cell immortalisation, the large T antigen and small t antigens which together form the SV40 early genomic region, with the Large T antigen specifically shown to be involved in the inactivation of crucial tumour suppressor genes including retinoblastoma and p53, and the small t antigen involved in inactivating PP2A, a crucial phosphatase involved in the negative regulation of both AKT and SGK, and the stabilisation of c-Myc. The final genetic element required for complete cell transformation is oncogenic H-Ras, which is able to signal through multiple effector pathways including PI3-K and MAPK (Zhao et al. 2004) to drive cell transformation.

The two genetically defined cell models used in this chapter include those generated from primary human BJ foreskin fibroblast cells and primary ovarian IOSE523 epithelial cells **(Figure 4.1 B)**. SGK-3 cell growth and proliferation studies, as described in Chapter 3, used BJ cells ectopically expressing hTERT only (BJ-hTERT), which leads to cell immortalisation but not transformation. In Chapter 2 the cell models recapitulate much of the physiology of a primary cell, hence allowing the characterisation of the potential role of SGK3 in growth and proliferation under cell physiological conditions. In contrast in Chapter 4 studies will use human BJ fibroblast cells ectopically expressing hTERT, as well as the large T and small t antigens (BJ-LST), and thus these cell lines more closely represent a pre-tumourigenic cell model, and allow the potential of additional ectopically expressed elements, such as SGK3 or AKT to recapitulate the effect of established drivers of cell transformation such as activated H-Ras (H-Ras ^{v12}) to be assessed. Of note the BJ-LST cells are isogenically matched with the BJ-hTERT cells used in Chapter 3. In addition to the BJ-LST cell model, an ovarian IOSE523 genetically defined cell model, a kind gift from the Canadian Ovarian Tissue Bank, generated from primary epithelial ovarian cells, was engineered to ectopically expresses the SV40 large T antigen and small t antigen from the SV40 early genomic region. However these cells are not defined as immortalised due to the absence of ectopically expressed hTERT, and therefore only survive up to approximately 20 passages.

The SGK3 mutants stably introduced into the BJ-LST and IOSE523 cells include those

previously described in Chapter 3.2, which include SGK3 WT, SGK3 CA, SGK3 CA PX and SGK3 KD. To further enhance SGK3 cell transformation studies, gain of function AKT mutant constructs were also stably introduced into both BJ-LST and IOSE523 cell lines to further define similarities and differences between the influence that both SGK3 and the AKT family have on key hallmarks of tumourigenesis. Furthermore as an experimental positive control, cells over-expressing H-Ras^{V12} were included in all experiments.

4.2.1 Characterisation of SGK3 and AKT genetically defined pre-tumourigenic stable cell lines

Following generation of the BJ-LST and IOSE523 stable cell lines through retroviral transduction (as described in Chapter 2.3), it was necessary to analyse cell lines to validate appropriate protein expression of ectopically expressed mutant constructs using western blot analysis. As described in Chapter 3, all SGK3 constructs used in these studies have been generated with a myc-tag, allowing exogenous protein expression to be detected using a myc-tag antibody. Similarly, all AKT constructs used in these studies were also generated with a haemagglutinin (HA) tag, allowing exogenous AKT expression to be detected using a HA-tag antibody. Also, while all SGK3 retroviral constructs were generated using only the retroviral MSCV-IRES-GFP (pMIG) as the vector backbone, the AKT retroviral constructs were generated using the retroviral pMIG vector in BJ-LST cells, and the MSCV-IRES-Cherry (pMIC) vector in IOSE523 cells.

As described, the BJ-LST fibroblast cells were retrovirally transduced with SGK3 and AKT isoform mutants in a pMIG vector backbone for all experiments. The SGK3 constructs stably expressed in the BJ-LST cells include SGK3 WT, SGK3 CA, SGK3 CA PX and SGK3 KD, and the three AKT isoform constructs stably expressed include myrAKT1, myrAKT2 and myrAKT3 (Chapter 2.2.3). In addition, H-Ras ^{v12} in a pMIG vector backbone was also stably expressed for use as a positive experimental control, and pMIG empty vector was stably expressed for use as a vector control. Following retroviral transduction of the BJ-LST cells with the above mutant constructs, each population of cells was sorted for the top 50% brightest GFP expressing cells using FACS, and all positive cells were pooled and individual cell lines were established.

Western blot analysis was performed on all BJ-LST cells to validate stable expression of all transduced constructs. Endogenous SGK3 protein expression was barely detectable in pMIG samples **(Figure 4.2, Lane 1)**, but a robust SGK3 band at 60 kDa motility was observed in SGK3 WT **(Figure 4.2, Lane 2),** SGK3 CA **(Figure 4.2, Lane 3)**, SGK3 CA PX **(Figure 4.2, Lane 4)**, and SGK3 KD **(Figure 4.2, Lane 5)** transduced cells. Similar to pMIG transduced BJ-LST cells endogenous SGK3 was barely detectable in cells stably expressing mutant AKT constructs **(Figure 4.2, Lane 6-8)**, or the BJ-LST cells stably expressing H-Ras^{v12} **(Figure 4.2, Lane 9)**. Using the Myc-tag antibody robust protein levels of all ectopically expressed myc-tagged SGK3 mutant constructs **(Figure 4.2, Lane 2-5)** were detected in the SGK3 transduced cells

Figure 4.1: Genetically defined cell models of malignant cell transformation

(A) Schematic showing the pathways that cooperate during human malignant cell transformation, where dysregulation of multiple pathways is required for complete cell transformation. hTERT expression contributes to telomere maintenance and cellular immortalisation. The SV40 early region (SV40 ER) encodes both Large T (LT) and small t (st) antigens. LT is able to inactivate RB and p53 tumour supressors to promote dysregulate cell cycle and apoptotic pathways. Additionally human papilloma virus (HPV) E6 and E7 are also able to act on these pathways. The st antigen is able to act through perturbation of protein phosphatase 2A (PP2A), which can lead to hyperactivation of the PI3-K pathway and stabilisation of MYC, promoting proliferation, survival and growth pathways. Lastly, expression of oncogenic H-Ras affects multiple pathways including PI3-K and MAPK pathways, further activating survival, growth and mitogenic signalling (Zhao et al. 2004). **(B)** Table shows the ectopically expressed genetic components present in each parental cell line used in these studies.

A

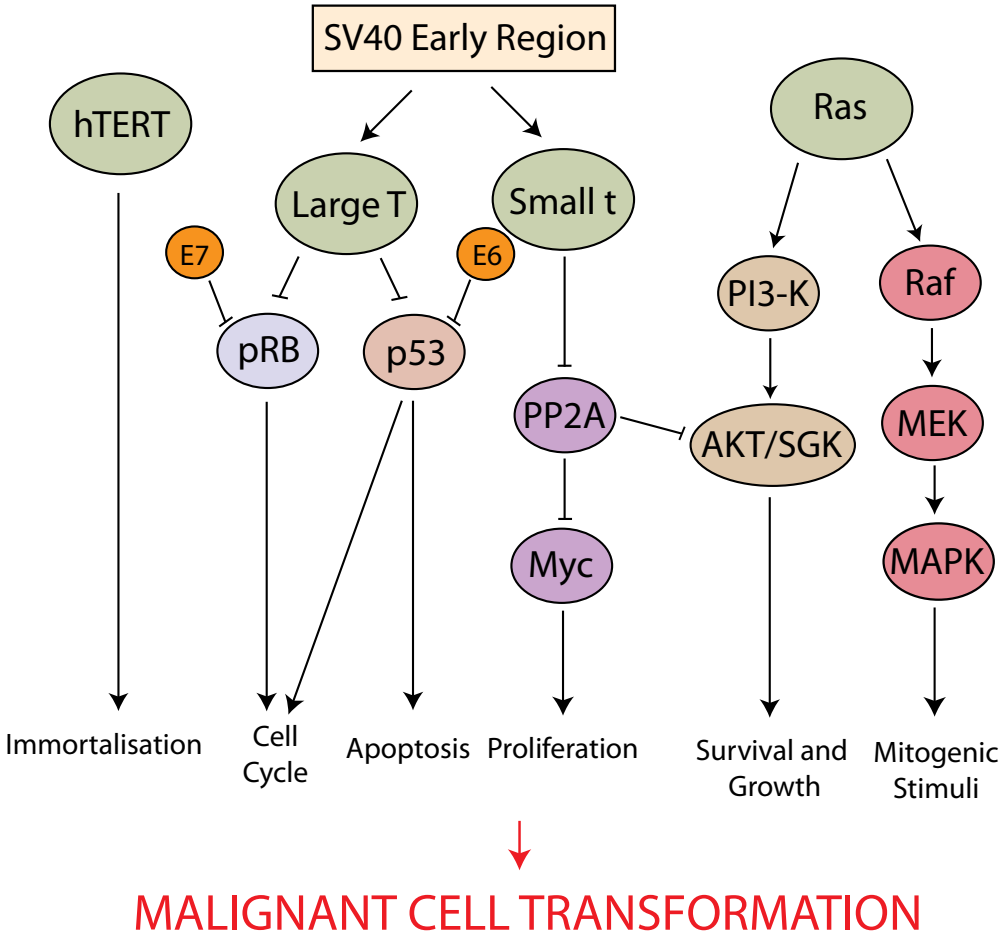

B

Cell Line	Genetic Components
BJ-LST	hTERT + Large T + small t
IOSE523	Large T + small t
HOSE	E6/E7

Figure 4.2: SGK3 and AKT mutant stable protein expression in BJ-LST cells

BJ-LST cells were stably transduced using virus generated from pMIG empty vector, SGK3 WT, SGK3 CA, SGK3 CA PX, SGK3 KD, myrAKT1, myrAKT2, and myrAKT3 and, H-Ras^{v12} retroviral constructs. The brightest 50% of GFP expressing cells were collected by FACS sorting, and subsequently pooled and expanded to establish cell lines. To validate correct protein expression cells were plated at low density in 100mm plates for 48 hr and harvested at approximately 70% confluency using WSB. Protein concentrations were determined using DC™ protein assay (Biorad). 20μg of protein was separated by SDS-PAGE (run on 10% gel) and expression of proteins determined by western analysis using indicated antibodies.

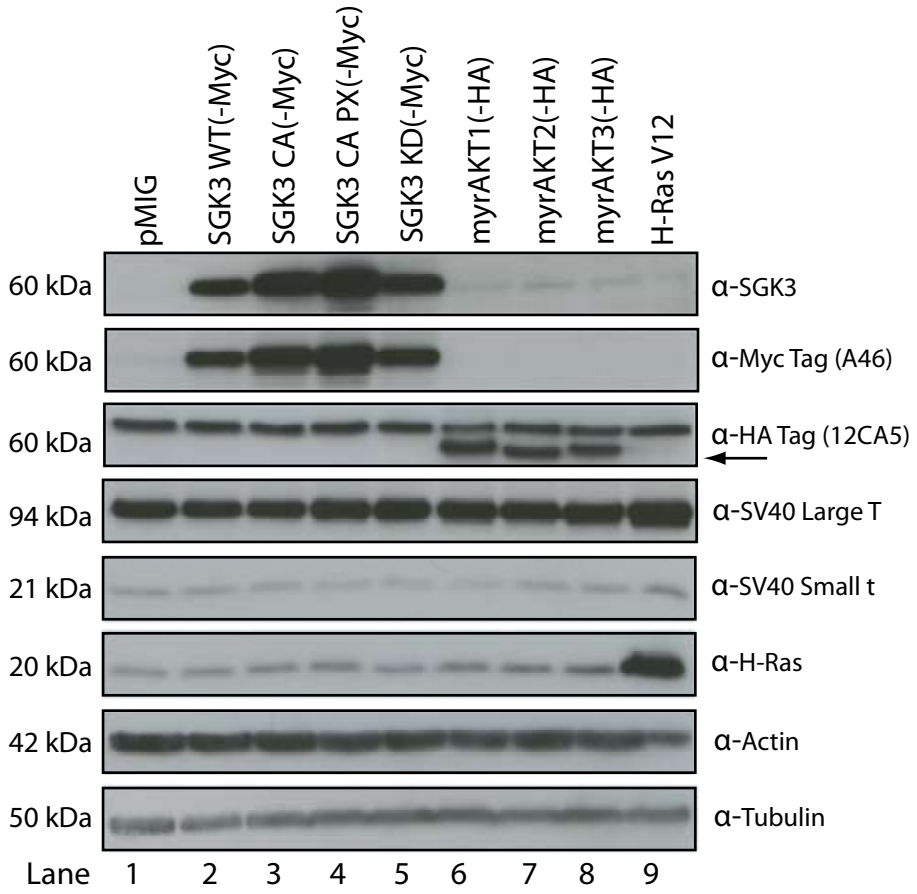
pMIG
SGK3 WT(-Myc)
SGK3 CA(-Myc)
SGK3 CA PX(-Myc)
SGK3 KD(-Myc)
myrAKT1(-HA)
myrAKT2(-HA)
myrAKT3(-HA)
H-Ras V12
60 kDa
α-SGK3
60 kDa
α-Myc Tag (A46)
60 kDa
α-HA Tag (12CA5)
94 kDa
α-SV40 Large T
21 kDa
α-SV40 Small t
20 kDa
α-H-Ras
42 kDa
α-Actin
50 kDa
α-Tubulin
Lane 1 2 3 4 5 6 7 8 9

and these levels mirrored the levels detected by the SGK3 antibody. Similarly, using the HA-Tag 12CA5 antibody detected robust protein levels of all ectopically expressed AKT isoform mutant constructs as shown by the arrow, as this antibody also produces a slightly larger non-specific band **(Figure 4.2, Lane 6-8).**

As previously described, the BJ-LST cells contain the early region SV40 large T and small t antigens, which along with hTERT are required components for cell transformation. All generated BJ-LST cell lines expressed similar protein expression of SV40 Large T **(Figure 4.2, Lane 1-9)**, and less robust but detectable levels of SV40 Small t **(Figure 4.2, Lane 1-9)**. Lastly, the BJ-LST cell line over-expressing H-Ras^{v12} exhibited strong expression levels of H-Ras protein **(Figure 4.2, Lane 9)**, compared with all other BJ-LST cell lines, which all expressed less robust, but similar levels of H-Ras protein **(Figure 4.2, Lane 1-8)**. In all samples the expression levels of the housekeeping proteins α -actin and α-tubulin were similar.

The ovarian epithelial genetically defined IOSE523 cells were transduced with the same SGK3 mutants as the BJ-LST cells (SGK3 WT, SGK3 CA, SGK3 CA PX and SGK3 KD), and following retroviral transduction were FACS sorted for the brightest 50% of GFP expressing cells. The IOSE523 SGK3 cell lines were then examined for stable protein expression using western blot analysis. A myc-tag antibody was used to detect protein expression of SGK3 mutant constructs, with robust expression of myc-tagged SGK3 shown in each WT and mutant cell line (lower band) **(Figure 4.3 A, Lane 2 – 5)**, compared with an absence of myc-tag expression in the pMIG control cells **(Figure 4.3 A, Lane 1)**.

The IOSE523 ovarian epithelial cells were retrovirally transduced with AKT constructs in a pMIC vector backbone for all experiments. The AKT constructs stably expressed in the IOSE523 cells were the same as those introduced into the BJ-LST cells, and included myrAKT1, myrAKT2 and myrAKT3. In addition, activated H-Ras ^{v12} in a pMIC vector, and pMIC vector only was expressed in these cells for use as a vector control. Following retroviral transduction of the IOSE523 cells with the above mutant constructs, each population of cells was sorted for the top 50% brightest Cherry expressing cells using FACS, and all positive cells were pooled and individual cell lines were established.

Western blot analysis was performed on all generated IOSE523 cell lines to detect stable protein expression of the transduced constructs. Using the HA Tag 12CA5 antibody to detect the HA Tag of the expressed AKT construct revealed robust expression of myrAKT1 **(Figure 4.3 B, Lane 3)**, myrAKT2 **(Figure 4.3 B, Lane 4)** and myrAKT3 **(Figure 4.3 B, Lane 5)**, but as expected was not detected in pMIC vector only **(Figure 4.3 B, Lane 1)** or H-Ras^{v12} **(Figure 4.3 B, Lane 2)**. Given that these cells also ectopically express large T antigen and small t antigen from the SV40 early genomic region, expression of these proteins was also confirmed. Western blot analysis detected equal expression of large T **(Figure 4.3 B, Lane 1-5) and** small t

(Figure 4.3 B, Lane 1-5) in all IOSE523 cell lines. Lastly, a H-Ras antibody was used to detect H-Ras protein expression in all IOSE523 cell lines. Endogenous H-Ras was detected in all IOSE523 cell lines **(Figure 4.3 B, Lane 1, 3-4)** with greater expression in the H-Ras^{v12} transduced cell line **(Figure 4.3 B, Lane 2)**.

In addition to the IOSE523 ovarian epithelial cells, we also used the HOSE cells stably transduced with SGK3 WT and SGK3 CA (Chapter 3.2.1) in the cell transformation studies as an alternative epithelial cell line, as these cells displayed robust growth and proliferation phenotypes with over-expression of SGK3 (Chapter 3). Additionally, several attempts were made to generate a HOSE AKT cell model and HOSE H-Ras^{v12} to complement the HOSE SGK3 cell model, however following retroviral transduction with the activated AKT constructs, it appeared that these cells stopped proliferating and displayed a senescent phenotype, however further studies would be required to confirm the senescent phenotype in these particular cells. Studies in our laboratory have demonstrated that high levels of AKT induces senescence in a variety of human non-transformed cells lines (Astle et al. 2011). However, despite the differences between the HOSE and IOSE523 ovarian epithelial cell lines, both were utilized in these studies in order to make broad comparisons between the roles of SGK3 and AKT in epithelial ovarian cell transformation.

4.2.2 Regulation of anchorage independent growth by SGK3 and AKT

In addition to uncontrolled growth and proliferation, a further common feature of tumourigenic cells is the capability of anchorage independent growth (Hanahan and Weinberg 2000). Cell anchorage to the extracellular matrix controls cell proliferation, with two distinct periods of the cell cycle subject to anchorage dependent regulation, including G1 phase progression and cytokinesis (Thullberg et al. 2007; Thullberg and Stromblad 2008). In order for cells to achieve anchorage independent growth the cell cycle anchorage requirements must be bypassed. Oncogenic H-Ras has demonstrated the ability to replace these required signals to promote anchorage independent growth, which is also consistent with H-Ras exhibiting hyperactivity in many types of human cancers (Thullberg et al. 2007).

Many recent studies have demonstrated that cells ectopically expressing hTERT, the early region SV40 large T and small t antigens, and activated H-Ras become transformed and thus easily produce large and numerous colonies when suspended in a semi-solid media (Hahn et al. 1999; Elenbaas et al. 2001; Zhao et al. 2003). If activated H-Ras is removed from this combination of elements, then the cells ability to transform is severely compromised, despite the presence of the remaining three elements (Hahn et al. 1999). Given that SGK3 is a downstream effector of H-Ras and PI3-K, studies presented in this section examined the potential of SGK3 to phenocopy activated H-Ras to promote anchorage independent growth *in vitro*. Furthermore, these studies also aimed to compare the ability of SGK3 and the AKT protein isoforms to promote anchorage independent growth. The anchorage independent growth assay used for these studies tested the ability of cells to proliferate and grow in a

Figure 4.3 SGK3 and AKT mutant stable protein expression in IOSE523 cells

The brightest 50% of GFP **(A)** or cherry **(B)** expressing cells were collected by FACS sorting, and subsequently pooled and expanded to establish cell lines. To validate correct protein expression cells were plated at low density in 100mm plates for 48 hr and harvested at approximately 70% confluency. Protein concentrations were determined using DC™ protein assay (Biorad). 20μg of protein was separated by SDS-PAGE (run on 10% gel). IOSE523 cells were stably transduced using virus generated **(A)** from pMIG empty vector, SGK3 CA, SGK3 WT, SGK3 CA PX and SGK3 KD retroviral constructs or **(B)** from pMIC empty vector, H-Ras^{v12}, myrAKT1, myrAKT2, and myrAKT3 retroviral constructs. Expression of proteins was determined by western analysis using indicated antibodies.

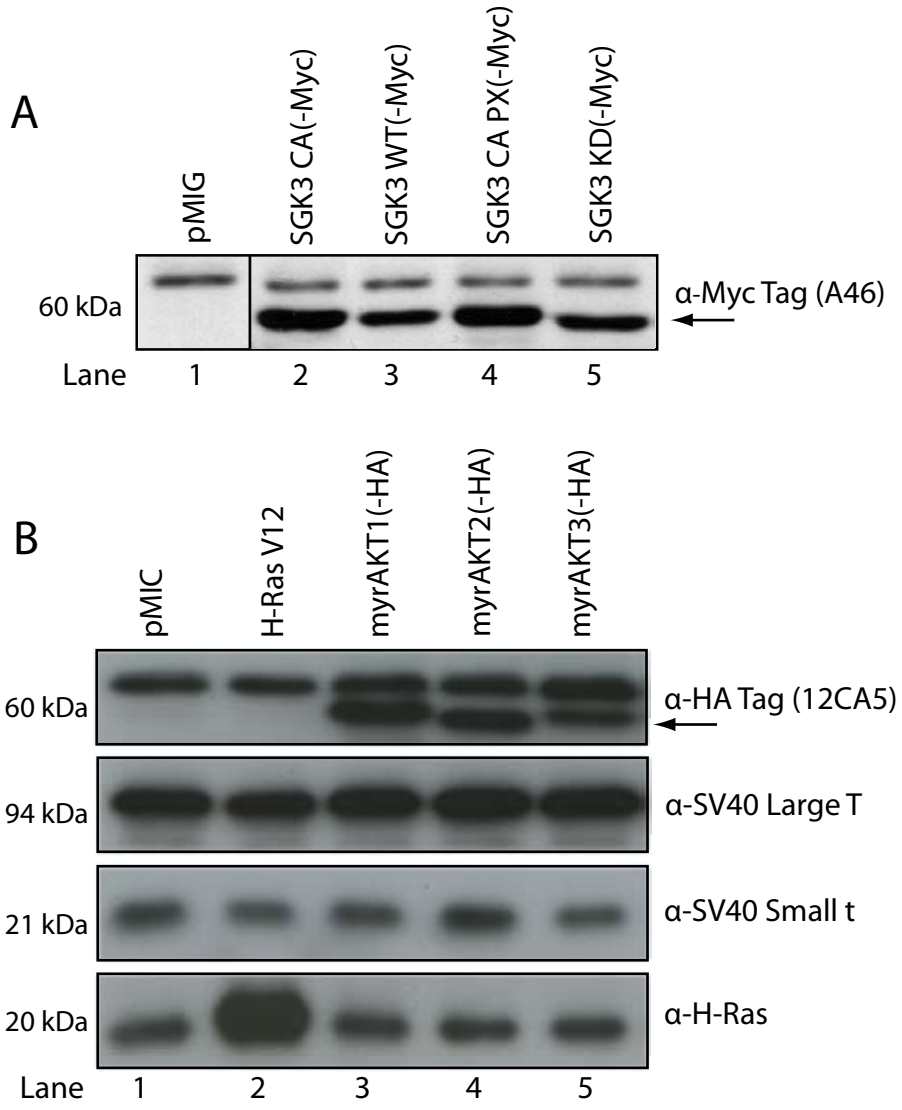
A
pMIG
SGK3 CA(-Myc)
SGK3 WT(-Myc)
SGK3 CA PX(-Myc)
SGK3 KD(-Myc)
60 kDa
α-Myc Tag (A46)
Lane 1 2 3 4 5
B
pMIC
H-Ras V12
myrAKT1(-HA)
myrAKT2(-HA)
myrAKT3(-HA)
60 kDa
α-HA Tag (12CA5)
94 kDa
α-SV40 Large T
21 kDa
α-SV40 Small t
20 kDa
α-H-Ras
Lane 1 2 3 4 5

semi-solid media, independently of the extracellular matrix, where it is likely that the molecular mechanisms that mediate anchorage independent growth are related to the mechanisms that underlie the aggressive growth properties of naturally occurring tumours *in vivo* (Kang and Krauss 1996; Hanahan and Weinberg 2000).

BJ-LST cells stably expressing SGK3 WT, SGK3 CA, SGK3 CA PX, SGK3 KD, myrAKT1, myrAKT2 and myrAKT3, along with pMIG empty vector control, and H-Ras^{v12} were used to perform colony formation assays (Chapter 2.16) to access anchorage independent growth. Analysis of colony number and size generated from BJ-LST cells stably expressing SGK3 mutants demonstrated that SGK3 CA was able to significantly increase colony growth and anchorage independent growth, however not to the same extent as activated H-Ras **(Figure 4.4 A, B and C)**. Furthermore, both SGK3 WT and SGK3 CA PX were unable to significantly induce more colonies than pMIG control **(Figure 4.4 A and C)**, demonstrating that the level of SGK3 activation and cellular localisation play a role in modulating the influence that SGK3 has on anchorage independent growth. SGK3 KD cells generated a greater than expected number of colonies, however this did not reach significance. Comparison of average colony area of colonies generated by each cell line determined no significant differences between sizes of colonies generated through stable over-expression of the SGK3 mutants, however stable over-expression of activated H-Ras had a clear advantage of generating significantly larger colonies **(Figure 4.4 D)**. Furthermore, these data show that there are more colonies generated by SGK3 CA cells when compared with pMIG cells, possibly demonstrating that the proliferative growth rate of the colonies is the same, but the SGK3 CA cells initially had a survival advantage to establish colonies, but once established they grow at the same rate.

Analysis of colony number and size generated from BJ-LST cells stably expressing activated AKT isoforms demonstrated that the stable over-expression of activated AKT1 displayed the most robust effect on anchorage independent growth out of the three AKT isoforms, generating in excess of 100 colonies, significantly more than both myrAKT2, and myrAKT3 cells **(Figure 4.5 A and B)**. These results also show that in the BJ-LST cells, myrAKT1 is able to generate similar colony numbers of that produced by the H-Ras^{v12} cells. However, despite similarities in colony numbers >2mm between myrAKT1 and H-Ras^{v12} cells, there is an observable difference in colony size between these two cell lines. Through measurement of average colony area, colonies are significantly larger in the H-Ras^{v12} cells compared with all other myrAKT cell lines **(Figure 4.5 C)**, demonstrating that in addition to promoting anchorage independent growth, H-Ras is also able to increase proliferative signals to a greater extent than any of the AKT isoforms in the BJ-LST cells, likely via signalling through other mitogenic pathways such as the MAPK pathway, in addition to the PI3-K pathways.

Anchorage independent growth studies were also extended into the IOSE523 genetically defined ovarian epithelial cell model, where unlike the BJ-LST cells, these cell ectopically express SV40 Large T and small t antigen, but not hTERT. The

IOSE523 cells stably expressing SGK3 WT, SGK3 CA, SGK3 CA PX, SGK3 KD, myrAKT1, myrAKT2 along with pMIG empty vector control, and H-Ras^{v12} were used to perform colony formation assays (Chapter 2.16). Analysis of colony numbers revealed that over-expression of SGK3 mutants did not promote anchorage independent growth, compared with H-Ras^{v12} cells that demonstrated an increase in colony number when compared with pMIG vector control cells **(Figure 4.6 A and B)**. Measurement of colony size also revealed that H-Ras^{v12} cells display the largest average colony size in addition to the highest colony numbers **(Figure 4.6 C)**. Taken together these results suggest that in a pre-tumourigenic epithelial background activated SGK3 is not sufficient as a single factor to promote anchorage independent growth.

Colony analysis of IOSE523 cells over-expressing myrAKT isoforms revealed that both activated AKT1 and AKT2 are able to promote anchorage independent growth, showing increases in colony number when compared with pMIG control cells **(Figure 4.7 A and B)**. However, increases in colony numbers by over-expression of both myrAKT1 and myrAKT2 were not equal to those generated through over-expression of H-Ras^{v12} **(Figure 4.7 A and B)**. Through measurement of average colony size both myrAKT1 and myrAKT2 cells demonstrated significantly larger colonies when compared with pMIG control cells, in addition to revealing a similar average colony area to those generated by H-Ras^{v12} cells **(Figure 4.7 C)**. These results suggest that activated AKT isoforms can promote anchorage independent growth as a single genetic factor, albeit to a lesser extent than oncogenic H-Ras.

Lastly, the ability of SGK3 to promote anchorage independent growth was investigated using another epithelial cell line, HOSE. HOSE cells were utilized in Chapter 3 to characterize the role of SGK3 in growth and proliferation, with over-expression of SGK3 in the HOSE cells demonstrating a robust increase in cell proliferation and growth. Given that we have been unable to stably express activated H-Ras in the HOSE cells as they display a senescent phenotype following transduction, we have been unable to determine if over-expression of H-Ras is able to promote robust anchorage independent growth in HOSE cells. However, given that HOSE cells already displayed increases in both proliferation and growth following over-expression of SGK3 CA in earlier studies, this cell line was also used for anchorage independent growth studies. The ability of SGK3 to drive anchorage independent growth in HOSE cells stably expressing SGK3 WT and SGK3 CA, along with pMIG vector control, was determined through performing colony formation assays (Chapter 2.16). Using a standard colony size regulation of >2mm, both HOSE SGK3 WT and SGK3 CA cells did not increase the number of colonies, compared to the pMIG control. In contrast the positive control, IOSE-523 H-Ras^{v12} cells, exhibited a significant increase in colony number colonies **(Figure 4.8 A and B)**. Furthermore, average size of colonies detected in the IOSE523 H-Ras^{v12} cells was also significantly larger than control **(Figure 4.8 C)**. Despite the immortalisation of the HOSE cells using HPV-E6E7 (Tsao et al. 1995), which has shown to inactivate key tumour suppressor genes including p53 and Retinoblastoma (Zhao et al. 2004), it is likely that these cells require further genetic aberrations such

Figure 4.4: SGK3 increases anchorage independent growth in BJ-LST cells

BJ-LST cells exhibiting stable protein expression of pMIG empty vector, SGK3 WT, SGK3 CA, SGK3 CA PX, SGK3 KD, and H-Ras^{v12} were seeded into semisolid 0.4% agarose media at a density of 1 x 10^4 in 35mm plates containing a base layer of 0.8% agarose. Cells were covered with 1ml of appropriate cell culture media and incubated at 37°C for 3 weeks, with cell culture media changed weekly. Liquid media was then removed, and colony formation was detected by staining with 500μl of 2mg/ml MTT at 37°C for 2 hr. **(A)** All plates were photographed from a fixed height on a light box. Each plate shown is representative of n=6. **(B)** Shows the BJ-LST SGK3 CA plate from **(A)** enlarged. **(C)** Detection and analysis of the number of colonies formed >2mm was by detecting all colonies from each image using Metamorph software (Molecular Devices). **(D)** Detection and analysis of colony area was performed using Metamorph software (Molecular Devices). n=6. ± SEM. * $p < 0.05$, *** $p < 0.001$.

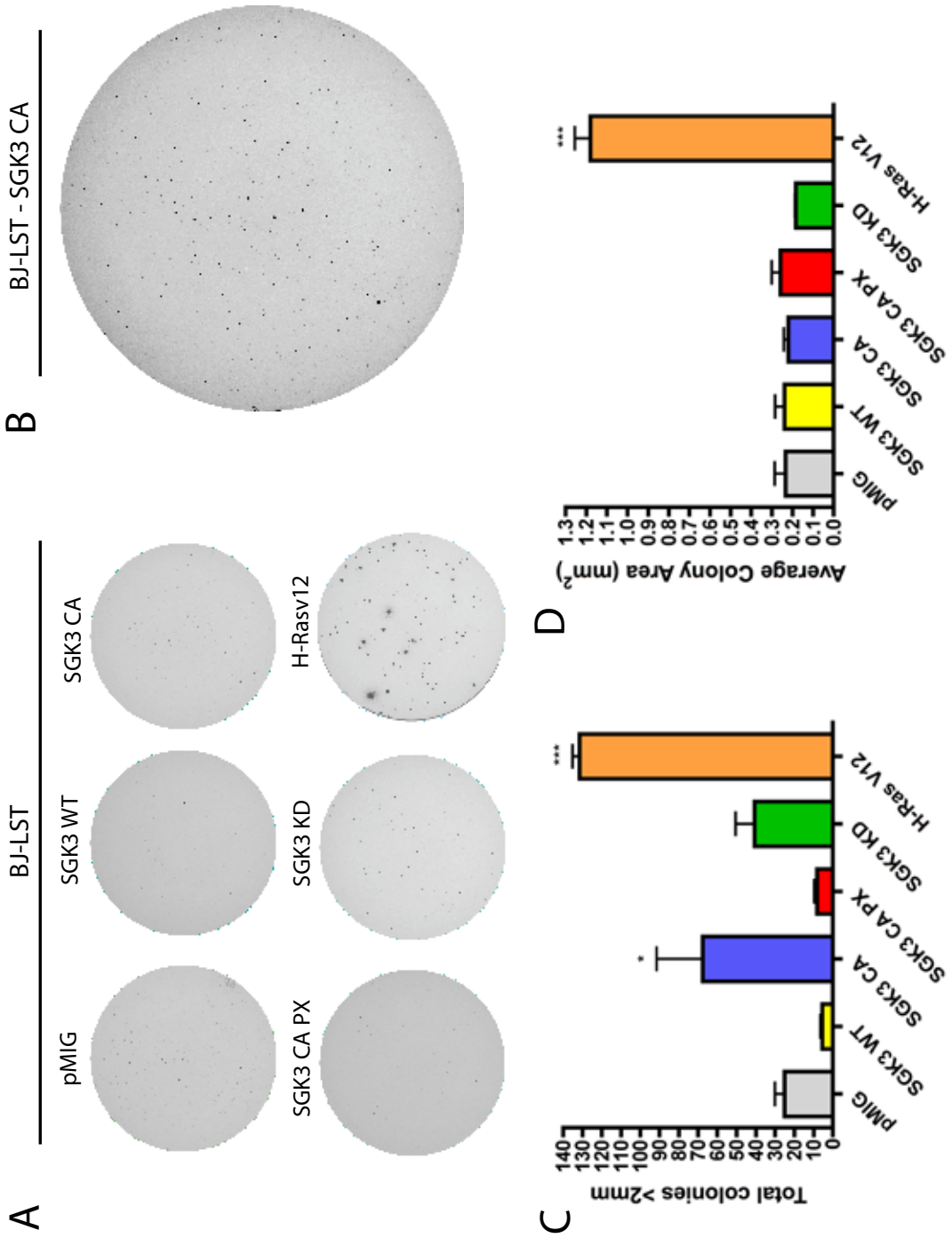
A
BJ-LST
pMIG
SGK3 WT
SGK3 CA
SGK3 CA PX
SGK3 KD
H-Rasv12
B
BJ-LST - SGK3 CA
C
Total colonies >2mm
pMIG
SGK3 WT
SGK3 CA
SGK3 CA PX
SGK3 KD
H-Ras V12
D
Average Colony Area (mm²)
pMIG
SGK3 WT
SGK3 CA
SGK3 CA PX
SGK3 KD
H-Ras V12

Figure 4.5: AKT increases anchorage independent growth in BJ-LST cells

BJ-LST cells exhibiting stable protein expression of pMIG empty vector, myrAKT1, myrAKT2, and myrAKT3 and H-Ras^{v12} were seeded into semisolid 0.4% agarose media at a density of 1 x 10^4 in 35mm plates containing a base layer of 0.8% agarose. Cells were then covered with 1ml of appropriate cell culture media and incubated at 37°C for 3 weeks, with cell culture media changed weekly. Liquid media was then removed, and colony formation was detected by staining with 500μl of 2mg/ml MTT at 37°C for 2 hr. **(A)** All plates were photographed from a fixed height on a light box. Each plate shown is representative of n=6. **(B)** Detection and analysis of the number of colonies formed >2mm was by detecting all colonies from each image using Metamorph software (Molecular Devices). **(C)** Detection and analysis of colony area was performed using Metamorph software (Molecular Devices). n=6. ± SEM. ** $p < 0.01$, *** $p < 0.001$.

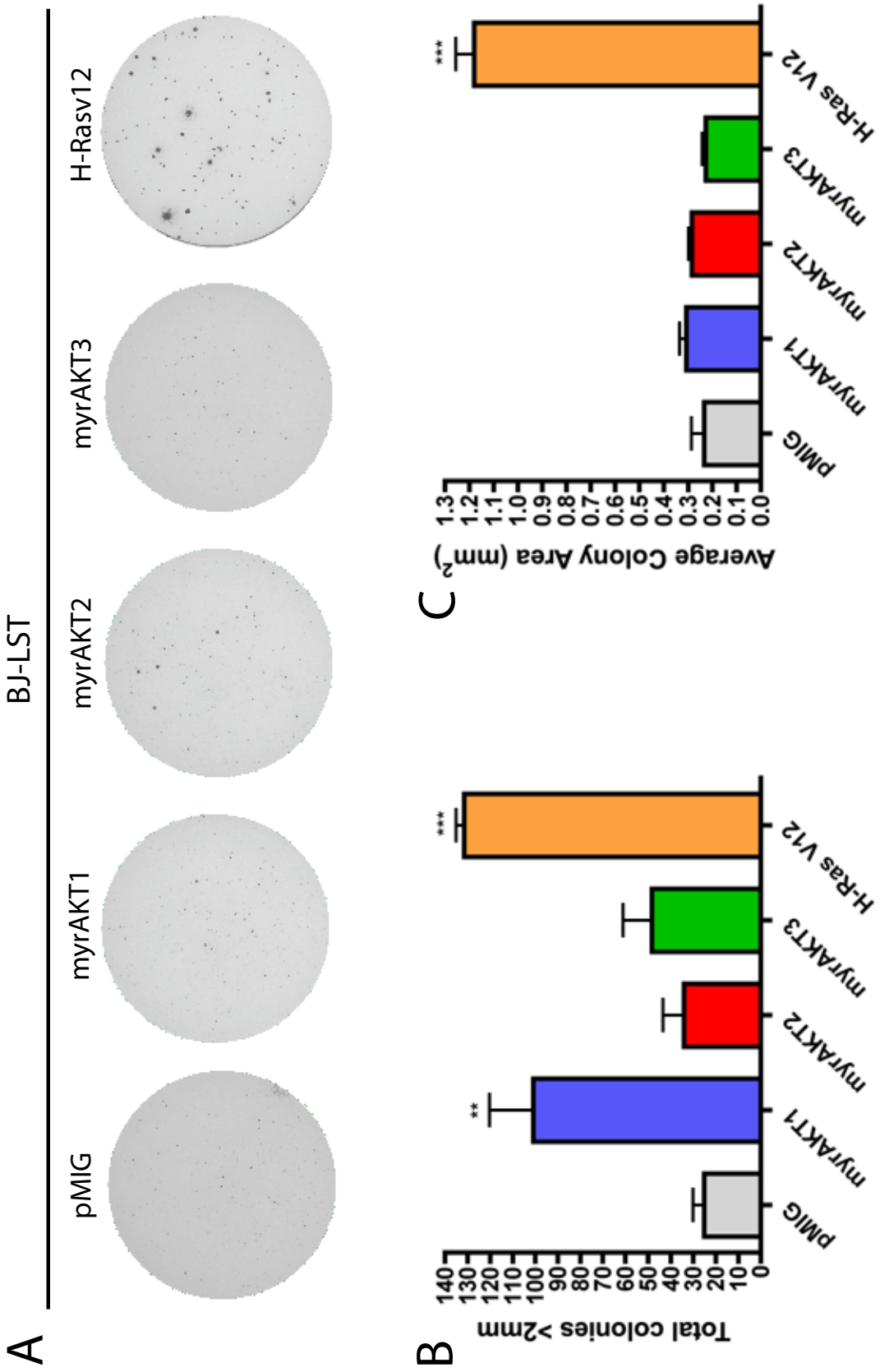
A
BJ-LST
pMIG
myrAKT1
myrAKT2
myrAKT3
H-Rasv12
B
Total colonies >2mm
pMIG
myrAKT1
myrAKT2
myrAKT3
H-Ras V12
C
Average Colony Area (mm²)
pMIG
myrAKT1
myrAKT2
myrAKT3
H-Ras V12

Figure 4.6: SGK3 does not increase anchorage independent growth in IOSE523 cells

IOSE523 cells exhibiting stable protein expression of pMIG empty vector, SGK3 WT, SGK3 CA, SGK3 CA PX, SGK3 KD, and H-Ras^{v12} were seeded into semisolid 0.4% agarose media at a density of 1 x 10^4 in 35mm plates containing a base layer of 0.8% agarose. Cells were then covered with 1ml of appropriate cell culture media and incubated at 37°C for 3 weeks, with cell culture media changed weekly. Liquid media was then removed, and colony formation was detected by staining with 500μl of 2mg/ml MTT at 37°C for 2 hr. **(A)** All plates were photographed from a fixed height on a light box. Each plate shown is representative of n=6. **(B)** Detection and analysis of the number of colonies formed >2mm was by detecting all colonies from each image using Metamorph software (Molecular Devices). **(C)** Detection and analysis of colony area was performed using Metamorph software (Molecular Devices). n=2-6. ± SEM.

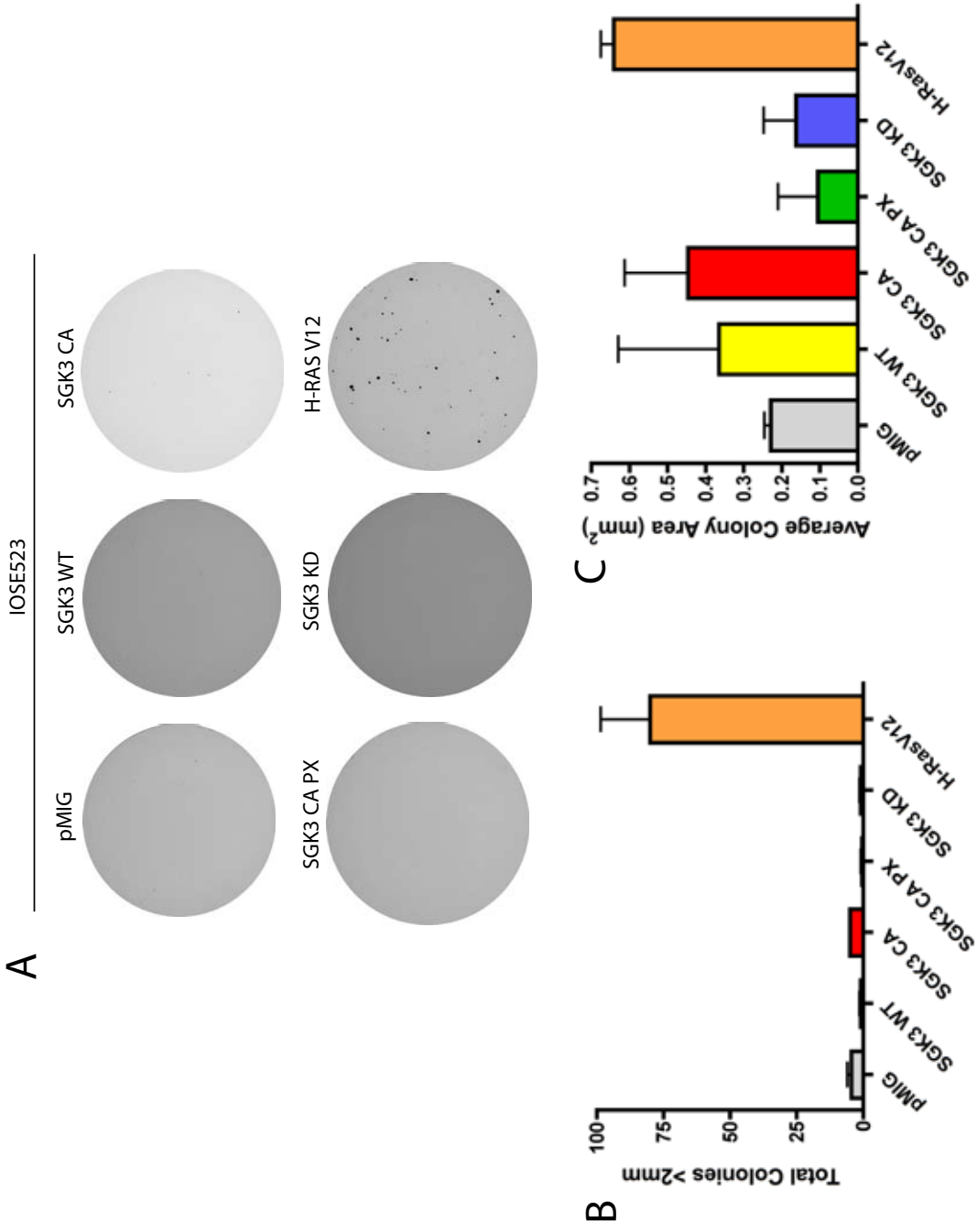
A
IOSE523
pMIG
SGK3 WT
SGK3 CA
SGK3 CA PX
SGK3 KD
H-RAS V12
B
Total Colonies >2mm
0
25
50
75
100
pMIG
SGK3 WT
SGK3 CA
SGK3 CA PX
SGK3 KD
H-RasV12
C
Average Colony Area (mm²)
0.0
0.1
0.2
0.3
0.4
0.5
0.6
0.7
pMIG
SGK3 WT
SGK3 CA
SGK3 CA PX
SGK3 KD
H-RasV12

Figure 4.7: AKT increases anchorage independent growth in IOSE523 cells

IOSE523 cells exhibiting stable protein expression of pMIC empty vector, myrAKT1, myrAKT2 and H-Ras^{v12} were seeded into semisolid 0.4% agarose media at a density of 1 x 10^4 in 35mm plates containing a base layer of 0.8% agarose. Cells were then covered with 1ml of appropriate cell culture media and incubated at 37°C for 3 weeks, with cell culture media changed weekly. Liquid media was then removed, and colony formation was detected by staining with 500μl of 2mg/ml MTT at 37°C for 2 hr. **(A)** All plates were photographed from a fixed height on a light box. Each plate shown is representative of n=6. **(B)** Detection and analysis of the number of colonies formed >2mm was by detecting all colonies from each image using Metamorph software (Molecular Devices). **(C)** Detection and analysis of colony area was performed using Metamorph software (Molecular Devices). n=6. ± SEM. ** $p < 0.01$, *** $p < 0.001$.

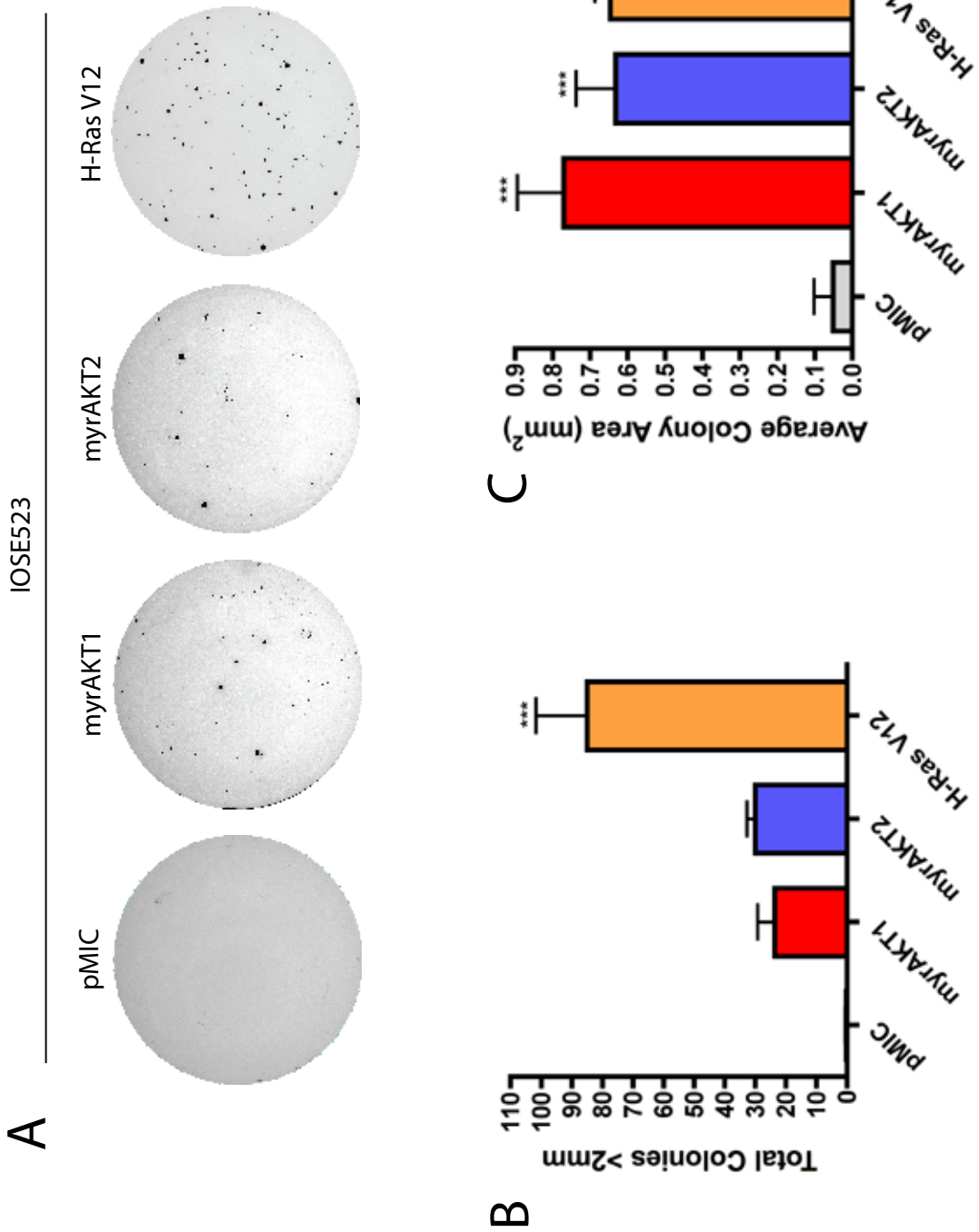
A
IOSE523
pMIC
myrAKT1
myrAKT2
H-Ras V12
B
Total Colonies >2mm
0
10
20
30
40
50
60
70
80
90
100
110
***
pMIC
myrAKT1
myrAKT2
H-Ras V12
C
Average Colony Area (mm²)
0.0
0.1
0.2
0.3
0.4
0.5
0.6
0.7
0.8
0.9
***
***
**
pMIC
myrAKT1
myrAKT2
H-Ras V12

as ectopic expression of small t in addition to increased expression of activated SGK3 to promote anchorage independent growth.

In summary these results suggest that in a pre-tumourigenic fibroblast cell line with hTERT, and both Large T and small t ectopically expressed, both activated SGK3 and AKT are able to promote tumourigenesis as single genetic factors, albeit to a lesser extent than oncogenic H-Ras. However, in an epithelial setting when hTERT, Large T and small t are not ectopically expressed together, activated AKT demonstrated an ability to promote colony formation, while over-expression of activated SGK3 was not sufficient to promote anchorage independent growth as a single genetic factor, suggesting that SGK3 is able to promote anchorage independent growth in a cell type specific manner. Furthermore it is likely that both SGK3 and the AKT isoforms require co-operation with other oncogenic signalling pathways to promote anchorage independent growth to the same extent as oncogenic H-Ras.

4.2.3 AKT but not SGK3 can increase cell migration

Cell migration is essential during the metastatic process, when tumour cells migrate from the primary tumour into circulation to invade other tissue and form secondary tumour sites. The process of conversion from epithelial to mesenchymal cell phenotypes, termed Epithelial-Mesenchymal Transition (EMT) has shown to be implicated in cancer metastasis, and facilitates tumour cells invasion, spread and metastasis, and potentially represents a major mechanism of tumour progression (Micalizzi et al. 2010). Further insight into key modulators of cell migration is a fundamental requirement to further understand the processes of tumour formation, metastasis and EMT, and will allow the development of more specific and targeted cancer therapeutics. To investigate a potential role for SGK3 in cell migration, and compare this to the established ability of AKT to drive cell migration (Cao et al. 2011; Ip et al. 2011; Yadav and Denning 2011), scratch wound assays were carried out.

The scratch wound assay is a well-established *in vitro* method of investigating cell migration through the observation of cells migrating into a scratch wound that is generated on a cell monolayer, known as the wound-healing scratch assay, which is able to mimic the behaviour of cells during migration *in vivo*. One caveat to accurately performing this assay is ensuring that images taken at all time points are of the exact same field of view each time, allowing quantitation of wound width to be an accurate indicator of migration. These studies used a live-cell imaging system known as an IncuCyte (Essen), therefore mitigating any potential issues with measurement inaccuracy, along with providing a secondary measurement of wound confluence for each well.

BJ-LST cells stably expressing SGK3 WT, SGK3 CA, SGK3 CA PX and SGK3 KD, along with pMIG empty vector control, and H-Ras^{v12} were used to perform scratch wound assays (Chapter 2.15) to examine cell migration. Following the scratch, images were taken at 0 hours, and then every 2 to 4 hours for 24 hours, recording changes

in wound confluency and width at each time point. Analysis of wound confluency and width at each time point revealed that stable over-expression of SGK3 WT, SGK3 CA, SGK3 CA PX and SGK3 KD were unable to substantially increase cell migration rate when compared with pMIG vector control **(Figure 4.9 A, B and C)**. Conversely, over-expression of H-Ras^{v12} in the BJ-LST cells were able to migrate to completely cover the wound width at 20 hours post-scratch **(Figure 4.9 A, B and C)**.

Both myrAKT1 and myrAKT2 were stably expressed in BJ-LST cells and analysed for their ability to promote cell migration using the scratch wound assay in the same way as described above. Results demonstrated that both myrAKT1 and myrAKT2 cells mimicked the ability of H-Ras^{v12} to promote wound closure within 20 hours, with a consistent increase of wound confluence and decrease in wound width at every time point, compared with pMIG cells which demonstrated only a subtle increase in wound confluence, and did not show complete closure of the wound area at 24 hours post-scratch **(Figure 4.10 A, B and C)**. BJ-LST cells stably expressing activated AKT3 were unable to be assayed for changes in migration rates using the scratch wound assay, as these cells would not maintain adherence on the plate following the scratch, which may have been due to the combination of serum starvation and anti-proliferative treatment of these cells causing toxicity. Taken together these results suggest that unlike activated AKT1 and 2, SGK3 is unable to promote cell migration in BJ-LST fibroblast cells.

Cell migration experiments were also extended into epithelial cell models, with both the HOSE SGK3 and IOSE523 AKT cell models used to further characterize the ability of these kinases to promote cell migration. The IOSE523 SGK3 cells were not utilised further for studies presented in this chapter following anchorage independent growth assays, as these cells did not demonstrate a phenotype with SGK3 over-expression. HOSE cells stably over-expressing SGK3 WT and SGK3 CA were analysed, using pMIG vector control, and IOSE523 cells stably expressing H-Ras^{v12} as an assay positive control. Following the scratch (Chapter 2.15), images were then taken at 0 hours, and then every 2 hours for 19 hours, recording changes in wound confluency and width at each time point. It was not possible to continue recording changes after 19 hours post-scratch, as the HOSE cells lost adherence and became apoptotic. Results from the HOSE cells revealed no substantial changes in the wound width or confluency of SGK3 WT or SGK3 CA cells after 19 hours post-scratch compared with pMIG vector control cells **(Figure 4.11 A, B and C)**. The IOSE-523 H-Ras^{v12} cells were included as an assay control, and demonstrated an ability to promote cell migration within 19 hours post-scratch.

To compliment the SGK3 ovarian epithelial migration studies, the IOSE523 cells stably expressing myrAKT1, myrAKT2 and myrAKT3, along with pMIC vector control and H-Ras^{v12} were analysed for differences in cell migration using the scratch wound assay also. Conditions used to perform this experiment were the same as described above for the HOSE cell culture model, with wound confluency and wound width monitored

Figure 4.8: SGK3 does not increase anchorage independent growth in HOSE cells

HOSE cells exhibiting stable protein expression of pMIG empty vector, SGK3 WT and SGK3 CA, along with positive experimental control IOSE-523 cells exhibiting stable protein expression of H-Ras^{v12} were seeded into semisolid 0.4% agarose media at a density of 1 x 10^4 in 35mm plates containing a base layer of 0.8% agarose. Cells were then covered with 1ml of appropriate cell culture media and incubated at 37°C for 3 weeks, with cell culture media changed weekly. Liquid media was then removed, and colony formation was detected by staining with 500μl of 2mg/ml MTT at 37°C for 2 hr. **(A)** All plates were photographed from a fixed height on a light box. Each plate shown is representative of n=6. **(B)** Detection and analysis of the number of colonies formed >2mm was by detecting all colonies from each image using Metamorph software (Molecular Devices). **(C)** Detection and analysis of colony area was performed using Metamorph software (Molecular Devices). n=8. ± SEM. *** $p < 0.001$.

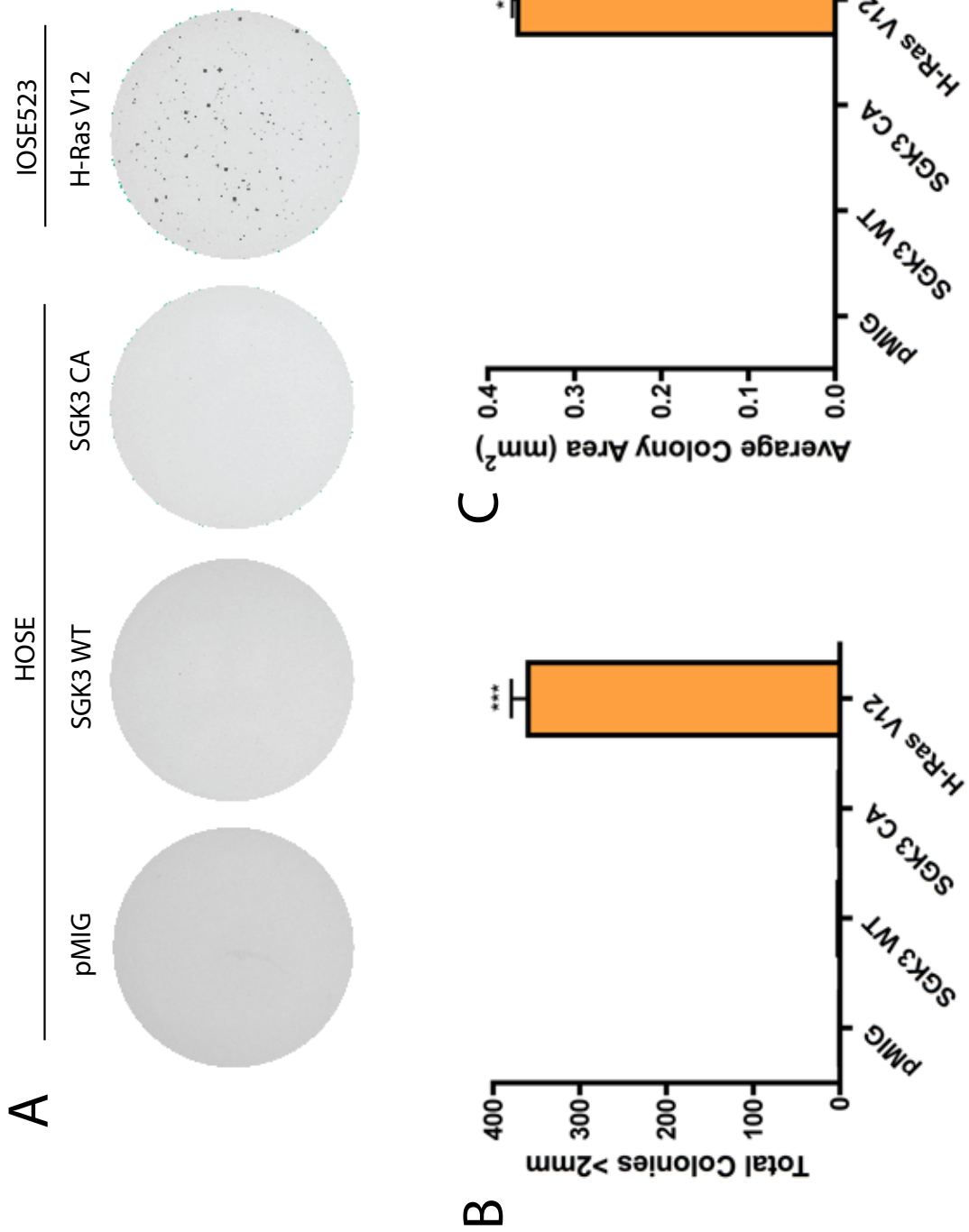
A
HOSE
IOSE523
pMIG
SGK3 WT
SGK3 CA
H-Ras V12
B
Total Colonies >2mm
0
100
200
300
400
***
pMIG
SGK3 WT
SGK3 CA
H-Ras V12
C
Average Colony Area (mm²)
0.0
0.1
0.2
0.3
0.4
***
pMIG
SGK3 WT
SGK3 CA
H-Ras V12

Figure 4.9: SGK3 does not increase cell migration in BJ-LST cells

BJ-LST cells exhibiting stable protein expression of pMIG empty vector, SGK3 WT, SGK3 CA, SGK3 CA PX, SGK3 KD and H-Ras^{v12} were plated at a density of 0.4 x 10^5 in 24 well plates. Cells were incubated for 48 hr and then serum starved overnight. All media was aspirated prior to making a single uniform scratch in each well of cells. Following the scratch, each well was replaced with media containing serum and anti-proliferative agent Mitomycin C. Images were taken of each well at 4 hr intervals from 0 hr 24 hr using the IncuCyte (Essen) and associated software. **(A)** Images of each cell line scratch at 0 hr time point, and at the final time point of 24 hr. **(B)** Graph showing average wound width as measured using IncuCyte (Essen) software. **(C)** Graph showing average wound confluence as measured using IncuCyte (Essen) software. n=3 ± SEM.

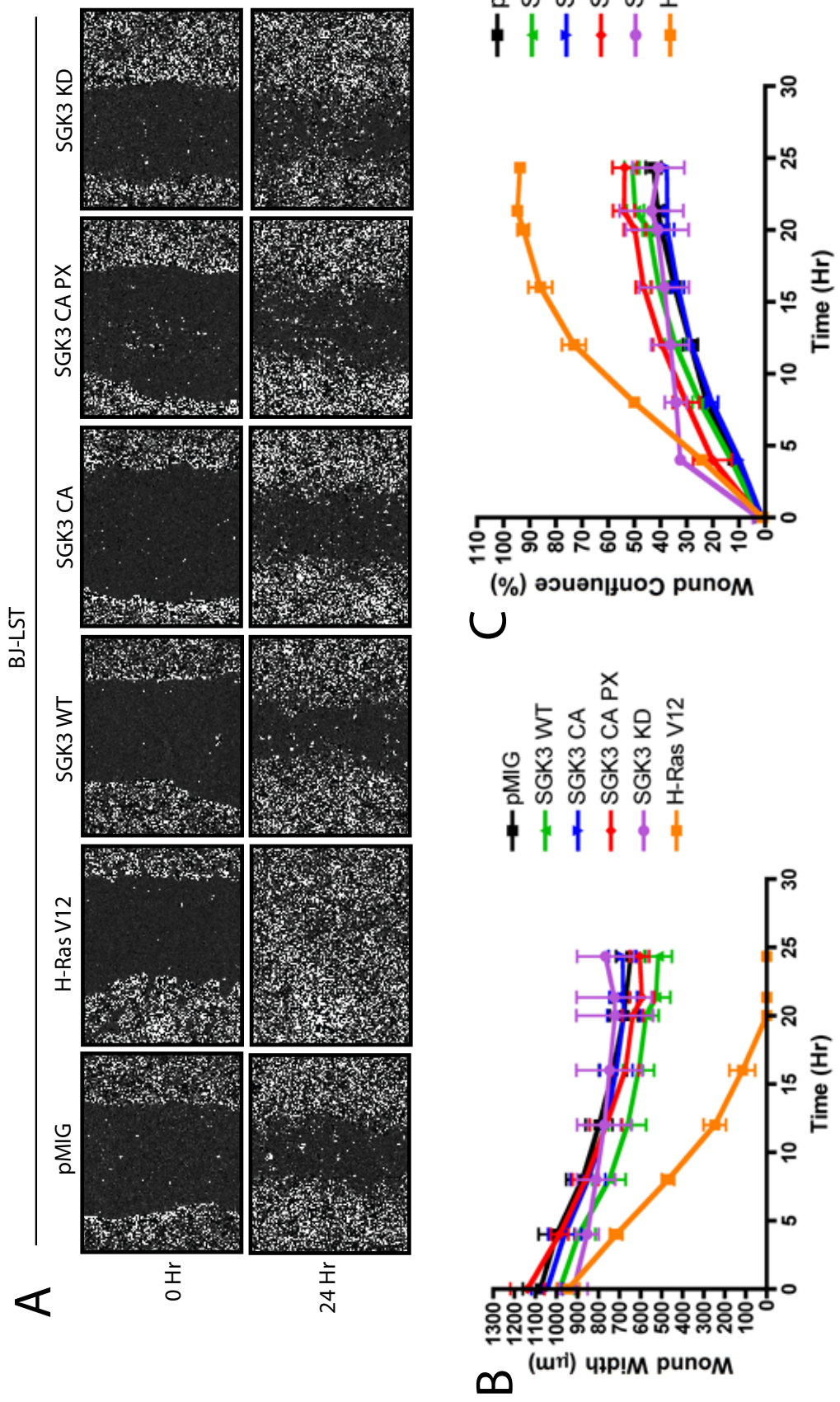
A
BJ-LST
pMIG
H-Ras V12
SGK3 WT
SGK3 CA
SGK3 CA PX
SGK3 KD
0 Hr
24 Hr
B
Wound Width (μm)
Time (Hr)
pMIG
SGK3 WT
SGK3 CA
SGK3 CA PX
SGK3 KD
H-Ras V12
C
Wound Confluence (%)
Time (Hr)

Figure 4.10: AKT increases cell migration in BJ-LST cells

BJ-LST cells exhibiting stable protein expression of pMIC empty vector, H-Ras^{v12}, myrAKT1, myrAKT2, and myrAKT3 were plated at a density of 0.4 x 10^5 in 24 well plates. Cells were incubated for 48 hr and then serum starved overnight. All media was aspirated prior to making a single uniform scratch in each well of cells. Following the scratch, each well was then replaced with media containing serum and anti-proliferative agent Mitomycin C. Images were taken of each well at 4 hr intervals from 0 hr 24 hr using the IncuCyte (Essen) and associated software. **(A)** Images of each cell line scratch at 0 hr time point, and at the final time point of 24 hr. **(B)** Graph showing average wound width as measured using IncuCyte (Essen) software. **(C)** Graph showing average wound confluence as measured using IncuCyte (Essen) software. n=3 ± SEM.

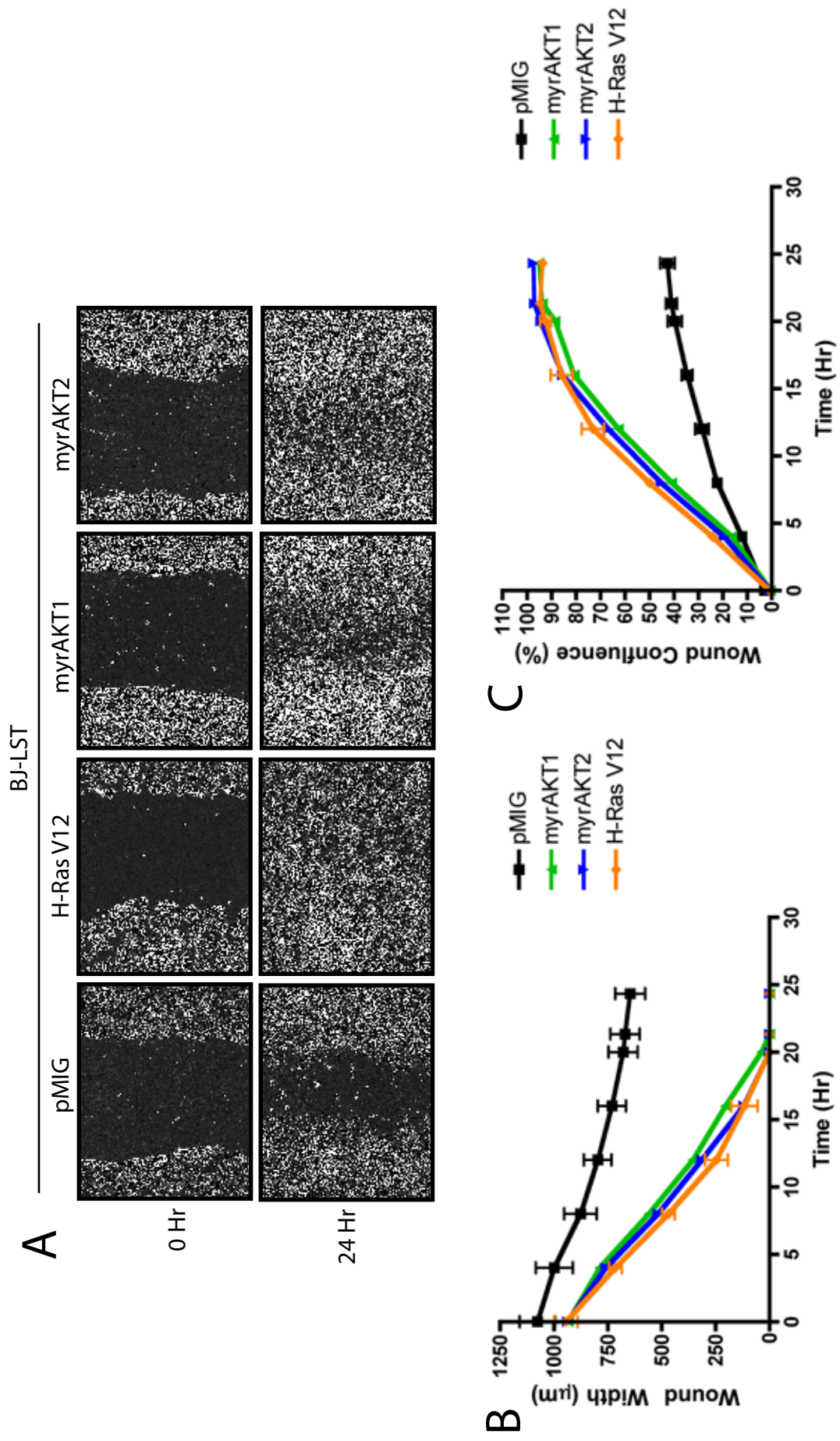
A
BJ-LST
pMIG
H-Ras V12
myrAKT1
myrAKT2
0 Hr
24 Hr
B
Wound Width (μm)
Time (Hr)
pMIG
myrAKT1
myrAKT2
H-Ras V12
C
Wound Confluence (%)
Time (Hr)
pMIG
myrAKT1
myrAKT2
H-Ras V12

Figure 4.11: SGK3 does not increase cell migration in HOSE cells

HOSE cells exhibiting stable protein expression of pMIG empty vector, SGK3 WT and SGK3 CA, together with experimental control cell line IOSE523 H-Ras^{v12} were plated at a density of 0.4 x 10^5 in 24 well plates. Cells were incubated for 48 hr and then serum starved overnight. All media was aspirated prior to making a single uniform scratch in each well of cells. Following the scratch, each well was then replaced with media containing serum and anti-proliferative agent Mitomycin C. Images were taken of each well at 2 hr intervals from 0 hr 19 hr using the IncuCyte (Essen) and associated software. **(A)** Images of each cell line scratch at 0 hr time point, and at the final time point of 19 hr. **(B)** Graph showing average wound width as measured using IncuCyte (Essen) software. **(C)** Graph showing average wound confluence as measured using IncuCyte (Essen) software. n=3 ± SEM.

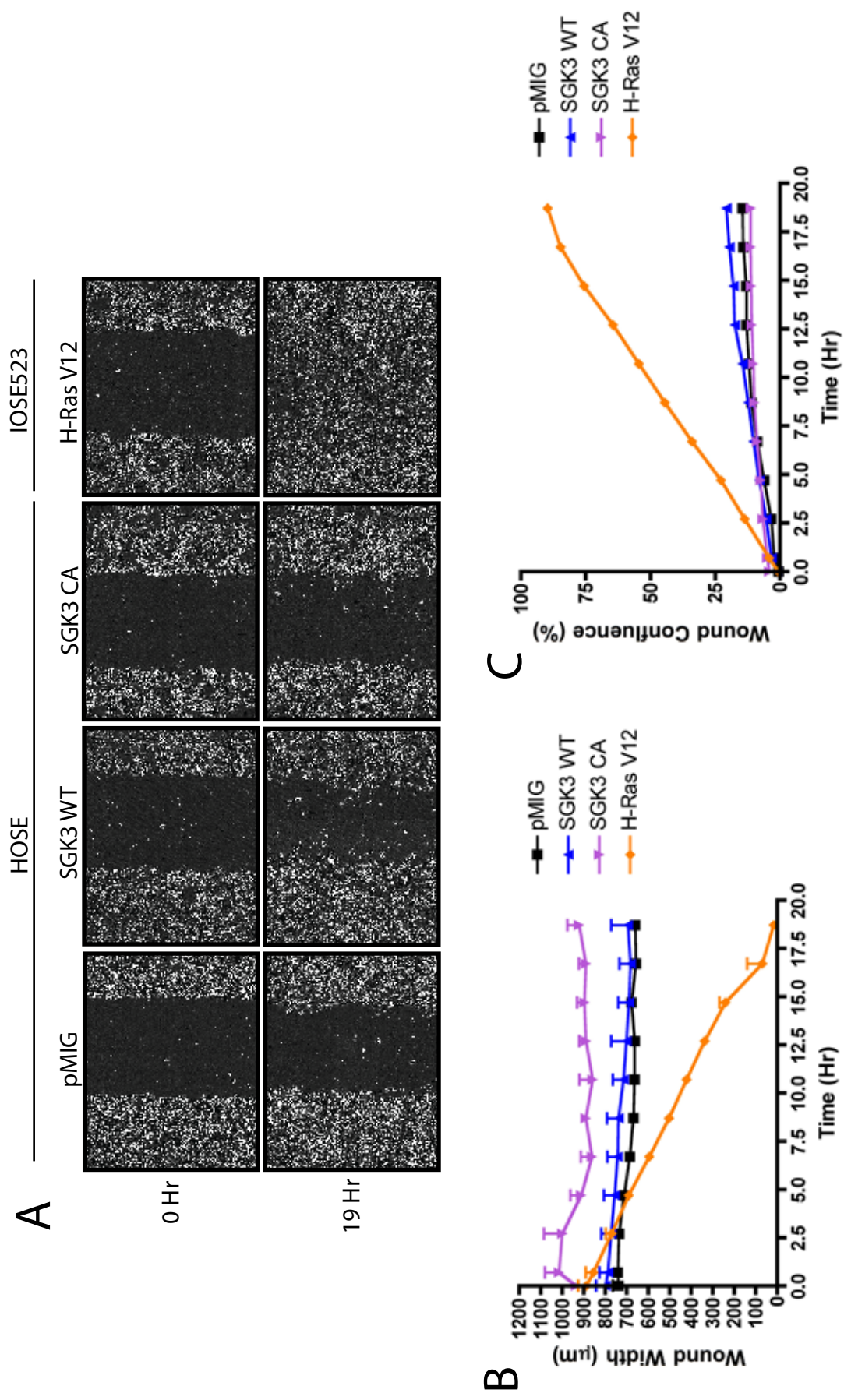
A
HOSE
IOSE523
pMIG
SGK3 WT
SGK3 CA
H-Ras V12
0 Hr
19 Hr
B
Wound Width (μm)
Time (Hr)
pMIG
SGK3 WT
SGK3 CA
H-Ras V12
C
Wound Confluence (%)
Time (Hr)

every 2 hours for 15 hours. IOSE523 cells exhibited a strong basal level of migratory ability, as reflected in the pMIC empty vector cells reaching nearly 80% confluency 15 hours post-scratch **(Figure 4.12 A and B)**. Furthermore, myrAKT1, myrAKT2 and H-Ras^{v12} cells also demonstrated similar increases in wound confluency at each 2 hour time point when compared with pMIC control cells, reaching nearly complete wound closure by 15 hours **(Figure 4.12 A, B and C)**, indicating that addition of other oncogenic factors does not increase migration rates in the IOSE523 cells. Strikingly, the stable expression of myrAKT3 in these cells revealed a decrease in cell migration when compared with both the pMIC vector control, H-Ras^{v12} and the other AKT isoform cells **(Figure 4.12 A, B and C)**, demonstrating that enforced expression of AKT3 may possibly produce dysregulation of adhesion and/or motility signalling.

Previous studies have demonstrated that in a variety of cell types AKT is able to promote cell migration, however to date only few studies have indirectly implicated SGK3 in the regulation of cell migration. Studies presented in this chapter demonstrate that SGK3 is not sufficient to promote cell migration in either an epithelial or fibroblast setting as a single factor. Furthermore, these studies also reveal that while AKT is able to promote cell migration in a pre-tumourigenic fibroblast setting, when over-expressed in epithelial cells it is unable to increase cell migration, with activated AKT3 actually impairing cell migration. It is possible that certain pathways required for cell migration may already hyperactivated in the IOSE523 cells, preventing further over-expression of activated AKT from increasing migration.

4.2.4 SGK3 does not increase cell viability following treatment with chemotherapeutic agents

The importance of signalling through the PI3-K pathway in regulating cell survival and modulating sensitivity to cytotoxic agents in human cancers has been demonstrated by several groups (Krystal et al. 2002; West et al. 2002; Tsurutani et al. 2005; Hartmann et al. 2009; Huang and Hung 2009). While many studies have shown that both SGK1 and SGK3 are able to promote cell survival (Liu et al. 2000; Brunet et al. 2001; Zhang et al. 2005; Endo et al. 2011; Wang et al. 2011), few studies have specifically investigated the ability of SGK3, or other SGK isoforms in promoting resistance to chemotherapeutic agents (Chapter 2.19). Studies presented in this section utilize BJ-LST, IOSE523 and HOSE cell lines stably over-expressing activated SGK3 and AKT isoforms, which have been treated with three different chemotherapeutic agents. These studies aimed firstly to determine if SGK3 is able to promote chemotherapeutic resistance, and secondly to further characterize possible differences in the ability of SGK3 and AKT isoforms to promote chemoresistance.

The first chemotherapeutic agent used in these studies was cisplatin (cis-diamminedichloroplatinum), a potent anti-tumour agent involved in the induction of cell cycle arrest and apoptosis through the formation of DNA adducts, which distort DNA conformation and inhibit replication and transcription (Peng et al. 2010). Cisplatin displays clinical activity against a variety of solid tumours, and is often used as a single

agent or in combination with other chemotherapeutics to treat a variety of tumours including, ovarian, lung, testicular and bladder (Peng et al. 2010). Furthermore studies have also demonstrated that signalling via the AKT/mTOR pathway is increased in cisplatin resistant ovarian tumour cell lines (Peng et al. 2010), which may also potentially involve SGK3 signalling.

To further determine a possible role for SGK3 in promoting increased cell survival following cisplatin treatment, a subset of SGK3 and AKT stable cell lines used in earlier studies presented in this chapter were utilized to conduct cell viability assays using cisplatin. The cell lines used for these studies included HOSE cells stably over-expressing SGK3 WT and SGK3 CA, IOSE523 cells stably over-expressing myrAKT1, myrAKT2, myrAKT3 and H-Ras^{v12}, in addition the BJ-LST fibroblast cells stably over-expressing SGK3 CA, SGK3 KD, myrAKT1, myrAKT2, myrAKT3 and H-Ras^{v12} were also used. Cells were seeded at low density into 6-well plates and allowed to reach 60% confluency before the addition of cisplatin at a range of concentrations between 0 and 500μM. The IC_{50} for cisplatin for each cell line utilized in these experiments was not specifically determined for these studies, however published reports have demonstrated that the IC_{50} for cisplatin is between 0.2μM and 55μM for many other ovarian epithelial tumour cell lines (Freeburg et al. 2009), therefore studies presented in this section used a large dose range to account for possible differences between ovarian and fibroblast cell lines.

Cells were incubated for 48 hours following drug treatment, based on published studies (Freeburg et al. 2009), before harvesting and subsequent addition of Propidium Iodide (PI) for analysis by flow cytometry. Stable over-expression of SGK3 mutant constructs did not produce a marked insensitivity to cisplatin in the HOSE cells, however with 500μM cisplatin treatment both SGK3 WT and SGK3 CA over-expression demonstrated minor rescue when compared with pMIG control cells **(Figure 4.13, A)**. The fibroblast BJ-LST model over-expressing SGK3 CA also revealed no difference in resistance to cisplatin when compared with pMIG control **(Figure 4.13, B)**. The IOSE523 cells stably over-expressing the three myrAKT isoform mutants displayed weak but inconsistent resistance to cisplatin in doses above 10μM compared with pMIC control cells **(Figure 4.13, C)**, while the BJ-LST cells over-expressing myrAKT isoforms displayed minor but consistent resistance to cisplatin in doses above 50μM when compared with pMIG control cells **(Figure 4.13, D).** Furthermore, these results demonstrate very minor, if any resistance to cisplatin with over-expression of oncogenic H-Ras in both epithelial and fibroblast cells **(Figure 4.13, B - C)**, which is consistent with reports suggesting that oncogenic H-Ras is unable to confer resistance to cisplatin in human ovarian tumour cell lines (Holford et al. 1998). Taken together these results indicate that both activated SGK3 and activated AKT can promote a trend towards resistance to cisplatin, however further replicates would need to be performed to determine if this is statistically significant.

Figure 4.12: AKT does not increase cell migration in IOSE523 cells

IOSE523 cells exhibiting stable protein expression of pMIC empty vector, H-Ras^{v12}, myrAKT1, myrAKT2, and myrAKT3 were plated at a density of 0.4 x 10^5 in 24 well plates. Cells were incubated for 48 hr and then serum starved overnight. All media was aspirated prior to making a single uniform scratch in each well of cells. Following the scratch, each well was then replaced with media containing serum and anti-proliferative agent Mitomycin C. Images were taken of each well at 2 hr intervals from 0 hr 15 hr using the IncuCyte (Essen) and associated software. **(A)** Images of each cell line scratch at 0 hr time point, and at the final time point of 15 hr. **(B)** Graph showing average wound width as measured using IncuCyte (Essen) software. **(C)** Graph showing average wound confluence as measured using IncuCyte (Essen) software. n=3 ± SEM.

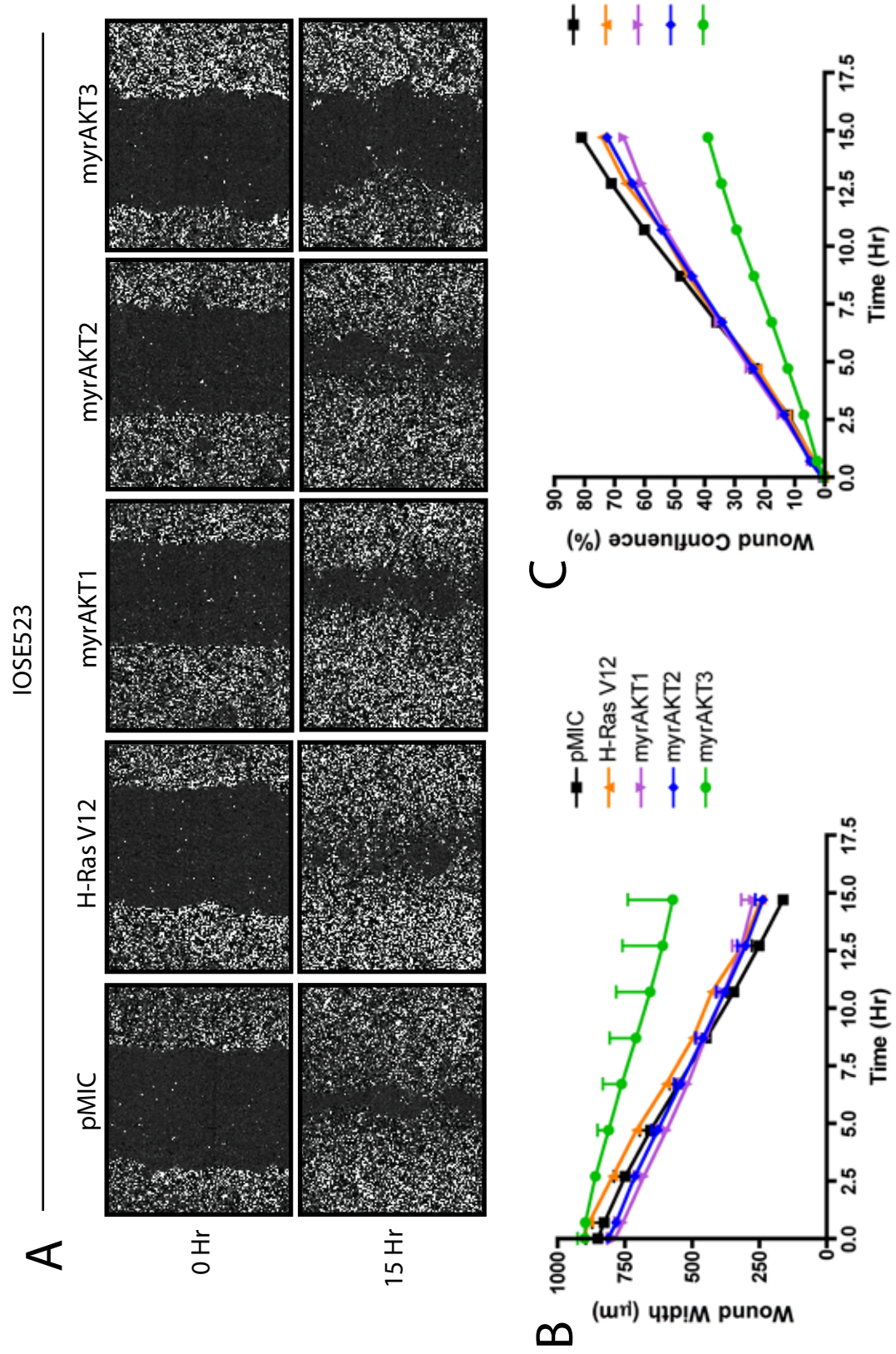
A
IOSE523
pMIC
H-Ras V12
myrAKT1
myrAKT2
myrAKT3
0 Hr
15 Hr
B
Wound Width (µm)
Time (Hr)
pMIC
H-Ras V12
myrAKT1
myrAKT2
myrAKT3
C
Wound Confluence (%)
Time (Hr)

Figure 4.13: The effect of SGK3 and AKT on cell viability following cisplatin treatment

HOSE, IOSE523 and BJ-LST cells exhibiting stable protein expression of a combination of SGK3 and AKT mutants were plated at a density of 1 x 10^5 in 6 well plates and incubated overnight. Cells were then treated with cisplatin at indicated doses and harvested at 48 hr. Following trypsinisation and multiple PBS washes, cells were resuspended in annexin V binding buffer and 2μl of propidium iodide citrate solution. Cells were then analysed for viability using the FACS Canto flowcytometer (BD Biosciences). **(A)** HOSE cells exhibiting stable protein expression of pMIG empty vector, SGK3 WT and SGK3 CA were analysed for cell viability following 48 hr of cisplatin treatment at indicated doses. n=1 **(B)** BJ-LST cells exhibiting stable protein expression of pMIG empty vector, SGK3 CA, SGK KD and H-Ras^{v12} were analysed for cell viability following 48 hr of cisplatin treatment at a indicated doses. n=1 **(C)** IOSE523 cells exhibiting stable protein expression of pMIG empty vector, myrAKT1, myrAKT2, and myrAKT3 and H-Ras^{v12} were analysed for cell viability following 48 hr of cisplatin treatment at indicated doses. n=1 **(D)** BJ-LST cells exhibiting stable protein expression of pMIG empty vector, myrAKT1, myrAKT2, and myrAKT3 and H-Ras^{v12} were analysed for cell viability following 48 hr of cisplatin treatment at indicated doses. n=1

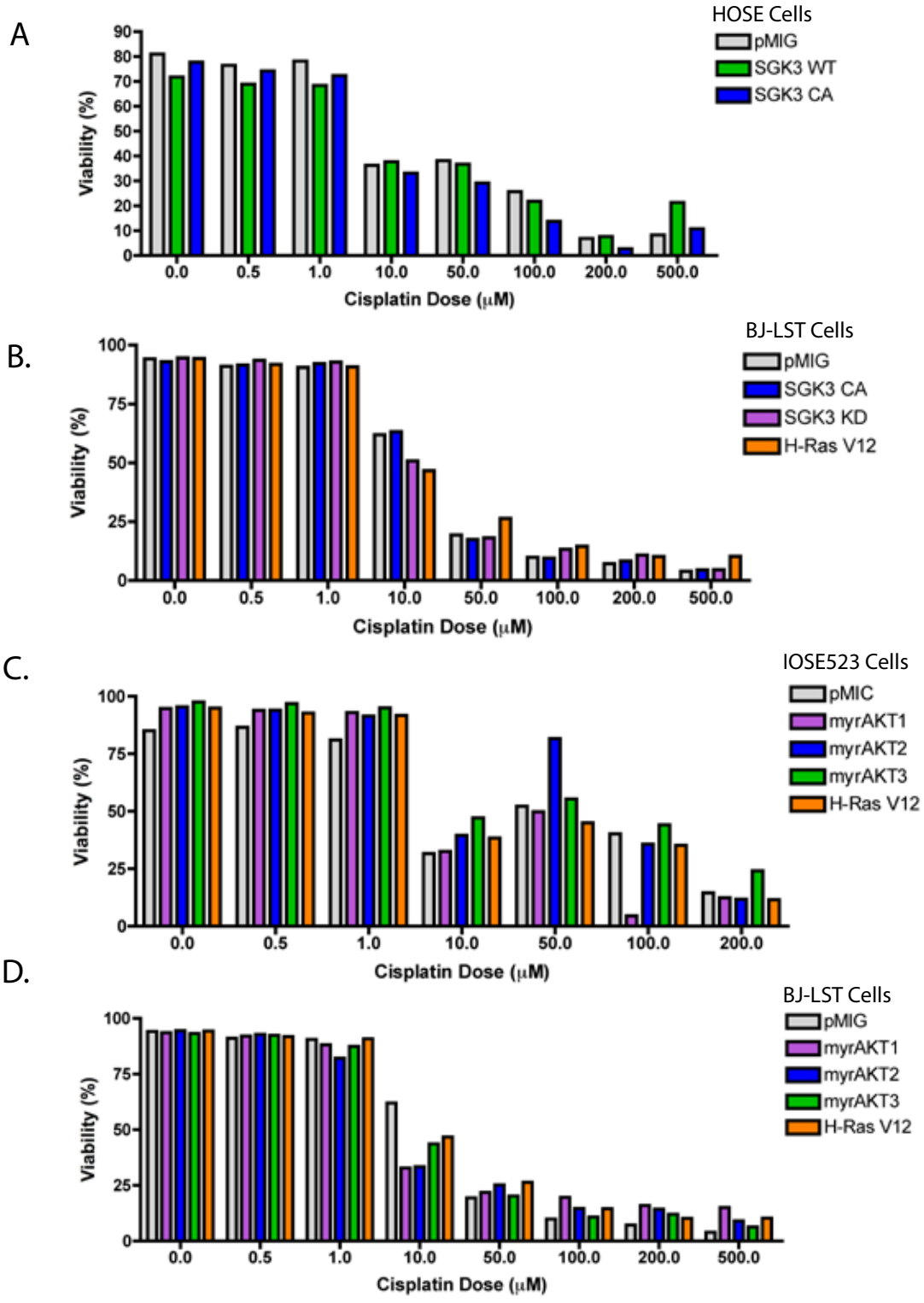
A
HOSE Cells
pMIG
SGK3 WT
SGK3 CA
Viability (%)
Cisplatin Dose (μM)
B.
BJ-LST Cells
pMIG
SGK3 CA
SGK3 KD
H-Ras V12
Viability (%)
Cisplatin Dose (μM)
C.
IOSE523 Cells
pMIC
myrAKT1
myrAKT2
myrAKT3
H-Ras V12
Viability (%)
Cisplatin Dose (μM)
D.
BJ-LST Cells
pMIG
myrAKT1
myrAKT2
myrAKT3
H-Ras V12
Viability (%)
Cisplatin Dose (μM)

The next chemotherapeutic agent to be tested on the same panel of cell lines as those used for cisplatin testing was taxol. Taxol is a commonly used first-line chemotherapeutic agent for many human cancers including ovarian, breast, lung and prostate cancers (McGuire et al. 1996; Ozols 2000; Chang et al. 2009; Rodriguez-Antona 2010). Taxol functions through stabilization of microtubules, which impairs mitosis and leads to cell cycle arrest in G_2/M-phase and the activation of pro-apoptotic signalling (Wang et al. 2000; Chang et al. 2009), with the involvement of Bcl-2 hyperphosphorylation (Blagosklonny et al. 1997; Haldar et al. 1997; Chang et al. 2009). Inhibition of PI3-K and AKT has shown to enhance sensitivity to taxol (Hu et al. 2002; Mabuchi et al. 2002; Luo et al. 2005), indicating the possibility that SGK3 may also promote taxol resistance if over-expressed.

To determine a possible role for SGK3 in promoting taxol resistance, cell lines were treated as described above using taxol as the cytotoxic agent using a 96 hour time point and a taxol dose range of between 0 and 3200nM. In the HOSE cells, lower doses of taxol displayed some minor increase in cell viability with over-expression of either SGK WT or SGK3 CA, however with the higher doses over-expression of SGK3 demonstrated a higher sensitivity to taxol **(Figure 4.14, A)**. In the BJ-LST cells over-expression of SGK3 CA and SGK3 WT, did not consistently increase cell viability to taxol at any dose compared with empty vector pMIG control **(Figure 4.14, B)**. Interestingly, at higher concentrations of taxol, both SGK3 CA and H-Ras^{v12} cell lines exhibited a trend towards an increase in sensitivity to taxol when compared with pMIG empty vector control. This increase in sensitivity to taxol was also evident in IOSE523 **(Figure 4.14, C)** and BJ-LST **(Figure 4.14, D)** cell lines stably over-expressing AKT mutant constructs.

A further cytotoxic agent utilized to determine the ability of SGK3 to promote resistance to cytotoxic agents is vincristine, a vinca alkaloid that inhibits the polymerisation of tubulin subunits, so microtubles do not form, thereby preventing the proper formation and function of the mitotic spindle, impeding mitotic progression (Dorsey et al. 2010). To determine the ability of SGK3 to promote resistance to vincristine, the same panel of cell lines used for the previous cytotoxic agent experiments described in this section were treated using vincristine for 48 hours using between 0 and 200 ng/mL dose range. Similar to the results demonstrating a lack of insensitivity to cisplatin and taxol, HOSE cells over-expressing SGK3 WT and SGK3 CA did not confer resistance to vincristine compared with pMIG control **(Figure 4.15, A).** Furthermore, BJ-LST cells over-expressing SGK3 CA also showed no consistent increase in resistance to vincristine compared with pMIG control cells **(Figure 4.15, B)**. In contrast over-expression of H-Ras^{v12} consistently increased cell viability of BJ-LST exposed to vincristine treatment compared to control cells **(Figure 4.15, B)**. Similarly, IOSE523 **(Figure 4.15, C)** and BJ-LST **(Figure 4.15, D)** cells over-expressing activated AKT isoforms exhibited a minor but consistent decrease in sensitivity to vincristine compared with empty vector control cells. Taken together these studies suggest that activated AKT is able to promote resistance to vincristine in a minor but consistent manner in both epithelial

and fibroblast cells, in contrast to SGK3, which demonstrates an inability to confer resistance to vincristine. However, these studies require further replicates to more conclusively determine the roles of these kinases in conferring resistance to cytotoxic agents.

4.3 Discussion

Studies presented in this chapter aimed to investigate the potential influence that both SGK3 and the AKT isoforms have on established hallmarks of cancer, with particular focus on the activation of invasion and metastasis, in addition to resistance to cell death (Hanahan and Weinberg 2011). These studies employed the use of epithelial (IOSE523) and fibroblast (BJ-LST) isogenic genetically defined cell lines to examine the influence of enforced expression of SGK3 gain of function mutant constructs on key functional readouts of these hallmarks, including anchorage independent growth, cell migration and cell viability following exposure to chemotherapeutic agents. Furthermore, parallel experiments using enforced expression of AKT gain of function mutant constructs in the same cell lines also enabled direct comparison between the effects that SGK3 and the AKT isoforms have on these readouts.

Several reports have implicated the PI3-K/AKT pathway in regulating a multitude of tumourigenic processes, however relatively few have focused on the influence that SGK3 has on malignant cell transformation and tumourigenesis. In this chapter a clear role for activated SGK3 in promoting anchorage independent growth in a pre-tumourigenic fibroblast cell line has been demonstrated. Indeed this role appears to be dependent on SGK3 endosomal localisation. However, despite reports indicating SGK3 association with cell migration and polarity regulation, these studies were unable to show a direct influence of SGK3 on cell migration. Furthermore, these studies were unable to conclusively determine a role for SGK3 in promoting chemoresistance. However, consistent with published data our results do validate the important role that the AKT family has on influencing key tumourigenic processes including anchorage independent growth and cell migration.

4.3.1 Activated SGK3 and AKT promote anchorage independent growth

The use of both IOSE523 epithelial and BJ-LST fibroblast genetically defined cell lines allowed a direct investigation on the ability of activated SGK3 and AKT as single elements to promote phenotypes associated with malignant cell transformation in a defined pre-tumourigenic background. While many studies have used other combinations of introduced genes to transform human cells (Brookes et al. 2002; Lazarov et al. 2002; Seger et al. 2002), studies presented in this chapter firstly utilized the BJ-LST cells, consisting of a combination of hTERT, and early region SV40 small t and Large T antigens, which when ectopically expressed together are considered to confer a pre-tumourigenic background (Hahn et al. 1999). Furthermore, ectopic expression of oncogenic H-Ras in the BJ-LST cells is able to transform these cells,

Figure 4.14: The effect of SGK3 and AKT on cell viability following taxol treatment

HOSE, IOSE523 and BJ-LST cells exhibiting stable protein expression of a combination of SGK3 and AKT mutants were plated at a density of 1 x 105 in 6 well plates and incubated overnight. Cells were then treated with taxol at a range of doses and harvested at 96 hr. Following trypsinisation and multiple PBS washes, cells were resuspended in annexin V binding buffer and 2μl of propidium iodide Citrate solution. Cells were then analysed for viability using the FACS Canto flow cytometer (BD Biosciences). **(A)** HOSE cells exhibiting stable protein expression of pMIG empty vector, SGK3 WT and SGK3 CA were analysed for cell viability following 96 hr of taxol treatment at indicated doses. n=1 **(B)** BJ-LST cells exhibiting stable protein expression of pMIG empty vector, SGK3 CA, SGK KD and H-Ras^{v12} were analysed for cell viability following 96 hr of taxol treatment at a indicated doses. n=1 **(C)** IOSE523 cells exhibiting stable protein expression of pMIG empty vector, myrAKT1, myrAKT2, and myrAKT3 and H-Ras^{v12} were analysed for cell viability following 96 hr of taxol treatment at indicated doses. n=1 **(D)** BJ-LST cells exhibiting stable protein expression of pMIG empty vector, myrAKT1, myrAKT2, and myrAKT3 and H-Ras^{v12} were analysed for cell viability following 96 hr of taxol treatment at indicated doses. n=1

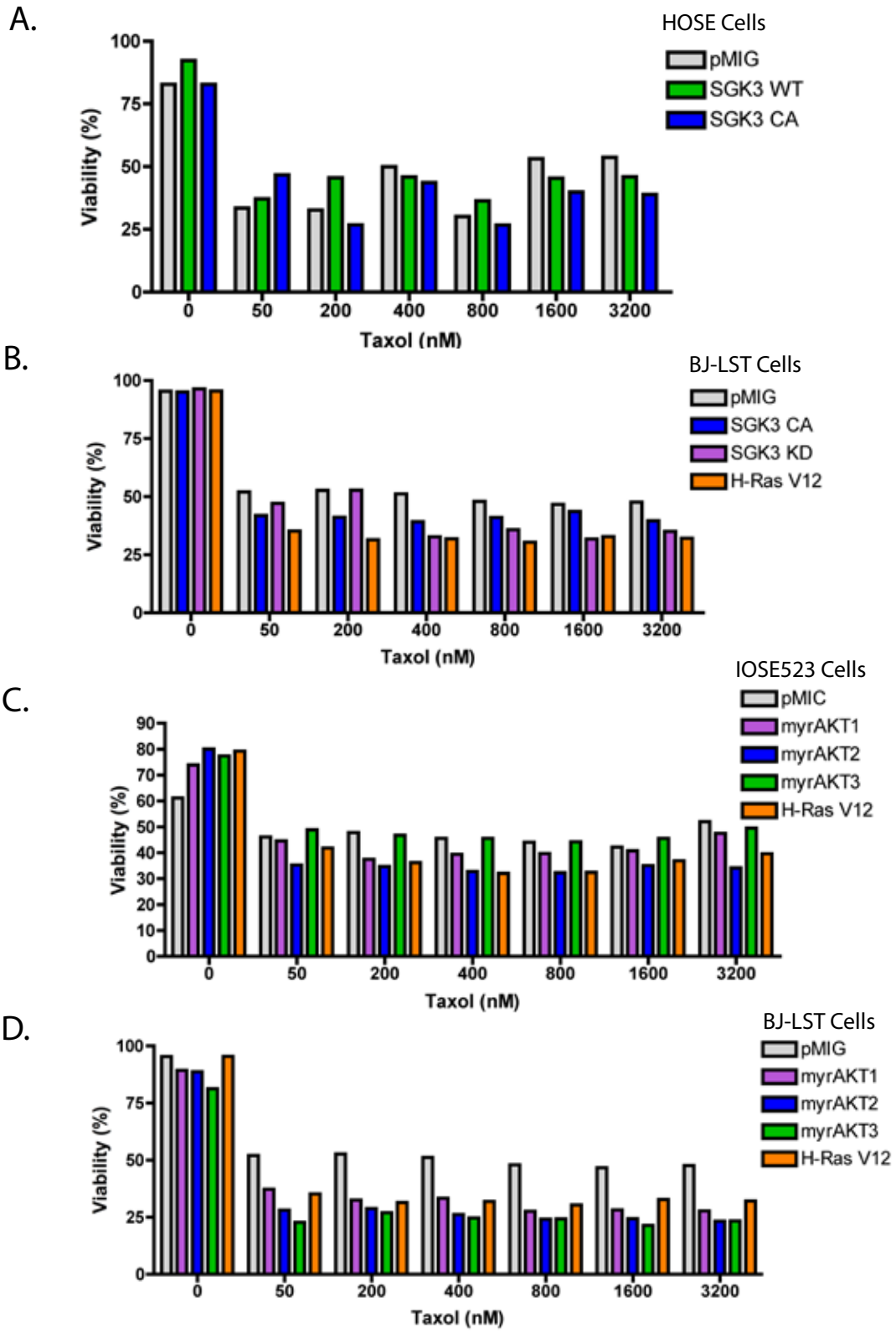
A.
HOSE Cells
pMIG
SGK3 WT
SGK3 CA
Viability (%)
Taxol (nM)
B.
BJ-LST Cells
pMIG
SGK3 CA
SGK3 KD
H-Ras V12
Viability (%)
Taxol (nM)
C.
IOSE523 Cells
pMIC
myrAKT1
myrAKT2
myrAKT3
H-Ras V12
Viability (%)
Taxol (nM)
D.
BJ-LST Cells
pMIG
myrAKT1
myrAKT2
myrAKT3
H-Ras V12
Viability (%)
Taxol (nM)

Figure 4.15: The effect of SGK3 and AKT on cell viability following vincristine treatment

HOSE, IOSE523 and BJ-LST cells exhibiting stable protein expression of a combination of SGK3 and AKT mutants were plated at a density of 1 x 10^5 in 6 well plates and incubated overnight. Cells were then treated with vincristine at a range of doses and harvested at 48 hr. Following trypsinisation and multiple PBS washes, cells were resuspended in annexin V binding buffer and 2μl of propidium iodide citrate solution. Cells were then analysed for viability using the Canto flow cytometer. **(A)** HOSE cells exhibiting stable protein expression of pMIG empty vector, SGK3 WT and SGK3 CA were analysed for cell viability following 48 hr of vincristine treatment at indicated doses. n=1 **(B)** BJ-LST cells exhibiting stable protein expression of pMIG empty vector, SGK3 CA, SGK KD and H-Ras^{v12} were analysed for cell viability following 48 hr of vincristine treatment at a indicated doses. n=1 **(C)** IOSE523 cells exhibiting stable protein expression of pMIG empty vector, myrAKT1, myrAKT2, and myrAKT3 and H-Ras^{v12} were analysed for cell viability following 48 hr of vincristine treatment at indicated doses. n=1 **(D)** BJ-LST cells exhibiting stable protein expression of pMIG empty vector, myrAKT1, myrAKT2, and myrAKT3 and H-Ras^{v12} were analysed for cell viability following 48 hr of vincristine treatment at indicated doses. n=1

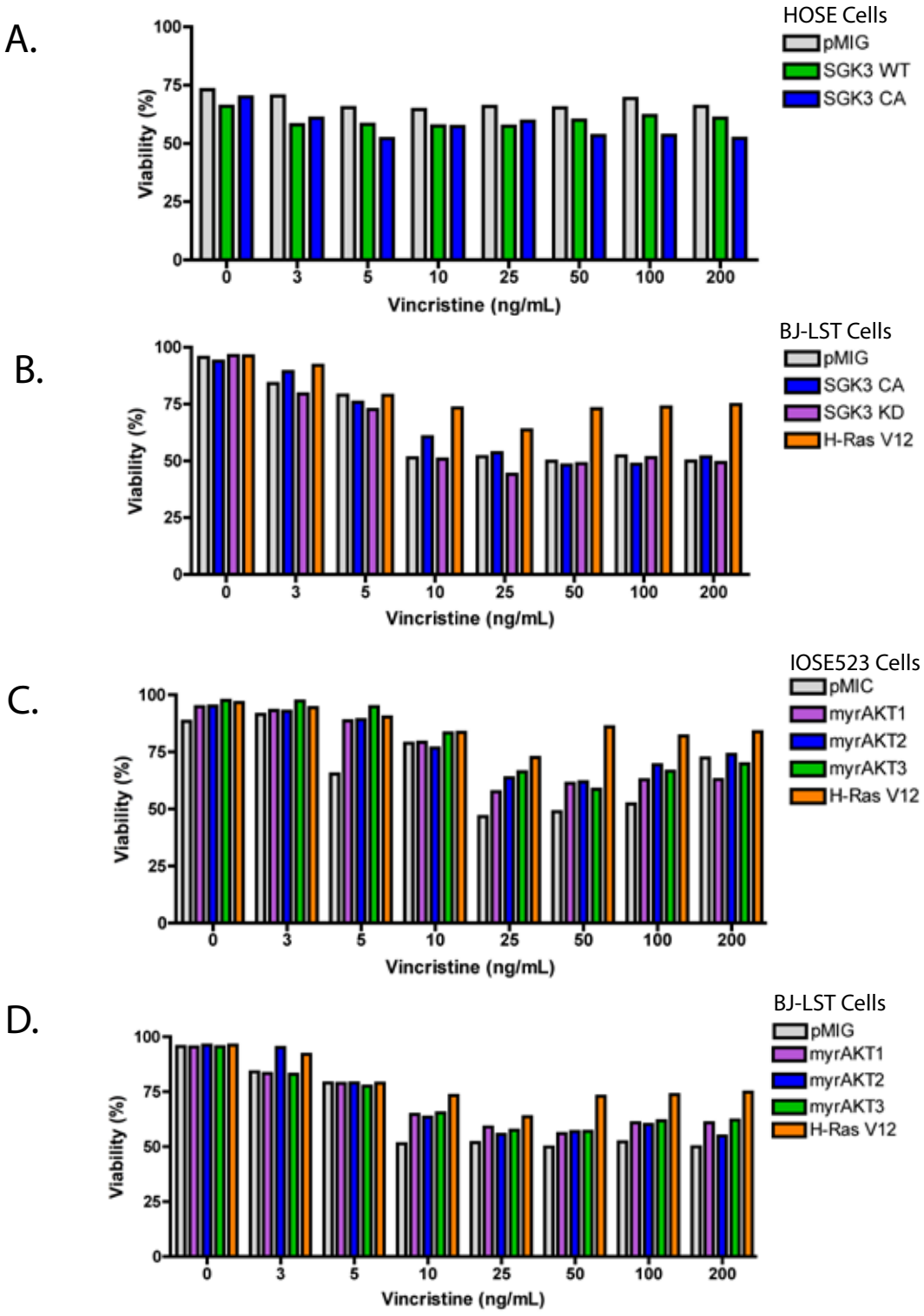
A.
HOSE Cells
pMIG
SGK3 WT
SGK3 CA
Viability (%)
Vincristine (ng/mL)
B.
BJ-LST Cells
pMIG
SGK3 CA
SGK3 KD
H-Ras V12
Viability (%)
Vincristine (ng/mL)
C.
IOSE523 Cells
pMIC
myrAKT1
myrAKT2
myrAKT3
H-Ras V12
Viability (%)
Vincristine (ng/mL)
D.
BJ-LST Cells
pMIG
myrAKT1
myrAKT2
myrAKT3
H-Ras V12
Viability (%)
Vincristine (ng/mL)

with anchorage independent growth indicative of cell transformation. By using the BJ-LST cell lines, we were able to individually introduce SGK3 and the AKT isoforms in order to determine the ability of these kinases to mimic activated H-Ras signalling, and promote cell transformation. Results presented in this chapter demonstrated that enforced expression of both activated SGK3 and the AKT isoforms were able to induce anchorage independent growth, with these cell lines producing significant colony numbers when compared with control cells in the BJ-LST cells.

Resistance to detachment-induced cell death (anoikis), leading to anchorage-independent growth has shown to be achieved through the activation of pro-survival pathways, and has been associated with several important players in integrin-mediated signal transduction, including focal adhesion kinase (FAK), integrin-linked kinase (ILK), PI3-K and ERK (Ilic et al. 1998; Hanks et al. 2003; Taddei et al. 2012). The AKT family have shown to be critical factors mediating the cell survival response, and have shown to be recruited and activated in a PI3-K-dependent manner by FAK and ILK to inhibit anoikis at several levels, including inactivation of caspase-9, phosphorylation of pro-apoptotic protein Bad and the FOXO transcription factors, and activation of NF-κB. As described (Chapter 1.4.5), the SGK family, and more specifically SGK3 have shown to be important mediators of cell survival, demonstrating key roles in regulating pro-apoptotic proteins Bad, the FOXO transcription factors, and the NF-κB pathway. It is possible that SGK3 is able to significantly promote anchorage-independent growth predominantly via its ability to promote resistance to anoikis, and act as a novel convergence point for integrin and growth factor signalling, and like AKT, mediate cell survival signalling in response to integrin ligation. Further characterising the role of SGK3 in anoikis resistance signalling may assist in further elucidating the mechanism behind the ability of SGK3 to induce anchorage-independent growth.

Furthermore, given that SGK3 has shown to be activated at the endosome where it remains, it is likely that SGK3 is able to convey oncogenic signalling from the endosomal compartment, suggesting the possibility of interaction with other endosomal based proteins that may further cooperate with SGK3 to drive malignant transformation. Evidence of this possibility comes from a recent report demonstrating that Na^+/H^+ exchangers (NHEs), important ion transporters that can shuttle between different cellular compartments including the endosomes to regulate cellular pH, cell volume and ion homeostasis, are involved in enhancing tumour progression through involvement in cell-cell adhesion, invasion and anchorage independent growth (Onishi et al. 2012). Furthermore, recent studies have demonstrated that SGK3 is able to co-localise with an NHE family member at the endosome to regulate its activity in a PI3-K-dependent manner (He et al. 2011). Taken together, these studies further suggest that SGK3 may be able to promote anchorage independent growth and oncogenic signalling via interaction with NHE family members from the endosomal compartment.

The importance of PI3-K/AKT signalling in malignant cell transformation has been demonstrated by several reports highlighting amplification and hyperactivation of

PI3-K pathway components in a number of cancer types (Chapter 1.6.1). PI3-K pathway activation has also shown to be crucial for transformation of several cell lines, including human mammary epithelial cells (HMEC) (Zhao et al. 2003), furthermore, inhibition of mTORC2, the complex that activates SGK1 and AKT via phosphorylation at the Ser site in the hydrophobic motif, is able to prevent proliferation and anchorage independent growth in breast tumour and prostate tumour cells (Hietakangas and Cohen 2008). Interestingly, experiments using HMECs have also demonstrated that activated AKT1 is not sufficient to replace active PI3-K to promote cell transformation, suggesting involvement of other PI3-K targets to induce cell transformation (Zhao et al. 2003). Moreover, additional evidence supporting AKT-independent PI3-K oncogenic signalling was demonstrated using *PIK3CA* mutant tumour cells, showing that in cells with low AKT activity, PDK-1 dependent SGK3 signalling was crucial for *PIK3CA* mutant cell viability. These studies, together with studies presented in this chapter demonstrate that SGK3 is likely to be an important factor involved in AKT-independent malignant cell transformation.

To date, despite the significant homology shared between the SGK and AKT families, few studies comparing the ability of these kinase families to regulate key cellular processes, in addition to exploring existing levels of functional redundancy, have been performed. Anchorage independent growth studies presented in this chapter demonstrate that while in identical backgrounds both activated SGK3 and AKT are able to induce colony formation to slightly different extents, neither was able to completely recapitulate the colony growth induced by oncogenic H-Ras. Although, given that H-Ras is able to activate multiple downstream pathways, including PI3-K and Raf, it is likely that the substitution of H-Ras with either SGK3 or AKT is unable to sufficiently drive all required survival and mitogenic pathways to the same extent as oncogenic H-Ras, thus leading to the generation of smaller and less numerous colonies.

Earlier studies demonstrated that activated AKT as a single factor is unable to replace PI3-K to promote cell transformation in HMECs, however additional studies have shown that AKT in combination with Rac1v12 is able to achieve efficient colony formation (Zhao et al. 2003). Moreover, further studies have demonstrated that other combinations of activated AKT with activated members of the MAPK pathway such as BRAF or MEK are also able to produce anchorage independent growth that is indistinguishable from that induced by activated H-Ras (Boehm et al. 2007). Given the results from studies presented in this chapter, it is likely that further studies investigating the ability of SGK3 to cooperate with activated Rac1 or members of the MAPK pathway would also reveal that like AKT, SGK3 is also able to functionally cooperate with other oncogenes to phenocopy activated H-Ras and induce malignant cell transformation. Similarly, it has been shown that the combination of enforced expression of c-myc with myr-AKT and Rac1v12 are sufficient to replace small t and to induce anchorage independent growth in cells expressing hTERT, Large T and H-Ras^{v12}. Hence, demonstrating a functional connection between the c-myc and PI3K pathways in human cell transformation (Zhao

et al. 2003). Further investigation into the ability of SGK3 to cooperate with c-myc and activated Rac1 to replace small t would also allow further characterisation of SGK3 associated malignant cell transformation, in addition to providing platforms relevant to the development of specific chemotherapeutic inhibitors.

Interestingly, an early study using murine fibroblast cells comparing the ability of SGK1 and AKT1 to drive colony formation demonstrated that activated AKT was able to form colonies in soft agar, but activated SGK1 was unable to generate colonies (Sakoda et al. 2003). While together, when compared with studies presented in this thesis, this may indicate an isoform specific role for SGK3 in promoting anchorage independent growth, it is possible that the expression of additional elements may have assisted in cooperating with SGK1 to promote colony formation. However, the level of redundancy existing between the SGK family, and more specifically SGK3 and the AKT isoforms in promoting cell transformation could potentially be more accurately explored through performing anchorage-independent growth assays using a genetically defined cell line which ectopically expressed all elements for complete transformation (hTERT, small t, Large t and H-Ras^{v12}), in addition to enforced SGK3 expression. Use of an AKT inhibitor on these cells would determine the ability of SGK3 to substitute for AKT activity in the context of malignant cell transformation. Based on the level of homology and targets shared between these kinases, it is likely that SGK3 is able to substitute for AKT activity to induce cell transformation.

The use of epithelial IOSE523 cells for anchorage-independent growth studies also provided a similar pre-tumourigenic background to that of the BJ-LST, however these cells were not engineered with ectopic expression of hTERT, thereby making these cells non-immortalised, potentially increasing the level of oncogenic signalling required to induce malignant cell transformation. While there have been no previous reports suggesting that the IOSE523 cells can promote colony growth in semi-solid media, in our hands over-expression of activated H-Ras was able to induce anchorage-independent growth in IOSE523 cells, demonstrating that these cells can be transformed, even without ectopic expression of hTERT. As an alternate model to the BJ-LST cells, the IOSE523 cell lines were useful to compare SGK3 and AKT isoforms in an epithelial background, and demonstrated that in the absence of hTERT, enforced expression of SGK3 cannot promote anchorage independent growth, in contrast to IOSE523 cells with enforced expression of activated AKT which demonstrated significant anchorage-independent growth. It is possible that the differences in subcellular localisation between SGK3 and AKT could potentially affect signalling to anchorage independent growth in the IOSE523 cells, with activated AKT targeted at the plasma membrane more able to access downstream targets and cooperate with other factors to drive malignant cell transformation, in comparison to endosomally localised SGK3.

Similarly, the HOSE cells, which have been immortalised with HPV E6/E7, and therefore contain the ectopic expression of even fewer genetic elements required to induce cell transformation than the BJ-LST or IOSE523 cells, have also not previously

been reported to grow colonies in semi-solid media with the over-expression of activated H-Ras. Furthermore, in our hands the HOSE cells developed a senescent phenotype following stable transduction of H-Ras into these cells, preventing the establishment of a stable HOSE cell line over-expressing H-Ras, thereby preventing further experiments to determine the ability of H-Ras to transform these cells. However, given that HOSE cells over-expressing SGK3 gain of function mutants demonstrated significant growth and proliferation phenotypes (Chapter 3) these cells were included in transformation studies, but like IOSE523 cells, HOSE cells with enforced expression of SGK3 demonstrated an inability to promote anchorage-independent growth. It is likely that despite immortalisation with HPV E6/E7, the HOSE cells are inadequate as a model for cell transformation potential given the absence of required factors demonstrated to confer a transformed phenotype.

Using the BJ-LST and IOSE523 genetically defined cell lines enabled studies presented in this chapter to mimic genetically compromised backgrounds common in tumourigenesis, allowed further investigation into enforced expression of activated SGK3 and AKT on malignant cell transformation. Importantly, in addition to demonstrating a novel role for SGK3 in cell transformation, these studies also further highlighted the requirement of SGK3 endosomal localisation for optimal functionality, as activated SGK3 at the endosome was able to drive anchorage independent growth, while activated but non-endosomally localised SGK3 was not in BJ-LST fibroblast cells. These data combined with cell growth and proliferation data detailed in Chapter 3 clearly demonstrate the importance of SGK3 signalling from the endosome to robustly drive multiple cell processes.

4.3.2 The regulation of cell migration and chemoresistance by SGK3 and AKT

To date studies have indirectly linked SGK3 to potential involvement in regulating cell migration machinery, demonstrating that *sgk3*$^{-/-}$ mice have disorganized hair follicles, suggesting a defect in cell polarity, in addition to a study showing SGK3 can co-localize, interact and phosphorylate the E3 ubiquitin ligase AIP4 in the early endosomes, thereby specifically attenuating the ubiquitin-dependent degradation of CXCR4, a key receptor involved in migration and metastasis (Muller et al. 2001; Scotton et al. 2002; Lapteva et al. 2005; Slagsvold et al. 2006). These studies indicate that SGK3 involvement in migration may only be through an indirect role in regulating receptor sorting. Studies presented in this chapter also demonstrate a lack of direct involvement of SGK3 in cell migration in both epithelial and fibroblast cell lines, with enforced expression of SGK3 unable to confer an increased cell migration response using scratch wound assays.

While studies presented in this chapter show that the scratch wound assay does not demonstrate a role for SGK3 in cell migration, the use of an alternative assay to investigate the ability of SGK3 to influence cell migration may be more useful to extend these studies. More specifically, the use of the Boyden Chamber assay to

measure the ability of cells with enforced expression of SGK3 to migrate towards a chemoattractant, such as a growth factor, where cell motility can be analysed without consideration of the effect from cell-cell interactions. Before a cell can migrate over a measurable distance it must first release cell-cell contacts, where cell migration and cell-cell interactions are controlled by different mechanisms (Sander et al. 1998; Royal et al. 2000; Chen 2005). By using the Boyden Chamber assay it may be possible to further determine if SGK3 is able to stimulate migration, even if unable to induce the disruption of cell-cell interactions.

In contrast to SGK3, activated AKT isoforms were able to increase cell migration in BJ-LST cells, consistent with previously reported role for this kinase family in cell migration, development of tumour invasiveness and metastasis. More specifically, AKT1 is implicated in cell migration through signalling downstream of Rac/Cdc42, a crucial mediator of actin cytoskeleton organization (Higuchi et al. 2001), and also by increasing cell motility in fibroblasts through phosphorylation of the actin binding protein Girdin (Enomoto et al. 2005). Furthermore, both AKT1 and AKT2 have been show to promote invasion of pancreatic cells through up-regulation of the IGF-I receptor (Tanno et al. 2001). However, in contrast to BJ-LST cells, enforced expression of activated AKT isoforms in the IOSE523 cell lines did not increase cell migration when compared with control. It is possible that signalling to migration in these cells may already be hyperactivated, where further activation does not further stimulate migration signalling, or it is also possible that like SGK3, the AKT kinases are not involved in directly regulating migration in IOSE523 cells. Furthermore, it is important to note that while the IOSE-523 cell model displayed a high basal level of cell migration, an obvious decrease is cell migration was observed in cells expressing activated AKT3, which displayed a much lower wound confluence compared with the other isoforms. Moreover, BJ-LST cells stably transduced with activated AKT3 also demonstrated an inability to maintain adherence under migration assay conditions. Taken together, these data suggest potential involvement for AKT3 in regulating adherence.

Accumulating evidence has demonstrated that in addition to dysregulation of cell growth, proliferation and migration, the ability of a cell to promote chemoresistance is an important characteristic of tumourigenesis. Many studies have implicated the AKT kinase family in eliciting a robust survival response following treatment with multiple types of chemotherapeutic agents, therefore implicating this kinase family in tumour chemoresistance. Whilst there are many reports providing evidence that SGK3 is indeed an important kinase involved in cell survival signalling, few studies have been performed demonstrating a role for SGK3 in inducing a chemoresistance response.

To further explore the role of SGK3 in chemoresistance, we utilized epithelial and fibroblast genetically defined cell models in a cell viability assay using three distinct cytotoxic agents; cisplatin, taxol and vincristine. These cytotoxic agents were selected as they each have unique mechanisms of action, and are also commonly used first-line chemotherapeutic drugs for a variety of human cancers. In our hands SGK3

had no influence on the resistance of either the ovarian or fibroblast cells to the chemotherapeutic agents used. Conversely, consistent with published literature, we demonstrated that enforced expression of activated AKT isoforms is able to possibly provide a moderate level of resistance to the cytotoxic agents used, however further experimentation is required to repeat these investigations for a conclusive analysis.

In summary, the results of studies presented in this chapter have demonstrated a novel role for SGK3 in inducing anchorage independent growth and malignant cell transformation, and further support the importance of SGK3 endosomal localisation for optimal functionality. Moreover, as expected, these data further support the already established role of AKT as a crucial element in promoting processes associated with tumourigenesis, and demonstrate that the AKT kinase family displays a more robust ability to influence important hallmarks of tumourigenesis such as cell migration when compared to SGK3. Further studies, potentially using a loss of function approach, in addition to extending cell transformation studies to incorporate *in vivo* models may more conclusively determine how necessary SGK3 signalling is for these processes. Together, studies presented in this chapter demonstrate the significance of SGK3 as an effector of PI3-K signalling in malignant cell transformation, and highlight the potential importance of SGK3 as a critical player in AKT-independent PI3-K signalling, and a novel chemotherapeutic target.

5. Gene expression studies using microarrays of epithelial and fibroblast cell lines over-expressing SGK3 and AKT

5.1 Introduction

SGK3 is involved in ion channel signalling, cell proliferation and cell survival signalling through negative regulation of a number of pro-apoptotic targets. Moreover, studies presented in this thesis have shown that SGK3 is involved not only in cell proliferation, but also in the regulation of cell growth and potentially transformation. Despite similarities in upstream regulation and downstream targets between AKT and the SGK's there are clear differences in phenotypes generated from over-expression of SGK3 and the AKT kinase family, suggesting potential differences between downstream targets and signalling networks.

Microarray technology has shown to be very effective in identifying diagnostic markers, as well as the intrinsic pathways implicated in the pathogenesis of various diseases, allowing greater insight into crucial biological processes in both health and disease. Using expression array analysis and bioinformatic interrogation of the data this chapter sought to identify global gene expression trends associated with over-expression of SGK3 in multiple cell lines, in an attempt to identify genes and pathways involved in SGK3 signalling and then correlate these changes with the phenotypes identified. In addition, expression array analysis of cell lines over-expressing AKT were analysed in parallel to determine potential signalling differences between SGK and AKT. The microarray gene expression data generated was interrogated using a variety of bioinformatic approaches in an attempt to identify genes associated with SGK3 signalling.

5.2 Methods

Studies outlined in this chapter utilized the same gain of function cell lines that have already been described and characterised extensively in Chapters 3 and 4. The cell lines included the epithelial ovarian cell lines HOSE, stably expressing both SGK3 WT and SGK3 CA (as described in Chapter 3.2), and the IOSE523 cell line stably expressing myrAKT1, myrAKT2 and myrAKT3 (as described in Chapter 4.2). The IOSE523 cells stably expressing SGK3 CA did not show any phenotypic changes compared with the control cell line (as described in Chapter 4.2), thus this cell line was not included in the microarray studies presented in this chapter. The fibroblast cell line BJ-hTERT stably expressing SGK3 CA, and BJ-hTERT cell lines stably expressing myrAKT1, myrAKT2 and myrAKT3 (as described in Chapter 3.2) were used for gene expression studies in order to gain a more direct comparison of expression differences existing between SGK3 CA and the AKT kinases.

Following the generation of stable cell lines through retroviral transduction and subsequent FACS (Chapter 2.3.3), cells were seeded at 1 x 10^6 in 100mm plates and harvested for RNA at 70% confluency. RNA was extracted (as described in Chapter 2.20.1), and subsequently assessed for purity using the Bioanalyzer (Agilent), all samples were then sent off-site to The Ramacotti Centre (Sydney, NSW) for microarray analysis. All samples were run on an Affymetrix 1.0 ST chip, with three independent samples processed for each cell line. All gene expression data was then returned and primary bioinformatic analysis of the raw data was conducted with the aid of the Peter MacCallum Cancer Centre Bioinfomatics core (Jason Ellul).

Using packages from Bioconductor (Gentleman et al. 2004), all data was loaded into the statistical program R (Team 2011). All chips were assessed for overall quality using the package affyPLM (as described in Chapter 2.20.2) (Bolstad 2004; Bolstad et al. 2005; Brettschneider et al. 2007), and all data was normalised and background corrected using the robust multi-array average (RMA) expression (Irizarry et al. 2003). Differential gene expression was assessed using the Affy (Gautier et al. 2004) and Limma (Smyth 2005) software packages (as described in Chapter 2.20.2), where any probesets that had a false discovery rate (FDR) adjusted p-value (p-val) (Benjamini and Hochberg 1995) less than 0.05 were considered differentially expressed. In addition to a FDR adjusted p-val of less than 0.05, all gene expression changes with a fold change greater than 2 for each cell line were also determined in order to more thoroughly investigate genes and pathways displaying the most robust changes.

The main aim of the gene expression studies was to investigate pathways regulated by SGK3 in both epithelial and fibroblast cells, and to determine the similarities between SGK3 and the AKT family. Two bioinformatic approaches were used. The first used the MetaCore™ platform by GeneGo (http://www.genego.com/metacore.php). This is an integrated knowledge database and software suite for pathway analysis of experimental data and gene lists. This platform allowed assessment of functional ontology categories of pathways enriched in the differential gene expression data, where a GeneGo pathway can be defined as a canonical map defining a signalling mechanism.

The second bioinformatic approach utilized was Gene Set Enrichment Analysis (GSEA) from the Broad Institute (http://www.broadinstitute.org/gsea) (Subramanian et al. 2005). The C2 (curated gene sets) Molecular Signatures Database (MSigDB) v3.0 (http://www.broadinstitute.org/gsea/msigdb/genesets.jsp?collection=C2) is a catalogue of hundreds of curated gene sets formatted for use with GSEA. Gene sets contained in the MSigDB are collected from published gene expression profiles, where a particular gene has been manipulated or a disease implicated, and provides an unbiased readout of biological state, reflecting transcriptional changes. The GSEA algorithm ranks all array genes according to their expression, and is able to integrate the known knowledge of a gene's functional role with the expression data

to detect concerted expression changes in a set of genes responsible for producing a phenotype. To determine the null distribution, gene permutation rather than sample permutation was used due to the small number of samples.

5.3 Results

5.3.1 Gene expression profiles in SGK3 transduced HOSE cells

The HOSE cell lines over-expressing SGK3 WT and SGK3 CA (as described in Chapter 3.2) were both used for gene expression studies, as these cell lines exhibited robust phenotypic changes, including an increase in cell proliferation, and increased signalling through the mTORC1 growth pathway. Some obvious differences were also detected between HOSE SGK3 WT and SGK3 CA (as described in Chapter 3.2); where activated SGK3 is able to increase both growth and proliferation in the HOSE cells, SGK3 WT can increase proliferation but increases growth to a lesser extent than activated SGK3. The analysis of gene expression data from the HOSE cells aimed to determine pathways and processes most robustly represented by both HOSE SGK3 WT and SGK3 CA cell lines, in an attempt to define differences that may account for differences in phenotype. All array data generated from HOSE SGK3 WT and SGK3 CA cell lines was initially normalised against the vector only control cell line HOSE-pMIG to control for expression changes not relevant to specific mutant expression.

5.3.1.1 Gene expression changes and pathway analysis in SGK3 WT over-expression

Gene expression data revealed that the stable over-expression of SGK3 WT in HOSE cells induced 687 differentially expressed genes, with the up-regulation of 364 genes and down-regulation of 323 genes. The majority of differentially regulated genes were concentrated within a +/- 4 fold change (FC) **(Figure 5.1)**. To increase the stringency of the analysis of the significantly regulated genes we applied a FC cut off of 2 and p-val of <0.05 to the significantly regulated genes data set, and found that this then gave 169 genes differentially expressed, with 71 genes up-regulated and 98 genes down-regulated. In order to provide a 'snapshot' of the most robustly regulated genes, the top 20 genes up-regulated and the top 20 genes down-regulated ranked according to FC are listed in **Table 5.1.** As expected, the positive control, SGK3 displayed the highest up-regulation, while most of the remaining top 20 differentially regulated genes do not have a previously reported association with SGK3. However, solute carrier family 14 (urea transporter) member 1 (Kidd blood group) (*SLC14A1*) did show significant down-regulation in these cells, consistent with SGK3's role in regulation of transporters (Bohmer et al. 2010).

All HOSE SGK3 WT data was loaded into the MetaCore™ platform for GeneGo pathway and network process analysis, producing results ranked by p-val, which was calculated using the formula for hypergeometric distribution. The significance cut off for all MetaCore™ analysis was selected at p <0.05. A FC of both 0 and 2 was applied

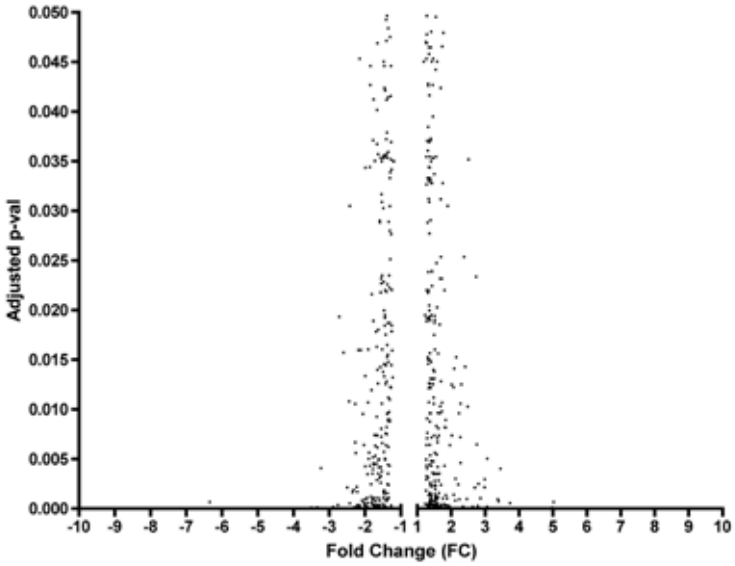

Figure 5.1: HOSE SGK3 WT compared with HOSE pMIG gene expression data. n=3. p-val <0.05.

Table 5.1: HOSE SGK3 WT compared with HOSE pMIG gene expression data. Ranked according to fold change. n=3, p-val <0.05. Top 20 up-regulated and top 20 down-regulated genes. See supplementary data DVD affixed to the back cover for complete list.

UP-REGULATED GENES			DOWN-REGULATED GENES		
Gene Symbol	**Fold Change**	**Adjusted P-Value**	**Gene Symbol**	**Fold Change**	**Adjusted P-Value**
SGK3	64.65147672	9.67E-63	RNF144B	-3.518094173	5.99E-11
FAM198B	7.618187207	5.81E-09	ADAM23	-3.612788628	2.63E-12
BEX1	7.529694401	3.06E-08	MIR492	-3.673194862	3.13E-07
STMN2	6.942220127	2.10E-13	TIMP3	-3.747219788	2.22E-06
C6orf138	5.935015059	3.88E-14	EMB	-3.764491685	5.99E-11
PI3	5.118971886	6.02E-08	DUOXA2	-3.803600304	1.14E-19
DCN	5.016165963	0.000662998	MALL	-3.892531438	9.36E-06
IFI44L	4.971955931	0.000125325	C4BPA	-4.39604058	2.82E-15
FGB	4.968675296	2.41E-19	PPP2R2B	-4.717024738	1.10E-24
ATP8B4	3.954684451	2.25E-22	ARHGAP29	-4.835353202	4.38E-12
H19	3.761662314	2.24E-12	GPR87	-4.860900854	2.93E-05
GFRA1	3.756409052	6.21E-07	SLC14A1	-4.864149978	2.69E-15
CXCL12	3.731912501	0.000559701	CD24	-4.98238992	3.68E-06
ADAMTS5	3.729579214	5.51E-07	DSP	-5.013026503	1.15E-15
C6orf138	3.476177214	1.40E-16	AKR1B10	-5.392100016	1.18E-09
FST	3.450730151	0.004040474	DUOX2	-6.312264419	2.36E-36
ENPP2	3.391205681	0.000749415	MMP1	-6.345552556	0.000662998
MX2	3.370337736	0.000962546	PLAT	-9.062078625	2.26E-16
GPR183	3.25476435	1.40E-16	PART1	-9.190938102	1.93E-34
DIO2	3.060363622	0.005038971	KRT19	-15.6524886	6.58E-18

to all MetaCore™ analyses in order to gain both a broad indication of pathways and process networks associated with SGK3 up-regulation, in addition to a more specific analysis of genes demonstrating robust differential expression.

Pathway analysis for HOSE SGK3 WT cells using a p-val of <0.05 and no FC cut off revealed a significant involvement of SGK3 WT in 37 pathways (**supplementary data Table S.1**), the top 10 are listed in **Table 5.2**. Generally these pathways are involved in tissue remodelling, inflammation and mitogenic signalling **(Table 5.2)**. Applying a FC cut off of 2 and a p-val of <0.05 indicated 17 pathways were significant in SGK3-WT cells (**supplementary data Table S.2**) with the majority of pathways associated with tissue remodelling, wound repair, and both the immune and inflammatory response. More specifically the changes in gene expression predict that SGK3 WT would modulate cell adhesion and increases in the immune and inflammatory responses **(Table 5.3)**.

GSEA was also used to analyse HOSE SGK3 WT gene expression. 736 out of 2526 gene sets from the Molecular Signatures Database were enriched in HOSE SGK3 WT cells, with 43 gene sets significant at FDR <25%. A FDR of <25% is recommended for interpreting GSEA, as given the small number of gene sets analysed, using a more stringent FDR cut off may result in potentially significant data being overlooked. Interestingly, many of the top 20 ranked enriched gene sets are described as interferon (*IFN*) -α and -β induced gene signatures, or related to immune or inflammatory responses **(Table 5.4)**. This analysis support the findings from the GeneGo analysis, and manual inspection reveal multiple genes in the IFN pathway to be differentially regulated including signal transducers and activators of transcription 1 (*STAT1)* and *STAT2*, interferon alpha-inducible protein 6 (*IFI6)* and interferon-stimulated gamma factor 3 (*ISGF3)*. These gene expression data have possibly uncovered a novel function of SGK3 placing it downstream of interferon signalling.

5.3.1.2 Gene Expression changes with SGK3 CA over-expression

Analysis of differential gene expression data generated from HOSE SGK3 CA cells following normalization with pMIG control, revealed that the stable over-expression of SGK3 CA induced differential regulation of 859 genes, with the up-regulation of 439 genes and down-regulation of 420 genes. Similar to the HOSE SGK3 WT cells, the majority of the differentially regulated genes were concentrated with a +/-4 FC **(Figure 5.2)**. To further identify genes with more robust FC, we applied FC cut off 2 to this data set, and found that this reduced significant total differential regulation to 172 genes, with 105 genes up-regulated and 67 genes down-regulated. The top 25 genes up-regulated and the top 25 genes down-regulated ranked according to FC are listed in **Table 5.5**.

MetaCore™ pathway and network process analysis of HOSE SGK3 CA data using p-val of <0.05 and FC of 0 produced only four statistically significant maps that were associated with processes related to cytoskeleton remodelling, cell adhesion and p53

Table 5.2: HOSE SGK3 WT Top 10 GeneGO pathways identified using a FC 0, p-val <0.05. Ranked according to p-val. See Appendix I for complete list.

#	GeneGO Pathways	P-Value
1	Signal transduction_IP3 signaling	5.535e-6
2	Development_PIP3 signaling in cardiac myocytes	3.331e-5
3	Immune response_IFN alpha/beta signaling pathway	3.382e-5
4	Cytoskeleton remodeling_TGF, WNT and cytoskeletal remodeling	4.484e-5
5	Immune response_IL-15 signaling	5.205e-5
6	Immune response_Function of MEF2 in T lymphocytes	5.302e-5
7	Neurophysiological process_Dopamine D2 receptor transactivation of PDGFR in CNS	5.527e-5
8	Cell adhesion_PLAU signaling	7.348e-5
9	Immune response_Fc epsilon RI pathway	1.070e-4
10	Development_HGF signaling pathway	2.498e-4

Table 5.3: HOSE SGK3 WT Top 10 GeneGO pathways identified using a FC >2, p-val <0.05. Ranked according to P-val. See Appendix I for complete list.

#	GeneGO Pathways	P-Value
1	Development_Regulation of epithelial-to-mesenchymal transition (EMT)	1.137e-5
2	Cell adhesion_PLAU signaling	1.365e-5
3	Blood coagulation_Blood coagulation	1.365e-5
4	Signal transduction_IP3 signaling	4.247e-5
5	Cell adhesion_ECM remodeling	5.682e-5
6	5Transport_Macropinocytosis regulation by growth factors	1.435e-4
7	Cell adhesion_Chemokines and adhesion	1.441e-4
8	Development_HGF signaling pathway	5.307e-4
9	Immune response_Antiviral actions of Interferons	7.815e-4
10	Immune response_IL-17 signaling pathways	1.341e-3

Table 5.4: Top 20 ranked GSEA gene sets enriched in HOSE-SGK3 WT. FDR <25%, ranked according to FWER p-val (http://www.broadinstitute.org/gsea/msigdb/). See supplementary data DVD affixed to the back cover for complete list.

Rank	GSEA set	Brief description of GSEA set	FDR q-val
1	RADAEVA_RESPONSE_TO_IFNA1_UP	Genes up-regulated in primary hepatocytes and Hep3B (hepatocyte) cells in response to IFNA.	0.000
2	MOSERLE_IFNA_RESPONSE	Top 50 genes up-regulated in ovarian cancer progenitor cells (also known as side population, SP, cells) in response to interferon alpha (IFNα).	0.000
3	ZHANG_INTERFERON_RESPONSE	Interferon-inducible genes up-regulated in A549 cells (lung cancer) infected with a respiratory syncytial virus (RSV) that had its NS1 gene knocked down by RNAi.	0.000
4	BROWNE_INTERFERON_RESPONSIVE_GENES	Genes up-regulated in primary fibroblast culture after treatment with interferon alpha for 6 h.	0.000
5	ZHU_CMV_ALL_UP	Up-regulated at any timepoint following infection of primary human foreskin fibroblasts with CMV	0.000
6	GEORGANTAS_HSC_MARKERS	Genes up-regulated in HSC (hematopoietic stem cells) compared to HPC (hematopoietic progenitor cells).	0.001
7	MAHADEVAN_RESPONSE_TO_MP470_UP	Top genes up-regulated in the GIST (gastrointestinal stromal tumor) cell line resistant to imatinib after treatment with MP470, a protein kinase inhibitor.	0.000
8	ZHU_CMV_8_HR_UP	Up-regulated at 8 h following infection of primary human foreskin fibroblasts with CMV	0.001
9	DER_IFN_ALPHA_RESPONSE_UP	Genes up-regulated in HT1080 cells (fibrosarcoma) by treatment with interferon alpha for 6 h.	0.001
10	EINAV_INTERFERON_SIGNATURE_IN_CANCER	A gene expression signature found in a subset of cancer patients suggestive of a deregulated immune or inflammatory response.	0.001
11	BENNETT_SYSTEMIC_LUPUS_ERYTHEMATOSUS	Genes significantly up-regulated in the blood mononuclear cells from patients with systemic lupus erythematosus compared to those from healthy persons.	0.001
12	NIKOLSKY_BREAST_CANCER_20Q11_AMPLICON	Genes within amplicon 20q11 identified in a copy number alterations study of 191 breast tumor samples.	0.001
13	REACTOME_P130CAS_LINKAGE_TO_MAPK_SIGNALING_FOR_INTEGRINS	Integrin signaling is linked to the MAP kinase pathway by recruiting p130cas and Crk to the FAK/Src activation complex.	0.002
14	REACTOME_GRB2_SOS_PROVIDES_LINKAGE_TO_MAPK_SIGNALING_FOR_INTERGRINS_	Genes involved in Grb2:SOS provides linkage to MAPK signaling for Integrins	0.002
15	REACTOME_PLATELET_AGGREGATION_PLUG_FORMATION	Genes involved in platelet aggregation (Plug Formation)	0.002
16	REACTOME_INTEGRIN_ALPHAIIBBETA3_SIGNALING	Genes involved in integrin alphaIIbbeta3 signaling	0.002
17	FARMER_BREAST_CANCER_CLUSTER_1	Interferon, T and B lymphocyte genes clustered together across breast cancer samples.	0.003
18	XU_AKT1_TARGETS_6HR	Genes up-regulated in DU-145 cells (prostate cancer) expressing a dominant negative form of AKT1 upon sham-treatment for 6 hr (as a control for the HGF experiments).	0.003
19	XU_HGF_TARGETS_INDUCED_BY_AKT1_6HR	Genes changed in DU-145 cells (prostate cancer) in the absence but not presence of a dominant negative form of AKT1 upon exposure to HGF for 6 hr.	0.003
20	NIKOLSKY_BREAST_CANCER_20Q12_Q13_AMPLICON	Genes within amplicon 20q12-q13 identified in a copy number alterations study of 191 breast tumor samples.	0.005

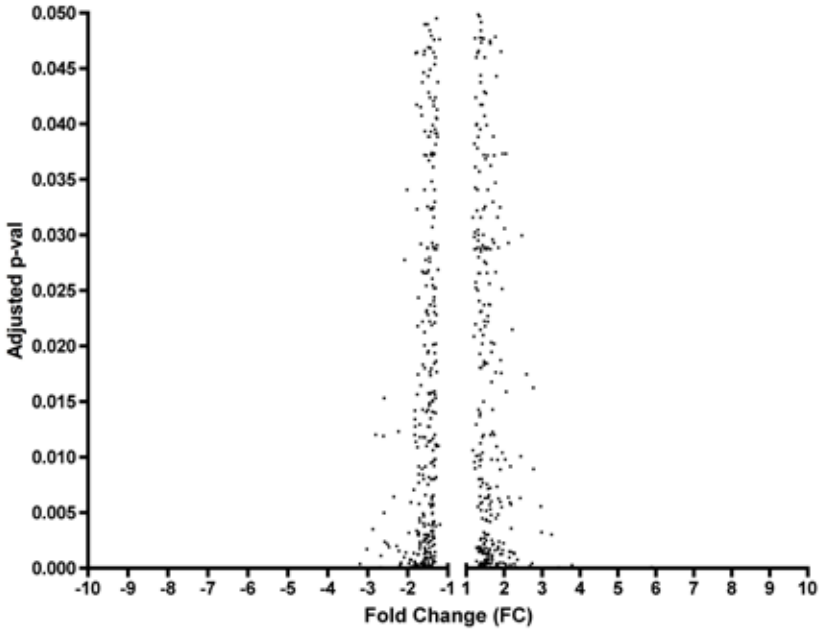

Figure 5.2: HOSE SGK3 CA compared with HOSE pMIG gene expression data. n=3. p-val <0.05.

Table 5.5: HOSE SGK3 CA compared with HOSE pMIG gene expression data. Ranked according to fold change. n=3, p-val <0.05. Top 20 up-regulated and top 20 down-regulated genes. See supplementary data DVD affixed to the back cover for complete list.

UP-REGULATED GENES			DOWN-REGULATED GENES		
Gene Symbol	**Fold Change**	**Adjusted P-Value**	**Gene Symbol**	**Fold Change**	**Adjusted P-Value**
SGK3	66.95812768	3.68E-63	SLC7A7	-2.806974505	0.012029999
HGF	18.74412432	1.48E-51	ITGB4	-2.860161305	4.82E-11
BEX1	8.129241418	6.33E-09	ITGA6	-2.873230336	5.88E-06
SERPINB2	6.886052521	5.30E-05	KIAA0040	-2.87827359	0.003517099
CACHD1	5.892896822	5.15E-21	TMC5	-2.890690412	4.63E-11
DCN	5.885040259	9.42E-05	ANXA4	-2.917331285	1.03E-08
ADD2	5.553799661	1.23E-16	PAPPA	-2.996545317	7.92E-10
MFAP4	5.069196473	1.02E-08	C8orf84	-3.022473637	1.06E-05
CPE	5.059275594	2.95E-13	C7orf69	-3.028136868	0.001721252
TDO2	4.966505706	3.84E-12	CRLF2	-3.08402784	6.77E-10
GFRA1	4.965624495	8.73E-10	LCN2	-3.198539759	0.000389735
FST	4.884841201	4.78E-05	ZNF626	-3.244746972	6.10E-08
VCAM1	4.287537155	2.76E-06	NR1H4	-3.955767895	3.50E-16
MCTP1	4.237907827	9.33E-11	DSP	-4.232627433	4.02E-13
ITGA4	3.992195871	2.57E-09	IDO1	-4.691722847	4.00E-08
TLL1	3.939574263	7.59E-06	STMN2	-4.704533742	2.73E-09
PRUNE2	3.857013182	1.78E-07	SLC14A1	-5.016703847	1.28E-15
ATP8B4	3.848589838	1.65E-21	C4BPA	-5.378305956	2.56E-18
DIO2	3.785216322	0.000291138	CD24	-5.447474686	6.53E-07
C1orf21	3.665782034	1.62E-16	AKR1B10	-7.464682162	4.34E-13

regulation **(Table 5.6)**. At a FC cut off of 2 there were only three significant pathways, two of which were involved in cell adhesion. In contrast to the gene expression profile in HOSE SGK3 WT cells a strong enrichment of pathways involved in immune function was not observed **(Table 5.7)**.

GSEA revealed 1030 out of 2526 gene sets to be enriched in HOSE SGK3 CA cells, with 74 gene sets significant at FDR <25%. Interestingly, GSEA showed that the top ranked gene set enriched in SGK3 CA were genes involved in ion-dependent neurotransmitter transporters **(Table 5.8)**, a function of SGK3 that has previously been reported (Shojaiefard et al. 2005). Furthermore, out of the top 20 ranked gene sets enriched in HOSE SGK3 CA cells, nine of those gene sets are described as either up or down-regulated gene sets in a specific tumour type compared to a normal control implicating SGK3 CA in tumourigenesis.

5.3.1.3 Comparative analysis of changes identified between SGK WT and CA datasets

In order to more thoroughly determine the genes regulated in response to SGK3 stable over-expression, a comparison of genes differentially expressed in both HOSE SGK3 WT and SGK3 CA was performed. Applying a p-val of <0.05, HOSE SGK3 WT and SGK3 CA share a total of 246 differentially regulated genes, 123 up-regulated genes and 123 down-regulated genes **(Figure 5.3)**. When a FC of 2 is applied, the number of shared genes is reduced to a total of 48 genes, 22 up-regulated genes and 26 down-regulated genes **(Figure 5.4)**. Unexpectedly, these data show that a large proportion of differentially regulated genes between HOSE SGK3 WT and HOSE SGK3 CA are not shared. It would be expected that the genes differentially regulated by SGK3 WT would likely be a subset of genes regulated by SGK3 CA, however this may possibly be indicative of the ability of hyperactivated SGK3 to induce regulation of novel targets not normally regulated by SGK3 under non-pathological conditions.

Manual inspection of the genes commonly up-regulated and down-regulated between HOSE SGK3 WT and HOSE SGK3 CA revealed important gene-sets that were not previously obvious via MetaCore ™ pathway analysis. Analysis of differentially regulated genes shared between HOSE SGK3 WT and HOSE SGK3 CA **(Table 5.9)** show that both of these cell lines share an up-regulation of ectonucleotide pyrophosphatase/ phosphodiesterase family member 2/Autotaxin (*ENPP2*) and lysophosphatidic acid receptor 3 (*LPAR3*), two crucial players in the lysophosphatidic acid (LPA) pathway. Autotaxin is an ectoenzyme important in LPA production, and plays an important role in LPA-mediated growth and motility of cancer cells (Umezu-Goto et al. 2002; Brettschneider et al. 2007; Liu et al. 2009b) Furthermore, over-expression of the LPA receptors enhances the production of IL-6, IL-8 and vacular endothelial growth factor (VEGF) in the tumourigenic ovarian cell lines SKOV-3 and OVCAR-3, establishing a strong correlation between LPA function and production of pro-inflammatory cytokines in ovarian cancer cells (Yu et al. 2008; Liu et al. 2009a). Our array studies have demonstrated that SGK increases expression of IFN-α and IFN-β signalling

Table 5.6: All HOSE SGK3 CA GeneGO pathways identified using a FC 0, p-val <0.05. Ranked according to p-val.

#	GeneGO Pathways	P-Value
1	Cytoskeleton remodeling_RalA regulation pathway	2.734e-6
2	Cell adhesion_PLAU signaling	2.248e-5
3	Cell adhesion_Endothelial cell contacts by junctional mechanisms	1.229e-4
4	DNA damage_Role of SUMO in p53 regulation	1.336e-4

Table 5.7: All HOSE SGK3 CA GeneGO pathways identified using a FC >2, p -val <0.05. Ranked according to p-val.

#	GeneGO Pathways	P-Value
1	Cell adhesion_PLAU signaling	1.088e-5
2	Role of alpha-6/beta-4 integrins in carcinoma progression	3.764e-4
3	Development_PIP3 signaling in cardiac myocytes	4.454e-4

Table 5.8: Top 20 ranked GSEA gene sets enriched in HOSE-SGK3 CA. FDR <25%, ranked according to FWER p-val (http://www.broadinstitute.org/gsea/msigdb/). See supplementary data DVD affixed to the back cover for complete list.

Rank	GSEA set	Brief description of GSEA set	FDR q-val
1	REACTOME_NA_CL_DEPENDENT_NEUROTRANSMITTER_TRANSPORTERS	Genes involved in Na+/Cl- dependent neurotransmitter transporters	0.121
2	DACOSTA_ERCC3_ALLELE_XPCS_VS_TTD_DN	Genes down-regulated in fibroblasts expressing different mutant forms of ERCC3 XP/CS (xeroderma pigmentosum (XP) and Cockraine's syndrome (CS)) vs TTD (trichothiodystrophy).	0.072
3	PICCALUGA_ANGIOIMMUNOBLASTIC_LYMPHOMA_UP	Up-regulated genes in angioimmunoblastic lymphoma (AILT) compared to normal T lymphocytes.	0.081
4	SABATES_COLORECTAL_ADENOMA_DN	Genes down-regulated in colorectal adenoma compared to normal mucosa samples.	0.067
5	BIOCARTA_IL17_PATHWAY	IL 17 Signaling Pathway	0.068
6	WONG_ENDMETRIUM_CANCER_DN	Genes down-regulated in cancer endometrium samples compared to the normal endometrium.	0.070
7	RIGGI_EWING_SARCOMA_PROGENITOR_DN	Genes down-regulated in mesenchymal stem cells (MSC) engineered to express EWS-FLI1 fusion protein.	0.067
8	RICKMAN_HEAD_AND_NECK_CANCER_C	Cluster c: genes identifying an intrinsic group in head and neck squamous cell carcinoma (HNSCC).	0.086
9	ROVERSI_GLIOMA_COPY_NUMBER_UP	Genes in the most frequently gained loci in a panel of glioma cell lines.	0.078
10	KEGG_INTESTINAL_IMMUNE_NETWORK_FOR_IGA_PRODUCTION	Brief description Intestinal immune network for IgA production	0.079
11	KORKOLA_YOLK_SAC_TUMOR	Genes predicting the yolk sac tumor (YS) subtype of nonseminomatous male germ cell tumors (NSGCT).	0.077
12	BIOCARTA_DC_PATHWAY	Dendritic cells in regulating TH1 and TH2 Development	0.088
13	MAHADEVAN_IMATINIB_RESISTANCE_DN	Top genes down-regulated in the GIST (gastrointestinal stromal tumor) cell line resistant to imatinib compared to the parental cell line sensitive to the drug.	0.094
14	BIOCARTA_INTRINSIC_PATHWAY	Intrinsic Prothrombin Activation Pathway	0.094
15	ABE_VEGFA_TARGETS_2HR	Genes up-regulated in HUVEC cells (endothelium) at 2 h after VEGFA stimulation.	0.096
16	VECCHI_GASTRIC_CANCER_EARLY_DN	Down-regulated genes distinguishing between early gastric cancer (EGC) and normal tissue samples.	0.132
17	SMID_BREAST_CANCER_NORMAL_LIKE_UP	Genes up-regulated in the normal-like subtype of breast cancer.	0.138
18	KANG_IMMORTALIZED_BY_TERT_UP	Up-regulated genes in the signature of adipose stromal cells (ADSC) immortalized by forced expression of telomerase (TERT).	0.131
19	HARRIS_HYPOXIA	Genes known to be induced by hypoxia	0.125
20	GEORGANTAS_HSC_MARKERS	Genes up-regulated in HSC (hematopoietic stem cells) compared to HPC (hematopoietic progenitor cells).	0.142

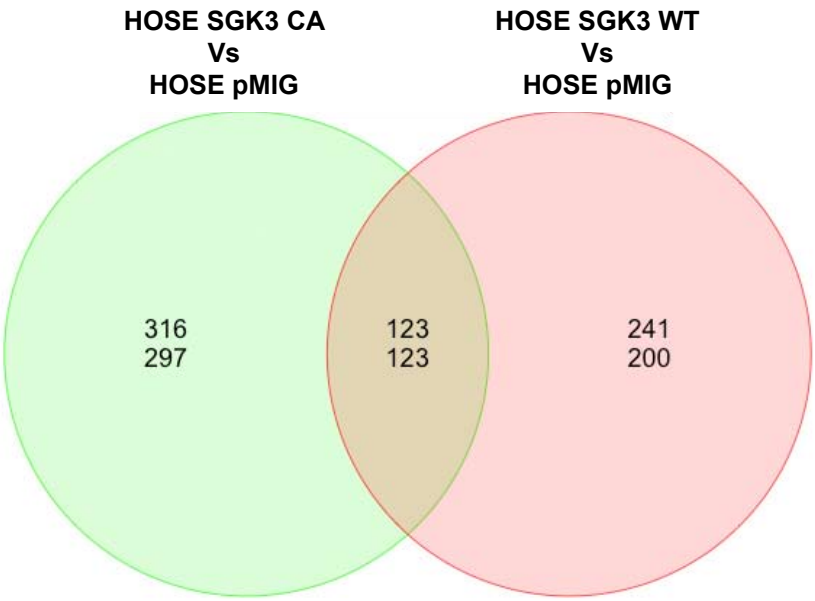

Figure 5.3: Venn Diagram showing common differentially regulated genes in HOSE-SGK3 CA Vs HOSE-SGK3 WT. FC 0, p-val <0.05. Top number represents number of up-regulated genes, while the bottom number represents down-regulated genes.

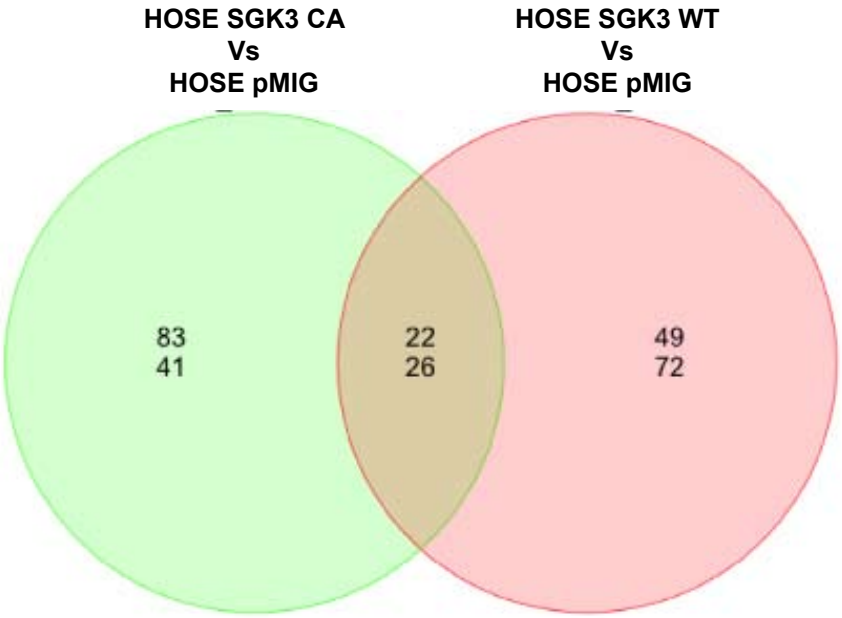

Figure 5.4: Venn Diagram showing common differentially regulated genes in HOSE-SGK3 CA vs HOSE-SGK3 WT. FC 2, p-val <0.05. Top number represents number of up-regulated genes, while the bottom number represents down-regulated genes.

Table 5.9: Differential expression between HOSE SGK3WT and HOSE SGK3CA cell lines. Common genes up-regulated (1) and down-regulated (-1).

Gene Symbol	HOSE SGK3 CA	HOSE SGK3 WT	Gene Symbol	HOSE SGK3 CA	HOSE SGK3 WT
HSD11B1	1	1	INADL	-1	-1
LPAR3	1	1	TMEM56	-1	-1
MASTL	1	1	C4BPA	-1	-1
CXCL12	1	1	DIRAS3	-1	-1
GFRA1	1	1	KIAA0040	-1	-1
DCN	1	1	AKR1C3	-1	-1
DIO2	1	1	SFMBT2	-1	-1
ATP8B4	1	1	SMPD1	-1	-1
MFAP4	1	1	PRKCDBP	-1	-1
DOK6	1	1	GNG2	-1	-1
C19orf63	1	1	ITGB4	-1	-1
PSG4	1	1	SLC14A1	-1	-1
FLRT3	1	1	C19orf21	-1	-1
FGB	1	1	LSR	-1	-1
FAM198B	1	1	ZNF626	-1	-1
FST	1	1	ADAM23	-1	-1
CAMK4	1	1	TIMP3	-1	-1
IL6	1	1	METT5D1	-1	-1
SGK3	1	1	CLDN1	-1	-1
ENPP2	1	1	AREG	-1	-1
BEX1	1	1	DSP	-1	-1
CDR1	1	1	AKR1B10	-1	-1
HGF	1	-1	C8orf84	-1	-1
ADAMTSL1	1	-1	LCN2	-1	-1
STMN2	-1	1	CRLF2	-1	-1
			CD24	-1	-1

components, in addition to increasing expression of other pro-inflammatory cytokines including interleukin 6 (*IL-6*) and chemokine (C-X-C motif) 12 (*CXCL12*) in both HOSE-SGK3 WT and HOSE-SGK3 CA cells. These data suggest that in addition to regulating cell growth and proliferation via mTORC1 activation as was demonstrated in Chapter 3, SGK3 may also influence normal cell physiology and tumourigenesis via cytokines.

Pathway analysis performed on both the HOSE SGK3 WT and HOSE SGK3 CA data sets revealed that both SGK3 WT and SGK3 CA are involved in tissue remodelling, whereas SGK3 WT also had a strong correlation with inflammation/immune signalling. Furthermore, analysis performed on the HOSE SGK3 CA gene expression data also revealed the involvement of SGK3 in already established process such as ion channel regulation, supporting the accuracy of this analysis. The analysis of HOSE gene expression data did not reveal differential regulation of direct pathways associated with regulation of growth and proliferation, even though over-expressed SGK3 CA and SGK3 WT demonstrated the ability to regulate growth and proliferation in the HOSE cells. A possible explanation for these changes not being detected in the gene expression data may be due to most components of this pathway regulated by post-translational modifications rather than transcriptional changes.

5.3.2 Gene expression profiles in AKT transduced IOSE523 cells

In order to make comparisons between the AKT kinase family and SGK family, the AKT stable cell lines were included in the gene expression studies. The IOSE523 cells stably expressing myrAKT1, myrAKT2 and myrAKT3 (as described in Chapter 4.2) were used for gene expression studies as it was not possible to generate HOSE cells stably expressing AKT as described in Chapter 4.2.1.

5.3.2.1 Gene expression changes with myr-AKT over-expression

For myrAKT1 cells compared with IOSE pMIC cells there was a total of 136 differentially regulated genes with 51 up-regulated and 85 down-regulated with a p-val <0.05 and no fold change cut-off applied. When a FC cut-off of 2 and a p-val <0.05 was applied, the number of regulated genes reduced to 46, with only 25 up-regulated and 21 down-regulated genes. The majority of regulated genes were within a +/-5 FC **(Figure 5.5 and Table 5.10)**. Pathway analysis using the MetaCore™ platform and a p-val <0.05, demonstrated that over-expression of myrAKT1 stimulates the significant regulation of 78 pathways, with the top 10 pathways shown in **Table 5.11, supplementary data Table S.3**. These data show strong enrichment of pathways involved mainly in immune response. Applying a FC cut off of 2 demonstrates an involvement of activated AKT1 in the significant regulation of 21 pathways, with six of the top ten pathways involved in immune response **(Table 5.12, supplementary data Table S.4)**.

GSEA was also used on IOSE523-myrAKT1 cells, with 1051 out of 2526 gene sets up-regulated, and 159 gene sets considered significant with a FDR<25% **(Table 5.13)**.

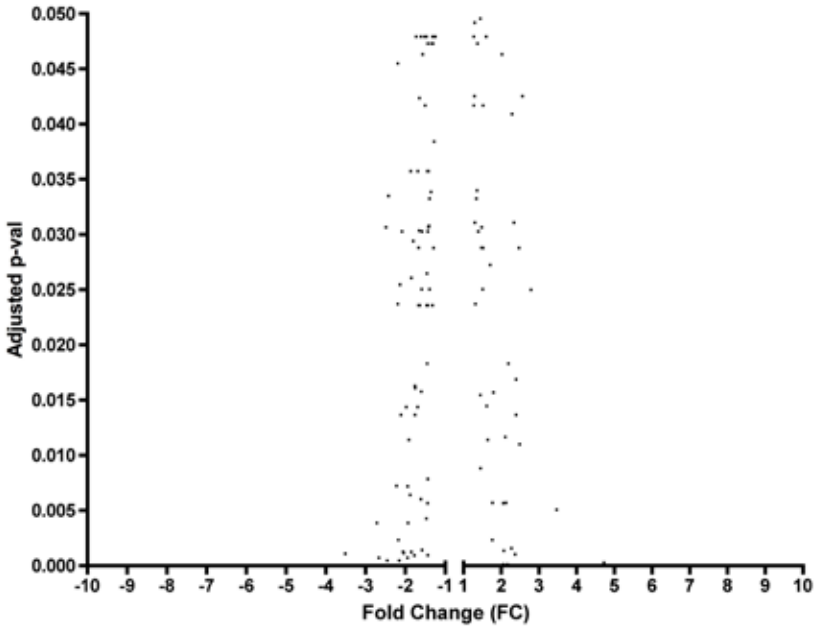

Figure 5.5: IOSE523-myrAKT1 compared with IOSE523-pMIC gene expression data. n=4, p-val <0.05.

Table 5.10: IOSE523-myrAKT1 compared with IOSE523-pMIC gene expression data. Ranked according to fold change. n=4, p-val <0.05. Top 20 up-regulated and top 20 down-regulated genes. See supplementary data DVD affixed to the back cover for complete list.

UP-REGULATED GENES			DOWN-REGULATED GENES		
Gene Symbol	Fold Change	Adjusted P-Value	Gene Symbol	Fold Change	Adjusted P-Value
PTGS2	5.289762809	3.66E-08	CHRM2	-2.065316093	0.001270178
AKT1	5.07772203	2.48E-53	BMP4	-2.089354439	0.030274265
HAS2	4.719490575	0.00028749	RBP7	-2.111785829	0.013671418
TNFAIP6	3.909080169	1.19E-06	EPHA5	-2.139789142	0.02546748
TNFSF15	3.541108761	5.56E-07	SDPR	-2.161740182	0.000459482
GREM1	3.470440269	0.00507582	CDH8	-2.18217673	0.002346244
STC1	3.389478941	3.47E-05	ODZ2	-2.193736893	0.023708323
TFPI2	2.786294305	0.025004748	TLL1	-2.194065016	0.045491496
IL6	2.55857526	0.042522803	PRUNE2	-2.224937696	0.007230585
IL1A	2.483029368	0.011005997	PTGIS	-2.430531955	0.033485994
TMEM156	2.467010481	0.028782022	RARRES1	-2.461056793	0.000459482
LCP1	2.396375451	0.016873886	PKP2	-2.490639148	0.03065827
DDIT4	2.396310139	0.013671418	PTN	-2.603629317	1.61E-07
SLC6A15	2.365958269	0.001036411	SCN9A	-2.652187411	1.66E-05
IL1B	2.334066349	0.031084338	OLFML1	-2.670125094	0.000724778
SLC22A3	2.286178766	0.040916297	GPR133	-2.673036584	2.21E-07
INHBA	2.271020681	0.001592119	OXTR	-2.719586977	0.003891537
CXCL5	2.191536727	0.018316768	PSG4	-2.798069852	3.64E-05
CD82	2.161497134	0.000121885	GFRA1	-3.459289722	5.56E-07
DNER	2.125977389	0.005697921	KIAA1199	-3.515136805	0.001099267

Closer inspection revealed that genes differentially regulated through over-expression of myrAKT1 were enriched in gene sets associated with inflammation, epidermal growth factor (EGF) and RAS signalling. Moreover, these cells also demonstrated an enrichment of gene sets associated with loss of histone deacetylase (HDAC) 1 and 2, both of which are involved in chromatin remodelling and regulation of gene transcription. Loss of HDAC1 and 2 has reported to be involved in cell cycle arrest and senescence (Zhou et al. 2008; Landreville et al. 2012), similarly Akt has previously been reported to induce cell senescence (Astle et al. 2011), and when over-expressed in HOSE cells it induces cell cycle arrest and senescence like phenotype (data not shown). Further enriched gene sets included genes regulated in response to environmental stress following exposure to ultraviolet B (UVB), and also genes regulated in response to knockdown of SRY (sex determining region Y)-box 4 (*SOX4*), a key gene required in tumour survival.

Analysis of differential gene expression in the IOSE523-myrAKT2 cells using a p-val of <0.05 revealed a total of 387 genes differentially regulated, with 149 up-regulated and 238 down-regulated. When a FC cut-off of 2 was applied to this data, the number of differentially regulated genes was reduced to 97, with 44 up-regulated and 53-downregulated. The majority of genes differentially regulated in IOSE523–myrAKT2 cells were within +/-5 FC **(Figure 5.6 and Table 5.14)**. Using a p-val <0.05, MetaCore™ pathway analysis revealed myrAKT2 is significantly involved in the regulation of 28 pathways **(Table 5.15, supplementary data Table S.5),** and similar to myrAKT1 cells, myrAKT2 is involved in pathways associated with immune response, but it also involved in several cell adhesion pathways. Applying a FC cut off of 2 reduced the number of pathways that myrAKT2 has significant involvement in to 18 **(Table 5.16, supplementary data Table S.6)**, with most of these pathways also involved in the immune response, along with development and cell adhesion. GSEA also revealed that many gene sets enriched in IOSE523-myrAKT1 cells were also enriched in myrAKT2 cells, including RAS oncogenic signature and genes regulated following HDAC1 and 2 or SOX4 knockdown **(Table 5.17)**.

Analysis of differential gene expression in the IOSE523-myrAKT3 cells using a p-val of <0.05 revealed a total of 85 genes differentially regulated, with 39 up-regulated and 46 down-regulated. Applying a FC cut off of 2 reduced the number of regulated genes to a total of 29, with 13 up-regulated and 16 down-regulated **(Figure 5.7 and Table 5.18)**. MetaCore™ pathway analysis revealed no significant involvement of myrAKT3 in any pathways using a p-val <0.05. When a FC cut off of 2 was applied, myrAKT3 showed significant involvement in 11 pathways, many involved in the immune response and development **(Table 5.19)**.

GSEA for IOSE523-myrAKT3 cells demonstrated 692 out of 2526 gene sets were enriched in the IOSE523-myrAKT3 cells, with 55 of those gene sets significant with a FDR <25% **(Table 5.20)**. The most significant gene set enriched in the myrAKT3 cells were genes involved in RNA Polymerase I promoter opening, suggesting genes regulated by AKT3 are involved in assembly of the transcription initiation complex.

Table 5.11: IOSE523-myrAKT1 GeneGO pathways identified using FC 0, p-val <0.05. Ranked according to p-val. See Appendix I for complete list.

#	GeneGO Pathways	P-Value
1	Immune response_IL-17 signaling pathways	1.15218E-09
2	Apoptosis and survival_NO synthesis and signaling	1.31075E-05
3	Immune response_TREM1 signaling pathway	1.85478E-05
4	Cell adhesion_Chemokines and adhesion	1.88261E-05
5	Muscle contraction_Oxytocin signaling in uterus and mammary gland	2.01487E-05
6	Immune response_Signaling pathway mediated by IL-6 and IL-1	2.21129E-05
7	Immune response_IL-15 signaling	2.76579E-05
8	Development_VEGF-family signaling	7.80754E-05
9	Immune response_IL-1 signaling pathway	0.000103368
10	Immune response_Inhibitory action of Lipoxins on pro-inflammatory TNF-alpha signalling	0.000112984

Table 5.12: IOSE523-myrAKT1 GeneGO pathways identified using FC >2, p-val <0.05. Ranked according to p-val. See Appendix I for complete list.

#	GeneGO Pathways	P-Value
1	Immune response_IL-17 signaling pathways	1.33563E-08
2	Immune response_IL-1 signaling pathway	6.72869E-06
3	Immune response_Inhibitory action of Lipoxins on pro-inflammatory TNF-alpha signalling	7.3709E-06
4	Immune response_MIF in innate immunity response	0.000195051
5	Development_PEDF signaling	0.000357574
6	Apoptosis and survival_NO synthesis and signaling	0.000503413
7	Immune response_TREM1 signaling pathway	0.000619093
8	Transcription_PPAR Pathway	0.000682792
9	Transcription_Role of VDR in regulation of genes involved in osteoporosis	0.000682792
10	Immune response_CD40 signaling	0.000785959

Table 5.13: Top 20 ranked GSEA gene sets enriched in IOSE523-myrAKT1. FDR <25%, ranked according to FWER p-val (http://www.broadinstitute.org/gsea/msigdb/). See supplementary data DVD affixed to the back cover for complete list.

Rank	GSEA set	Brief description of GSEA set	FDR q-val
1	MCLACHLAN_DENTAL_CARIES_UP	Genes up-regulated in pulpal tissue extracted from carious teeth.	0.000
2	SENESE_HDAC2_TARGETS_UP	Genes up-regulated in U2OS cells (osteosarcoma) upon knockdown of HDAC2 by RNAi.	0.000
3	PRAMOONJAGO_SOX4_TARGETS_UP	Genes up-regulated in ACC3 cells (adenoid cystic carcinoma) after knockdown of SOX4 by RNAi.	0.000
4	SENESE_HDAC1_AND_HDAC2_TARGETS_UP	Genes up-regulated in U2OS cells (osteosarcoma) upon knockdown of both HDAC1 and HDAC2 by RNAi.	0.000
5	HAHTOLA_MYCOSIS_FUNGOIDES_CD4_UP	Genes up-regulated in T helper cells (defines as CD4+) isolated from patients with mucosis fungoides compared to those from normal control donors.	0.002
6	GRAHAM_CML_QUIESCENT_VS_NORMAL_DIVIDING_UP	Genes up-regulated in quescent CD34+ cells isolated from peripheral blood of CML (chronic myeloblastic leukemia) patients compared to the dividing cells from normal donors.	0.002
7	MCLACHLAN_DENTAL_CARIES_DN	Genes down-regulated in pulpal tissue extracted from carious teeth.	0.003
8	AMIT_EGF_RESPONSE_120_MCF10A	Genes whose expression peaked at 120 min after stimulation of MCF10A cells with EGF.	0.004
9	SESTO_RESPONSE_TO_UV_C3	Cluster 3: genes changed in primary keratinocytes by UVB irradiation.	0.004
10	LY_AGING_PREMATURE_DN	Genes down-regulated in fibroblasts from patients with Hutchinson-Gilford progeria (premature aging), compared to those from normal young individuals.	0.004
11	RAS_ONCOGENIC_SIGNATURE_UP		0.004
12	NEWMAN_ERCC6_TARGETS_UP	Genes up-regulated in Cockayne syndrome fibroblasts rescued by expression of ERCC6 off a plasmid vector.	0.005
13	SEITZ_NEOPLASTIC_TRANSFORMATION_BY_8P_DELETION_DN	Genes down-regulated in CT60/4 cells (breast cancer reverted to normal by transfer of chromosome 8p region) vs parental MDA-MB-231 cells (deleted chromosome 8p).	0.005
14	HINATA_NFKB_TARGETS_FIBROBLAST_UP	Genes up-regulated in primary fibroblast cells by expression of p50 (NFKB1) and p65 (RELA) components of NFKB.	0.007
15	DASU_IL6_SIGNALING_UP	Genes up-regulated in normal fibroblasts in response to IL6.	0.007
16	MAHADEVAN_RESPONSE_TO_MP470_UP	Top genes up-regulated in the GIST (gastrointestinal stromal tumor) cell line resistant to imatinib after treatment with MP470, a protein kinase inhibitor.	0.009
17	MENSE_HYPOXIA_UP	Hypoxia response genes in both astrocytes and HeLa cell line.	0.010
18	HINATA_NFKB_TARGETS_KERATINOCYTE_UP	Genes up-regulated in primary keratinocytes by expression of p50 (NFKB1) and p65 (RELA) components of NFKB.	0.016
19	DORSEY_GAB2_TARGETS	Genes up-regulated by expression of GAB2 in K562 cells (chronic myeloid leukemia (CML) cell line with p210 BCR-ABL.	0.017
20	LU_TUMOR_ENDOTHELIAL_MARKERS_UP	Genes specifically up-regulated in tumor endothelium.	0.017

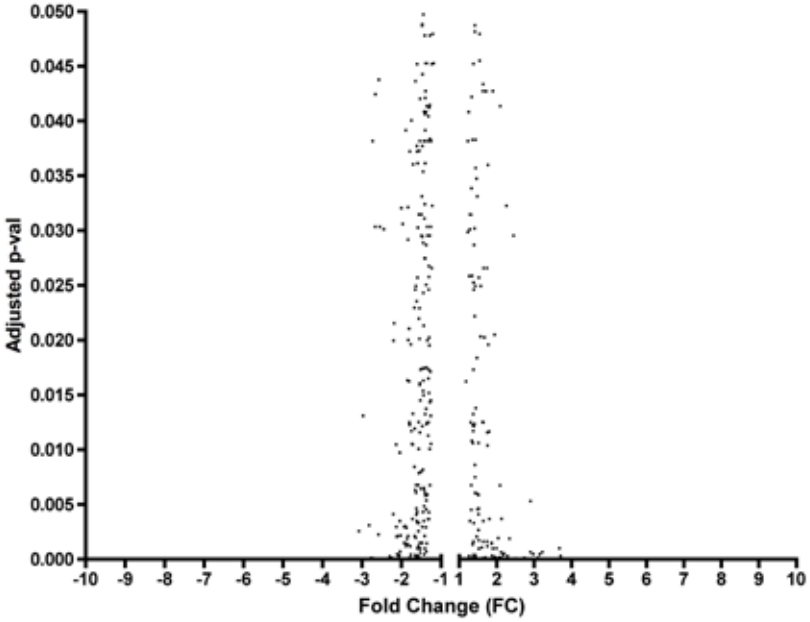

Figure 5.6: IOSE523-myrAKT2 gene expression data compared with IOSE523-pMIC gene expression data. n=4, p-val <0.05.

Table 5.14: IOSE523-myrAKT2 compared with IOSE523-pMIC gene expression data. Ranked according to fold change. n=4, p-val <0.05. Top 20 up-regulated and top 20 down-regulated genes. See supplementary data DVD affixed to the back cover for complete list.

UP-REGULATED GENES			DOWN-REGULATED GENES		
Gene Symbol	**Fold Change**	**Adjusted P-Value**	**Gene Symbol**	**Fold Change**	**Adjusted P-Value**
PTGS2	8.640093193	2.96E-13	PTN	-2.550108972	1.46E-07
HAS2	6.401056785	1.71E-06	SULF1	-2.550236291	0.030354754
AKT2	5.861676907	5.89E-54	SDPR	-2.558443751	1.95E-06
STC1	5.488441797	4.42E-10	---	-2.577155804	0.043757421
TNFSF15	4.738547515	2.87E-10	TLL1	-2.589888463	0.002277095
IL6	4.68788325	5.60E-06	UPK1B	-2.665532195	0.042433697
TNFAIP6	4.476247154	5.08E-08	EPCAM	-2.671404274	0.030354754
TFPI2	3.705072609	0.000318974	PRUNE2	-2.711006345	7.50E-05
GREM1	3.670749875	0.001021234	IL18	-2.735787475	0.038168051
IL1B	3.626450456	1.70E-05	OLFML1	-2.772162953	0.000138167
INHBA	3.268663518	1.35E-07	PKP2	-2.821517332	0.003105991
DDIT4	3.221494115	4.32E-05	EPHA5	-2.92866373	4.98E-05
IL33	3.215162179	0.000670482	ANKRD1	-2.978057241	0.013102825
TMEM156	3.145965442	0.000465494	KIAA1199	-3.081499094	0.002587671
IL1A	3.102840171	0.000129418	PDE1C	-3.11150121	1.46E-07
SLC6A15	2.98322068	2.09E-06	PSG4	-3.113052246	1.45E-06
CXCL5	2.976806222	3.68E-05	GPR133	-3.135355131	5.45E-10
SLC22A3	2.976183044	0.000490821	OXTR	-3.372930335	4.92E-05
CD82	2.913895385	4.99E-09	SCN9A	-3.82468941	2.87E-10
IL8	2.899916084	0.005320364	GFRA1	-4.089661603	5.56E-09

Table 5.15: IOSE523-myrAKT2 GeneGO pathways identified using FC 0, p-val 0.05. Ranked according to p-val. See Appendix I for complete list.

#	GeneGO Pathways	P-Value
1	Immune response_IL-17 signaling pathways	1.78265E-08
2	Cell adhesion_Endothelial cell contacts by junctional mechanisms	1.93776E-06
3	Cell adhesion_Chemokines and adhesion	2.45452E-06
4	Muscle contraction_GPCRs in the regulation of smooth muscle tone	3.40635E-05
5	Transcription_Role of Akt in hypoxia induced HIF1 activation	4.57476E-05
6	Immune response_IL-1 signaling pathway	4.75232E-05
7	Immune response_Gastrin in inflammatory response	7.71659E-05
8	Development_BMP signalling	0.000125045
9	Regulation of lipid metabolism_Regulation of fatty acid synthase activity in hepatocytes	0.000163801
10	Cell adhesion_Tight junctions	0.000191531

Table 5.16: IOSE523-myrAKT2 GeneGO pathways identified using FC >2, p-val 0.05. Ranked according to p-val. See Appendix I for complete list.

#	GeneGO Pathways	P-Value
1	Immune response_IL-17 signaling pathways	1.17907E-10
2	Cell adhesion_Chemokines and adhesion	3.80019E-06
3	Cytokine production by Th17 cells in CF	2.19139E-05
4	Immune response_IL-1 signaling pathway	3.56144E-05
5	Cytokine production by Th17 cells in CF (Mouse model)	5.47356E-05
6	Apoptosis and survival_NO synthesis and signalling	8.64927E-05
7	Immune response_TREM1 signaling pathway	0.000114007
8	Immune response_Gastrin in inflammatory response	0.000209983
9	Immune response_MIF in innate immunity response	0.000661081
10	Immune response_PGE2 signaling in immune response	0.000935465

Table 5.17: Top 20 ranked GSEA gene sets enriched in IOSE523-myrAKT2. FDR <25%, ranked according to FWER p-val (http://www.broadinstitute.org/gsea/msigdb/). See supplementary data DVD affixed to the back cover for complete list.

Rank	GSEA set	Brief description of GSEA set	FDR q-val
1	HAHTOLA_MYCOSIS_FUNGOIDES_CD4_UP	Genes up-regulated in T helper cells (defines as CD4+) isolated from patients with mucosis fungoides compared to those from normal control donors.	0.000
2	SENESE_HDAC2_TARGETS_UP	Genes up-regulated in U2OS cells (osteosarcoma) upon knockdown of HDAC2 by RNAi.	0.000
3	PRAMOONJAGO_SOX4_TARGETS_UP	Genes up-regulated in ACC3 cells (adenoid cystic carcinoma) after knockdown of SOX4 by RNAi.	0.000
4	SESTO_RESPONSE_TO_UV_C3	Cluster 3: genes changed in primary keratinocytes by UVB irradiation.	0.000
5	SENESE_HDAC1_AND_HDAC2_TARGETS_UP	Genes up-regulated in U2OS cells (osteosarcoma) upon knockdown of both HDAC1 and HDAC2 by RNAi.	0.000
6	MCLACHLAN_DENTAL_CARIES_UP	Genes up-regulated in pulpal tissue extracted from carious teeth.	0.000
7	MENSE_HYPOXIA_UP	Hypoxia response genes in both astrocytes and HeLa cell line.	0.000
8	HINATA_NFKB_TARGETS_FIBROBLAST_UP	Genes up-regulated in primary fibroblast cells by expression of p50 (NFKB1) and p65 (RELA) components of NFKB.	0.000
9	RAS_ONCOGENIC_SIGNATURE_UP		0.000
10	LY_AGING_PREMATURE_DN	Genes down-regulated in fibroblasts from patients with Hutchinson-Gilford progeria (premature aging), compared to those from normal young individuals.	0.001
11	GRAHAM_CML_QUIESCENT_VS_NORMAL_DIVIDING_UP	Genes up-regulated in quescent CD34+ cells isolated from peripheral blood of CML (chronic myeloblastic leukemia) patients compared to the dividing cells from normal donors.	0.001
12	ELVIDGE_HIF1A_TARGETS_DN	Genes down-regulated in MCF7 cells (breast cancer) after knockdown of HIF1A by RNAi.	0.001
13	MAHADEVAN_RESPONSE_TO_MP470_UP	Top genes up-regulated in the GIST (gastrointestinal stromal tumor) cell line resistant to imatinib after treatment with MP470, a protein kinase inhibitor.	0.002
14	HINATA_NFKB_TARGETS_KERATINOCYTE_UP	Genes up-regulated in primary keratinocytes by expression of p50 (NFKB1) and p65 (RELA) components of NFKB.	0.003
15	MCLACHLAN_DENTAL_CARIES_DN	Genes down-regulated in pulpal tissue extracted from carious teeth.	0.003
16	DASU_IL6_SIGNALING_UP	Genes up-regulated in normal fibroblasts in response to IL6.	0.003
17	ELVIDGE_HIF1A_AND_HIF2A_TARGETS_DN	Genes down-regulated in MCF7 cells (breast cancer) after knockdown of both HIF1A and HIF2A by RNAi.	0.003
18	DORSEY_GAB2_TARGETS	Genes up-regulated by expression of GAB2 in K562 cells (chronic myeloid leukemia (CML) cell line with p210 BCR-ABL).	0.003
19	AMIT_EGF_RESPONSE_60_MCF10A	Genes whose expression peaked at 60 min after stimulation of MCF10A cells with EGF.	0.004
20	ELVIDGE_HYPOXIA_BY_DMOG_UP	Genes up-regulated in MCF7 cells (breast cancer) treated with hypoxia mimetic DMOG.	0.004

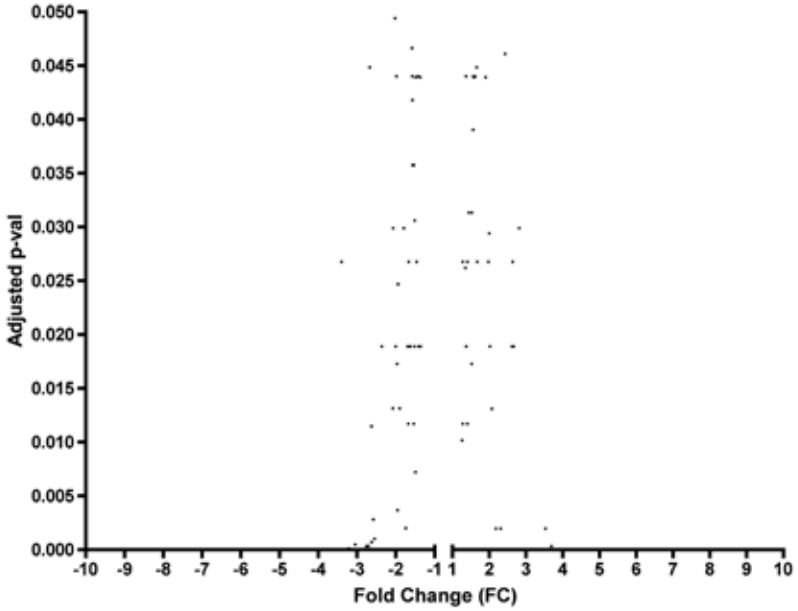

Figure 5.7: IOSE523-myrAKT3 gene expression data compared with IOSE523-pMIC gene expression data. n=4, p-val <0.05.

Table 5.18: All IOSE523-myrAKT3 compared with IOSE523-pMIC gene expression data. Ranked according to fold change. n=4, P-val <0.05. Up-regulated and down-regulated genes.

UP-REGULATED GENES			DOWN-REGULATED GENES		
Gene Symbol	**Fold Change**	**Adjusted P-Value**	**Gene Symbol**	**Fold Change**	**Adjusted P-Value**
AKT3	5.062563237	1.37E-10	ARHGAP20	-1.961649271	0.00368955
TNFAIP6	3.688778903	0.000347909	GPR133	-1.971322292	0.017278014
PTGS2	3.526632179	0.001973042	CPS1	-1.986372069	0.043996374
RNU5E	2.811258183	0.029886787	SDPR	-2.007324687	0.018903395
IFI44	2.663611544	0.018903395	PRUNE2	-2.009609338	0.018903395
CYP2B6	2.638075094	0.026763701	FBXO25	-2.022385951	0.049395838
---	2.615710667	0.018903395	VGLL3	-2.075662023	0.029886787
AADAC	2.432089767	0.046092146	KCNK2	-2.077030588	0.013153734
---	2.307194684	0.001973042	SFRP1	-2.362361855	0.018903395
CD82	2.176986187	0.001973042	AOX1	-2.555120196	0.001024054
OASL	2.070749723	0.0131076	KCNAB1	-2.582219965	0.002816617
RNU1-1	2.017372241	0.018903395	PSG7	-2.626591077	0.000721061
CYP2B7P1	1.996977091	0.029406537	OLFML1	-2.630443906	0.011468906
RNU4ATAC	1.900308187	0.043912639	PSG5	-2.67540019	0.04485001
IL11	1.671743914	0.026763701	SCN9A	-2.708192102	0.000364269
HCG27	1.657891041	0.04485001	PDE1C	-2.765851233	0.000347909
CAPNS2	1.617171851	0.043996374	GFRA1	-3.050639306	0.000491795
---	1.589580086	0.043912639	PSG4	-3.219485816	0.000112717
---	1.568294753	0.043996374	EPCAM	-3.403421526	0.026763701

Table 5.19: All IOSE523-myrAKT3 GeneGO pathways identified using FC >2, P-val 0.05.

#	GeneGO Pathways	P-Value
1	Development_GDNF family signalling	0.001311774
2	Development_HGF signaling pathway	0.001369195
3	G-protein signaling_Proinsulin C-peptide signaling	0.001674125
4	Immune response_PGE2 common pathways	0.001674125
5	Apoptosis and survival_NO synthesis and signaling	0.001871258
6	PGE2 pathways in cancer	0.001871258
7	Nicotine metabolism in liver	0.001936000
8	Immune response_IL-17 signaling pathways	0.002223234
9	Transcription_PPAR Pathway	0.002297121
10	Immune response_CD40 signaling	0.002525726
11	Immune response_Gastrin in inflammatory response	0.002929734

The genes that form this particular gene set include numerous histone cluster genes, upstream binding transcription factor RNA polymerase I (UBTF/*UBF*), methy-CpG binding domain protein 2 (*MBD2*), and mitogen-activated protein kinase 3 (*MAPK3*). These data demonstrating regulation of RNA Pol I promoter opening is consist with a recent publication from our laboratory showing that AKT is able to regulate Pol I initiation (Chan et al. 2011). Other enriched gene sets ranked highly included those involved in the regulation of chemokine receptors, and genes involved in packaging of telomere ends.

The differences in the GSEA between the IOSE523-myrAKT3 cells and both the IOSE523-myrAKT1 and 2 cells was reflected in a comparison of differentially regulated genes between all IOSE523-myrAKT cell lines, revealing that all three isoforms share a total of 24 significantly (p-val <0.05) regulated genes, 6 of which are up-regulated and 18 are down-regulated **(Figure 5.8)**. The highest number of genes shared are between myrAKT1 and myrAKT2 only, with a total of 111 genes, 42 up-regulated and 69 down-regulated. The least amount of similarity appears between myrAKT1 and myrAKT3 cell lines, as there are no genes commonly regulated specifically between these two cell lines. These similarities between AKT 1 and 2, and differences with AKT3 may be reflected in previous studies demonstrating similarities in AKT isoform specific signalling, where AKT 1 and 2 have shown to be required for TSC2 phosphorylation while AKT3 is not, in addition to showing that AKT3 is required for p27 phosphorylation, but AKT 1 and 2 are not (Brognard et al. 2007), together possibly suggesting a greater level of similarity between AKT 1 and 2.

5.3.3 Comparative analysis of gene expression differences between IOSE523-myrAKT and HOSE-SGK3CA cells

Given that microarray studies were not performed on the IOSE523-SGK3 cells, as stable SGK3CA over-expression did not elicit an observable phenotype, a comparative analysis between the HOSE SGK3CA and IOSE523 myrAKT cells were carried out to gain further insight into the similarities and/or differences in signalling between these kinases in epithelial ovarian cells. Individual analyses, using a p-val <0.05 determined that HOSE SGK3 CA cells shared a total of nine, 25 and three differentially regulated genes with IOSE523 myrAKT1 and IOSE523 myrAKT2 cell lines, respectively **(Figure 5.9, Figure 5.10)**. IOSE523 myrAKT1 and HOSE SGK3 CA shared nine differentially regulated genes, five being up-regulated and four being down-regulated, IOSE523-myrAKT2 and HOSE-SGK3CA shared 25 differentially regulated genes, 13 being up-regulated and 12 being down-regulated.

Interestingly, three of the shared up-regulated genes between both myrAKT1 and SGK3 CA, and myrAKT2 and SGK3 CA are the same, which include Leupaxin (*LPXN*), a focal adhesion-associated adaptor protein, solute carrier family 6 (neutral amino acid transporter) member 15 (*SLC6A15*), an amino acid transporter, and *IL-6*, which is involved in the induction of an inflammatory response. A comparison between IOSE523-myrAKT3 and HOSE-SGK3CA revealed that there were only three genes

Table 5.20: Top 20 ranked gene sets enriched in IOSE523-myrAKT3. FDR <25%, ranked according to FWER p-val (http://www.broadinstitute.org/gsea/msigdb/). See supplementary data DVD affixed to the back cover for complete list.

Rank	GSEA set	Brief description of GSEA set	FDR q-val
1	REACTOME_RNA_POLYMERASE_I_PROMOTER_OPENING	Genes involved in RNA Polymerase I Promoter Opening	0.001
2	REACTOME_CHEMOKINE_RECEPTORS_BIND_CHEMOKINES	Genes involved in Chemokine receptors bind chemokines	0.016
3	REACTOME_PACKAGING_OF_TELOMERE_ENDS	Genes involved in Packaging Of Telomere Ends	0.013
4	SHEN_SMARCA2_TARGETS_DN	Genes whose expression negatively correlated with that of SMARCA2 in prostate cancer samples.	0.013
5	KLEIN_TARGETS_OF_BCR_ABL1_FUSION	Brief description Genes changed in pre-B lymphoblastic leukemia cells with BCR-ABL1 fusion vs normal pre-B lymphocytes.	0.012
6	REACTOME_GPCR_LIGAND_BINDING	Genes involved in GPCR ligand binding	0.012
7	KEGG_SYSTEMIC_LUPUS_ERYTHEMATOSUS	Systemic lupus erythematosus	0.018
8	FARMER_BREAST_CANCER_CLUSTER_1	Cluster 1: interferon, T and B lymphocyte genes clustered together across breast cancer samples.	0.018
9	REACTOME_PEPTIDE_LIGAND_BINDING_RECEPTORS	Brief description Genes involved in Peptide ligand-binding receptors	0.019
10	REACTOME_CLASS_A1_RHODOPSIN_LIKE_RECEPTORS	Genes involved in Class A/1 (Rhodopsin-like receptors)	0.021
11	BIOCARTA_IL17_PATHWAY	IL 17 Signaling Pathway	0.029
12	KEGG_MATURITY_ONSET_DIABETES_OF_THE_YOUNG	Maturity onset diabetes of the young	0.038
13	SCHLESINGER_H3K27ME3_IN_NORMAL_AND_METHYLATED_IN_CANCER	Genes bearing the H3K27me3 mark in normal cells; their DNA is methylated in cancer cells.	0.042
14	KIM_LRRC3B_TARGETS	Immune response genes up-regulated in zenograft tumors formed by SNU-601 cells (gastric cancer) made to express LRRC3B.	0.049
15	KEGG_NEUROACTIVE_LIGAND_RECEPTOR_INTERACTION	Neuroactive ligand-receptor interaction	0.047
16	MAHADEVAN_RESPONSE_TO_MP470_UP	Top genes up-regulated in the GIST (gastrointestinal stromal tumor) cell line resistant to imatinib after treatment with MP470, a protein kinase inhibitor.	0.055
17	BIOCARTA_INFLAM_PATHWAY	Cytokines and Inflammatory Response	0.057
18	REACTOME_IMMUNOREGULATORY_INTERACTIONS_BETWEEN_A_LYMPHOID_AND_A_NON_LYMPHOID_CELL	Genes involved in Immunoregulatory interactions between a Lymphoid and a non-Lymphoid cell	0.086
19	REACTOME_NCAM1_INTERACTIONS	Genes involved in NCAM1 interactions	0.082
20	MCLACHLAN_DENTAL_CARIES_UP	Genes up-regulated in pulpal tissue extracted from carious teeth.	0.100

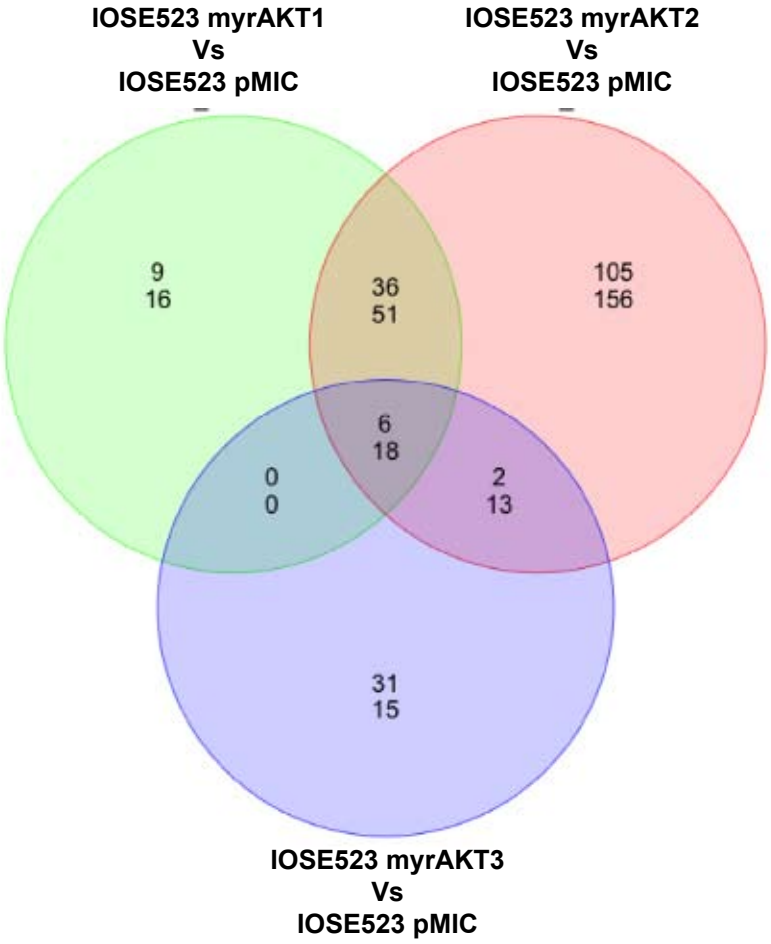

Figure 5.8: Venn diagram showing common differentially regulated genes between all three IOSE523-myrAKT cell lines. P-val <0.05 FC 0. Top number represents up-regulated genes and bottom number represents down-regulated genes.

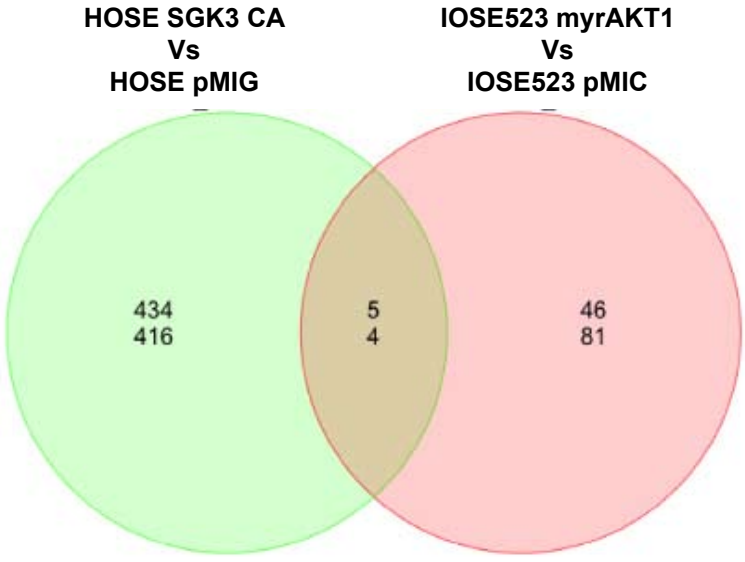

Figure 5.9: Venn diagram showing common differentially regulated genes between IOSE523-myrAKT1 and HOSE SGK3CA cell lines. P-val <0.05 FC 0. Top number represents up-regulated genes and bottom number represents down-regulated genes.

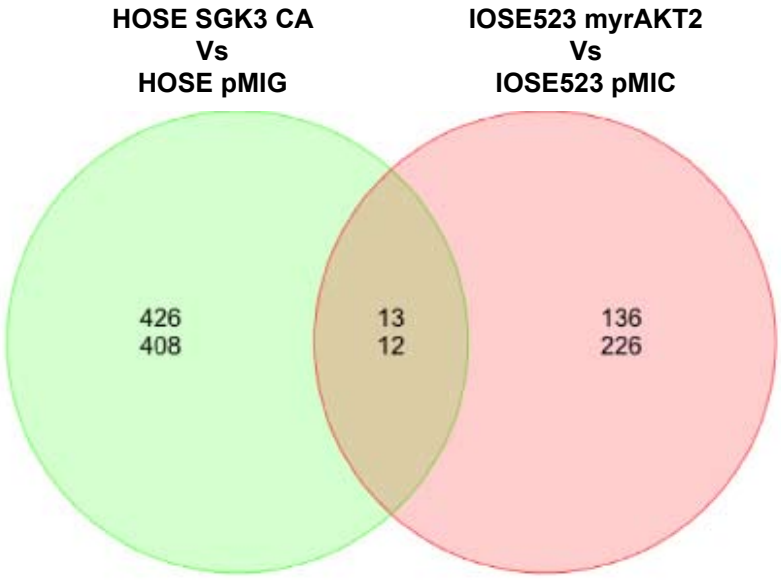

Figure 5.10: Venn diagram showing common differentially regulated genes between IOSE523-myrAKT2 and HOSE SGK3CA cell lines. P-val <0.05 FC 0. Top number represents up-regulated genes and bottom number represents down-regulated genes.

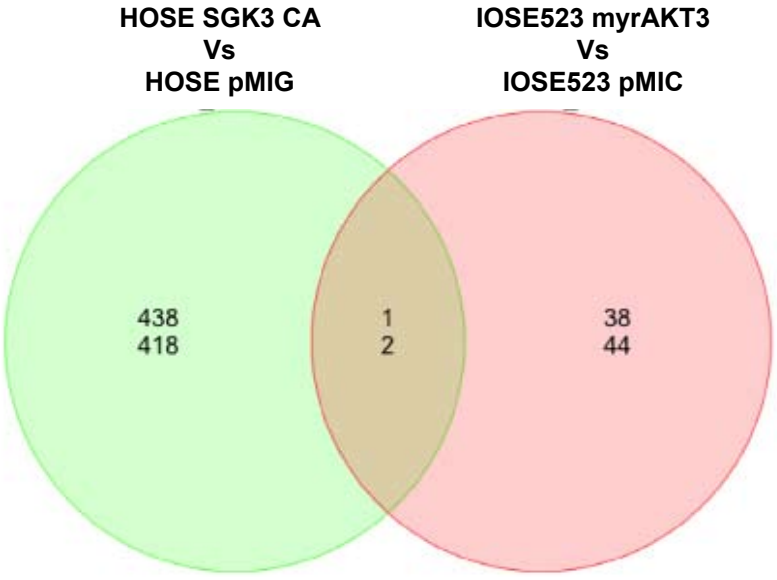

Figure 5.11: Venn diagram showing common differentially regulated genes between IOSE523-myrAKT3 and HOSE SGK3CA cell lines. P-val <0.05 FC 0. Top number represents up-regulated genes and bottom number represents down-regulated genes.

differentially regulated, with one up-regulated and two down-regulated (p-val <0.05) **(Figure 5.11)**. The gene expression data indicate that in ovarian epithelial cells SGK3 induced signalling is more comparable to AKT1 and AKT2 induced signalling than that of AKT3.

5.3.4 Differential gene expression in over-expression of SGK3 mutants in BJ-hTERT cells

To further understand SGK3 signalling we used a second model, BJ-hTERT fibroblast cells stably over-expressing SGK3 CA (as described in Chapter 3.2), to determine gene expression changes associated with SGK3 signalling. In these cells SGK3 CA increased cell size, demonstrated to be associated with increased rDNA transcription and both RNA and protein per cell (as shown in Chapter 3) but unlike the phenotype in HOSE cells did not increase cell proliferation. Analysis of the BJ-hTERT SGK3 CA cells revealed a total of 31 genes were significantly (p<0.05) differentially regulated, with 20 up-regulated and 11 down-regulated. The majority of regulated genes were within a +/-2 FC range **(Figure 5.12 and Table 5.21)**.

MetaCore™ pathway analysis using a p-val of <0.05 reveal SGK3 CA to be significantly involved in 86 pathways in BJ-hTERT cells **(Table 5.22 and supplementary data Table S.7)**, and only eight after applying a FC cut off of 2 **(Table 5.23)**. Many of these pathways demonstrated involvement of SGK3 CA in PI3-K signalling, through regulation of PI3-K subunits, development and immune response. Manual inspection of differentially regulated genes also detected the increased expression of genes associated with lipid metabolism apolipoprotein D (*APOD*) (Do Carmo et al. 2009), cell adhesion cluster of differentiation 36 (*CD36*) (Trinh-Trang-Tan et al. 2010), and polarity prickle homolog 2 (Drosophila) (*PRICKLE2*) (Katoh 2005). Interestingly, the hypoxia induced gene DNA-damage-inducible transcript 4 (*DDIT4*) was also detected at a 2.63 fold change in the BJ-hTERT SGK3CA cells, which is an established negative regulator of mTOR activity through TSC1/2 (Brugarolas et al. 2004; Reiling and Hafen 2004). GSEA of BJ-hTERT SGK3 CA revealed 933 out of 2526 gene sets that were enriched, however none of those gene sets were significant with a FDR <25%.

5.3.5 Gene expression changes with myr-AKT over-expression in BJ-hTERT cells

The BJ-hTERT myrAKT cell lines were not used in functional work outlined in this thesis, however recent publications from our laboratory have reported that these cell lines do have a robust cell growth (Chan et al. 2011) and senescence phenotype (Astle et al. 2011). Analysis of BJ-hTERT myrAKT1 gene expression data revealed a total of 71 differentially regulated genes, with 65 up-regulated and six down-regulated **(Figure 5.13 and Table 5.24)**. MetaCore™ pathway analysis using a p-val <0.05 demonstrated significant involvement of myrAKT1 45 pathways **(Table 5.25 and supplementary data Table S.8)** in the immune and inflammation response through the regulation of complement component 3 (*C3*), and PI3-K signalling**.** Applying a

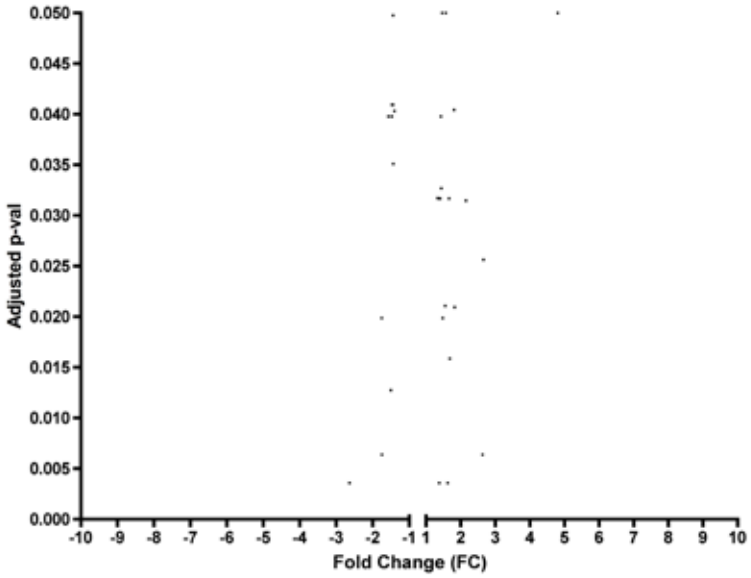

Figure 5.12: BJ-hTERT SGK3 CA gene expression data compared with BJ-hTERT pMIG gene expression data. n=3, P-val <0.05.

Table 5.21: All BJ-hTERT SGK3 CA compared with BJ-hTERT-pMIG gene expression data. Ranked according to fold change. n=3, p-val <0.05. Up-regulated and down-regulated.

UP-REGULATED GENES			DOWN-REGULATED GENES		
Gene Symbol	Fold Change	Adjusted P-Value	Gene Symbol	Fold Change	Adjusted P-Value
SGK3	37.75910482	1.85E-17	EMP2	-1.412963932	0.040311507
APOD	4.799126685	0.049988753	RASA3	-1.442668413	0.035086071
CD36	2.657687932	0.025615983	BST1	-1.443801166	0.040930983
DDIT4	2.630592118	0.006376957	STMN1	-1.446911294	0.049758414
COL14A1	2.153790015	0.031470006	PIK3CD	-1.4791803	0.040930983
PIK3R3	1.826076336	0.020933321	CCDC80	-1.482329846	0.039781983
---	1.807171473	0.040413281	SPRY2	-1.505141887	0.012750754
SORBS1	1.683940515	0.015876016	ARNT2	-1.572522344	0.039781983
PCDH10	1.661981629	0.031671362	GLI3	-1.751520369	0.006376957
CORO2B	1.626385595	0.003595145	PTN	-1.759224618	0.019879513
---	1.57476722	0.049988753	KIAA1199	-2.638421123	0.003595145
MLLT11	1.551794563	0.021061041			
ITGA6	1.478300063	0.019879513			
GALNT1	1.465627545	0.049988753			
---	1.440269773	0.032682506			
---	1.425539526	0.039781983			
PRICKLE2	1.412997023	0.031671362			
GYS1	1.38104888	0.003595145			
ENDOD1	1.37685154	0.031671362			
CTPS	1.329833157	0.031699214			

Table 5.22: BJ-hTERT SGK3 CA GeneGO pathways identified using FC 0, P-val <0.05. Ranked according to p-val. See Appendix I for complete list.

#	GeneGO Pathways	P-Value
1	Signal transduction_AKT signaling	4.517e-5
2	Development_PIP3 signaling in cardiac myocytes	5.911e-5
3	Development_IGF-1 receptor signaling	7.562e-5
4	Regulation of lipid metabolism_Insulin regulation of glycogen metabolism	1.002e-4
5	Development_EGFR signaling via PIP3	6.537e-4
6	Development_Dopamine D2 receptor transactivation of EGFR	7.124e-4
7	Immune response_IL-23 signaling pathway	7.736e-4
8	Immune response_IL-10 signaling pathway	8.373e-4
9	Apoptosis and survival_NGF signaling pathway	8.373e-4
10	NGF activation of NF-kB	1.041e-3

Table 5.23: All BJ-hTERT SGK3 CA GeneGO pathways identified using FC >2, P-val <0.05. Ranked according to P-val.

#	GeneGO Pathways	P-Value
1	Niacin-HDL metabolism	9.362e-5
2	Transport_Intracellular cholesterol transport in norm	3.082e-4
3	Atherosclerosis_Role of ZNF202 in regulation of expression of genes involved in Atherosclerosis	7.564e-3
4	Cholesterol and Sphingolipids transport / Recycling to plasma membrane in lung (normal and CF)	8.282e-3
5	Development_Thrombospondin-1 signaling	1.008e-2
6	Transport_FXR-regulated cholesterol and bile acids cellular transport	1.509e-2
7	Regulation of lipid metabolism_PPAR regulation of lipid metabolism	1.509e-2
8	Regulation of lipid metabolism_G-alpha(q) regulation of lipid metabolism	2.115e-2

p-val of <0.05 in addition to a FC cut off of 2 revealed 83 pathways that myrAKT1 is significantly involved in **(Table 5.26 and supplementary data Table S.9)**. GSEA analysis demonstrated 1603 out of 2526 gene sets enriched in BJ-hTERT myrAKT1, with 210 gene sets significant with FDR <25% **(Table 5.27)**.

Many of the highly ranked gene sets enriched in myrAKT1 induced genes were genes expressed in a variety of tumour types, including endothelial tumours, head and neck squamous cell carcinoma, acute myeloid leukaemia, and prostate tumours implicating AKT signalling in these tumour types. The "BIOCARTA _AKT_PATHWAY" gene signature fell within the FDR < 25% cut off and was the 141st pathway listed. Increased signalling through the PI3K/AKT pathway leads to negative feedback loops one of these being decreased transcription of growth factor receptors (Sheppard, unpublished data) in fibroblast cells AKT1 induced a decrease in insulin-like growth factor receptor (*IGFR*) mRNA, suggesting that this feedback loop is active in these cells.

Analysis of BJ-hTERT myrAKT2 gene expression data showed a total of 352 genes differentially regulated, with 249 up-regulated and 103 down-regulated **(Figure 5.14 and Table 5.28)**. MetaCore™ pathway analysis revealed significant involvement of myrAKT2 in 64 pathways **(Table 5.29, supplementary data Table S.10),** associated mainly with cell adhesion pathways through up-regulation of a number of genes including osteonectin (*SPARC*), matrix metallopeptidase *(MMP) 7*, laminin 1 (*LAMC1*), *MMP-14*, serpin peptidase inhibitor clade E (nexin plasminogen activator inhibitor type 1) member 2 (*SERPINE2*) and plasminogen activator urokinase (*PLAU*). In addition, pathways involved in immune response were also present through the regulation of interleukin 1 (*IL-1*) and *C3*. Applying a FC cut off of 2 demonstrated myrAKT2 to be significantly involved in 27 pathways **(Table 5.30, supplementary data Table S.11)**, many of which also involved in the immune response, cell adhesion and development.

BJ-hTERT myrAKT2 GSEA revealed 1657 out of 2526 gene sets enriched, and 618 gene sets significant with a FDR>25% **(Table 5.31)**. The two most highly ranked gene sets were both sets induced by treatment with IFN-α. Closer analysis of the top 20 ranked gene sets revealed a list similar to that of gene sets enriched in BJ-hTERT myrAKT1 cells with many of the same tumour gene sets enriched.

Analysis of BJ-hTERT myrAKT3 gene expression data demonstrated a total of 601 genes, with 373 up-regulated and 228 down-regulated **(Figure 5.15 and Table 5.32)**. As with BJ-hTERT myrAKT1 and myrAKT2 gene expression, MetaCore™ pathway analysis (p-val <0.05) revealed the significant involvement of myrAKT3 in only 11 pathways **(Table 5.33)**, and applying a FC cut off of 2 showed significant involvement in 22 pathways **(Table 5.34)**. Significant pathways were associated with immune response through C3, revealed that myrAKT3 is implicated in regulating genes involved in the production of arachidonic acid, a lipid second messenger and key inflammatory intermediate, through the up-regulation of several molecules including

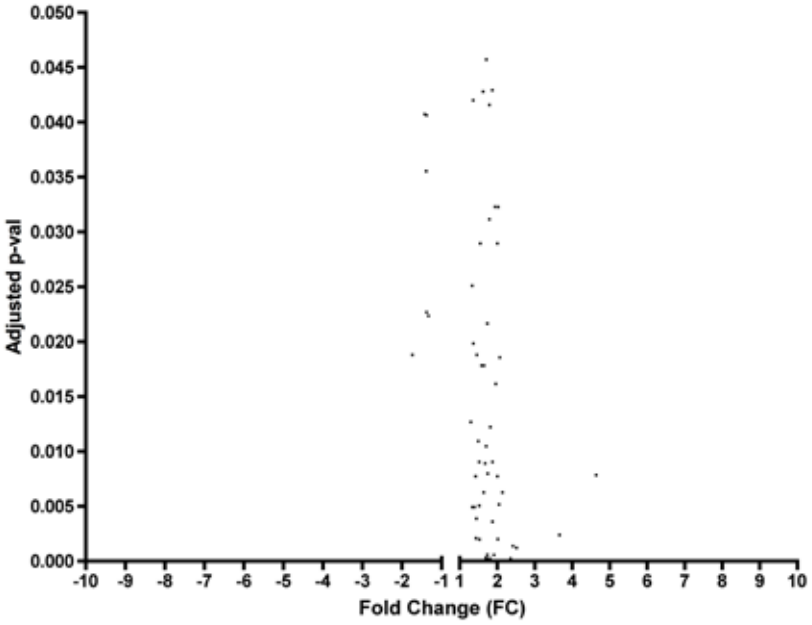

Figure 5.13: BJ-hTERT myrAKT1 gene expression data compared with BJ-hTERT pMIC gene expression data. n=3, p-val <0.05.

Table 5.24: BJ-hTERT myrAKT1 compared with BJ-hTERT-pMIC gene expression data. Ranked according to fold change. n=3, p-val <0.05. Up-regulated and down-regulated genes. See supplementary data DVD affixed to the back cover for complete list.

UP-REGULATED GENES			DOWN-REGULATED GENES		
Gene Symbol	Fold Change	Adjusted P-Value	Gene Symbol	Fold Change	Adjusted P-Value
C3	11.00426167	1.19E-06	IGF1R	-1.33176138	0.022347744
AKT1	5.134613006	3.18E-15	NFATC3	-1.381946017	0.040635429
IL13RA2	4.655983443	1.46E-09	---	-1.381951065	0.02269137
SERPINB2	4.633723292	0.007852621	MAMLD1	-1.388386709	0.03554462
CD36	4.216904665	3.93E-05	MEIS1	-1.43295021	0.040725338
TRPA1	4.004780721	9.40E-07	SNORD115-42	-1.743605985	0.018811183
IL1A	3.659412075	0.002394498			
TDO2	3.654952239	1.91E-07			
DPP4	3.135343233	1.46E-05			
IL1B	2.760990783	1.93E-06			
CH25H	2.665422898	2.86E-06			
SEMA3C	2.601866916	3.84E-05			
COL14A1	2.514087548	0.00122494			
PIK3R3	2.481133259	2.03E-05			
CLDN1	2.413230803	0.001381302			
SPON2	2.350915022	0.000239987			
SLC2A12	2.134958237	0.006277265			
APCDD1	2.068364633	0.018562633			
SOD3	2.043925753	0.005167483			
SYT1	2.031729469	4.85E-06			

Table 5.25: BJ-hTERT myrAKT1 GeneGO pathways identified using FC 0, p-val <0.05. Ranked according to p-val. See Appendix I for complete list.

#	GeneGO Pathways	P-Value
1	Immune response_Alternative complement pathway	2.085e-8
2	Immune response_Lectin induced complement pathway	8.635e-8
3	Immune response_Classical complement pathway	1.244e-7
4	Development_PEDF signaling	7.544e-5
5	Signal transduction_IP3 signaling	7.544e-5
6	Immune response_IL-17 signaling pathways	1.673e-4
7	Development_Delta-type opioid receptor mediated cardioprotection	6.653e-4
8	Cell adhesion_PLAU signaling	7.774e-4
9	Apoptosis and survival_BAD phosphorylation	9.671e-4
10	Neurophysiological process_HTR1A receptor signaling in neuronal cells	9.671e-4

Table 5.26: BJ-hTERT myrAKT1 GeneGO pathways identified using FC >2, p-val <0.05. Ranked according to p-val. See Appendix I for complete list.

#	GeneGO Pathways	P-Value
1	Immune response_Alternative complement pathway	1.27431E-10
2	Immune response_Lectin induced complement pathway	5.39429E-10
3	Immune response_Classical complement pathway	7.8241E-10
4	Development_Delta-type opioid receptor mediated cardioprotection	6.33517E-05
5	Cell adhesion_PLAU signalling	7.43119E-05
6	Immune response_Inhibitory action of Lipoxins on pro-inflammatory TNF-alpha signalling	0.000114448
7	Development_PEDF signalling	0.000147794
8	Immune response_TREM1 signaling pathway	0.000257269
9	Immune response_IL-17 signaling pathways	0.000270443
10	Development_FGF2-dependent induction of EMT	0.000822984

Table 5.27: Top 20 ranked GSEA gene sets enriched in BJhTERT-myrAKT1. FDR <25%, ranked according to FWER p-val (http://www.broadinstitute.org/gsea/msigdb/). See supplementary data DVD affixed to the back cover for complete list.

Rank	GSEA set	Brief description of GSEA set	FDR q-val
1	LU_TUMOR_ENDOTHELIAL_MARKERS_UP	Genes specifically up-regulated in tumor endothelium.	0.001
2	LU_TUMOR_VASCULATURE_UP	Genes up-regulated in endothelial cells derived from invasive ovarian cancer tissue.	0.000
3	KANG_IMMORTALIZED_BY_TERT_UP	Up-regulated genes in the signature of adipose stromal cells (ADSC) immortalized by forced expression of telomerase (TERT).	0.000
4	AMIT_EGF_RESPONSE_120_MCF10A	Genes whose expression peaked at 120 min after stimulation of MCF10A cells with EGF	0.001
5	BOQUEST_STEM_CELL_CULTURED_VS_FRESH_DN	Genes down-regulated in cultured stromal stem cells from adipose tissue, compared to the freshly isolated cells.	0.001
6	CROMER_TUMORIGENESIS_UP	Tumorigenesis markers of head and neck squamous cell carcinoma (HNSCC): up-regulated in the 'early' tumors vs normal samples.	0.005
7	MACLACHLAN_BRCA1_TARGETS_DN	Genes down-regulated in SW480 cells (colon cancer with mutated p53) upon expression of BRCA1 off an adenovirus vector.	0.005
8	VERHAAK_AML_WITH_NPM1_MUTATED_UP	Genes up-regulated in acute myeloid leukemia (AML) patients with mutated NPM1.	0.013
9	ONDER_CDH1_SIGNALING_VIA_CTNNB1	Genes changed in HMLE cells (mmortalized nontransformed mammary epithelium) after RNAi knockdown of both CDH1 and CTNNB1, compared to the knockdown of CDH1 alone.	0.017
10	CLASPER_LYMPHATIC_VESSELS_DURING_METASTASIS_DN	Selected genes down-regulated during invasion of lymphatic vessels during metastasis.	0.021
11	HINATA_NFKB_TARGETS_KERATINOCYTE_UP	Genes up-regulated in primary keratinocytes by expression of p50 (NFKB1) and p65 (RELA) components of NFKB.	0.023
12	COLIN_PILOCYTIC_ASTROCYTOMA_VS_GLIOBLASTOMA_UP	Genes up-regulated in pilocytic astrocytoma compared to glioblastoma samples.	0.022
13	BIOCARTA_LAIR_PATHWAY	Cells and Molecules involved in local acute inflammatory response	0.020
14	LIU_VAV3_PROSTATE_CARCINOGENESIS_UP	Selected genes up-regulated in prostate tumors developed by transgenic mice overexpressing VAV3 in prostate epithelium.	0.019
15	HINATA_NFKB_TARGETS_FIBROBLAST_UP	Genes up-regulated in primary fibroblast cells by expression of p50 (NFKB1) and p65 (RELA) components of NFKB.	0.023
16	HUPER_BREAST_BASAL_VS_LUMINAL_UP	Genes up-regulated in basal mammary epithelial cells compared to the luminal ones.	0.023
17	KEGG_TRYPTOPHAN_METABOLISM	Tryptophan metabolism	0.026
18	GERY_CEBP_TARGETS	Genes changed in NIH 3T3 cells (embryonic fibroblast) by expression of one or more of C/EBP proteins: CEBPA, CEBPB, CEBPG, and CEBPD.	0.026
19	KEGG_STEROID_HORMONE_BIOSYNTHESIS	Steroid hormone biosynthesis	0.027
20	THUM_MIR21_TARGETS_HEART_DISEASE_UP	Genes up-regulated in a mouse model of heart disease whose expression reverted to normal by silencing of MIR21 microRNA.	0.026

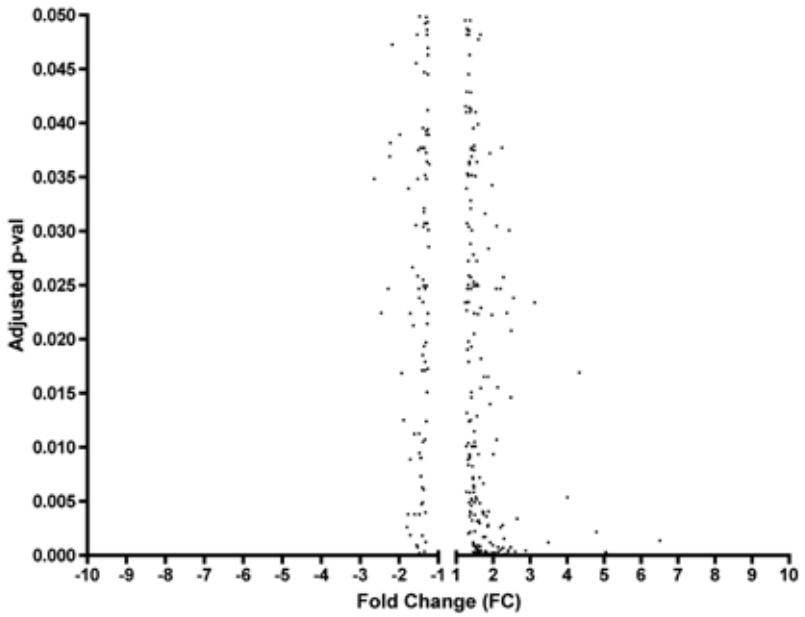

Figure 5.14: BJ-hTERT myrAKT2 gene expression data compared with BJ-hTERT pMIC gene expression data. n=3, p-val <0.05.

Table 5.28: BJ-hTERT myrAKT2 compared with BJ-hTERT-pMIC gene expression data. Ranked according to fold change. n=3, p-val <0.05. Top 20 up-regulated and down-regulated genes. See supplementary data DVD affixed to the back cover for complete list.

UP-REGULATED GENES			DOWN-REGULATED GENES		
Gene Symbol	Fold Change	Adjusted P-Value	Gene Symbol	Fold Change	Adjusted P-Value
POSTN	31.41594919	0.001783949	CHML	-1.555510604	0.000970309
C3	15.44233777	3.03E-08	GPR137C	-1.567019376	0.045524976
IL1A	13.21549767	1.29E-08	SORT1	-1.575135118	0.030544782
TRPA1	12.19843052	1.37E-12	ARNT2	-1.608890869	0.003807439
TDO2	10.68993248	1.90E-13	NEDD1	-1.613650233	0.011231134
AKT2	9.127722343	3.89E-20	SNORD115-6	-1.640647111	0.021278824
CH25H	8.440178622	1.90E-13	CWH43	-1.667817044	0.026652096
IL1B	6.965363543	1.37E-12	SNORD115-42	-1.719002393	0.008877654
APOD	6.504751489	0.00136962	DSP	-1.720219569	0.00188396
COL14A1	6.361736208	3.86E-09	FRMD4B	-1.723321228	0.022394114
IL13RA2	6.194211904	9.37E-12	UCP2	-1.767867048	0.033956192
RANBP3L	5.125693132	7.63E-09	ADAMTS6	-1.775358488	0.003812639
FRZB	5.043714597	0.000305705	IL17RB	-1.801485431	0.002626951
SERPINB2	4.788626271	0.00217753	MBOAT1	-1.890211495	0.012515067
CYP1B1	4.328736625	0.016912118	KIAA1199	-1.93979645	0.016865334
PRSS35	4.216107284	8.65E-06	SNORD115-20	-1.984606144	0.038921279
APCDD1	4.205623267	3.97E-07	SNORD115-26	-2.231038464	0.038164999
TNFSF18	4.004903386	0.005376179	SNORD115-12	-2.24545789	0.036905071
DPP4	3.823852353	3.31E-07	GRIA1	-2.46668704	0.022429012
CD36	3.744278273	6.22E-05	SNORD115-11	-2.645904479	0.034822358

Table 5.29: BJ-hTERT myrAKT2 GeneGO pathways identified using FC 0, p-val <0.05. Ranked according to p-val. See Appendix I for complete list.

#	GeneGO Pathways	P-Value
1	Cell adhesion_ECM remodelling	1.77228E-05
2	Cell adhesion_Chemokines and adhesion	3.10152E-05
3	Immune response_Alternative complement pathway	3.31371E-05
4	Immune response_IL-17 signaling pathways	4.59631E-05
5	Transport_RAB3 regulation pathway	5.71133E-05
6	Immune response_Lectin induced complement pathway	0.000124456
7	Immune response_Classical complement pathway	0.000174163
8	Development_Role of HDAC and calcium/calmodulin-dependent kinase (CaMK) in control of skeletal myogenesis	0.000215197
9	Immune response_TREM1 signaling pathway	0.0003515
10	Cell adhesion_PLAU signalling	0.000375206

Table 5.30: BJ-hTERT myrAKT2 GeneGO pathways identified using FC >2, p-val <0.05. Ranked according to p-val. See Appendix I for complete list.

#	GeneGO Pathways	P-Value
1	Immune response_Alternative complement pathway	5.84337E-08
2	Immune response_Lectin induced complement pathway	2.40292E-07
3	Immune response_Classical complement pathway	3.45514E-07
4	Immune response_IL-17 signaling pathways	8.21969E-07
5	Cell adhesion_PLAU signalling	5.86955E-05
6	Development_PEDF signalling	0.000145208
7	Cell adhesion_Chemokines and adhesion	0.000211686
8	Immune response_TREM1 signaling pathway	0.00029957
9	Immune response_Gastrin in inflammatory response	0.00054652
10	Androstenedione and testosterone biosynthesis and metabolism p.2	0.00091816

Table 5.31: Top 20 ranked GSEA gene sets enriched in BJhTERT-myrAKT2. FDR <25%, ranked according to FWER p-val (http://www.broadinstitute.org/gsea/msigdb/). See supplementary data DVD affixed to the back cover for complete list.

Rank	GSEA set	Brief description of GSEA set	FDR q-val
1	MOSERLE_IFNA_RESPONSE	Brief description Top 50 genes up-regulated in ovarian cancer progenitor cells (also known as side population, SP, cells) in response to interferon alpha (IFNA).	0.000
2	BROWNE_INTERFERON_RESPONSIVE_GENES	Genes up-regulated in primary fibroblast culture after treatment with interferon alpha for 6 h.	0.000
3	LIANG_SILENCED_BY_METHYLATION_2	Genes up-regulated in T24 cells (bladder carcinoma) after treatment with decitabine (5-aza-2'-deoxycytidine).	0.000
4	VERHAAK_AML_WITH_NPM1_MUTATED_UP	Genes up-regulated in acute myeloid leukemia (AML) patients with mutated NPM1.	0.000
5	MAHADEVAN_RESPONSE_TO_MP470_UP	Top genes up-regulated in the GIST (gastrointestinal stromal tumor) cell line resistant to imatinib after treatment with MP470, a protein kinase inhibitor.	0.000
6	GRAHAM_CML_QUIESCENT_VS_NORMAL_DIVIDING_UP	Genes up-regulated in quescent CD34+ cells isolated from peripheral blood of CML (chronic myeloblastic leukemia) patients compared to the dividing cells from normal donors.	0.000
7	SANA_TNF_SIGNALING_UP	Genes up-regulated in five primary endothelial cell types (lung, aortic, iliac, dermal, and colon) by TNF.	0.000
8	NAKAYAMA_SOFT_TISSUE_TUMORS_PCA1_UP	Top 100 probe sets contrubuting to the positive side of the 1st principal component; predominantly associated with spindle cell and pleomorphic sarcoma samples.	0.000
9	SEITZ_NEOPLASTIC_TRANSFORMATION_BY_8P_DELETION_UP	Genes up-regulated in CT60/4 cells (breast cancer reverted to normal by transfer of chromosome 8p region) vs parental MDA-MB-231 cells (deleted chromosome 8p).	0.000
10	LU_TUMOR_VASCULATURE_UP	Genes up-regulated in endothelial cells derived from invasive ovarian cancer tissue.	0.000
11	HINATA_NFKB_TARGETS_KERATINOCYTE_UP	Genes up-regulated in primary keratinocytes by expression of p50 (NFKB1) and p65 (RELA) components of NFKB.	0.000
12	LU_TUMOR_ENDOTHELIAL_MARKERS_UP	Genes specifically up-regulated in tumor endothelium.	0.000
13	HUPER_BREAST_BASAL_VS_LUMINAL_UP	Genes up-regulated in basal mammary epithelial cells compared to the luminal ones.	0.000
14	CROMER_TUMORIGENESIS_UP	Tumorigenesis markers of head and neck squamous cell carcinoma (HNSCC): up-regulated in the 'early' tumors vs normal samples.	0.000
15	DAUER_STAT3_TARGETS_DN	Top 50 genes down-regulated in A549 cells (lung cancer) expressing STAT3 off an adenovirus vector.	0.000
16	BOQUEST_STEM_CELL_CULTURED_VS_FRESH_DN	Genes down-regulated in cultured stromal stem cells from adipose tissue, compared to the freshly isolated cells.	0.000
17	AMIT_EGF_RESPONSE_120_MCF10A	Genes whose expression peaked at 120 min after stimulation of MCF10A cells with EGF.	0.000
18	HAHTOLA_MYCOSIS_FUNGOIDES_CD4_UP	Genes up-regulated in T helper cells (defines as CD4+) isolated from patients with mucosis fungoides compared to those from normal control donors.	0.000
19	GAURNIER_PSMD4_TARGETS	Inflammatory cytokines, chemokines and their cognate receptors up-regulated in THP-1 cells (monocyte) after treatment with PSMD4.	0.000
20	BIOCARTA_IL1R_PATHWAY	Signal transduction through IL1R	0.000

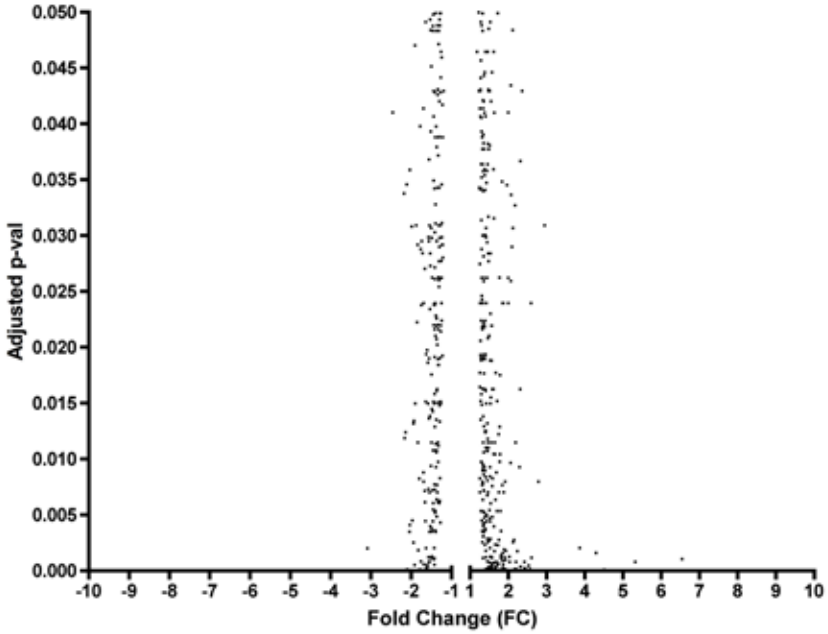

Figure 5.15: BJ-hTERT myrAKT3 gene expression data compared with BJ-hTERT pMIC gene expression data. n=3, p-val <0.05.

Table 5.32: BJ-hTERT myrAKT3 compared with BJ-hTERT-pMIC gene expression data. Ranked according to fold change. n=3, p-val <0.05. Top 20 up-regulated and down-regulated genes. See supplementary data DVD affixed to the back cover for complete list.

UP-REGULATED GENES			DOWN-REGULATED GENES		
Gene Symbol	**Fold Change**	**Adjusted P-Value**	**Gene Symbol**	**Fold Change**	**Adjusted P-Value**
POSTN	15.26385816	0.013365358	SNORD115-1	-1.859619527	0.022237742
TRPA1	11.36718645	4.14E-12	HIST1H1E	-1.879930715	0.030913162
CD36	9.782495972	7.75E-09	KIAA1199	-1.9042809	0.014963736
C3	9.275917336	1.40E-06	DUSP4	-1.909090245	0.0470209
IL13RA2	8.515994591	6.06E-13	NMI	-1.917894645	0.000516328
AKT3	7.20790787	8.03E-14	CCDC109B	-1.937368833	0.013430228
APOD	6.539718157	0.001056647	---	-1.944822804	0.002523723
SERPINB2	5.315832779	0.000803928	PM20D2	-1.946285707	0.013191653
IL1A	4.507910583	9.85E-05	FLJ30064	-1.974715694	0.004505746
SYTL5	4.386047529	7.39E-06	---	-1.990226298	0.030814741
INMT	4.289161407	0.001610695	CD274	-2.037303342	0.035870672
DPP4	4.266703751	1.15E-07	GFRA1	-2.039373647	0.004099899
FRZB	3.864816639	0.002041191	TGFBR3	-2.047023552	0.003492868
IL1B	3.795998378	7.75E-09	IL17RB	-2.102836974	0.00011091
COL14A1	3.496185107	4.41E-06	SULF1	-2.14345307	0.012399519
PIK3R3	3.480926943	4.47E-08	SLIT2	-2.162937272	0.01188163
SPON2	3.476681223	2.43E-07	SNORD115-26	-2.180033882	0.033763088
ITGB3	3.183963225	1.42E-05	ADAMTS6	-2.393632262	1.34E-05
APCDD1	3.161655485	1.47E-05	SNORD115-11	-2.45982894	0.041005205
SOD3	3.090641107	2.78E-06	GRIA1	-3.086417447	0.002008702

hepatic triacylglycerol lipase (*LIPC*), endothelial lipase (*LIPE*) and phospholipase A2 (*PLA2*). Cell adhesion pathways through differential regulation of caludin-1 (*CLDN1*), connexin 40 (*GJA5*), desmoplakin (*DSP*) and plakoglobin (*JUP*) were also ranked highly in pathway analysis results.

GSEA of the BJ-hTERT myrAKT3 gene expression data revealed 1562 out of 2526 gene sets to be enriched, with 424 of those genes sets significant with a FDR <25% **(Table 5.35)**. Similar to BJ-hTERT myrAKT1 and myrAKT2, a number of the highly ranked gene sets were of genes enriched in tumour tissue. Consistent with a previously reported phenotype of BJ-hTERT myrAKT3 (Astle et al. 2011) is the enrichment of genes up-regulated in a senescent phenotype.

To more specifically determine the similarity between gene expression of the three AKT isoforms in BJ-hTERT cells, a comparative analysis was performed. A total of 59 differentially regulated genes were common to all three AKT cell lines with 56 genes up- regulated and three genes down-regulated. Furthermore, the majority of genes regulated by AKT1 were the genes commonly regulated between all AKT isoforms, with only five genes being unique to AKT1. Both myrAKT2 and myrAKT3 induced many genes that were in common (226 genes), as well as distinct, 126 for myrAKT2 and 375 genes for myrAKT3 **(Figure 5.16)**.

5.3.6 Comparative analysis of gene expression differences between BJ-hTERT myrAKT and BJ-hTERT SGK3CA cells

A comparative analysis between the BJ-hTERT SGK3CA and BJ-hTERT myrAKT cells were carried out to more specifically determine similarities and differences between SGK3 and the AKT kinases in the same background. Individual analyses using a p-val <0.05 revealed that all three AKT kinases share very few commonly regulated genes with SGK3 CA in the BJ-hTERT cells, with myrAKT1 sharing a total of five genes with SGK3 CA **(Figure 5.17)**, myrAKT2 sharing a total of 13 genes with SGK3 CA **(Figure 5.18)**, and myrAKT3 sharing a total of 14 commonly regulated genes with SGK3 CA **(Figure 5.19)**. **Table 5.36** lists all genes common between SGK3 CA and the myrAKT cell lines.

Over all, from the total 59 genes commonly regulated by the AKT isoforms, only five of these are also commonly regulated by SGK3 CA (p-val <0.05), all of which are up-regulated genes **(Figure 5.20)**. Through closer investigation of all five shared genes it was found that two of these genes have been associated with tumourigenesis. Over-expressed myeloid/lymphoid or mixed-lineage leukemia (trithorax homolog Drosophila) translocated to 11 (MLLT11) has been reported to increase proliferation and metastases in human breast cancer cell lines (Chang et al. 2008), in addition to being a poor prognostic marker for patients with acute myeloid leukemia with normal cytogenics (Strunk et al. 2009). The PI3-K regulatory subunit *PIK3R3* has also been identified as a crucial regulator of various cancer associated signal transduction pathways. The remaining genes up-regulated by all myrAKT isoforms and SGK3 CA

Table 5.33: BJ-hTERT myrAKT3 GeneGO pathways identified using FC 0, p-val <0.05. Ranked according to p-val. See Appendix I for complete list.

#	GeneGO Pathways	P-Value
1	Immune response_Alternative complement pathway	3.04147E-07
2	Immune response_Lectin induced complement pathway	2.38343E-06
3	Immune response_Classical complement pathway	4.00448E-06
4	Arachidonic acid production	2.5476E-05
5	Muscle contraction_Regulation of eNOS activity in endothelial cells	0.000156493
6	Transport_RAB3 regulation pathway	0.000291088
7	Cell adhesion_Endothelial cell contacts by junctional mechanisms	0.000366879
8	Apoptosis and survival_BAD phosphorylation	0.000510486
9	Role of alpha-6/beta-4 integrins in carcinoma progression	0.000745638
10	Transport_Alpha-2 adrenergic receptor regulation of ion channels	0.000943769
11	Cell cycle_Role of Nek in cell cycle regulation	9.923e-4

Table 5.34: BJ-hTERT myrAKT3 GeneGO pathways identified using FC >2, p-val <0.05. Ranked according to p-val. See Appendix I for complete list.

#	GeneGO Pathways	P-Value
1	Immune response_Alternative complement pathway	8.63465E-08
2	Immune response_Lectin induced complement pathway	3.53977E-07
3	Immune response_Classical complement pathway	5.08506E-07
4	Immune response_MIF - the neuroendocrine-macrophage connector	0.000145208
5	Development_PEDF signaling	0.000186103
6	Immune response_IL-17 signaling pathways	0.000408417
7	Neurophysiological process_NMDA-dependent postsynaptic long-term potentiation in CA1 hippocampal neurons	0.001215033
8	Cell adhesion_PLAU signaling	0.001517334
9	Apoptosis and survival_BAD phosphorylation	0.001882519
10	Development_A2A receptor signaling	0.002015365

Table 5.35: Top 20 ranked GSEA gene sets enriched in BJhTERT-myrAKT3. FDR <25%, ranked according to FWER p-val (http://www.broadinstitute.org/gsea/msigdb/). See supplementary data DVD affixed to the back cover for complete list.

Rank	GSEA set	Brief description of GSEA set	FDR q-val
1	LU_TUMOR_ENDOTHELIAL_MARKERS_UP	Genes specifically up-regulated in tumor endothelium.	0.000
2	LU_TUMOR_VASCULATURE_UP	Genes up-regulated in endothelial cells derived from invasive ovarian cancer tissue.	0.000
3	HUPER_BREAST_BASAL_VS_LUMINAL_UP	Genes up-regulated in basal mammary epithelial cells compared to the luminal ones.	0.001
4	KANG_IMMORTALIZED_BY_TERT_UP	Up-regulated genes in the signature of adipose stromal cells (ADSC) immortalized by forced expression of telomerase (TERT).	0.002
5	VERHAAK_AML_WITH_NPM1_MUTATED_UP	Genes up-regulated in acute myeloid leukemia (AML) patients with mutated NPM1.	0.002
6	LIU_VAV3_PROSTATE_CARCINOGENESIS_UP	Selected genes up-regulated in prostate tumors developed by transgenic mice overexpressing VAV3 in prostate epithelium.	0.005
7	TANG_SENESCENCE_TP53_TARGETS_UP	Genes up-regulated in WI-38 cells (senescent primary fibroblasts) after inactivation of TP53 by GSE56 polypeptide.	0.005
8	BOQUEST_STEM_CELL_CULTURED_VS_FRESH_DN	Genes down-regulated in cultured stromal stem cells from adipose tissue, compared to the freshly isolated cells.	0.005
9	KEGG_TYPE_I_DIABETES_MELLITUS	Type I diabetes mellitus	0.006
10	CROMER_TUMORIGENESIS_UP	Tumorigenesis markers of head and neck squamous cell carcinoma (HNSCC): up-regulated in the 'early' tumors vs normal samples.	0.006
11	KEGG_ABC_TRANSPORTERS	ABC transporters	0.008
12	SCHUETZ_BREAST_CANCER_DUCTAL_INVASIVE_UP	Genes up-regulated in invasive ductal carcinoma (IDC) relative to ductal carcinoma in situ (DCIS, non-invasive).	0.009
13	PIEPOLI_LGI1_TARGETS_DN	Down-regulated genes in U87 cells (glioblastoma multiforme, GBM) engineered to stably express LGI1.	0.009
14	WANG_SMARCE1_TARGETS_UP	Genes up-regulated in BT549 cells (breast cancer) by expression of SMARCE1 off a retroviral vector.	0.008
15	KEGG_COMPLEMENT_AND_COAGULATION_CASCADES	Complement and coagulation cascades	0.013
16	KEGG_GRAFT_VERSUS_HOST_DISEASE	Graft-versus-host disease	0.013
17	VECCHI_GASTRIC_CANCER_ADVANCED_VS_EARLY_UP	Up-regulated genes distinguishing between two subtypes of gastric cancer: advanced (AGC) and early (EGC).	0.017
18	GRAHAM_CML_QUIESCENT_VS_NORMAL_DIVIDING_UP	Genes up-regulated in quescent CD34+ cells isolated from peripheral blood of CML (chronic myeloblastic leukemia) patients compared to the dividing cells from normal donors.	0.016
19	STOSSI_RESPONSE_TO_ESTRADIOL	Genes up-regulated by estradiol (E2) in U2OS cells (osteosarcoma) expressing ESR1 or ESR2.	0.025
20	AMIT_EGF_RESPONSE_120_MCF10A	Genes whose expression peaked at 120 min after stimulation of MCF10A cells with EGF.	0.025

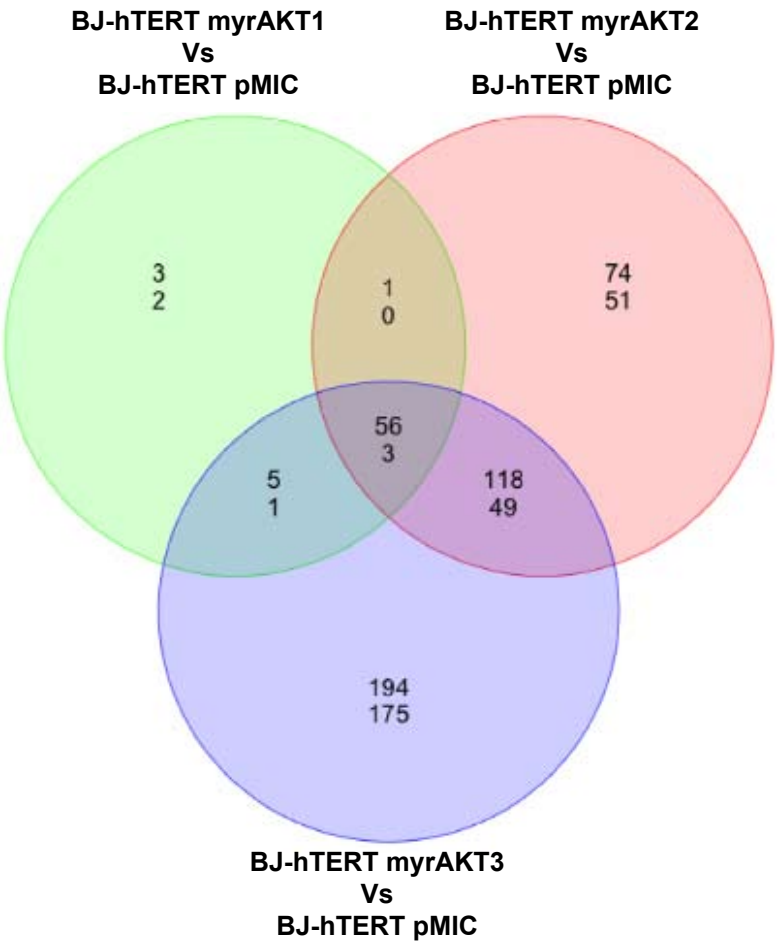

Figure 5.16: Venn diagram showing common differentially regulated genes between all three BJ-hTERT-myrAKT cell lines. P-val <0.05, FC 0. Top number represents up-regulated genes and bottom number represents down-regulated genes.

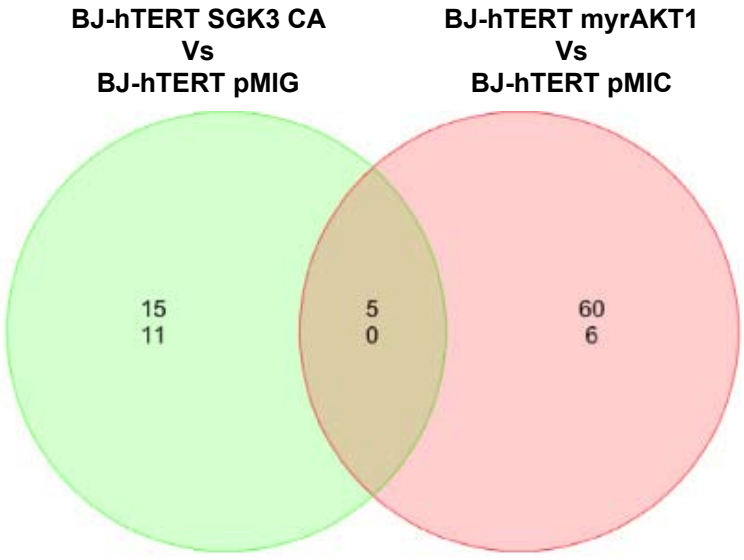

Figure 5.17: Venn diagram showing common differentially regulated genes between BJ-hTERT SGK3CA and BJ-hTERT myrAKT1 cell lines. P-val <0.05, FC 0. Top number represents up-regulated genes and bottom number represents down-regulated genes.

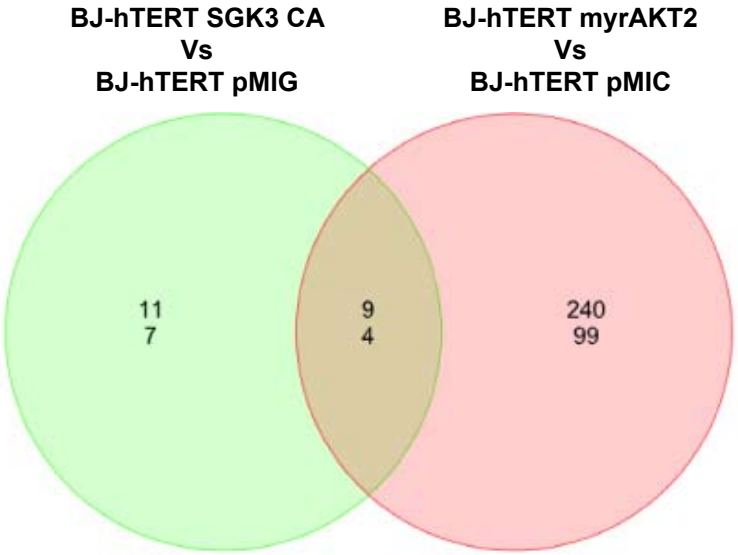

Figure 5.18: Venn diagram showing common differentially regulated genes between BJ-hTERT SGK3CA and BJ-hTERT myrAKT2 cell lines. P-val <0.05, FC 0. Top number represents up-regulated genes and bottom number represents down-regulated genes.

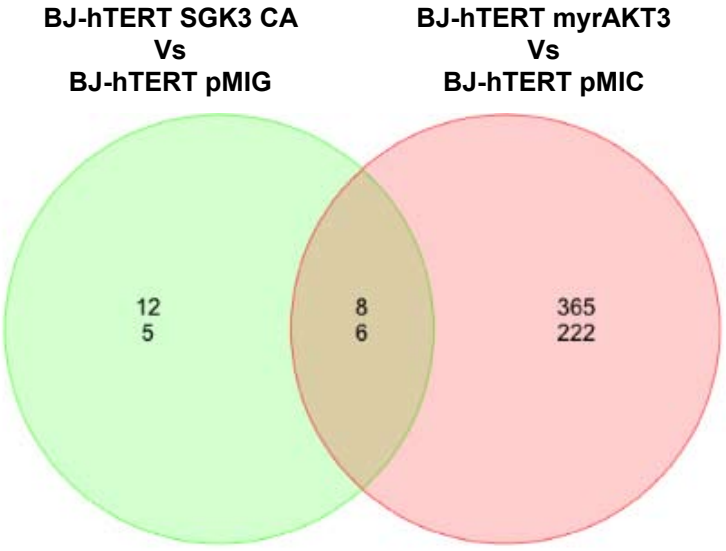

Figure 5.19: Venn diagram showing common differentially regulated genes between BJ-hTERT SGK3CA and BJ-hTERT myrAKT3 cell lines. P-val <0.05, FC 0. Top number represents up-regulated genes and bottom number represents down-regulated genes.

Table 5.36: Differential expression between BJ-hTERT SGK3 amd BJ-hTERT myrAKT cell lines. Common genes up-regulated (1) and down-regulated (-1).

GeneSymbol	BJ-hTERT SGK3 CA	BJ-hTERT-myrAKT1	BJ-hTERT-myrAKT2	BJ-hTERT-myrAKT3
MLLT11	1	1	1	1
STMN1	-1	0	0	-1
PIK3R3	1	1	1	1
DDIT4	1	0	1	0
ARNT2	-1	0	-1	-1
KIAA1199	-1	0	-1	-1
EMP2	-1	0	-1	-1
GALNT1	1	0	1	1
PRICKLE2	1	1	1	1
CCDC80	-1	0	0	-1
APOD	1	0	1	1
BST1	-1	0	-1	-1
PCDH10	1	0	1	1
CD36	1	1	1	1
COL14A1	1	1	1	1

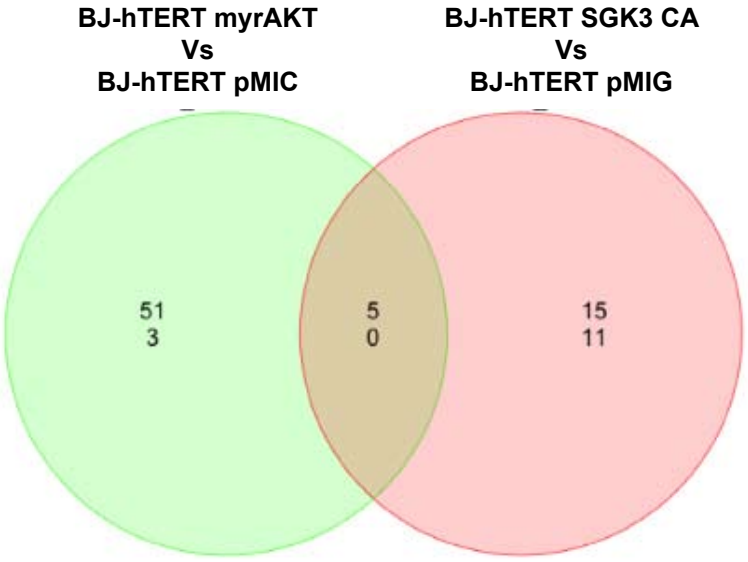

Figure 5.20: Venn diagram showing common differentially regulated genes between all genes commonly regulated by all three BJ-hTERT myrAKT isoforms (BJ-hTERT-myrAKT) and BJ-hTERT SGK3CA. P-val <0.05, FC 0. Top number represents up-regulated genes and bottom number represents down-regulated genes.

include *CD36*, *PRICKLE2* and collagen type XIV alpha 1 (*COL14A1)*, which have shown to be involved in the regulation of fatty acid transport (Lynes and Widmaier 2011), polarity (Katoh and Katoh 2006) and fibrillogenesis (Ansorge et al. 2009) respectively.

5.4 Discussion

Microarray technology is a valuable tool for generating global gene expression profiles, in addition to being a useful platform for further elucidating functions of specific genes. In this chapter, the use of gene expression microarray technology facilitated the analysis of global gene expression changes induced by ectopic expression of different SGK3 and AKT mutants in both fibroblast and epithelial backgrounds. Studies outlined here have focused on the analysis of data generated utilizing Affymetrix gene chip arrays, using samples generated from the same stable cell lines used to conduct functional studies highlighted in Chapters 3 and 4 of this thesis. Collectively these studies have allowed broad gene expression analysis to be coupled with functional data to gain further insight into the function of SGK3, and to identify further similarities and differences between SGK3 and the AKT kinase family.

Importantly, the expression array experiments were conducted in cells stably over expressing SGK3 or AKT or mutants thereof. Thus the observed changes in gene expression reflect not only direct targets downstream of SGK/AKT signalling but also secondary responses to the consequences of the physiological changes that occur in response to SGK/AKT manipulation. For this reason more emphasis was put on identifying functional ontology categories of signalling pathways that were regulated by SGK/AKT rather than simply examining the hits in terms of fold change in expression and investigating only those most robustly regulated. However in some cases where only limited numbers of genes exhibited significant changes in expression, more manual approaches were used.

Two platforms were used to analyse this gene expression data. MetaCore™ platform by GeneGo allowed assessment of functional ontology categories of pathways enriched in the differential gene expression data. The second platform, GSEA, ranks published gene expression profiles based on similarity of enriched gene sets in expression data. The MetaCore™ platform demonstrated a useful approach to determine possible ontologist, however limitations associated with this platform involved using known signalling pathways for analysis of gene expression data. The second platform used was GSEA, which utilizes a MSigDB of curated gene sets to evaluate microarray data, ranking genes according to their expression. The use of GSEA was useful in that it is based on changes in gene expression associated with disease or cell manipulation, and is complimentary for analysis of changes in gene expression.

5.4.1 SGK3 gene expression in ovarian epithelial cells

Analysis of gene expression data generated from the HOSE SGK3 WT cells indicated

through both pathway analysis and GSEA that SGK3 may potentially be in involved in immune response signalling, particularly through the IFN-α and -β pathways. To date, a direct connection between the SGK family and IFN signalling has not been demonstrated, however AKT signalling has been implicated in IFN signalling where it has been shown to connect both type I IFN (IFN-α and -β) and type II IFN (IFN-γ) signalling to the regulation of translation through the mTOR pathway (Kaur et al. 2008a). Studies have shown that activation of AKT is required for IFN-inducible engagement of the mTOR/p70 S6 kinase pathway and in AKT knockout animals a dramatic reduction in IFN-induced antiviral response is observed, taken together these studies suggest that AKT plays an important role in IFN signalling (Kaur et al. 2008a), suggesting the possibility that SGK3 may also be involved in the regulation of IFN signalling in ovarian surface epithelial cells. Moreover, recent studies have also demonstrated that there is defective transcription of IFN-stimulated genes in PI3-K knockout cells, which has shown to be AKT-independent, further suggesting a possible link between SGK3 and IFN signalling (Kaur et al. 2008b).

Through manual inspection of differentially regulated genes shared between HOSE SGK3 WT and HOSE SGK3 CA cells it was evident that over-expressed SGK3 is able to induce an increase in components of the LPA pathway in HOSE cells, most notably LPAR3, one of six G-protein coupled receptors that binds LPA (Hama and Aoki 2010), and is able to signal through both the PI3-K and Ras pathways to a number of downstream effectors (Moolenaar and Perrakis 2011). Previous studies have demonstrated *LPAR3* mRNA expression to be elevated in ovarian cancer cell lines in comparison with normal ovarian epithelial cell lines (Fang et al. 2000), in addition to high expression in ovarian cancer tissue compared with tissue from normal ovaries, with over-expression of *LAPR3* in between 44% and 49% of early stage ovarian cancers (Fang et al. 2002). These data suggest that over-expression of SGK3 is able to increase LPA signalling, potentially through a positive feedback mechanism incorporating autotaxin secretion. Furthermore, increased signalling through LPAR3 has shown to increase production of cytokines IL-6 and IL-8 (Liu et al. 2009a), both of which were identified as up-regulated in HOSE SGK3 CA cells and not HOSE SGK3 WT, suggesting that activated SGK3 is potentially able to drive cytokine production via LPAR3 implicating SGK3 in associated pro-inflammatory signalling.

A comparison of the GSEA conducted between HOSE SGK3 WT and HOSE SGK3 CA gene expression data highlighted marked differences between the enriched gene sets in these cell lines. Analysis of the top 20 enriched gene sets in both cell lines revealed that HOSE SGK3 CA was strongly association with a variety of tumour gene sets when compared to those enriched in HOSE SGK3 WT cells. These difference are also consistent with functional data presented in Chapter 3 demonstrating that in HOSE cells SGK3 CA is able to drive cell growth and proliferation, two core cell processes and two key hallmarks of cancer, to a greater extent than SGK3 WT. Thus taken together both gene expression and functional data suggest that activated SGK3 is able to influence oncogenic signalling to a greater extent.

Comparison of the differential gene expression lists between HOSE SGK3 CA and HOSE SGK3 WT revealed that hepatocyte growth factor (HGF) is the second highest up-regulated gene in the HOSE SGK3 CA cells at a FC increase of 18.74, but down-regulated in SGK3 WT cells at a FC decrease of 2.21. Through binding to its receptor, met, HGF is able to activate many pathways including ERK1/2 and PI3-K to stimulate proliferation, growth and survival (Wong et al. 2001; Tulasne and Foveau 2008; Menakongka and Suthiphongchai). Furthermore, HGF is also involved in cytoskeletal organization and promoting transition through the cell cycle via multiple effectors including Rho, Rac, cell division cycle 42 (GTP binding protein, 25kDa) (CDC42) and retinoblastoma protein (Leshem and Halevy 2002; Bosse et al. 2007; Chianale et al. 2010).

To date, many studies have demonstrated a connection between HGF over-expression and tumourigenesis, establishing HGF/Met as an important target for cancer therapeutics (Parrott and Skinner 2000; Wong et al. 2001; Lee et al. 2004). The marked difference in *HGF* expression levels between the HOSE SGK3 WT and HOSE SGK3 CA cell lines may explain the differences in cell growth and proliferation observed in Chapter 3. Furthermore, HGF production is primarily limited to cells of mesenchymal or stromal origin (Parrott and Skinner 2000), suggesting that the HOSE SGK3 CA cells have the ability to stimulate their own growth in an autocrine manner, potentially demonstrating that these cells have developed early characteristics of malignant cell transformation.

Taken together comparisons between SGK3 WT and SGK3 CA in ovarian epithelial cell lines reveal a potential novel link between SGK3 and IFN signalling. Additionally, differential regulation of important components of the LPA pathway in both HOSE SGK3 WT and HOSE SGK3 CA further also suggest a potential link with SGK3 and cytokine regulation. Moreover, analysis between these two cell lines also revealed that HOSE SGK3 CA cells show a robust increase in HGF expression, in addition to demonstrating regulation of more tumour-related gene sets in GSEA, which together suggest that activated SGK3 may be more involved in oncogenic signalling and malignant cell transformation.

5.4.2 Comparison between SGK3 and AKT gene regulation in ovarian cell lines

Components of the LPA pathway up-regulated in HOSE-SGK3 cells were not found to be up-regulated in any of the IOSE523-AKT cells. It is possible that given these cells already express early region SV40 small t and large T antigens, that many of these pathways are already maximally regulated. Analysis of gene expression data from the IOSE523 cells stably over-expressing the AKT isoforms revealed a marked difference between the number of differentially regulated genes shared between the AKT isoforms, with IOSE523 myrAKT3 cells sharing very few regulated genes with either IOSE523 myrAKT1 or IOSE523 myrAKT2. The similarities between the

IOSE523 myrAKT1 and IOSE523 myrAKT2 cells lines were also evident from the GSEA, which revealed very similar enriched gene sets for both of these cell lines.

Interestingly, GSEA of IOSE523 myrAKT1 and IOSE523 myrAKT2 gene expression data both show enrichment of gene sets associated with senescence, recently reported to be induced by AKT in fibroblast cells (Astle et al. 2011), but GSEA of IOSE523 myrAKT3 did not show enrichment of these same gene sets. Not surprisingly a number of studies have reported both functional redundancy and isoform-specific functions for the AKT kinase family, although the basis for these differences remains unclear, cellular localisation upon stimulation has been implicated.

Given that gene expression data was not generated using IOSE523 SGK3 stable cell lines due to preliminary function data demonstrating an absence of phenotype, broad comparisons between HOSE stable cell lines and IOSE523 stable cell lines were performed. There were far less genes differentially regulated in the IOSE523 cells expressing AKT compared with the SGK3 expressing HOSE stable cell lines, potentially indicating that many pathways activated by AKT may have already been activated in the IOSE523 cells. This is a distinct possibility given that IOSE523 cells are immortalized via the ectopic expression of small t and large T antigen, and small t antigen inhibits protein phosphatase 2A (PP2A), the phosphatase responsible for decreasing AKT signalling. The higher basal proliferation and migratory rate of control IOSE523 pMIG cells compared to control HOSE cells (Chapter 4) also indicates that IOSE523 cells do have greater activation of certain pathways. Closer analysis between the epithelial cell lines also revealed that HOSE SGK3 CA cells shows slightly more similarity with IOSE523 myrAKT1 and IOSE523 myrAKT2 than IOSE523 myrAKT3 based on the number of commonly regulated genes. Recent studies using *sgk3*$^{-/-}$/*akt2*$^{-/-}$ mice have demonstrated that these two kinases may share significant redundancy, given that single knockout mice of both kinases demonstrate comparatively mild phenotypes, but simultaneous deletion of both genes produces a stronger phenotype (Mauro et al. 2009; Yao et al. 2011).

Through analysis of gene expression profiles in the HOSE cells, it is evident that over-expression of both WT and CA SGK3 produces the differential regulation of hundreds of genes, likely impacting a variety off cellular processes, some of which are reflected in results obtained from functional studies presented in earlier chapters. Furthermore, studies using the IOSE523 cells have demonstrated the most similarities between AKT1 and AKT2, which are further reflected in reports describing AKT isoform specific signalling (Brognard et al. 2007). Importantly, gene expression studies using epithelial cells have demonstrated possible novel associations with SGK3 and cytokine signalling, as demonstrated by analysis using two different bioinformatic platforms, however further investigation and validation is required to explore this link.

5.4.3 SGK and AKT gene expression in fibroblast cells

BJ-hTERT fibroblast cell lines over-expressing both activated SGK3 and the activated

AKT isoforms allowed a more direct comparison between gene expression profiles in an isogenic background that was not possible with the epithelial cell lines. Initial analysis comparing total number of differentially regulated genes between BJ-hTERT cell lines revealed striking differences, with SGK3 CA cells significantly regulating 31 genes compared with myrAKT1 where it was 71 genes, myrAKT2 was 352 genes and myrAKT3 was 601 genes. However, despite SGK3CA regulating a comparatively lower number of total genes when compared with the activated AKT isoforms, SGK3CA was still able to significantly increase key readouts of growth in the BJ-hTERT cell line as demonstrated in Chapter 3. Strikingly the ability of SGK3 to regulate cell growth processes as shown in Chapter 3, was not directly reflected in the gene expression data presented in this chapter; i.e. we did not observe robust transcriptional changes in components directly involved in ribosome biogenesis, processing, and assembly or cell cycle markers. One possible explanation is that SGK3 might affect growth and cell cycle pathways at the post-translational levels by modulating the activity of specific factors rather than inducing signalling cascades that result in their increased expression. In addition as the studies were performed under steady state conditions, much of the expression changes clearly reflect the physiological response to altered growth, proliferation and anchorage independent growth rather than the transcriptional cause of those process. These findings are in marked contrast to another master regulator of ribosome biogenesis and growth, c-myc that directly transcriptionally up regulates all components of the ribosome and in its over expression or amplification is invariably linked to a ribosome signature in malignancy (Chan et al. 2011).

In BJ-hTERT SGK3 CA cells, manual inspection of the gene list together with MetaCore™ analysis indicated that in these cells SGK3 CA signalling was associated with glucose and lipid metabolism, cell adhesion and polarity. These functions have previously been associated with SGK signalling. SGK3 has demonstrated involvement in glucose metabolism through phosphorylation of GSK3β (Liu et al. 2000), and polarity through alteration of β-catenin dynamics leading to formation of adherens junctions and tight junction sealing, also through phosphorylation of GSK3β (Failor et al. 2007). Evidence suggesting SGK3 involvement in polarity comes from studies using *sgk3*$^{-/-}$ mice, which displayed disorganisation of hair follicles and cells in the outer root sheath, indicating a dysregulation of cell polarity (McCormick et al. 2004; Alonso et al. 2005).

Unexpectedly, expression of hypoxia-induced negative regulator of mTOR activity, *DDIT4*, was increased in the BJ-hTERT SGK3 CA cells. DDIT4 was first identified as an essential factor required for regulation of mTOR by hypoxia in *Drosophila* (Reiling and Hafen 2004), and subsequent studies in mammalian cells have also demonstrated induction of DDIT4 by hypoxia, along with a concurrent down-regulation of mTOR substrate phosphorylation (Brugarolas et al. 2004). Further studies have also demonstrated that DDIT4 is able to regulate mTOR in response to hypoxia via upstream regulation of the TSC1/2 complex (Sofer et al. 2005).

Given that DDIT4 is essentially a negative regulator of mTOR activity, ultimately leading to a decrease in protein synthesis and cell growth, it is unexpected that it has been identified as positively regulated in BJ-hTERT SGK3 CA cells, as these cells exhibit a robust increase in cell growth (Chapter 3). A possible explanation may be that SGK3 is involved in a previously identified feedback loop (Ellisen 2005). DDIT4 is transcriptionally activated by hypoxia inducible factor (HIF) (Ellisen 2005), which is positively regulated by mTOR (Brugarolas et al. 2003). Thus increased mTORC1 activity as a result of over-activation of the PI3-K/SGK3 pathway in the BJ-hTERT SGK3 CA cells would ultimately induce DDIT4 via HIF, and thus dampening mTOR signalling.

Further examination of the BJ-hTERT SGK3 CA gene list also shows that SGK3 may increase Ras/Erk pathway signalling, a pathway also involved in cell proliferation. Both RASA3 and SPRY2 are decreased in BJ-hTERT SGK3 CA cells, these genes encode proteins that are negative regulators of Ras (Hacohen et al. 1998; Lee et al. 2004; Frank et al. 2009) and tyrosine kinase receptor signalling (Casci et al. 1999) respectively. Thus by decreasing expression of these negative regulators it is likely that you have increased signalling via the Ras/Raf/Erk pathway.

Analysis of BJ-hTERT myrAKT cell lines demonstrated an involvement in immune response pathways and cell adhesion pathways, in addition to GSEA highlighting enrichment of several tumour associated gene sets. Many of these pathways and functions have previously been attributed to AKT activation, and hyperactivity of the PI-3K/AKT pathway has shown to be a common factor in many cancers. Despite SGK3 differentially regulating a comparatively low number of genes in the BJ-hTERT cells when compared to the number regulated by the AKT isoforms, functional data presented in Chapter 3 demonstrates SGK3's ability to influence key parameters of cell growth in a similar way to AKT. Moreover, comparative analysis shows that despite SGK3 differentially regulating a low number of genes in the BJ-hTERT cells, many of these genes are commonly regulated by individual AKT isoforms, with the exception of myrAKT1, which shares the least number of commonly regulated genes with SGK3 CA.

5.4.4 Limitations on data interpretation

Some caution needs to be used when applying gene expression data for identification and characterization of gene sets regulated by a protein kinase such as SGK3, given that correlation between mRNA and protein levels is highly variable. Furthermore, as outlined at the start of this discussion the expression array experiments were conducted in cells stably over expressing SGK3 or AKT or mutants thereof. Thus the observed changes in gene expression reflect not only direct targets downstream of SGK/AKT signalling but also secondary responses to the consequences of the physiological changes that occur in response to SGK/AKT manipulation.

In addition, subcellular localisation and/or other posttranslational modifications may

be altered in response to enforced over-expression and again neither of these are addressed by transcriptional analysis. In light of the aforementioned caveats, gene expression analysis presented in this chapter aimed to identify global gene expression trends in an attempt to determine potential novel associations with SGK3 regulation, which can be used as a platform for further validation and characterisation in future studies. Additionally, a future approaches that may allow a more comprehensive view of the transcriptome in response to enforced SGK3 expression might combine temporal analysis of the changes in gene expression following enforced SGK3 expression. In this way the specific and immediately down stream targets of SGK3 signalling versus chronically modulated as an indirect consequence to changes in physiology might be able to be separated. Moreover, in order to counteract possible artefacts experienced with over-expression studies, expression analysis could also be performed after SGK3 or AKT knockdown. The use of RNA-Seq as opposed to expression arrays may also be of utility. RNA-Seq is advantageous for studying gene expression as it incorporates all RNA expression changes, allows greater sensitivity of sequencing data, unlimited dynamic range of expression, and reduced background compared with microarray techniques (Wang et al. 2009). Finally, to directly determine changes in phosphoproteins levels in response to SGK3 manipulation, approaches such as stable isotope labelling by amino acids in cell culture (SILAC) could be implemented. SILAC is a method that allows identification and quantification of relative differential changes in complex protein samples. This method uses the *in vivo* metabolic incorporation of ^{13}C- or ^{15}N-labelled amino acids into proteins, followed by mass spectrometry to identify and characterise proteins.

5.4.5 Summary

Despite caveats in gene expression analysis, studies presented in this chapter have allowed identification of global gene expression trends associated with over-expression of SGK3. Gene expression data was interrogated using two distinct bioinformatic approaches, which included the MetaCore™ platform by GeneGo, along with GSEA. Taken together, these approaches identified possible novel pathway connections associated with SGK3 including IFN and LPA signalling, potentially suggesting a role in cytokine regulation, which may also add another important level of SGK3 involvement in tumourigenesis. Studies presented in this chapter were also able to link SGK3 involvement in already established processes including metabolism and cell adhesion. Furthermore, parallel studies using AKT over-expression also linked AKT regulation with already reported processes, such as Pol I regulation and senescence. Moreover, direct comparison between SGK3 and AKT isoform regulation in the fibroblast cells showed AKT isoforms to differentially regulate substantially more genes than SGK3. While individual validation of regulated genes is still required, these studies have provided an important basis for future investigation into SGK3 function.

6. Summary and future directions

6.1 Overview

The PI3-K signalling pathway plays an important role in a wide variety of fundamental cellular process, largely mediated signalling via the AKT isoforms. Given the crucial role of PI3-K/AKT signalling in regulating processes such as cell growth, proliferation and survival, it is not surprising that components of this pathway are frequently dysregulated in cancer, making the AKT kinase family important therapeutic targets. This is further emphasized by the large number of clinical trials currently testing AKT inhibitors as a therapeutic strategy for tumours with hyperactivity of PI3-K/AKT (Mehta et al. 2011; Reid et al. 2011; Yap et al. 2011). Importantly, over the last decade increasing evidence has emerged revealing that in addition to the AKT kinase family, the lesser-known SGK kinase family are also important downstream effectors of PI3-K signalling, showing similar structural homology, in addition to similarities in activation and downstream targets, when compared with AKT.

Despite some similarities in activation and downstream targets between SGK and AKT, substantial differences in SGK and AKT isoform cellular localisation suggests the potential for specialised cellular functions. Moreover, comparisons between SGK and AKT single knockout mice also suggest important differences in signalling mechanisms existing between these families. Recent reports have also demonstrated SGK3 to play an important role in AKT-independent oncogenic signalling (Vasudevan et al. 2009; Liu et al. 2012). Together, accumulating evidence supports a convincing role for SGK3 in regulating important cellular processes, in addition to involvement in oncogenic signalling. Thus, studies to further characterise SGK3 function, in addition to elucidating key differences in signalling between both SGK3 and AKT, are of considerable relevance to elucidating key signalling mechanisms in cancer.

The studies presented in this thesis allowed development of robust, stable gain-of-function cell models that were used to investigate the potential role of SGK3 in cell growth and proliferation, two key process involved in tumourigenesis, while simultaneously exploring the importance of SGK3's reported endosomal localisation on functionality. In addition, genetically defined pre-tumourigenic cell models were also used in these studies to investigate the influence of SGK3 over-expression on key readouts of tumourigenesis, in order to further define SGK3's role in these processes, in addition to further distinguishing between SGK3 and AKT's role in oncogenic signalling. Finally, as an extension of our functional studies, gene expression arrays were performed using Affymetrix chips to determine differences in global gene expression profiles between cell lines over-expressing SGK3 and AKT. In addition, the gene expression profiling of SGK3 activated cells also enabled mechanisms of action associated with SGK3 phenotypes to be further defined, in addition to investigation of possible novel associations existing between SGK3 and other important signalling nodes. Differences

in global gene expressing patterns between SGK3 and AKT activated cells were also used to assess both common and uniquely regulated pathways between SGK3 and AKT.

6.2 SGK3 regulates cell growth

Initial studies presented in chapter 3 focused on defining a possible role for SGK3 in regulating cell growth, a process previously not associated with SGK3 signalling, but widely established to be modulated in a PI3-K/AKT dependent manner, via AKT/mTORC1 signalling. Using non-tumourigenic immortalised fibroblast and epithelial cell lines, we demonstrated that enforced expression of activated SGK3 significantly increased key readouts of cell growth, including cell size and macromolecular content (RNA and protein per cell). Further studies revealed that the ability of SGK3 to impact these growth parameters was mediated, in part, via regulation of rDNA transcription, the rate-limiting step in ribosome biogenesis and cell growth. Importantly, using enforced expression of SGK3 in serum-starved cell it was shown that SGK3 is sufficient to drive rDNA transcription without the requirement of additional factors. Furthermore, through investigation of cell signalling using rapamycin, our studies were able to determine that a component of SGK3 regulation of rDNA transcription and growth is likely via signalling through mTORC1, a well-established convergence point of nutrient and growth factor signalling to cell growth.

While regulation of rDNA transcription is a novel function for SGK3, as discovered in this thesis, several studies have shown AKT to be a crucial mediator of rDNA transcription and growth, with more recent studies in our laboratory demonstrating that AKT regulates rDNA transcription through both mTORC1-dependent and –independent mechanisms (Chan et al. 2011). Importantly, these studies revealed that AKT is involved in rDNA transcription via loading RNA polymerase I (Pol I) onto the rDNA, in addition to involvement in transcription elongation and rRNA processing, with more immediate AKT inhibition leading to defects in rRNA processing and accumulation of unprocessed 45S rRNA, and more sustained AKT inhibition reducing Pol I loading (Chan et al. 2011). Given the importance of AKT regulation of rDNA transcription via Pol I regulation, it is possible that SGK3's ability to regulate rDNA transcription may also be via similar mechanisms. Moreover, the PI3-K/mTOR signalling pathway is involved in Pol I regulation in response to IGF-1 and nutrients, via increasing the amount of SL1, a specific Pol I factor, on the rDNA promoter and activating Pol I activity (James and Zomerdijk 2004). Thus, as a downstream effector of PI3-K, SGK3 may be involved in regulation of rDNA transcription via modulating components of the Pol I transcription apparatus, in addition to a possible involvement in regulating elongation and processing.

While studies presented in this thesis were able to demonstrate that SGK3 is sufficient to increase 45S transcription rates using the RPA to detect changes in 5' ETS levels, further studies using siRNA knockdown tools would assist in determining if SGK3 is

required for these processes. Furthermore, labelling cells with ^{32}P-orthophosphate to allow visualization of all newly synthesised rRNA species, would allow a more specific investigation into the requirement of SGK3 for regulation in the generation of the 45S precursor rRNA, in addition to further defining involvement in elongation and processing into the mature 28S, 18S and 5.8S rRNA (Chan et al. 2011). To date only AKT (Ruggero and Sonenberg 2005; Chan et al. 2011) and MYC (Arabi et al. 2005; Grandori et al. 2005; Grewal et al. 2005; Dai and Lu 2008) have been shown to be sufficient, in the absence of other growth factors to drive the enormously complex process of ribosome biogenesis, which requires the coordinated effort of all three RNA Polymerases, and over 1000 accessory processors and non-coding RNAs. Thus, the work presented in this thesis suggests that like AKT and myc, SGK3 is an important central player in the modulation of cellular growth, warranting further investigation into the mechanisms behind SGK3 regulation of cell growth machinery.

Using the mTORC1 inhibitor rapamycin, studies presented in Chapter 3 were also able to show that a component of SGK3 signalling to rDNA transcription and cell growth is likely to be mTORC1-dependent, given the robust reduction in phosphorylation of downstream effectors rpS6 and 4EBP1, and reduction in rDNA transcription following rapamycin treatment in cells with enforced expression of SGK3. However, these studies also indicate a possible mTORC1-independent component of SGK3 signalling to cell growth, which requires further investigation using more specific model systems. As described in chapter 3, the use of *raptor*$^{-/-}$ murine embryonic fibroblasts (MEFs), which lack raptor, a required component of functional mTORC1, could be used with enforced expression of SGK3 to directly test the requirement for SGK3 to promote rDNA transcription in an mTORC1-independent manner. Moreover, studies to investigate the possibility that SGK3 may directly target components of the Pol I complex to drive rDNA transcription would further assist in elucidating possible mTORC1-independent mechanisms behind SGK3's ability to regulate growth. Two approaches could be used for further investigation, which include firstly determining SGK3 motifs in core Pol I components, which could then be expressed to determine if they are phosphorylated by SGK3 *in vitro*. Furthermore, phosphospecific antibodies could also be raised to the specific sites in order to determine if they are also phosphorylated *in vivo*. The second approach would incorporate SILAC proteomics to determine if any components are phosphorylated in response to the manipulation of SGK3.

Future studies should examine to what extent SGK3 interacts with other modulators of growth. For example, recent studies from our laboratory have demonstrated that AKT co-operates with c-myc to synergistically activate rDNA transcription and cell growth (Chan et al. 2011). The ability of SGK3 to co-operate with c-myc could be studied using already established gain-of-function mutant constructs for SGK and myc available in our laboratory. Moreover, recent studies in our laboratory have also demonstrated that AKT repression, but not mTORC1 inhibition led to repression of rDNA transcription and increased apoptosis in a c-myc-driven model of murine B cell lymphoma (Eμ-*Myc*) (Chan et al. 2011). This finding suggests that AKT activity is an important component

of the survival of myc driven tumours. Further studies to examine whether SGK3 is similarly required for c-myc driven malignant transformation could also be performed using SGK3 knockdown tools on cultured Eμ-*Myc* cells. Additionally, pre-malignant haematopoetic stem cells derived from Eμ-*Myc* mice fetal livers could be retrovirally transduced with a constitutively activated SGK3 construct, and used to reconstitute the haematopoietic compartment of irradiated C57BL/6 mice to determine the ability of SGK3 to accelerate lymphomagenesis, which has been demonstrated by activated AKT1 (Wendel et al. 2004).

The importance of endosomal localisation of SGK3 for optimal regulation of cell growth was also demonstrated in Chapter 3 by comparing the functionality of a constitutively active SGK3 mutant with and without a functional phox homology domain. Endosomal localisation has shown to be of particular relevance to cell growth given that the endosomally localised class III PI3-K Vps34 has an important role in regulating mTORC1 downstream of amino acids (Nobukuni et al. 2005), raising the question of what other factors are involved in this process, given that the mechanism remains largely undefined. Studies have shown that amino acids induce an increase in cystolic calcium, leading to binding of Ca^{2+}/calmodulin to Vps34, which subsequently elevates PtdIns3P levels, and then goes on to recruit FYVE or PX domain-containing proteins to the early endosomes (Gulati et al. 2008), which includes SGK3 given the presence of a PX domain in its N-terminal region. It is possible that endosomally localised SGK3 is able to regulate cell growth via mediating nutrient signalling to mTORC1, possibly through interaction with other endosomally localised factors such as the Rab proteins, or through phosphorylation and inactivation of TSC2. Extending these studies to determine factors that SGK3 directly interacts with in the endosomal compartment may assist in more specifically defining mechanisms in which SGK3 contributes to growth signalling from the endosome. Identification of novel protein interactions with SGK3 could be accomplished by using cells over-expressing myc-tagged SGK3 and performing co-immunoprecipitation with a myc-tag antibody, protein components could then be size fractionated using SDS-PAGE, and subsequently digested and analysed by high sensitivity mass spectrometry.

Finally, our growth studies also demonstrated that SGK3 is able to increase proliferation rates of immortalised ovarian epithelial HOSE cells but not of BJ-hTERT foreskin fibroblast cells. Investigation into cell cycle phase distribution showed that SGK3 is able to increase cells in S phase in HOSE cells, compared with the BJ-hTERT cells which demonstrated no changes in cell cycle phase distribution. A recent report has demonstrated that SGK3 is able to promote G1/S transition in hepatocellular carcinoma cells, providing a proliferative advantage, which is likely to be via SGK3 direct phosphorylation and inactivation of GSK3-β, and subsequent inhibition of cyclin D1 (CCND1) degradation, a major cyclin involved in regulation of G1/S checkpoint (Liu et al. 2012). Signalling results presented in chapter 3 demonstrate that SGK3 is able to regulate GSK3-β activity in all cell lines analysed suggesting that the coupling of SGK3 regulation of GSK3-B is not coupled to proliferation responses in all cells. Indeed

results from chapter 3 demonstrate that SGK3-mediated growth and proliferation in these cells is uncoupled, with SGK3 preferentially signalling to cell growth.

Recent studies have demonstrated the dependency for ongoing cell cycle progression on growth, where it is thought that critical cell size thresholds are imposed at the G1/S phase transition and/or the G2/M phase transition (Jorgensen and Tyers 2004). Cell size thresholds enforce a minimal cell size, and it has been observed in many cell types that smaller cells delay cell cycle progression until they have reached a certain size (Fantes 1977; Johnston et al. 1977; Shields et al. 1978; Dolznig et al. 2004; Jorgensen and Tyers 2004). Studies presented in this thesis demonstrate that SGK3 is able to uncouple this cell size threshold, resulting in cell growth driving larger cells with the same proliferation rate, suggesting that SGK3 signalling is able to reset the cell size threshold at which cells proliferate.

This suggests that additional factors may be necessary for SGK3 to recouple cell cycle progression with the cell size threshold. The BJ isogenic cell lines would be useful to further delineate SGK3 signalling in the context of cell proliferation as they are a series of genetically matched cells that represent combinations of hTERT, SV40 LT and st, and H-Ras (as described in chapter 4.2) and therefore could be used to determine the additional molecular changes that are required to allow SGK3 to translate increased growth into a concurrent proliferative advantage. This would provide valuable information about how SGK3 in a malignant setting drives accelerated proliferative growth. More specifically enforced expression of SGK3 in the BJ-hTERT + small t antigen cells would allow further investigation into the ability of MYC stabilisation to reconnect SGK3-mediated growth increases with proliferation. Additionally, the use of BJ-hTERT + LT would allow further investigation into the effect that loss of important tumour suppressor proteins and cell cycle regulators pRB and p53 have on proliferation in cells with enforced expression of SGK3. Alternatively, a functional genome wide RNAi screen may provide an unbiased approach to explore signals required to couple growth and proliferation in response to SGK3 signalling. More specifically BJ-hTERT cells over-expressing SGK3, exhibit a larger cell size but proliferate at the same rate as parental cells. The Dharmacon RNAi library could be used to individually knock out each gene in the genome to identify to those genes whose loss of expression can convert the large SGK3 driven BJ-hTERT cells to normal size cells proliferating at a faster rate. Such screens are feasible as Petermac using the Victorian Centre for Functional Genomics located at the Peter Mac that has the RNAi libraries arrayed into 364 cell plates suitable for reverse transfection and the appropriate robotics and high content analysers required for such studies.

6.3 SGK3 can promote some hallmarks of malignant cell transformation

To investigate the extent to which SGK3 is able to regulate certain well-characterised hallmarks of tumourigenesis, we used genetically defined pre-tumourigenic ovarian

epithelial and foreskin fibroblast cell lines. Additionally, parallel studies using gain-of-function AKT isoform constructs in these cell lines also enabled a comprehensive comparison between SGK3 and the AKT mediated effects. Results from these studies demonstrated that activated SGK3 can promote anchorage independent growth in fibroblast cells, and is consistent with recent studies indicating a role for SGK3 as a critical regulator of AKT-independent anchorage independent growth and *in vivo* tumour formation (Vasudevan et al. 2009; Liu et al. 2012). Together, these studies suggest that SGK3 is likely to promote anchorage independent growth via activation of established pro-survival pathways, in addition to growth and proliferation signalling, leading to anoikis-resistance, an important step in malignant cell transformation. This is further highlighted by results shown in chapter 5 demonstrating the involvement of enforced expression of SGK3 in the differential regulation of genes associated with integrins and adhesion pathways.

Anchorage independent growth studies presented in chapter 4 also indicate that both activated SGK3 and AKT require additional factors to maximally drive malignant cell transformation. This was evident from experiments comparing anchorage independent growth of fibroblast cells expressing oncogenic H-Ras with fibroblasts expressing activated SGK3 or activated AKT, whereby oncogenic H-Ras induced greater colony numbers and size. Additional experiments utilizing the genetically defined fibroblast cell lines over-expressing SGK3 in combination with other genetic factors previously shown to cooperate with AKT to drive anchorage independent growth would allow further insight into SGK3-mediated malignant transformation. Previous studies have shown that AKT in combination with either activated MEK, or c-myc and activated Rac1 (Zhao et al. 2003; Boehm et al. 2007) are able to induce anchorage-independent growth. Thus, over-expressing these genetic factors in combinations with activated SGK3 would further determine other signalling pathways that SGK3 is able cooperate with to further drive malignant cell transformation. Additionally, loss-of-function experiments could be performed to confirm gain-of-function experiments, and to definitively determine to what extent SGK3 is required in both normal and tumourigenic cells for the phenotypes observed for cell lines utilised in chapter 4.

Furthermore, complimenting *in vitro* studies using genetically defined cell models systems with *in vivo* xenograft models would also determine the ability of SGK3 (with and without additional factors) to drive cell transformation in a system more able to recapitulate the tumour microenvironment. Interestingly, amplification of broad regions of 8q is one of the most frequent alterations in some cancers, including hepatocellular carcinoma (Liu et al. 2012). SGK3 has shown to be localised to 8q13.1, in addition to Myc at 8q24.21, suggesting the possibility that in certain cancers genomic dysregulation of both SGK3 and MYC, in addition to other oncogenes in this region such as FAK may cooperate to promote tumourigenesis. Further elucidating possible signalling connections between these important oncogenes may also further define SGK3's role in malignant cell transformation.

A murine model of ovarian cancer would more specifically explore the role of SGK3

dysregulation in ovarian tumourigenesis, and compliment our ovarian *in vitro* studies, providing a more physiologically relevant analysis of SGK3 involvement in human ovarian tumour biology. There are several published murine models of ovarian cancer, however possibly the most relevant to study the role of SGK3 in tumourigenesis is a model of human ovarian endometrioid adenocarcinoma based on somatic defects in the Wnt/β-Catenin and PI3-K/PTEN signalling pathways, which have shown to frequently occur together in a subset of human ovarian endometrioid adenocarcinoma (Wu et al. 2007). Importantly, signalling in this model demonstrates equivalent pPDK1 and pRPS6 levels, but relatively low levels of pAKT (Kinross et al. 2012), suggesting that this these mutations drive tumour formation via an AKT-independent mechanism.

Recent studies using PIK3CA mutant cancer cell lines and human breast tumours exhibiting robust PDK1 activation, but minimal AKT activation, demonstrated a critical reliance on SGK3 for anchorage independent growth (Vasudevan et al. 2009), demonstrating that in the absence of AKT signalling SGK3 is able to drive malignant cell transformation. Using the $PTEN^{-/-}/APC^{-/-}$ murine model studies further investigation of the role of SGK3 in tumour formation could be achieved through analysing tumour morphology and possible immunohistochemical analysis. Furthermore, isolation of tumour cells and subsequent knockdown of SGK3 would also allow further investigation into the contribution of SGK3 in AKT-independent oncogenic signalling.

6.4 SGK3 impact on global gene expression

As an extension of our functional studies characterising SGK3 in both normal physiology and pathophysiology, we also utilized microarray technology to couple functional studies with broad gene expression analysis, in order to gain further insight into SGK3 function, and to identify further similarities and/or differences between SGK3 and the AKT family. Moreover, given that SGK3 is a kinase involved in post-translational modification, its was assumed that a majority of the changes in gene expression were an indirect consequence of enforced SGK expression and thus rather than ranking and focusing on specific genes with the greatest change in expression, the data was interrogated to identify ontological categories of signalling pathways controlled by SGK. Specifically using two bioinformatic approaches (GeneGo and GSEA) to interrogate gene expression data we were able to identify several novel signalling modules/pathways that SGK3 can modulate, in addition to identifying some known effectors. Through over-expression of SGK3 our data revealed a robust immune response, including the significant differential regulation of genes involved in IFN signalling and pro-inflammatory cytokine production.

Studies have demonstrated that pro-inflammatory signalling is critical in neoplastic transformation (Allavena et al. 2008), with oncogenes such as Ras (Liu et al. 2004) and myc (Shchors et al. 2006) showing an ability to build up inflammatory pro-tumourigenic microenvironments. Further studies to more specifically validate and delineate SGK3 regulation of inflammatory signalling will assist in further elucidating

the role that SGK3 plays in malignant cell transformation. Furthermore, our studies also revealed a possible role for SGK3 in regulation of LPA signalling. Lysophosphatidic acids have shown to promote many of the hallmarks of cancer such as proliferation, survival, migration and invasion, with these studies marking LPA receptors as potential therapeutic targets (Gendaszewska-Darmach 2008). Further validating our results demonstrating that SGK3 over-expression is able to induce differential expression of multiple components of the LPA pathway, in addition to further extending these studies to define a potential mechanism involved in regulation will also further assist in defining SGK3's role in malignant cell transformation.

Despite results in earlier chapters demonstrating an involvement of SGK3 in rDNA transcription and cell growth, a robust ribosome biogenesis gene expression signature was not observed in cells over-expressing activated SGK3. This is in contrast to enforced expression of c-myc, which demonstrates massive transcriptional up-regulation of many ribosome components. While both SGK3 and c-myc can regulate ribosome biogenesis, the lack of transcriptional regulation elicited by SGK3 over-expression suggests that SGK3 and AKT may effect ribosome biogenesis via post-translationally modifying the RNA Pol I transcription components. Moreover, this may also assist in explaining the synergy demonstrated between AKT and c-myc to regulate rDNA transcription (Chan et al. 2011), whereby AKT is able to phosphorylate the RNA Pol I components that c-MYC is able to transcriptionally up-regulate. Experiments described earlier, including proteomics and candidate analysis of targets would also further test this hypothesis.

Furthermore, our genomic and functional studies have identified differences between SGK3 and the AKT. Functional data demonstrated that both SGK3 and AKT isoforms are able to induce anchorage independent growth, however only AKT was able to drive cell migration, while neither conferred consistent chemoresistance, indicating that while SGK3 and the AKT isoforms share similar upstream activation and downstream targets, fundamental differences in localisation are likely to be involved in their ability to regulate certain processes. Consistent with this, recent reports have demonstrated that SGK3 mainly affects proliferation and survival processes, while effects on cell motility and metastasis are weak in hepatocellular carcinoma cancer (Liu et al. 2012), while AKT studies have demonstrated a direct role for AKT in cell migration (Stambolic and Woodgett 2006). A comparison of differential gene expression in both epithelial and fibroblast cells demonstrated overall that SGK3 shared very few differentially regulated genes with the AKT isoforms despite some functional similarities. Further validation and analysis of genes that are shared between SGK3 and the three AKT isoforms may assist in further delineating signalling mechanisms shared between these kinases. Moreover, conducting gain-of-function experiments involving over-expression of both SGK3 and AKT together may assist in determining if these kinases are able to have an additive effect on key functional outcomes. Additionally, generating SGK3 knock-in models where AKT has been knocked out could also more definitively determine how much SGK3 is able to phenotype AKT.

6.5 Conclusion

Together, the studies presented in this thesis show for the first time that SGK3 is able to regulate cell growth and proliferation. These effects of SGK3 are likely to be cell specific and mediated largely via mTORC1. Moreover, SGK3's ability to optimally regulate growth requires endosomal localisation, where it potentially interacts with endosomal factors such as the class III PI3-K hVps34 to mediate fundamental growth processes. The ability to regulate cell growth and proliferation together with the ability to induce anchorage independent growth strongly support a role for SGK3 in malignant cell transformation, moreover recent reports demonstrating that SGK3 is a critical factor in PI3-K AKT-independent signalling to anchorage-independent growth and *in vivo* tumour formation in multiple cell systems (Vasudevan et al. 2009; Liu et al. 2012) further support an important role for SGK3 in oncogenic signalling, potentially making it a key therapeutic target. Taken together, both functional and genomic studies presented in this thesis were able to build upon our current knowledge of SGK3, in addition to providing key novel observations that can be used as a platform to further elucidate SGK3 functionality in both health and disease.

Appendix I: Chapter 5 supplementary data

Tables presented in this appendix are supplementary tables from GeneGo pathway analysis referred to in Chapter 5. Complete tables showing a list of all differentially regulated genes from cell lines with more than 20 up- or down-regulated genes presented in Chapter 5, in addition to all GSEA data from cell lines enriched with more than 20 significant gene sets can be found on the DVD affixed on the inside back cover of this thesis.

Table S.1: HOSE SGK3 WT remaining GeneGO pathways. Identified using a FC 0, p-val <0.05. Ranked according to p-val.

#	GeneGO Pathways	P-Value
11	Immune response_Histamine H1 receptor signaling in immune response	2.998e-4
12	Cytoskeleton remodeling_RalB regulation pathway	3.237e-4
13	Immune response_Oncostatin M signaling via MAPK in mouse cells	3.312e-4
14	Development_Regulation of epithelial-to-mesenchymal transition (EMT)	3.323e-4
15	Some pathways of EMT in cancer cells	4.396e-4
16	Immune response_Oncostatin M signaling via MAPK in human cells	4.532e-4
17	Cytoskeleton remodeling_Cytoskeleton remodeling	4.614e-4
18	Cell adhesion_ECM remodeling	4.964e-4
19	Immune response_BCR pathway	6.273e-4
20	Apoptosis and survival_Apoptotic TNF-family pathways	9.122e-4
21	Apoptosis and survival_BAD phosphorylation	9.122e-4
22	Immune response_TREM1 signaling pathway	1.076e-3
23	Role of alpha-6/beta-4 integrins in carcinoma progression	1.323e-3
24	Signal transduction_Calcium signaling	1.323e-3
25	Cell adhesion_Chemokines and adhesion	1.629e-3
26	Development_PDGF signaling via STATs and NF-kB	1.630e-3
27	Development_VEGF signaling via VEGFR2 - generic cascades	2.048e-3
28	Signal transduction_Erk Interactions: Inhibition of Erk	2.154e-3
29	G-protein signaling_G-Protein alpha-q signaling cascades	2.154e-3
30	Development_EPO-induced Jak-STAT pathway	2.458e-3
31	Cell adhesion_Plasmin signaling	2.458e-3
32	Development_Growth hormone signaling via STATs and PLC/IP3	2.458e-3
33	Cell cycle_Role of 14-3-3 proteins in cell cycle regulation	2.728e-3
34	Immune response_Antiviral actions of Interferons	2.820e-3
35	Apoptosis and survival_Endoplasmic reticulum stress response pathway	3.109e-3
36	G-protein signaling_G-Protein alpha-12 signaling pathway	3.157e-3
37	Reproduction_GnRH signaling	3.442e-3

Table S.2: HOSE SGK3 WT remaining GeneGO pathways. Identified using a FC >2, p-val <0.05. Ranked according to P-val.

#	GeneGO Pathways	P-Value
11	Immune response_Signaling pathway mediated by IL-6 and IL-1	1.812e-3
12	Cytoskeleton remodeling_TGF, WNT and cytoskeletal remodeling	2.067e-3
13	Development_HGF-dependent inhibition of TGF-beta-induced EMT	2.188e-3
14	Development_PDGF signaling via STATs and NF-kB	2.188e-3
15	Normal and pathological TGF-beta-mediated regulation of cell proliferation	2.393e-3
16	Cell adhesion_Plasmin signaling	2.838e-3
17	Immune response_Oncostatin M signaling via MAPK in mouse cells	2.838e-3

Table S.3: IOSE523-myrAKT1 remaining GeneGO pathways. Identified using FC 0, p-val <0.05. Ranked according to p-val.

#	GeneGO Pathways	P-Value
11	Transcription_Androgen Receptor nuclear signaling	1.126e-4
12	Immune response_Inhibitory action of Lipoxins on pro-inflammatory TNF-alpha signaling	1.336e-4
13	Immune response_Histamine H1 receptor signaling in immune response	1.452e-4
14	Development_PEDF signaling	1.575e-4
15	Immune response_Histamine signaling in dendritic cells	1.704e-4
16	Development_A2B receptor: action via G-protein alpha s	1.704e-4
17	G-protein signaling_Proinsulin C-peptide signaling	1.987e-4
18	Immune response_PGE2 common pathways	1.987e-4
19	Cytoskeleton remodeling_FAK signaling	2.840e-4
20	Apoptosis and survival_Apoptotic Activin A signaling	3.566e-4
21	Transcription_PPAR Pathway	3.691e-4
22	Muscle contraction_Regulation of eNOS activity in endothelial cells	4.438e-4
23	Regulation of lipid metabolism_Alpha-1 adrenergic receptors signaling via arachidonic acid	6.248e-4
24	Regulation of lipid metabolism_Alpha-1 adrenergic receptors signaling via arachidonic acid	8.952e-4
25	Development_Delta-type opioid receptor mediated cardioprotection	1.149e-3
26	Muscle contraction_GPCRs in the regulation of smooth muscle tone	1.187e-3
27	Development_VEGF signaling via VEGFR2 - generic cascades	1.241e-3
28	Immune response_Human NKG2D signaling	1.242e-3
29	Cytokine production by Th17 cells in CF	1.340e-3
30	Transcription_Receptor-mediated HIF regulation	1.340e-3
31	Translation_Non-genomic (rapid) action of Androgen Receptor	1.443e-3
32	Immune response_MIF in innate immunity response	1.443e-3
33	Immune response_Murine NKG2D signaling	1.664e-3
34	Neurophysiological process_HTR1A receptor signaling in neuronal cells	1.664e-3
35	Development_ACM2 and ACM4 activation of ERK	1.782e-3
36	Development_VEGF signaling and activation	1.782e-3
37	Immune response_PGE2 in immune and neuroendocrine system interactions	1.904e-3
38	Development_S1P1 signaling pathway	1.904e-3
39	Role of alpha-6/beta-4 integrins in carcinoma progression	2.032e-3
40	Immune response_PGE2 signaling in immune response	2.032e-3
41	G-protein signaling_Regulation of cAMP levels by ACM	2.032e-3
42	Development_GDNF family signaling	2.166e-3
43	Development_Endothelin-1/EDNRA transactivation of EGFR	2.166e-3
44	Development_HGF signaling pathway	2.304e-3
45	Muscle contraction_Relaxin signaling pathway	2.448e-3
46	Development_A3 receptor signaling	2.598e-3
47	Signal transduction_IP3 signaling	2.598e-3
48	Cytokine production by Th17 cells in CF (Mouse model)	2.598e-3
49	Development_GM-CSF signaling	2.753e-3
50	Development_EDNRB signaling	2.753e-3
51	Signal transduction_Activation of PKC via G-Protein coupled receptor	3.079e-3
52	Cell cycle_Influence of Ras and Rho proteins on G1/S Transition	3.251e-3
53	Development_WNT signaling pathway. Part 2	3.251e-3
54	Cytoskeleton remodeling_TGF, WNT and cytoskeletal remodeling	3.447e-3
55	PGE2 pathways in cancer	3.612e-3

#	GeneGO Pathways	P-Value
56	Muscle contraction_ACM regulation of smooth muscle contraction	3.802e-3
57	Immune response_CCR5 signaling in macrophages and T lymphocytes	4.199e-3
58	Transcription_Role of VDR in regulation of genes involved in osteoporosis	4.840e-3
59	Development_Regulation of epithelial-to-mesenchymal transition (EMT)	5.537e-3
60	Development_FGF2-dependent induction of EMT	5.566e-3
61	Immune response_CD40 signaling	5.782e-3
62	Development_S1P4 receptor signaling pathway	6.719e-3
63	Immune response_MIF-mediated glucocorticoid regulation	6.719e-3
64	Immune response_Gastrin in inflammatory response	6.828e-3
65	G-protein signaling_Cross-talk between Ras-family GTPases	7.332e-3
66	Regulation of lipid metabolism_Stimulation of Arachidonic acid production by ACM receptors	7.681e-3
67	Development_Dopamine D2 receptor transactivation of EGFR	7.970e-3
68	Development_GDNF signaling	7.970e-3
69	Development_Leptin signaling via JAK/STAT and MAPK cascades	8.633e-3
70	Cell adhesion_Endothelial cell contacts by junctional mechanisms	9.318e-3
71	PDGF activation of prostacyclin synthesis	1.003e-2
72	Transcription_Role of Akt in hypoxia induced HIF1 activation	1.003e-2
73	Neurophysiological process_NMDA-dependent postsynaptic long-term potentiation in CA1 hippocampal neurons	1.025e-2
74	Development_Mu-type opioid receptor regulation of proliferation	1.076e-2
75	Development_Delta-type opioid receptor signaling via G-protein alpha-14	1.076e-2
76	Immune response_Delta-type opioid receptor signaling in T-cells	1.152e-2
77	NGF activation of NF-kB	1.152e-2
78	Immune response_IL-6 signaling pathway	1.152e-2

Table S.4: IOSE523-myrAKT1 remaining GeneGO pathways. Identified using FC >2, p-val <0.05. Ranked according to p-val.

#	GeneGO Pathways	P-Value
11	Immune response_CD40 signaling	8.202e-4
12	Development_FGF2-dependent induction of EMT	1.469e-3
13	Muscle contraction_GPCRs in the regulation of smooth muscle tone	1.667e-3
14	Immune response_MIF-mediated glucocorticoid regulation	1.780e-3
15	Apoptosis and survival_Apoptotic Activin A signaling	2.299e-3
16	PDGF activation of prostacyclin synthesis	2.681e-3
17	Cell adhesion_Chemokines and adhesion	2.842e-3
18	Immune response_Signaling pathway mediated by IL-6 and IL-1	3.305e-3
19	Immune response_Th17 cell differentiation	3.526e-3
20	Development_BMP signaling	3.990e-3
21	Development_Delta-type opioid receptor mediated cardioprotection	4.998e-3

Table S.5: IOSE523-myrAKT2 remaining GeneGO pathways. Identified using FC 0, p-val 0.05. Ranked according to P-val.

#	GeneGO Pathways	P-Value
11	Cytoskeleton remodeling_TGF, WNT and cytoskeletal remodeling	2.518e-4
12	Cytokine production by Th17 cells in CF	2.706e-4
13	Immune response_MIF in innate immunity response	3.056e-4
14	Immune response_IL-15 signaling	3.758e-4
15	Immune response_CD40 signaling	4.089e-4
16	Development_PEDF signaling	7.951e-4
17	Cytokine production by Th17 cells in CF (Mouse model)	7.951e-4
18	Immune response_Histamine signaling in dendritic cells	8.729e-4
19	Development_Slit-Robo signaling	9.847e-4
20	Cytoskeleton remodeling_FAK signaling	1.587e-3
21	Immune response_TREM1 signaling pathway	1.852e-3
22	Cell adhesion_Tight junctions	1.974e-3
23	Muscle contraction_Oxytocin signaling in uterus and mammary gland	1.997e-3
24	Regulation of lipid metabolism_Insulin regulation of fatty acid methabolism	2.147e-3
25	Regulation of lipid metabolism_Regulation of lipid metabolism via LXR, NF-Y and SREBP	2.418e-3
26	Muscle contraction_Regulation of eNOS activity in endothelial cells	2.658e-3
27	Glycolysis and gluconeogenesis (short map)	3.042e-3
28	Cytoskeleton remodeling_Role of Activin A in cytoskeleton remodeling	3.134e-3

Table S.6: IOSE523-myrAKT2 remaining GeneGO pathways. Identified using FC >2, p-val 0.05. Ranked according to p-val.

#	GeneGO Pathways	P-Value
11	Immune response_Inhibitory action of Lipoxins on pro-inflammatory TNF-alpha signaling	1.060e-3
12	Development_PEDF signaling	1.197e-3
13	Development_WNT signaling pathway. Part 2	1.504e-3
14	PGE2 pathways in cancer	1.674e-3
15	Development_Role of IL-8 in angiogenesis	1.952e-3
16	Immune response_CD40 signaling	2.706e-3
17	Development_FGF2-dependent induction of EMT	3.296e-3
18	Atherosclerosis_Role of ZNF202 in regulation of expression of genes involved in Atherosclerosis	3.633e-3

Table S.7: BJ-hTERT SGK3 CA remaining GeneGO pathways. Identified using FC 0, p-val <0.05. Ranked according to P-val.

#	GeneGO Pathways	P-Value
11	Immune response_IL-4 - antiapoptotic action	1.114e-3
12	Development_Transactivation of PDGFR in non-neuronal cells by Dopamine D2 receptor	1.190e-3
13	Cell cycle_Role of Nek in cell cycle regulation	1.268e-3
14	Development_PDGF signaling via STATs and NF-kB	1.268e-3
15	Development_EGFR signaling via small GTPases	1.349e-3
16	Development_CNTF receptor signaling	1.431e-3
17	Development_Angiopoietin - Tie2 signaling	1.517e-3
18	Cell adhesion_Plasmin signaling	1.517e-3
19	Immune response_IL-9 signaling pathway	1.604e-3
20	G-protein signaling_H-RAS regulation pathway	1.694e-3
21	Development_Beta-adrenergic receptors transactivation of EGFR	1.694e-3
22	Development_Delta-type opioid receptor mediated cardioprotection	1.694e-3
23	Immune response_Human NKG2D signaling	1.787e-3
24	Cell adhesion_PLAU signaling	1.882e-3
25	Development_ERBB-family signaling	1.882e-3
26	Transcription_Receptor-mediated HIF regulation	1.882e-3
27	Translation _Regulation of EIF2 activity	1.882e-3
28	Development_Neurotrophin family signaling	1.979e-3
29	Immune response_TCR and CD28 co-stimulation in activation of NF-kB	1.979e-3
30	Development_VEGF-family signaling	2.078e-3
31	Immune response_PIP3 signaling in B lymphocytes	2.180e-3
32	Translation_Insulin regulation of translation	2.180e-3
33	Immune response_Murine NKG2D signaling	2.180e-3
34	Apoptosis and survival_BAD phosphorylation	2.180e-3
35	Development_S1P3 receptor signaling pathway	2.284e-3
36	Development_VEGF signaling and activation	2.284e-3
37	Immune response_IL-4 signaling pathway	2.391e-3
38	Development_Ligand-independent activation of ESR1 and ESR2	2.500e-3
39	Development_Membrane-bound ESR1: interaction with growth factors signaling	2.500e-3
40	Development_Thrombopoietin-regulated cell processes	2.500e-3
41	Development_Hedgehog signaling	2.611e-3
42	Immune response_ICOS pathway in T-helper cell	2.611e-3
43	Signal transduction_PTEN pathway	2.611e-3
44	Development_Endothelin-1/EDNRA transactivation of EGFR	2.611e-3
45	Development_Angiotensin activation of Akt	2.611e-3
46	Regulation of lipid metabolism_Insulin signaling:generic cascades	2.724e-3
47	Transcription_CREB pathway	2.724e-3
48	Niacin-HDL metabolism	2.724e-3
49	Development_Leptin signaling via PI3K-dependent pathway	2.724e-3
50	Development_HGF signaling pathway	2.724e-3
51	Development_PDGF signaling via MAPK cascades	2.724e-3
52	Immune response_Fc gamma R-mediated phagocytosis in macrophages	2.724e-3
53	Development_Melanocyte development and pigmentation	2.958e-3
54	Signal transduction_IP3 signaling	2.958e-3
55	Development_PEDF signaling	2.958e-3

#	GeneGO Pathways	P-Value
56	Nicotine signaling in cholinergic neurons	3.078e-3
57	Some pathways of EMT in cancer cells	3.201e-3
58	Immune response_NFAT in immune response	3.201e-3
59	G-protein signaling_Proinsulin C-peptide signaling	3.325e-3
60	Development_FGF-family signaling	3.325e-3
61	Cell cycle_Influence of Ras and Rho proteins on G1/S Transition	3.453e-3
62	Development_Endothelin-1/EDNRA signaling	3.453e-3
63	Translation _Regulation of EIF4F activity	3.453e-3
64	Immune response_CD28 signaling	3.582e-3
65	Immune response_Role of DAP12 receptors in NK cells	3.582e-3
66	Immune response _IFN gamma signaling pathway	3.582e-3
67	Development_Role of HDAC and calcium/calmodulin-dependent kinase (CaMK) in control of skeletal myogenesis	3.582e-3
68	Development_FGFR signaling pathway	3.582e-3
69	Immune response_BCR pathway	3.582e-3
70	Immune response_Fc epsilon RI pathway	3.713e-3
71	Cytoskeleton remodeling_FAK signaling	3.983e-3
72	Immune response_TREM1 signaling pathway	4.262e-3
73	Immune response_Immunological synapse formation	4.262e-3
74	Immune response_IL-17 signaling pathways	4.405e-3
75	Transcription_PPAR Pathway	4.550e-3
76	Development_Alpha-2 adrenergic receptor activation of ERK	4.697e-3
77	Muscle contraction_Regulation of eNOS activity in endothelial cells	4.998e-3
78	Cardiac Hypertrophy_NF-AT signaling in Cardiac Hypertrophy	5.152e-3
79	Immune response_CD16 signaling in NK cells	5.788e-3
80	Development_VEGF signaling via VEGFR2 - generic cascades	8.478e-3
81	Regulation of lipid metabolism_Insulin regulation of fatty acid methabolism	9.478e-3
82	Transport_Intracellular cholesterol transport in norm	9.684e-3
83	Cell adhesion_Chemokines and adhesion	1.185e-2
84	Cytoskeleton remodeling_Cytoskeleton remodeling	1.231e-2
85	Cytoskeleton remodeling_TGF, WNT and cytoskeletal remodeling	1.447e-2
86	G-protein signaling_Rap1B regulation pathway	1.837e-2

Table S.8: BJ-hTERT myrAKT1 remaining GeneGO pathways. Identified using FC 0, p-val <0.05. Ranked according to p-val.

#	GeneGO Pathways	P-Value
11	Immune response_PIP3 signaling in B lymphocytes	9.645e-4
12	Development_S1P3 receptor signaling pathway	1.033e-3
13	Development_A2A receptor signaling	1.033e-3
14	Development_S1P1 signaling pathway	1.105e-3
15	Development_Ligand-independent activation of ESR1 and ESR2	1.181e-3
16	Development_Endothelin-1/EDNRA transactivation of EGFR	1.259e-3
17	Development_Angiotensin activation of Akt	1.259e-3
18	Transcription_CREB pathway	1.340e-3
19	Development_Leptin signaling via PI3K-dependent pathway	1.340e-3
20	Immune response_Inhibitory action of Lipoxins on pro-inflammatory TNF-alpha signaling	1.340e-3
21	Regulation of lipid metabolism_Insulin signaling:generic cascades	1.340e-3
22	Immune response_Antigen presentation by MHC class II	1.373e-3
23	Development_Melanocyte development and pigmentation	1.513e-3
24	Development_A3 receptor signaling	1.513e-3
25	Immune response_Histamine signaling in dendritic cells	1.605e-3
26	Development_A2B receptor: action via G-protein alpha s	1.605e-3
27	Immune response_NFAT in immune response	1.699e-3
28	G-protein signaling_Proinsulin C-peptide signaling	1.798e-3
29	Immune response_PGE2 common pathways	1.798e-3
30	Immune response_CD28 signaling	2.005e-3
31	Muscle contraction_Regulation of eNOS activity in cardiomyocytes	2.226e-3
32	Regulation of lipid metabolism_Insulin regulation of glycogen metabolism	2.226e-3
33	Cytoskeleton remodeling_FAK signaling	2.342e-3
34	Immune response_TREM1 signaling pathway	2.585e-3
35	Transcription_PPAR Pathway	2.843e-3
36	Muscle contraction_Regulation of eNOS activity in endothelial cells	3.260e-3
37	Development_FGF2-dependent induction of EMT	3.860e-3
38	Immune response_Gastrin in inflammatory response	4.034e-3
39	Apoptosis and survival_Beta-2 adrenergic receptor anti-apoptotic action	5.094e-3
40	Development_EGFR signaling via PIP3	5.094e-3
41	Development_Dopamine D2 receptor transactivation of EGFR	5.541e-3
42	Immune response_IL-23 signaling pathway	6.005e-3
43	Apoptosis and survival_NGF signaling pathway	6.486e-3
44	Immune response_IL-10 signaling pathway	6.486e-3
45	Cell adhesion_Endothelial cell contacts by junctional mechanisms	6.486e-3

Table S.9: BJ-hTERT myrAKT1 remaining GeneGO pathways. Identified using FC >2, p-val <0.05. Ranked according to p-val.

#	GeneGO Pathways	P-Value
11	Development_FGF2-dependent induction of EMT	8.162e-4
12	Development_EGFR signaling via PIP3	1.083e-3
13	Development_Dopamine D2 receptor transactivation of EGFR	1.180e-3
14	Immune response_IL-23 signaling pathway	1.280e-3
15	Immune response_IL-10 signaling pathway	1.385e-3
16	Apoptosis and survival_NGF signaling pathway	1.385e-3
17	NGF activation of NF-kB	1.724e-3
18	Immune response_IL-4 - antiapoptotic action	1.845e-3
19	Development_PDGF signaling via STATs and NF-kB	2.098e-3
20	Development_CNTF receptor signaling	2.367e-3
21	Development_Angiopoietin - Tie2 signaling	2.507e-3
22	Immune response_Human NKG2D signaling	2.951e-3
23	Development_ERBB-family signaling	3.107e-3
24	Transcription_Receptor-mediated HIF regulation	3.107e-3
25	Translation _Regulation of EIF2 activity	3.107e-3
26	Transcription_NF-kB signaling pathway	3.107e-3
27	Development_Neurotrophin family signaling	3.266e-3
28	Immune response_TCR and CD28 co-stimulation in activation of NF-kB	3.266e-3
29	Development_VEGF-family signaling	3.429e-3
30	Immune response_HMGB1 release from the cell	3.429e-3
31	Immune response_PIP3 signaling in B lymphocytes	3.596e-3
32	Translation_Insulin regulation of translation	3.596e-3
33	Immune response_Murine NKG2D signaling	3.596e-3
34	Apoptosis and survival_BAD phosphorylation	3.596e-3
35	Development_S1P3 receptor signaling pathway	3.767e-3
36	Signal transduction_AKT signaling	3.767e-3
37	Development_VEGF signaling and activation	3.767e-3
38	Immune response_IL-4 signaling pathway	3.941e-3
39	Development_S1P1 signaling pathway	3.941e-3
40	Immune response_IL-1 signaling pathway	3.941e-3
41	Development_Ligand-independent activation of ESR1 and ESR2	4.119e-3
42	Development_Membrane-bound ESR1: interaction with growth factors signaling	4.119e-3
43	Role of alpha-6/beta-4 integrins in carcinoma progression	4.119e-3
44	Development_Thrombopoietin-regulated cell processes	4.119e-3
45	Immune response_ICOS pathway in T-helper cell	4.301e-3
46	Signal transduction_PTEN pathway	4.301e-3
47	Development_TGF-beta-dependent induction of EMT via RhoA, PI3K and ILK.	4.301e-3
48	Development_Endothelin-1/EDNRA transactivation of EGFR	4.301e-3
49	Development_Angiotensin activation of Akt	4.301e-3
50	Regulation of lipid metabolism_Insulin signaling:generic cascades	4.486e-3
51	Transcription_CREB pathway	4.486e-3
52	Development_Leptin signaling via PI3K-dependent pathway	4.486e-3
53	Development_PIP3 signaling in cardiac myocytes	4.486e-3
54	Development_HGF signaling pathway	4.486e-3
55	Development_Melanocyte development and pigmentation	4.868e-3

#	GeneGO Pathways	P-Value
56	Signal transduction_IP3 signaling	4.868e-3
57	Nicotine signaling in cholinergic neurons	5.064e-3
58	Some pathways of EMT in cancer cells	5.264e-3
59	Immune response_NFAT in immune response	5.264e-3
60	Development_IGF-1 receptor signaling	5.468e-3
61	G-protein signaling_Proinsulin C-peptide signaling	5.468e-3
62	Development_FGF-family signaling	5.468e-3
63	Cell cycle_Influence of Ras and Rho proteins on G1/S Transition	5.675e-3
64	Development_Endothelin-1/EDNRA signaling	5.675e-3
65	Translation _Regulation of EIF4F activity	5.675e-3
66	Immune response_CD28 signaling	5.886e-3
67	Immune response _IFN gamma signaling pathway	5.886e-3
68	Development_Role of HDAC and calcium/calmodulin-dependent kinase (CaMK) in control of skeletal myogenesis	5.886e-3
69	Development_FGFR signaling pathway	5.886e-3
70	Immune response_BCR pathway	5.886e-3
71	Apoptosis and survival_NO synthesis and signaling	6.100e-3
72	Immune response_Fc epsilon RI pathway	6.100e-3
73	Regulation of lipid metabolism_Insulin regulation of glycogen metabolism	6.318e-3
74	Cytoskeleton remodeling_FAK signaling	6.540e-3
75	Transcription_PPAR Pathway	7.460e-3
76	Transcription_Role of VDR in regulation of genes involved in osteoporosis	7.460e-3
77	Development_Alpha-2 adrenergic receptor activation of ERK	7.699e-3
78	Immune response_IL-15 signaling	8.187e-3
79	Muscle contraction_Regulation of eNOS activity in endothelial cells	8.187e-3
80	Development_Regulation of epithelial-to-mesenchymal transition (EMT)	8.187e-3
81	Cardiac Hypertrophy_NF-AT signaling in Cardiac Hypertrophy	8.436e-3
82	Immune response_Gastrin in inflammatory response	9.467e-3
83	Development_VEGF signaling via VEGFR2 - generic cascades	1.380e-2
84	Regulation of lipid metabolism_Insulin regulation of fatty acid methabolism	1.541e-2
85	Cell adhesion_Chemokines and adhesion	1.920e-2

Table S.10: BJ-hTERT myrAKT2 GeneGO pathways. Identified using FC 0, p-val <0.05. Ranked according to p-val.

#	GeneGO Pathways	P-Value
56	Immune response_MIF-mediated glucocorticoid regulation	4.988e-3
57	Blood coagulation_GPCRs in platelet aggregation	5.530e-3
58	Cell adhesion_Histamine H1 receptor signaling in the interruption of cell barrier integrity	5.693e-3
59	Development_Ligand-independent activation of ESR1 and ESR2	5.693e-3
60	Signal transduction_Calcium signaling	5.693e-3
61	Neurophysiological process_ACM regulation of nerve impulse	6.159e-3
62	Development_Endothelin-1/EDNRA transactivation of EGFR	6.159e-3
63	Development_PIP3 signaling in cardiac myocytes	6.650e-3
64	Transport_Alpha-2 adrenergic receptor regulation of ion channels	6.650e-3

Table S.11: BJ-hTERT myrAKT2 remaining GeneGO pathways. Identified using FC >2, p-val <0.05. Ranked according to p-val.

#	GeneGO Pathways	P-Value
11	Androstenedione and testosterone biosynthesis and metabolism p.2	9.071e-4
12	Androstenedione and testosterone biosynthesis and metabolism p.2/ Rodent version	9.858e-4
13	Cytokine production by Th17 cells in CF	1.247e-3
14	Development_VEGF signaling and activation	1.659e-3
15	Immune response_IL-1 signaling pathway	1.773e-3
16	Development_Leptin signaling via PI3K-dependent pathway	2.146e-3
17	Immune response_Inhibitory action of Lipoxins on pro-inflammatory TNF-alpha signaling	2.146e-3
18	Regulation of lipid metabolism_Insulin signaling:generic cascades	2.146e-3
19	Development_HGF signaling pathway	2.146e-3
20	Chemotaxis_Inhibitory action of lipoxins on IL-8- and Leukotriene B4-induced neutrophil migration	2.714e-3
21	Cytoskeleton remodeling_TGF, WNT and cytoskeletal remodeling	3.149e-3
22	Immune response _IFN gamma signaling pathway	3.195e-3
23	Regulation of lipid metabolism_Insulin regulation of glycogen metabolism	3.544e-3
24	Inhibitory action of Lipoxins on neutrophil migration	3.726e-3

Bibliography

2011. Integrated genomic analyses of ovarian carcinoma. Nature 474(7353): 609-615.

Ackermann, T.F., Boini, K.M., Beier, N., Scholz, W., Fuchss, T., and Lang, F. 2011. EMD638683, a novel SGK inhibitor with antihypertensive potency. Cell Physiol Biochem 28(1): 137-146.

Adeyinka, A., Emberley, E., Niu, Y., Snell, L., Murphy, L.C., Sowter, H., Wykoff, C.C., Harris, A.L., and Watson, P.H. 2002. Analysis of gene expression in ductal carcinoma in situ of the breast. Clin Cancer Res 8(12): 3788-3795.

Allavena, P., Garlanda, C., Borrello, M.G., Sica, A., and Mantovani, A. 2008. Pathways connecting inflammation and cancer. Curr Opin Genet Dev 18(1): 3-10.

Alliston, T.N., Maiyar, A.C., Buse, P., Firestone, G.L., and Richards, J.S. 1997. Follicle stimulating hormone-regulated expression of serum/glucocorticoid-inducible kinase in rat ovarian granulosa cells: a functional role for the Sp1 family in promoter activity. Mol Endocrinol 11(13): 1934-1949.

Alonso, L., Okada, H., Pasolli, H.A., Wakeham, A., You-Ten, A.I., Mak, T.W., and Fuchs, E. 2005. Sgk3 links growth factor signaling to maintenance of progenitor cells in the hair follicle. J Cell Biol 170(4): 559-570.

Alvarez de la Rosa, D., Zhang, P., Naray-Fejes-Toth, A., Fejes-Toth, G., and Canessa, C.M. 1999. The serum and glucocorticoid kinase sgk increases the abundance of epithelial sodium channels in the plasma membrane of Xenopus oocytes. J Biol Chem 274(53): 37834-37839.

Amato, R., D'Antona, L., Porciatti, G., Agosti, V., Menniti, M., Rinaldo, C., Costa, N., Bellacchio, E., Mattarocci, S., Fuiano, G., Soddu, S., Paggi, M.G., Lang, F., and Perrotti, N. 2009. Sgk1 activates MDM2-dependent p53 degradation and affects cell proliferation, survival, and differentiation. J Mol Med 87(12): 1221-1239.

Amato, R., Menniti, M., Agosti, V., Boito, R., Costa, N., Bond, H.M., Barbieri, V., Tagliaferri, P., Venuta, S., and Perrotti, N. 2007. IL-2 signals through Sgk1 and inhibits proliferation and apoptosis in kidney cancer cells. J Mol Med (Berl) 85(7): 707-721.

Ansorge, H.L., Meng, X., Zhang, G., Veit, G., Sun, M., Klement, J.F., Beason, D.P., Soslowsky, L.J., Koch, M., and Birk, D.E. 2009. Type XIV Collagen Regulates Fibrillogenesis: PREMATURE COLLAGEN FIBRIL GROWTH AND TISSUE DYSFUNCTION IN NULL MICE. J Biol Chem 284(13): 8427-8438.

Aoki, M., Blazek, E., and Vogt, P.K. 2001. A role of the kinase mTOR in cellular transformation induced by the oncoproteins P3k and Akt. Proc Natl Acad Sci U S A 98(1): 136-141.

Aoyama, T., Matsui, T., Novikov, M., Park, J., Hemmings, B., and Rosenzweig, A. 2005. Serum and glucocorticoid-responsive kinase-1 regulates cardiomyocyte survival and hypertrophic response. Circulation 111(13): 1652-1659.

Arabi, A., Wu, S., Ridderstrale, K., Bierhoff, H., Shiue, C., Fatyol, K., Fahlen, S., Hydbring, P., Soderberg, O., Grummt, I., Larsson, L.G., and Wright, A.P. 2005. c-Myc associates with ribosomal DNA and activates RNA polymerase I transcription. Nat Cell Biol 7(3): 303-310.

Aronova, S., Wedaman, K., Aronov, P.A., Fontes, K., Ramos, K., Hammock, B.D., and Powers, T. 2008. Regulation of ceramide biosynthesis by TOR complex 2. Cell Metab 7(2): 148-158.

Arteaga, M.F., Alvarez de la Rosa, D., Alvarez, J.A., and Canessa, C.M. 2007. Multiple Translational Isoforms Give Functional Specificity to Serum- and Glucocorticoid-induced Kinase 1. Mol Biol Cell 18(6): 2072-2080.

Arteaga, M.F., Wang, L., Ravid, T., Hochstrasser, M., and Canessa, C.M. 2006. An amphipathic helix targets serum and glucocorticoid-induced kinase 1 to the endoplasmic reticulum-associated ubiquitin-conjugation machinery. Proc Natl Acad Sci U S A 103(30): 11178-11183.

Asher, C., Sinha, I., and Garty, H. 2003. Characterization of the interactions between Nedd4-2, ENaC, and sgk-1 using surface plasmon resonance. Biochim Biophys Acta 1612(1): 59-64.

Astle, M.V., Hannan, K.M., Ng, P.Y., Lee, R.S., George, A.J., Hsu, A.K., Haupt, Y., Hannan, R.D., and Pearson, R.B. 2011. AKT induces senescence in human cells via mTORC1 and p53 in the absence of DNA damage: implications for targeting mTOR during malignancy. Oncogene.

Backer, J.M. 2008. The regulation and function of Class III PI3Ks: novel roles for Vps34. Biochem J 410(1): 1-17.

Backman, S.A., Ghazarian, D., So, K., Sanchez, O., Wagner, K.U., Hennighausen, L., Suzuki, A., Tsao, M.S., Chapman, W.B., Stambolic, V., and Mak, T.W. 2004. Early onset of neoplasia in the prostate and skin of mice with tissue-specific deletion of Pten. Proc Natl Acad Sci U S A 101(6): 1725-1730.

Bader, A.G., Kang, S., Zhao, L., and Vogt, P.K. 2005. Oncogenic PI3K deregulates transcription and translation. Nat Rev Cancer 5(12): 921-929.

Baltaev, R., Strutz-Seebohm, N., Korniychuk, G., Myssina, S., Lang, F., and Seebohm, G. 2005. Regulation of cardiac shal-related potassium channel Kv 4.3 by serum- and glucocorticoid-inducible kinase isoforms in Xenopus oocytes. Pflugers Arch 450(1): 26-33.

Barbet, N.C., Schneider, U., Helliwell, S.B., Stansfield, I., Tuite, M.F., and Hall, M.N. 1996. TOR controls translation initiation and early G1 progression in yeast. Mol Biol Cell 7(1): 25-42.

BelAiba, R.S., Djordjevic, T., Bonello, S., Artunc, F., Lang, F., Hess, J., and Gorlach, A. 2006. The serum- and glucocorticoid-inducible kinase Sgk-1 is involved in pulmonary vascular remodeling: role in redox-sensitive regulation of tissue factor by thrombin. Circ Res 98(6): 828-836.

Bell, L.M., Leong, M.L., Kim, B., Wang, E., Park, J., Hemmings, B.A., and Firestone, G.L. 2000. Hyperosmotic stress stimulates promoter activity and regulates cellular utilization of the serum- and glucocorticoid-inducible protein kinase (Sgk) by a p38 MAPK-dependent pathway. J Biol Chem 275(33): 25262-25272.

Bellacosa, A., de Feo, D., Godwin, A.K., Bell, D.W., Cheng, J.Q., Altomare, D.A., Wan, M., Dubeau, L., Scambia, G., Masciullo, V., Ferrandina, G., Benedetti Panici, P., Mancuso, S., Neri, G., and Testa, J.R. 1995. Molecular alterations of the AKT2 oncogene in ovarian and breast carcinomas. Int J Cancer 64(4): 280-285.

Belova, L., Brickley, D.R., Ky, B., Sharma, S.K., and Conzen, S.D. 2008. Hsp90 regulates the phosphorylation and activity of serum- and glucocorticoid-regulated kinase-1. J Biol Chem 283(27): 18821-18831.

Belova, L., Sharma, S., Brickley, D.R., Nicolarsen, J.R., Patterson, C., and Conzen, S.D. 2006. Ubiquitin-proteasome degradation of serum- and glucocorticoid-regulated kinase-1 (SGK-1) is mediated by the chaperone-dependent E3 ligase CHIP. Biochem J 400(2): 235-244.

Benjamini, Y. and Hochberg, Y. 1995. Controlling the false discovery rate: a practical and powerful approach to multiple testing. Journal of the Royal Statistical Society Series B 57: 289-300.

Bertog, M., Cuffe, J.E., Pradervand, S., Hummler, E., Hartner, A., Porst, M., Hilgers, K.F., Rossier, B.C., and Korbmacher, C. 2008. Aldosterone responsiveness of the epithelial sodium channel (ENaC) in colon is increased in a mouse model for Liddle's syndrome. J Physiol 586(2): 459-475.

Bhandaru, M., Kempe, D.S., Rotte, A., Capuano, P., Pathare, G., Sopjani, M., Alesutan, I., Tyan, L., Huang, D.Y., Siraskar, B., Judenhofer, M.S., Stange, G., Pichler, B.J., Biber, J., Quintanilla-Martinez, L., Wagner, C.A., Pearce, D., Foller, M., and Lang, F. 2011. Decreased bone density and increased phosphaturia in gene-targeted mice lacking functional serum- and glucocorticoid-inducible kinase 3. Kidney Int 80(1): 61-67.

Biondi, R.M., Kieloch, A., Currie, R.A., Deak, M., and Alessi, D.R. 2001. The PIF-binding pocket in PDK1 is essential for activation of S6K and SGK, but not PKB. Embo J 20(16): 4380-4390.

Blagosklonny, M.V., Giannakakou, P., el-Deiry, W.S., Kingston, D.G., Higgs, P.I., Neckers, L., and Fojo, T. 1997. Raf-1/bcl-2 phosphorylation: a step from microtubule damage to cell death. Cancer Res 57(1): 130-135.

Boehm, J.S., Zhao, J.J., Yao, J., Kim, S.Y., Firestein, R., Dunn, I.F., Sjostrom, S.K.,

Garraway, L.A., Weremowicz, S., Richardson, A.L., Greulich, H., Stewart, C.J., Mulvey, L.A., Shen, R.R., Ambrogio, L., Hirozane-Kishikawa, T., Hill, D.E., Vidal, M., Meyerson, M., Grenier, J.K., Hinkle, G., Root, D.E., Roberts, T.M., Lander, E.S., Polyak, K., and Hahn, W.C. 2007. Integrative genomic approaches identify IKBKE as a breast cancer oncogene. Cell 129(6): 1065-1079.

Boehmer, C., Embark, H.M., Bauer, A., Palmada, M., Yun, C.H., Weinman, E.J., Endou, H., Cohen, P., Lahme, S., Bichler, K.H., and Lang, F. 2004. Stimulation of renal Na+ dicarboxylate cotransporter 1 by Na+/H+ exchanger regulating factor 2, serum and glucocorticoid inducible kinase isoforms, and protein kinase B. Biochem Biophys Res Commun 313(4): 998-1003.

Boehmer, C., Henke, G., Schniepp, R., Palmada, M., Rothstein, J.D., Broer, S., and Lang, F. 2003a. Regulation of the glutamate transporter EAAT1 by the ubiquitin ligase Nedd4-2 and the serum and glucocorticoid-inducible kinase isoforms SGK1/3 and protein kinase B. J Neurochem 86(5): 1181-1188.

Boehmer, C., Okur, F., Setiawan, I., Broer, S., and Lang, F. 2003b. Properties and regulation of glutamine transporter SN1 by protein kinases SGK and PKB. Biochem Biophys Res Commun 306(1): 156-162.

Boehmer, C., Palmada, M., Rajamanickam, J., Schniepp, R., Amara, S., and Lang, F. 2006. Post-translational regulation of EAAT2 function by co-expressed ubiquitin ligase Nedd4-2 is impacted by SGK kinases. J Neurochem 97(4): 911-921.

Boehmer, C., Rajamanickam, J., Schniepp, R., Kohler, K., Wulff, P., Kuhl, D., Palmada, M., and Lang, F. 2005. Regulation of the excitatory amino acid transporter EAAT5 by the serum and glucocorticoid dependent kinases SGK1 and SGK3. Biochem Biophys Res Commun 329(2): 738-742.

Boehmer, C., Wilhelm, V., Palmada, M., Wallisch, S., Henke, G., Brinkmeier, H., Cohen, P., Pieske, B., and Lang, F. 2003c. Serum and glucocorticoid inducible kinases in the regulation of the cardiac sodium channel SCN5A. Cardiovasc Res 57(4): 1079-1084.

Bogusz, A.M., Brickley, D.R., Pew, T., and Conzen, S.D. 2006. A novel N-terminal hydrophobic motif mediates constitutive degradation of serum- and glucocorticoid-induced kinase-1 by the ubiquitin-proteasome pathway. Febs J 273(13): 2913-2928.

Bohmer, C., Philippin, M., Rajamanickam, J., Mack, A., Broer, S., Palmada, M., and Lang, F. 2004. Stimulation of the EAAT4 glutamate transporter by SGK protein kinase isoforms and PKB. Biochem Biophys Res Commun 324(4): 1242-1248.

Bohmer, C., Sopjani, M., Klaus, F., Lindner, R., Laufer, J., Jeyaraj, S., Lang, F., and Palmada, M. 2010. The serum and glucocorticoid inducible kinases SGK1-3 stimulate the neutral amino acid transporter SLC6A19. Cell Physiol Biochem 25(6): 723-732.

Bolstad, B. 2004. Low Level Analysis of High-density Oligonucleotide Array Data: Background, Normalization and Summarization. In. University of California, Berkeley.

Bolstad, B.M., Collin, F., Brettschneider, J., Simpson, K., Cope, L., Irizarry, R.A., and Speed, T.P. 2005. Quality Assessment of Affymetrix GeneChip Data in Bioinformatics and Computational Biology Solutions Using R and Bioconductor. Springer.

Borst, O., Schmidt, E.M., Munzer, P., Schonberger, T., Towhid, S.T., Elvers, M., Leibrock, C., Schmid, E., Eylenstein, A., Kuhl, D., May, A.E., Gawaz, M., and Lang, F. 2012. The serum- and glucocorticoid-inducible kinase 1 (SGK1) influences platelet calcium signaling and function by regulation of Orai1 expression in megakaryocytes. Blood.

Bosse, T., Ehinger, J., Czuchra, A., Benesch, S., Steffen, A., Wu, X., Schloen, K., Niemann, H.H., Scita, G., Stradal, T.E., Brakebusch, C., and Rottner, K. 2007. Cdc42 and phosphoinositide 3-kinase drive Rac-mediated actin polymerization downstream of c-Met in distinct and common pathways. Mol Cell Biol 27(19): 6615-6628.

Brettschneider, J., Collin, F., Bolstad, B.M., and Speed, T.P. 2007. Quality assessment for short oligonucleotide arrays. Technometrics 50(3).

Brickley, D.R., Mikosz, C.A., Hagan, C.R., and Conzen, S.D. 2002. Ubiquitin modification of serum and glucocorticoid-induced protein kinase-1 (SGK-1). J Biol Chem 277(45): 43064-43070.

Brognard, J., Sierecki, E., Gao, T., and Newton, A.C. 2007. PHLPP and a second isoform, PHLPP2, differentially attenuate the amplitude of Akt signaling by regulating distinct Akt isoforms. Mol Cell 25(6): 917-931.

Brookes, S., Rowe, J., Ruas, M., Llanos, S., Clark, P.A., Lomax, M., James, M.C., Vatcheva, R., Bates, S., Vousden, K.H., Parry, D., Gruis, N., Smit, N., Bergman, W., and Peters, G. 2002. INK4a-deficient human diploid fibroblasts are resistant to RAS-induced senescence. Embo J 21(12): 2936-2945.

Brugarolas, J., Lei, K., Hurley, R.L., Manning, B.D., Reiling, J.H., Hafen, E., Witters, L.A., Ellisen, L.W., and Kaelin, W.G., Jr. 2004. Regulation of mTOR function in response to hypoxia by REDD1 and the TSC1/TSC2 tumor suppressor complex. Genes Dev 18(23): 2893-2904.

Brugarolas, J.B., Vazquez, F., Reddy, A., Sellers, W.R., and Kaelin, W.G., Jr. 2003. TSC2 regulates VEGF through mTOR-dependent and -independent pathways. Cancer Cell 4(2): 147-158.

Brunet, A., Park, J., Tran, H., Hu, L.S., Hemmings, B.A., and Greenberg, M.E. 2001. Protein kinase SGK mediates survival signals by phosphorylating the forkhead transcription factor FKHRL1 (FOXO3a). Mol Cell Biol 21(3): 952-965.

Buse, P., Maiyar, A.C., Failor, K.L., Tran, S., Leong, M.L., and Firestone, G.L. 2007.

The stimulus-dependent co-localization of serum- and glucocorticoid-regulated protein kinase (Sgk) and Erk/MAPK in mammary tumor cells involves the mutual interaction with the importin-alpha nuclear import protein. Exp Cell Res 313(15): 3261-3275.

Buse, P., Tran, S.H., Luther, E., Phu, P.T., Aponte, G.W., and Firestone, G.L. 1999. Cell cycle and hormonal control of nuclear-cytoplasmic localization of the serum- and glucocorticoid-inducible protein kinase, Sgk, in mammary tumor cells. A novel convergence point of anti-proliferative and proliferative cell signaling pathways. J Biol Chem 274(11): 7253-7263.

Busjahn, A., Aydin, A., Uhlmann, R., Krasko, C., Bahring, S., Szelestei, T., Feng, Y., Dahm, S., Sharma, A.M., Luft, F.C., and Lang, F. 2002. Serum- and glucocorticoid-regulated kinase (SGK1) gene and blood pressure. Hypertension 40(3): 256-260.

Busjahn, A. and Luft, F.C. 2003. Twin studies in the analysis of minor physiological differences between individuals. Cell Physiol Biochem 13(1): 51-58.

Byfield, M.P., Murray, J.T., and Backer, J.M. 2005. hVps34 is a nutrient-regulated lipid kinase required for activation of p70 S6 kinase. J Biol Chem 280(38): 33076-33082.

Cao, L., Graue-Hernandez, E.O., Tran, V., Reid, B., Pu, J., Mannis, M.J., and Zhao, M. 2011. Down-Regulation of PTEN at Corneal Wound Sites Accelerates Wound Healing Through Increased Cell Migration. Invest Ophthalmol Vis Sci.

Carpten, J.D., Faber, A.L., Horn, C., Donoho, G.P., Briggs, S.L., Robbins, C.M., Hostetter, G., Boguslawski, S., Moses, T.Y., Savage, S., Uhlik, M., Lin, A., Du, J., Qian, Y.W., Zeckner, D.J., Tucker-Kellogg, G., Touchman, J., Patel, K., Mousses, S., Bittner, M., Schevitz, R., Lai, M.H., Blanchard, K.L., and Thomas, J.E. 2007. A transforming mutation in the pleckstrin homology domain of AKT1 in cancer. Nature 448(7152): 439-444.

Casci, T., Vinos, J., and Freeman, M. 1999. Sprouty, an intracellular inhibitor of Ras signaling. Cell 96(5): 655-665.

Chan, J.C., Hannan, K.M., Riddell, K., Ng, P.Y., Peck, A., Lee, R.S., Hung, S., Astle, M.V., Bywater, M., Wall, M., Poortinga, G., Jastrzebski, K., Sheppard, K.E., Hemmings, B.A., Hall, M.N., Johnstone, R.W., McArthur, G.A., Hannan, R.D., and Pearson, R.B. 2011. AKT promotes rRNA synthesis and cooperates with c-MYC to stimulate ribosome biogenesis in cancer. Sci Signal 4(188): ra56.

Chang, F., Lee, J.T., Navolanic, P.M., Steelman, L.S., Shelton, J.G., Blalock, W.L., Franklin, R.A., and McCubrey, J.A. 2003. Involvement of PI3K/Akt pathway in cell cycle progression, apoptosis, and neoplastic transformation: a target for cancer chemotherapy. Leukemia 17(3): 590-603.

Chang, M.C., Chen, C.A., Hsieh, C.Y., Lee, C.N., Su, Y.N., Hu, Y.H., and Cheng, W.F. 2009. Mesothelin inhibits paclitaxel-induced apoptosis through the PI3K pathway. Biochem J 424(3): 449-458.

Chang, X.Z., Li, D.Q., Hou, Y.F., Wu, J., Lu, J.S., Di, G.H., Jin, W., Ou, Z.L., Shen, Z.Z., and Shao, Z.M. 2008. Identification of the functional role of AF1Q in the progression of breast cancer. Breast Cancer Res Treat 111(1): 65-78.

Chen, H.C. 2005. Boyden chamber assay. Methods Mol Biol 294: 15-22.

Chen, S.Y., Bhargava, A., Mastroberardino, L., Meijer, O.C., Wang, J., Buse, P., Firestone, G.L., Verrey, F., and Pearce, D. 1999. Epithelial sodium channel regulated by aldosterone-induced protein sgk. Proc Natl Acad Sci U S A 96(5): 2514-2519.

Cheng, J., Wang, Y., Ma, Y., Chan, B.T., Yang, M., Liang, A., Zhang, L., Li, H., and Du, J. 2010. The mechanical stress-activated serum-, glucocorticoid-regulated kinase 1 contributes to neointima formation in vein grafts. Circ Res 107(10): 1265-1274.

Cheng, J.Q., Lindsley, C.W., Cheng, G.Z., Yang, H., and Nicosia, S.V. 2005. The Akt/PKB pathway: molecular target for cancer drug discovery. Oncogene 24(50): 7482-7492.

Chianale, F., Rainero, E., Cianflone, C., Bettio, V., Pighini, A., Porporato, P.E., Filigheddu, N., Serini, G., Sinigaglia, F., Baldanzi, G., and Graziani, A. 2010. Diacylglycerol kinase alpha mediates HGF-induced Rac activation and membrane ruffling by regulating atypical PKC and RhoGDI. Proc Natl Acad Sci U S A 107(9): 4182-4187.

Cho, H., Mu, J., Kim, J.K., Thorvaldsen, J.L., Chu, Q., Crenshaw, E.B., 3rd, Kaestner, K.H., Bartolomei, M.S., Shulman, G.I., and Birnbaum, M.J. 2001a. Insulin resistance and a diabetes mellitus-like syndrome in mice lacking the protein kinase Akt2 (PKB beta). Science 292(5522): 1728-1731.

Cho, H., Thorvaldsen, J.L., Chu, Q., Feng, F., and Birnbaum, M.J. 2001b. Akt1/PKBalpha is required for normal growth but dispensable for maintenance of glucose homeostasis in mice. J Biol Chem 276(42): 38349-38352.

Chomczynski, P. and Sacchi, N. 1987. Single-step method of RNA isolation by acid guanidinium thiocyanate-phenol-chloroform extraction. Anal Biochem 162(1): 156-159.

Chong, H., Vikis, H.G., and Guan, K.L. 2003. Mechanisms of regulating the Raf kinase family. Cell Signal 15(5): 463-469.

Chu, S., Rushdi, S., Zumpe, E.T., Mamers, P., Healy, D.L., Jobling, T., Burger, H.G., and Fuller, P.J. 2002. FSH-regulated gene expression profiles in ovarian tumours and normal ovaries. Mol Hum Reprod 8(5): 426-433.

Chun, J., Kwon, T., Kim, D.J., Park, I., Chung, G., Lee, E.J., Hong, S.K., Chang, S.I., Kim, H.Y., and Kang, S.S. 2003. Inhibition of mitogen-activated kinase kinase kinase 3 activity through phosphorylation by the serum- and glucocorticoid-induced kinase 1. J Biochem 133(1): 103-108.

Chun, J., Kwon, T., Lee, E., Suh, P.G., Choi, E.J., and Sun Kang, S. 2002. The Na(+)/H(+) exchanger regulatory factor 2 mediates phosphorylation of serum- and glucocorticoid-induced protein kinase 1 by 3-phosphoinositide-dependent protein kinase 1. Biochem Biophys Res Commun 298(2): 207-215.

Chun, J., Kwon, T., Lee, E.J., Kim, C.H., Han, Y.S., Hong, S.K., Hyun, S., and Kang, S.S. 2004. 14-3-3 Protein mediates phosphorylation of microtubule-associated protein tau by serum- and glucocorticoid-induced protein kinase 1. Mol Cells 18(3): 360-368.

Chung, E.J., Sung, Y.K., Farooq, M., Kim, Y., Im, S., Tak, W.Y., Hwang, Y.J., Kim, Y.I., Han, H.S., Kim, J.C., and Kim, M.K. 2002. Gene expression profile analysis in human hepatocellular carcinoma by cDNA microarray. Mol Cells 14(3): 382-387.

Collins, B.J., Deak, M., Arthur, J.S., Armit, L.J., and Alessi, D.R. 2003. In vivo role of the PIF-binding docking site of PDK1 defined by knock-in mutation. Embo J 22(16): 4202-4211.

Collins, B.J., Deak, M., Murray-Tait, V., Storey, K.G., and Alessi, D.R. 2005. In vivo role of the phosphate groove of PDK1 defined by knockin mutation. J Cell Sci 118(Pt 21): 5023-5034.

Conti, B., Maier, R., Barr, A.M., Morale, M.C., Lu, X., Sanna, P.P., Bilbe, G., Hoyer, D., and Bartfai, T. 2007. Region-specific transcriptional changes following the three antidepressant treatments electro convulsive therapy, sleep deprivation and fluoxetine. Mol Psychiatry 12(2): 167-189.

Cordas, E., Naray-Fejes-Toth, A., and Fejes-Toth, G. 2007. Subcellular location of serum- and glucocorticoid-induced kinase-1 in renal and mammary epithelial cells. Am J Physiol Cell Physiol 292(5): C1971-1981.

Corradetti, M.N. and Guan, K.L. 2006. Upstream of the mammalian target of rapamycin: do all roads pass through mTOR? Oncogene 25(48): 6347-6360.

Cowling, R.T. and Birnboim, H.C. 2000. Expression of serum- and glucocorticoid-regulated kinase (sgk) mRNA is up-regulated by GM-CSF and other proinflammatory mediators in human granulocytes. J Leukoc Biol 67(2): 240-248.

Dai, F., Yu, L., He, H., Chen, Y., Yu, J., Yang, Y., Xu, Y., Ling, W., and Zhao, S. 2002. Human serum and glucocorticoid-inducible kinase-like kinase (SGKL) phosphorylates glycogen syntheses kinase 3 beta (GSK-3beta) at serine-9 through direct interaction. Biochem Biophys Res Commun 293(4): 1191-1196.

Dai, F., Yu, L., He, H., Zhao, Y., Yang, J., Zhang, X., and Zhao, S. 1999. Cloning and mapping of a novel human serum/glucocorticoid regulated kinase-like gene, SGKL, to chromosome 8q12.3-q13.1. Genomics 62(1): 95-97.

Dai, M.S. and Lu, H. 2008. Crosstalk between c-Myc and ribosome in ribosomal

biogenesis and cancer. J Cell Biochem 105(3): 670-677.

Debonneville, C., Flores, S.Y., Kamynina, E., Plant, P.J., Tauxe, C., Thomas, M.A., Munster, C., Chraibi, A., Pratt, J.H., Horisberger, J.D., Pearce, D., Loffing, J., and Staub, O. 2001. Phosphorylation of Nedd4-2 by Sgk1 regulates epithelial Na(+) channel cell surface expression. Embo J 20(24): 7052-7059.

Dehner, M., Hadjihannas, M., Weiske, J., Huber, O., and Behrens, J. 2008. Wnt signaling inhibits Forkhead box O3a-induced transcription and apoptosis through up-regulation of serum- and glucocorticoid-inducible kinase 1. J Biol Chem 283(28): 19201-19210.

Diakov, A. and Korbmacher, C. 2004. A novel pathway of epithelial sodium channel activation involves a serum- and glucocorticoid-inducible kinase consensus motif in the C terminus of the channel's alpha-subunit. J Biol Chem 279(37): 38134-38142.

Dieter, M., Palmada, M., Rajamanickam, J., Aydin, A., Busjahn, A., Boehmer, C., Luft, F.C., and Lang, F. 2004. Regulation of glucose transporter SGLT1 by ubiquitin ligase Nedd4-2 and kinases SGK1, SGK3, and PKB. Obes Res 12(5): 862-870.

Do Carmo, S., Fournier, D., Mounier, C., and Rassart, E. 2009. Human apolipoprotein D overexpression in transgenic mice induces insulin resistance and alters lipid metabolism. Am J Physiol Endocrinol Metab 296(4): E802-811.

Dolznig, H., Grebien, F., Sauer, T., Beug, H., and Mullner, E.W. 2004. Evidence for a size-sensing mechanism in animal cells. Nat Cell Biol 6(9): 899-905.

Dorsey, J.F., Dowling, M.L., Kim, M., Voong, R., Solin, L.J., and Kao, G.D. 2010. Modulation of the anti-cancer efficacy of microtubule-targeting agents by cellular growth conditions. Cancer Biol Ther 9(10): 809-818.

Dow, L.E., Elsum, I.A., King, C.L., Kinross, K.M., Richardson, H.E., and Humbert, P.O. 2008. Loss of human Scribble cooperates with H-Ras to promote cell invasion through deregulation of MAPK signalling. Oncogene 27(46): 5988-6001.

Easton, R.M., Cho, H., Roovers, K., Shineman, D.W., Mizrahi, M., Forman, M.S., Lee, V.M., Szabolcs, M., de Jong, R., Oltersdorf, T., Ludwig, T., Efstratiadis, A., and Birnbaum, M.J. 2005. Role for Akt3/protein kinase Bgamma in attainment of normal brain size. Mol Cell Biol 25(5): 1869-1878.

Elenbaas, B., Spirio, L., Koerner, F., Fleming, M.D., Zimonjic, D.B., Donaher, J.L., Popescu, N.C., Hahn, W.C., and Weinberg, R.A. 2001. Human breast cancer cells generated by oncogenic transformation of primary mammary epithelial cells. Genes Dev 15(1): 50-65.

Ellisen, L.W. 2005. Growth control under stress: mTOR regulation through the REDD1-TSC pathway. Cell Cycle 4(11): 1500-1502.

Ellson, C.D., Andrews, S., Stephens, L.R., and Hawkins, P.T. 2002. The PX domain: a

new phosphoinositide-binding module. J Cell Sci 115(Pt 6): 1099-1105.

Embark, H.M., Bohmer, C., Palmada, M., Rajamanickam, J., Wyatt, A.W., Wallisch, S., Capasso, G., Waldegger, P., Seyberth, H.W., Waldegger, S., and Lang, F. 2004a. Regulation of CLC-Ka/barttin by the ubiquitin ligase Nedd4-2 and the serum- and glucocorticoid-dependent kinases. Kidney Int 66(5): 1918-1925.

Embark, H.M., Bohmer, C., Vallon, V., Luft, F., and Lang, F. 2003. Regulation of KCNE1-dependent K(+) current by the serum and glucocorticoid-inducible kinase (SGK) isoforms. Pflugers Arch 445(5): 601-606.

Embark, H.M., Setiawan, I., Poppendieck, S., van de Graaf, S.F., Boehmer, C., Palmada, M., Wieder, T., Gerstberger, R., Cohen, P., Yun, C.C., Bindels, R.J., and Lang, F. 2004b. Regulation of the epithelial Ca2+ channel TRPV5 by the NHE regulating factor NHERF2 and the serum and glucocorticoid inducible kinase isoforms SGK1 and SGK3 expressed in Xenopus oocytes. Cell Physiol Biochem 14(4-6): 203-212.

Endo, T., Kusakabe, M., Sunadome, K., Yamamoto, T., and Nishida, E. 2011. The kinase SGK1 in the endoderm and mesoderm promotes ectodermal survival by down-regulating components of the death-inducing signaling complex. Sci Signal 4(156): ra2.

Engelman, J.A., Luo, J., and Cantley, L.C. 2006. The evolution of phosphatidylinositol 3-kinases as regulators of growth and metabolism. Nat Rev Genet 7(8): 606-619.

Engelsberg, A., Kobelt, F., and Kuhl, D. 2006. The N-terminus of the serum- and glucocorticoid-inducible kinase Sgk1 specifies mitochondrial localization and rapid turnover. Biochem J 399(1): 69-76.

Enomoto, A., Murakami, H., Asai, N., Morone, N., Watanabe, T., Kawai, K., Murakumo, Y., Usukura, J., Kaibuchi, K., and Takahashi, M. 2005. Akt/PKB regulates actin organization and cell motility via Girdin/APE. Dev Cell 9(3): 389-402.

Eylenstein, A., Gehring, E.M., Heise, N., Shumilina, E., Schmidt, S., Szteyn, K., Munzer, P., Nurbaeva, M.K., Eichenmuller, M., Tyan, L., Regel, I., Foller, M., Kuhl, D., Soboloff, J., Penner, R., and Lang, F. 2011. Stimulation of Ca2+-channel Orai1/STIM1 by serum- and glucocorticoid-inducible kinase 1 (SGK1). Faseb J 25(6): 2012-2021.

Failor, K.L., Desyatnikov, Y., Finger, L.A., and Firestone, G.L. 2007. Glucocorticoid-induced degradation of glycogen synthase kinase-3 protein is triggered by serum- and glucocorticoid-induced protein kinase and Akt signaling and controls beta-catenin dynamics and tight junction formation in mammary epithelial tumor cells. Mol Endocrinol 21(10): 2403-2415.

Fakitsas, P., Adam, G., Daidie, D., van Bemmelen, M.X., Fouladkou, F., Patrignani, A., Wagner, U., Warth, R., Camargo, S.M., Staub, O., and Verrey, F. 2007. Early aldosterone-induced gene product regulates the epithelial sodium channel by deubiquitylation. J Am Soc Nephrol 18(4): 1084-1092.

Fang, X., Gaudette, D., Furui, T., Mao, M., Estrella, V., Eder, A., Pustilnik, T., Sasagawa, T., Lapushin, R., Yu, S., Jaffe, R.B., Wiener, J.R., Erickson, J.R., and Mills, G.B. 2000. Lysophospholipid growth factors in the initiation, progression, metastases, and management of ovarian cancer. Ann N Y Acad Sci 905: 188-208.

Fang, X., Schummer, M., Mao, M., Yu, S., Tabassam, F.H., Swaby, R., Hasegawa, Y., Tanyi, J.L., LaPushin, R., Eder, A., Jaffe, R., Erickson, J., and Mills, G.B. 2002. Lysophosphatidic acid is a bioactive mediator in ovarian cancer. Biochim Biophys Acta 1582(1-3): 257-264.

Fantes, P.A. 1977. Control of cell size and cycle time in Schizosaccharomyces pombe. J Cell Sci 24: 51-67.

Faroqui, S., Sheriff, S., and Amlal, H. 2006. Metabolic acidosis has dual effects on sodium handling by rat kidney. Am J Physiol Renal Physiol 291(2): F322-331.

Feroze-Zaidi, F., Fusi, L., Takano, M., Higham, J., Salker, M.S., Goto, T., Edassery, S., Klingel, K., Boini, K.M., Palmada, M., Kamps, R., Groothuis, P.G., Lam, E.W., Smith, S.K., Lang, F., Sharkey, A.M., and Brosens, J.J. 2007. Role and regulation of the serum- and glucocorticoid-regulated kinase 1 in fertile and infertile human endometrium. Endocrinology 148(10): 5020-5029.

Fillon, S., Klingel, K., Warntges, S., Sauter, M., Gabrysch, S., Pestel, S., Tanneur, V., Waldegger, S., Zipfel, A., Viebahn, R., Haussinger, D., Broer, S., Kandolf, R., and Lang, F. 2002. Expression of the serine/threonine kinase hSGK1 in chronic viral hepatitis. Cell Physiol Biochem 12(1): 47-54.

Fillon, S., Warntges, S., Matskevitch, J., Moschen, I., Setiawan, I., Gamper, N., Feng, Y.X., Stegen, C., Friedrich, B., Waldegger, S., Broer, S., Wagner, C.A., Huber, S.M., Klingel, K., Vereninov, A., and Lang, F. 2001. Serum- and glucocorticoid-dependent kinase, cell volume, and the regulation of epithelial transport. Comp Biochem Physiol A Mol Integr Physiol 130(3): 367-376.

Fingar, D.C., Richardson, C.J., Tee, A.R., Cheatham, L., Tsou, C., and Blenis, J. 2004. mTOR controls cell cycle progression through its cell growth effectors S6K1 and 4E-BP1/eukaryotic translation initiation factor 4E. Mol Cell Biol 24(1): 200-216.

Fingar, D.C., Salama, S., Tsou, C., Harlow, E., and Blenis, J. 2002. Mammalian cell size is controlled by mTOR and its downstream targets S6K1 and 4EBP1/eIF4E. Genes Dev 16(12): 1472-1487.

Firestone, G.L., Giampaolo, J.R., and O'Keeffe, B.A. 2003. Stimulus-dependent regulation of serum and glucocorticoid inducible protein kinase (SGK) transcription, subcellular localization and enzymatic activity. Cell Physiol Biochem 13(1): 1-12.

Flores, S.Y., Debonneville, C., and Staub, O. 2003. The role of Nedd4/Nedd4-like dependant ubiquitylation in epithelial transport processes. Pflugers Arch 446(3): 334-338.

Foster, K.G. and Fingar, D.C. 2010. Mammalian target of rapamycin (mTOR): conducting the cellular signaling symphony. J Biol Chem 285(19): 14071-14077.

Frank, M.J., Dawson, D.W., Bensinger, S.J., Hong, J.S., Knosp, W.M., Xu, L., Balatoni, C.E., Allen, E.L., Shen, R.R., Bar-Sagi, D., Martin, G.R., and Teitell, M.A. 2009. Expression of sprouty2 inhibits B-cell proliferation and is epigenetically silenced in mouse and human B-cell lymphomas. Blood 113(11): 2478-2487.

Freeburg, E.M., Goyeneche, A.A., Seidel, E.E., and Telleria, C.M. 2009. Resistance to cisplatin does not affect sensitivity of human ovarian cancer cell lines to mifepristone cytotoxicity. Cancer Cell Int 9: 4.

Frodin, M., Antal, T.L., Dummler, B.A., Jensen, C.J., Deak, M., Gammeltoft, S., and Biondi, R.M. 2002. A phosphoserine/threonine-binding pocket in AGC kinases and PDK1 mediates activation by hydrophobic motif phosphorylation. Embo J 21(20): 5396-5407.

Fruman, D.A. 2010. Regulatory subunits of class IA PI3K. Curr Top Microbiol Immunol 346: 225-244.

Gaertner, R.F., Wyss-Coray, T., Von Euw, D., Lesne, S., Vivien, D., and Lacombe, P. 2005. Reduced brain tissue perfusion in TGF-beta 1 transgenic mice showing Alzheimer's disease-like cerebrovascular abnormalities. Neurobiol Dis 19(1-2): 38-46.

Gamper, N., Fillon, S., Feng, Y., Friedrich, B., Lang, P.A., Henke, G., Huber, S.M., Kobayashi, T., Cohen, P., and Lang, F. 2002a. K+ channel activation by all three isoforms of serum- and glucocorticoid-dependent protein kinase SGK. Pflugers Arch 445(1): 60-66.

Gamper, N., Fillon, S., Huber, S.M., Feng, Y., Kobayashi, T., Cohen, P., and Lang, F. 2002b. IGF-1 up-regulates K+ channels via PI3-kinase, PDK1 and SGK1. Pflugers Arch 443(4): 625-634.

Gangloff, Y.G., Mueller, M., Dann, S.G., Svoboda, P., Sticker, M., Spetz, J.F., Um, S.H., Brown, E.J., Cereghini, S., Thomas, G., and Kozma, S.C. 2004. Disruption of the mouse mTOR gene leads to early postimplantation lethality and prohibits embryonic stem cell development. Mol Cell Biol 24(21): 9508-9516.

Gao, D., Wan, L., Inuzuka, H., Berg, A.H., Tseng, A., Zhai, B., Shaik, S., Bennett, E., Tron, A.E., Gasser, J.A., Lau, A., Gygi, S.P., Harper, J.W., DeCaprio, J.A., Toker, A., and Wei, W. 2010a. Rictor forms a complex with Cullin-1 to promote SGK1 ubiquitination and destruction. Mol Cell 39(5): 797-808.

Gao, D., Wan, L., and Wei, W. 2010b. Phosphorylation of Rictor at Thr1135 impairs the Rictor/Cullin-1 complex to ubiquitinate SGK1. Protein Cell 1(10): 881-885.

Gao, X., Lowry, P.R., Zhou, X., Depry, C., Wei, Z., Wong, G.W., and Zhang, J. 2011. PI3K/Akt signaling requires spatial compartmentalization in plasma membrane microdomains. Proc Natl Acad Sci U S A 108(35): 14509-14514.

Garcia-Martinez, J.M. and Alessi, D.R. 2008. mTOR complex 2 (mTORC2) controls hydrophobic motif phosphorylation and activation of serum- and glucocorticoid-induced protein kinase 1 (SGK1). Biochem J 416(3): 375-385.

Gassmann, P., Haier, J., Schluter, K., Domikowsky, B., Wendel, C., Wiesner, U., Kubitza, R., Engers, R., Schneider, S.W., Homey, B., and Muller, A. 2009. CXCR4 regulates the early extravasation of metastatic tumor cells in vivo. Neoplasia 11(7): 651-661.

Gautier, L., Cope, L., Bolstad, B.M., and Irizarry, R.A. 2004. affy--analysis of Affymetrix GeneChip data at the probe level. Bioinformatics 20(3): 307-315.

Gendaszewska-Darmach, E. 2008. Lysophosphatidic acids, cyclic phosphatidic acids and autotaxin as promising targets in therapies of cancer and other diseases. Acta Biochim Pol 55(2): 227-240.

Gentleman, R.C., Carey, V.J., Bates, D.M., Bolstad, B., Dettling, M., Dudoit, S., Ellis, B., Gautier, L., Ge, Y., Gentry, J., Hornik, K., Hothorn, T., Huber, W., Iacus, S., Irizarry, R., Leisch, F., Li, C., Maechler, M., Rossini, A.J., Sawitzki, G., Smith, C., Smyth, G., Tierney, L., Yang, J.Y., and Zhang, J. 2004. Bioconductor: open software development for computational biology and bioinformatics. Genome Biol 5(10): R80.

Gillooly, D.J., Raiborg, C., and Stenmark, H. 2003. Phosphatidylinositol 3-phosphate is found in microdomains of early endosomes. Histochem Cell Biol 120(6): 445-453.

Gingras, A.C., Raught, B., and Sonenberg, N. 2001. Regulation of translation initiation by FRAP/mTOR. Genes Dev 15(7): 807-826.

Grahammer, F., Artunc, F., Sandulache, D., Rexhepaj, R., Friedrich, B., Risler, T., McCormick, J.A., Dawson, K., Wang, J., Pearce, D., Wulff, P., Kuhl, D., and Lang, F. 2006. Renal function of gene-targeted mice lacking both SGK1 and SGK3. Am J Physiol Regul Integr Comp Physiol 290(4): R945-950.

Grandori, C., Gomez-Roman, N., Felton-Edkins, Z.A., Ngouenet, C., Galloway, D.A., Eisenman, R.N., and White, R.J. 2005. c-Myc binds to human ribosomal DNA and stimulates transcription of rRNA genes by RNA polymerase I. Nat Cell Biol 7(3): 311-318.

Grewal, S.S., Li, L., Orian, A., Eisenman, R.N., and Edgar, B.A. 2005. Myc-dependent regulation of ribosomal RNA synthesis during Drosophila development. Nat Cell Biol 7(3): 295-302.

Guan, K.L., Figueroa, C., Brtva, T.R., Zhu, T., Taylor, J., Barber, T.D., and Vojtek, A.B. 2000. Negative regulation of the serine/threonine kinase B-Raf by Akt. J Biol Chem 275(35): 27354-27359.

Guertin, D.A. and Sabatini, D.M. 2005. An expanding role for mTOR in cancer. Trends Mol Med 11(8): 353-361.

Gulati, P., Gaspers, L.D., Dann, S.G., Joaquin, M., Nobukuni, T., Natt, F., Kozma, S.C., Thomas, A.P., and Thomas, G. 2008. Amino acids activate mTOR complex 1 via Ca2+/CaM signaling to hVps34. Cell Metab 7(5): 456-465.

Gusella, J.F. and MacDonald, M.E. 2000. Molecular genetics: unmasking polyglutamine triggers in neurodegenerative disease. Nat Rev Neurosci 1(2): 109-115.

Gymnopoulos, M., Elsliger, M.A., and Vogt, P.K. 2007. Rare cancer-specific mutations in PIK3CA show gain of function. Proc Natl Acad Sci U S A 104(13): 5569-5574.

Hacohen, N., Kramer, S., Sutherland, D., Hiromi, Y., and Krasnow, M.A. 1998. sprouty encodes a novel antagonist of FGF signaling that patterns apical branching of the Drosophila airways. Cell 92(2): 253-263.

Hahn, W.C., Counter, C.M., Lundberg, A.S., Beijersbergen, R.L., Brooks, M.W., and Weinberg, R.A. 1999. Creation of human tumour cells with defined genetic elements. Nature 400(6743): 464-468.

Haldar, S., Basu, A., and Croce, C.M. 1997. Bcl2 is the guardian of microtubule integrity. Cancer Res 57(2): 229-233.

Hama, K. and Aoki, J. 2010. LPA(3), a unique G protein-coupled receptor for lysophosphatidic acid. Prog Lipid Res 49(4): 335-342.

Hanahan, D. and Weinberg, R.A. 2000. The hallmarks of cancer. Cell 100(1): 57-70.

Hanahan, D. and Weinberg, R.A. 2011. Hallmarks of cancer: the next generation. Cell 144(5): 646-674.

Hanks, S.K., Ryzhova, L., Shin, N.Y., and Brabek, J. 2003. Focal adhesion kinase signaling activities and their implications in the control of cell survival and motility. Front Biosci 8: d982-996.

Hannan, K.M., Brandenburger, Y., Jenkins, A., Sharkey, K., Cavanaugh, A., Rothblum, L., Moss, T., Poortinga, G., McArthur, G.A., Pearson, R.B., and Hannan, R.D. 2003. mTOR-dependent regulation of ribosomal gene transcription requires S6K1 and is mediated by phosphorylation of the carboxy-terminal activation domain of the nucleolar transcription factor UBF. Mol Cell Biol 23(23): 8862-8877.

Hartmann, W., Kuchler, J., Koch, A., Friedrichs, N., Waha, A., Endl, E., Czerwitzki, J., Metzger, D., Steiner, S., Wurst, P., Leuschner, I., von Schweinitz, D., Buettner, R., and Pietsch, T. 2009. Activation of phosphatidylinositol-3'-kinase/AKT signaling is essential in hepatoblastoma survival. Clin Cancer Res 15(14): 4538-4545.

Haruta, T., Uno, T., Kawahara, J., Takano, A., Egawa, K., Sharma, P.M., Olefsky, J.M., and Kobayashi, M. 2000. A rapamycin-sensitive pathway down-regulates insulin signaling via phosphorylation and proteasomal degradation of insulin receptor substrate-1. Mol Endocrinol 14(6): 783-794.

Haslam, R.J., Koide, H.B., and Hemmings, B.A. 1993. Pleckstrin domain homology. Nature 363(6427): 309-310.

Hay, N. 2005. The Akt-mTOR tango and its relevance to cancer. Cancer Cell 8(3): 179-183.

Hay, N. and Sonenberg, N. 2004. Upstream and downstream of mTOR. Genes Dev 18(16): 1926-1945.

Hayashi, M., Tapping, R.I., Chao, T.H., Lo, J.F., King, C.C., Yang, Y., and Lee, J.D. 2001. BMK1 mediates growth factor-induced cell proliferation through direct cellular activation of serum and glucocorticoid-inducible kinase. J Biol Chem 276(12): 8631-8634.

He, P., Lee, S.J., Lin, S., Seidler, U., Lang, F., Fejes-Toth, G., Naray-Fejes-Toth, A., and Yun, C.C. 2011. Serum- and glucocorticoid-induced kinase 3 in recycling endosomes mediates acute activation of Na+/H+ exchanger NHE3 by glucocorticoids. Mol Biol Cell 22(20): 3812-3825.

Heise, C.J., Xu, B.E., Deaton, S.L., Cha, S.K., Cheng, C.J., Earnest, S., Sengupta, S., Juang, Y.C., Stippec, S., Xu, Y., Zhao, Y., Huang, C.L., and Cobb, M.H. 2010. Serum and glucocorticoid-induced kinase (SGK) 1 and the epithelial sodium channel are regulated by multiple with no lysine (WNK) family members. J Biol Chem 285(33): 25161-25167.

Henke, G., Maier, G., Wallisch, S., Boehmer, C., and Lang, F. 2004. Regulation of the voltage gated K+ channel Kv1.3 by the ubiquitin ligase Nedd4-2 and the serum and glucocorticoid inducible kinase SGK1. J Cell Physiol 199(2): 194-199.

Hennessy, B.T., Smith, D.L., Ram, P.T., Lu, Y., and Mills, G.B. 2005. Exploiting the PI3K/AKT pathway for cancer drug discovery. Nat Rev Drug Discov 4(12): 988-1004.

Hietakangas, V. and Cohen, S.M. 2008. TOR complex 2 is needed for cell cycle progression and anchorage-independent growth of MCF7 and PC3 tumor cells. BMC Cancer 8: 282.

Higuchi, M., Masuyama, N., Fukui, Y., Suzuki, A., and Gotoh, Y. 2001. Akt mediates Rac/Cdc42-regulated cell motility in growth factor-stimulated cells and in invasive PTEN knockout cells. Curr Biol 11(24): 1958-1962.

Ho, K.K., Myatt, S.S., and Lam, E.W. 2008. Many forks in the path: cycling with FoxO. Oncogene 27(16): 2300-2311.

Holford, J., Rogers, P., and Kelland, L.R. 1998. ras mutation and platinum resistance in human ovarian carcinomas in vitro. Int J Cancer 77(1): 94-100.

Hong, F., Larrea, M.D., Doughty, C., Kwiatkowski, D.J., Squillace, R., and Slingerland, J.M. 2008. mTOR-raptor binds and activates SGK1 to regulate p27 phosphorylation. Mol Cell 30(6): 701-711.

Hu, L., Hofmann, J., Lu, Y., Mills, G.B., and Jaffe, R.B. 2002. Inhibition of phosphatidylinositol 3'-kinase increases efficacy of paclitaxel in in vitro and in vivo ovarian cancer models. Cancer Res 62(4): 1087-1092.

Hu, P., Margolis, B., Skolnik, E.Y., Lammers, R., Ullrich, A., and Schlessinger, J. 1992. Interaction of phosphatidylinositol 3-kinase-associated p85 with epidermal growth factor and platelet-derived growth factor receptors. Mol Cell Biol 12(3): 981-990.

Huang, D.Y., Wulff, P., Volkl, H., Loffing, J., Richter, K., Kuhl, D., Lang, F., and Vallon, V. 2004. Impaired regulation of renal K+ elimination in the sgk1-knockout mouse. J Am Soc Nephrol 15(4): 885-891.

Huang, W.C. and Hung, M.C. 2009. Induction of Akt activity by chemotherapy confers acquired resistance. J Formos Med Assoc 108(3): 180-194.

Humbert, S., Bryson, E.A., Cordelieres, F.P., Connors, N.C., Datta, S.R., Finkbeiner, S., Greenberg, M.E., and Saudou, F. 2002. The IGF-1/Akt pathway is neuroprotective in Huntington's disease and involves Huntingtin phosphorylation by Akt. Dev Cell 2(6): 831-837.

Iadevaia, V., Huo, Y., Zhang, Z., Foster, L.J., and Proud, C.G. 2012. Roles of the mammalian target of rapamycin, mTOR, in controlling ribosome biogenesis and protein synthesis. Biochem Soc Trans 40(1): 168-172.

Ilic, D., Almeida, E.A., Schlaepfer, D.D., Dazin, P., Aizawa, S., and Damsky, C.H. 1998. Extracellular matrix survival signals transduced by focal adhesion kinase suppress p53-mediated apoptosis. J Cell Biol 143(2): 547-560.

Imai, S., Okayama, N., Shimizu, M., and Itoh, M. 2003. Increased intracellular calcium activates serum and glucocorticoid-inducible kinase 1 (SGK1) through a calmodulin-calcium calmodulin dependent kinase kinase pathway in Chinese hamster ovary cells. Life Sci 72(20): 2199-2209.

Imaizumi, K., Tsuda, M., Wanaka, A., Tohyama, M., and Takagi, T. 1994. Differential expression of sgk mRNA, a member of the Ser/Thr protein kinase gene family, in rat brain after CNS injury. Brain Res Mol Brain Res 26(1-2): 189-196.

Ip, C.K., Cheung, A.N., Ngan, H.Y., and Wong, A.S. 2011. p70 S6 kinase in the control of actin cytoskeleton dynamics and directed migration of ovarian cancer cells. Oncogene.

Irizarry, R.A., Bolstad, B.M., Collin, F., Cope, L.M., Hobbs, B., and Speed, T.P. 2003. Summaries of Affymetrix GeneChip probe level data. Nucleic Acids Res 31(4): e15.

Isakoff, S.J., Engelman, J.A., Irie, H.Y., Luo, J., Brachmann, S.M., Pearline, R.V., Cantley, L.C., and Brugge, J.S. 2005. Breast cancer-associated PIK3CA mutations are oncogenic in mammary epithelial cells. Cancer Res 65(23): 10992-11000.

Ivanchuk, S.M. and Rutka, J.T. 2004. The cell cycle: accelerators, brakes, and checkpoints. Neurosurgery 54(3): 692-699; discussion 699-700.

Jacinto, E., Loewith, R., Schmidt, A., Lin, S., Ruegg, M.A., Hall, A., and Hall, M.N. 2004. Mammalian TOR complex 2 controls the actin cytoskeleton and is rapamycin insensitive. Nat Cell Biol 6(11): 1122-1128.

James, M.J. and Zomerdijk, J.C. 2004. Phosphatidylinositol 3-kinase and mTOR signaling pathways regulate RNA polymerase I transcription in response to IGF-1 and nutrients. J Biol Chem 279(10): 8911-8918.

Jefferies, H.B., Fumagalli, S., Dennis, P.B., Reinhard, C., Pearson, R.B., and Thomas, G. 1997. Rapamycin suppresses 5'TOP mRNA translation through inhibition of p70s6k. Embo J 16(12): 3693-3704.

Jeyaraj, S., Boehmer, C., Lang, F., and Palmada, M. 2007. Role of SGK1 kinase in regulating glucose transport via glucose transporter GLUT4. Biochem Biophys Res Commun 356(3): 629-635.

Johnston, G.C., Pringle, J.R., and Hartwell, L.H. 1977. Coordination of growth with cell division in the yeast Saccharomyces cerevisiae. Exp Cell Res 105(1): 79-98.

Jones, K.T., Greer, E.R., Pearce, D., and Ashrafi, K. 2009. Rictor/TORC2 regulates Caenorhabditis elegans fat storage, body size, and development through sgk-1. PLoS Biol 7(3): e60.

Jorgensen, P. and Tyers, M. 2004. How cells coordinate growth and division. Curr Biol 14(23): R1014-1027.

Jung, C.H., Ro, S.H., Cao, J., Otto, N.M., and Kim, D.H. 2010. mTOR regulation of autophagy. FEBS Lett 584(7): 1287-1295.

Kamynina, E. and Staub, O. 2002. Concerted action of ENaC, Nedd4-2, and Sgk1 in transepithelial Na(+) transport. Am J Physiol Renal Physiol 283(3): F377-387.

Kang, J.S. and Krauss, R.S. 1996. Ras induces anchorage-independent growth by subverting multiple adhesion-regulated cell cycle events. Mol Cell Biol 16(7): 3370-3380.

Katoh, M. 2005. WNT/PCP signaling pathway and human cancer (review). Oncol Rep 14(6): 1583-1588.

Katoh, Y. and Katoh, M. 2006. Comparative integromics on FAT1, FAT2, FAT3 and FAT4. Int J Mol Med 18(3): 523-528.

Kaur, S., Sassano, A., Dolniak, B., Joshi, S., Majchrzak-Kita, B., Baker, D.P., Hay, N., Fish, E.N., and Platanias, L.C. 2008a. Role of the Akt pathway in mRNA translation of interferon-stimulated genes. Proc Natl Acad Sci U S A 105(12):

4808-4813.

Kaur, S., Sassano, A., Joseph, A.M., Majchrzak-Kita, B., Eklund, E.A., Verma, A., Brachmann, S.M., Fish, E.N., and Platanias, L.C. 2008b. Dual regulatory roles of phosphatidylinositol 3-kinase in IFN signaling. J Immunol 181(10): 7316-7323.

Kim, M.J., Chae, J.S., Kim, K.J., Hwang, S.G., Yoon, K.W., Kim, E.K., Yun, H.J., Cho, J.H., Kim, J., Kim, B.W., Kim, H.C., Kang, S.S., Lang, F., Cho, S.G., and Choi, E.J. 2007. Negative regulation of SEK1 signaling by serum- and glucocorticoid-inducible protein kinase 1. Embo J 26(13): 3075-3085.

Kinross, K.M., Montgomery, K.G., Kleinschmidt, M., Waring, P., Ivetac, I., Tikoo, A., Saad, M., Hare, L., Roh, V., Mantamadiotis, T., Sheppard, K.E., Ryland, G.L., Campbell, I.G., Gorringe, K.L., Christensen, J.G., Cullinane, C., Hicks, R.J., Pearson, R.B., Johnstone, R.W., McArthur, G.A., and Phillips, W.A. 2012. An activating Pik3ca mutation coupled with Pten loss is sufficient to initiate ovarian tumorigenesis in mice. J Clin Invest.

Klaus, F., Palmada, M., Lindner, R., Laufer, J., Jeyaraj, S., Lang, F., and Boehmer, C. 2008. Up-regulation of hypertonicity-activated myo-inositol transporter SMIT1 by the cell volume-sensitive protein kinase SGK1. J Physiol 586(6): 1539-1547.

Klingel, K., Warntges, S., Bock, J., Wagner, C.A., Sauter, M., Waldegger, S., Kandolf, R., and Lang, F. 2000. Expression of cell volume-regulated kinase h-sgk in pancreatic tissue. Am J Physiol Gastrointest Liver Physiol 279(5): G998-G1002.

Kobayashi, T. and Cohen, P. 1999. Activation of serum- and glucocorticoid-regulated protein kinase by agonists that activate phosphatidylinositide 3-kinase is mediated by 3-phosphoinositide-dependent protein kinase-1 (PDK1) and PDK2. Biochem J 339 (Pt 2): 319-328.

Kobayashi, T., Deak, M., Morrice, N., and Cohen, P. 1999. Characterization of the structure and regulation of two novel isoforms of serum- and glucocorticoid-induced protein kinase. Biochem J 344 Pt 1: 189-197.

Kops, G.J., de Ruiter, N.D., De Vries-Smits, A.M., Powell, D.R., Bos, J.L., and Burgering, B.M. 1999. Direct control of the Forkhead transcription factor AFX by protein kinase B. Nature 398(6728): 630-634.

Kozma, S.C. and Thomas, G. 2002. Regulation of cell size in growth, development and human disease: PI3K, PKB and S6K. Bioessays 24(1): 65-71.

Krasil'nikov, M.A., Shatskaya, V.A., Stavrovskaya, A.A., Erohina, M., Gershtein, E.S., and Adler, V.V. 1999. The role of phosphatidylinositol 3-kinase in the regulation of cell response to steroid hormones. Biochim Biophys Acta 1450(3): 434-443.

Krystal, G.W., Sulanke, G., and Litz, J. 2002. Inhibition of phosphatidylinositol 3-kinase-

Akt signaling blocks growth, promotes apoptosis, and enhances sensitivity of small cell lung cancer cells to chemotherapy. Mol Cancer Ther 1(11): 913-922.

Kumari, S., Liu, X., Nguyen, T., Zhang, X., and D'Mello, S.R. 2001. Distinct phosphorylation patterns underlie Akt activation by different survival factors in neurons. Brain Res Mol Brain Res 96(1-2): 157-162.

Landreville, S., Agapova, O.A., Matatall, K.A., Kneass, Z.T., Onken, M.D., Lee, R.S., Bowcock, A.M., and Harbour, J.W. 2012. Histone deacetylase inhibitors induce growth arrest and differentiation in uveal melanoma. Clin Cancer Res.

Lang, F., Bohmer, C., Palmada, M., Seebohm, G., Strutz-Seebohm, N., and Vallon, V. 2006a. (Patho)physiological significance of the serum- and glucocorticoid-inducible kinase isoforms. Physiol Rev 86(4): 1151-1178.

Lang, F., Busch, G.L., Ritter, M., Volkl, H., Waldegger, S., Gulbins, E., and Haussinger, D. 1998. Functional significance of cell volume regulatory mechanisms. Physiol Rev 78(1): 247-306.

Lang, F. and Cohen, P. 2001. Regulation and physiological roles of serum- and glucocorticoid-induced protein kinase isoforms. Sci STKE 2001(108): RE17.

Lang, F., Gorlach, A., and Vallon, V. 2009. Targeting SGK1 in diabetes. Expert Opin Ther Targets 13(11): 1303-1311.

Lang, U.E., Wolfer, D.P., Grahammer, F., Strutz-Seebohm, N., Seebohm, G., Lipp, H.P., McCormick, J.A., Hellweg, R., Dawson, K., Wang, J., Pearce, D., and Lang, F. 2006b. Reduced locomotion in the serum and glucocorticoid inducible kinase 3 knock out mouse. Behav Brain Res 167(1): 75-86.

Lapteva, N., Yang, A.G., Sanders, D.E., Strube, R.W., and Chen, S.Y. 2005. CXCR4 knockdown by small interfering RNA abrogates breast tumor growth in vivo. Cancer Gene Ther 12(1): 84-89.

Lauring, J., Cosgrove, D.P., Fontana, S., Gustin, J.P., Konishi, H., Abukhdeir, A.M., Garay, J.P., Mohseni, M., Wang, G.M., Higgins, M.J., Gorkin, D., Reis, M., Vogelstein, B., Polyak, K., Cowherd, M., Buckhaults, P.J., and Park, B.H. 2010. Knock in of the AKT1 E17K mutation in human breast epithelial cells does not recapitulate oncogenic PIK3CA mutations. Oncogene 29(16): 2337-2345.

Lazarov, M., Kubo, Y., Cai, T., Dajee, M., Tarutani, M., Lin, Q., Fang, M., Tao, S., Green, C.L., and Khavari, P.A. 2002. CDK4 coexpression with Ras generates malignant human epidermal tumorigenesis. Nat Med 8(10): 1105-1114.

Lee, C.C., Putnam, A.J., Miranti, C.K., Gustafson, M., Wang, L.M., Vande Woude, G.F., and Gao, C.F. 2004. Overexpression of sprouty 2 inhibits HGF/SF-mediated cell growth, invasion, migration, and cytokinesis. Oncogene 23(30): 5193-5202.

Lee, C.T., Tyan, S.W., Ma, Y.L., Tsai, M.C., Yang, Y.C., and Lee, E.H. 2006. Serum- and

glucocorticoid-inducible kinase (SGK) is a target of the MAPK/ERK signaling pathway that mediates memory formation in rats. Eur J Neurosci 23(5): 1311-1320.

Lee, E.H., Hsu, W.L., Ma, Y.L., Lee, P.J., and Chao, C.C. 2003. Enrichment enhances the expression of sgk, a glucocorticoid-induced gene, and facilitates spatial learning through glutamate AMPA receptor mediation. Eur J Neurosci 18(10): 2842-2852.

Lenertz, L.Y., Lee, B.H., Min, X., Xu, B.E., Wedin, K., Earnest, S., Goldsmith, E.J., and Cobb, M.H. 2005. Properties of WNK1 and implications for other family members. J Biol Chem 280(29): 26653-26658.

Leong, M.L., Maiyar, A.C., Kim, B., O'Keeffe, B.A., and Firestone, G.L. 2003. Expression of the serum- and glucocorticoid-inducible protein kinase, Sgk, is a cell survival response to multiple types of environmental stress stimuli in mammary epithelial cells. J Biol Chem 278(8): 5871-5882.

Leshem, Y. and Halevy, O. 2002. Phosphorylation of pRb is required for HGF-induced muscle cell proliferation and is p27kip1-dependent. J Cell Physiol 191(2): 173-182.

Lessi, F., Beggs, A., de Palo, M., Anti, M., Macarone Palmieri, R., Francesconi, S., Gomes, V., Bevilacqua, G., Tomlinson, I., and Segditsas, S. 2010. Down-regulation of serum/glucocorticoid regulated kinase 1 in colorectal tumours is largely independent of promoter hypermethylation. PLoS One 5(11): e13840.

Li, G., Robinson, G.W., Lesche, R., Martinez-Diaz, H., Jiang, Z., Rozengurt, N., Wagner, K.U., Wu, D.C., Lane, T.F., Liu, X., Hennighausen, L., and Wu, H. 2002. Conditional loss of PTEN leads to precocious development and neoplasia in the mammary gland. Development 129(17): 4159-4170.

Li, J., Yen, C., Liaw, D., Podsypanina, K., Bose, S., Wang, S.I., Puc, J., Miliaresis, C., Rodgers, L., McCombie, R., Bigner, S.H., Giovanella, B.C., Ittmann, M., Tycko, B., Hibshoosh, H., Wigler, M.H., and Parsons, R. 1997. PTEN, a putative protein tyrosine phosphatase gene mutated in human brain, breast, and prostate cancer. Science 275(5308): 1943-1947.

Li, L., Wingo, C.S., and Xia, S.L. 2007. Downregulation of SGK1 by nucleotides in renal tubular epithelial cells. Am J Physiol Renal Physiol 293(5): F1751-1757.

Liu, D., Yang, X., and Songyang, Z. 2000. Identification of CISK, a new member of the SGK kinase family that promotes IL-3-dependent survival. Curr Biol 10(19): 1233-1236.

Liu, J., Yang, G., Thompson-Lanza, J.A., Glassman, A., Hayes, K., Patterson, A., Marquez, R.T., Auersperg, N., Yu, Y., Hahn, W.C., Mills, G.B., and Bast, R.C., Jr. 2004. A genetically defined model for human ovarian cancer. Cancer Res 64(5): 1655-1663.

Liu, M., Chen, L.L., Chan, T.H., Wang, J., Li, Y., Zeng, T.T., Yuan, Y.F., and Guan, X.Y.

2012. Serum and glucocorticoid kinase 3 at 8q13.1 promotes cell proliferation and survival in hepatocellular carcinoma. Hepatology.

Liu, S., Murph, M., Panupinthu, N., and Mills, G.B. 2009a. ATX-LPA receptor axis in inflammation and cancer. Cell Cycle 8(22): 3695-3701.

Liu, S., Umezu-Goto, M., Murph, M., Lu, Y., Liu, W., Zhang, F., Yu, S., Stephens, L.C., Cui, X., Murrow, G., Coombes, K., Muller, W., Hung, M.C., Perou, C.M., Lee, A.V., Fang, X., and Mills, G.B. 2009b. Expression of autotaxin and lysophosphatidic acid receptors increases mammary tumorigenesis, invasion, and metastases. Cancer Cell 15(6): 539-550.

Lu, M., Wang, J., Ives, H.E., and Pearce, D. 2011. mSIN1 protein mediates SGK1 protein interaction with mTORC2 protein complex and is required for selective activation of the epithelial sodium channel. J Biol Chem 286(35): 30647-30654.

Lu, M., Wang, J., Jones, K.T., Ives, H.E., Feldman, M.E., Yao, L.J., Shokat, K.M., Ashrafi, K., and Pearce, D. 2010. mTOR complex-2 activates ENaC by phosphorylating SGK1. J Am Soc Nephrol 21(5): 811-818.

Lu, Y., Wang, H., and Mills, G.B. 2003. Targeting PI3K-AKT pathway for cancer therapy. Rev Clin Exp Hematol 7(2): 205-228.

Luo, Y., Shoemaker, A.R., Liu, X., Woods, K.W., Thomas, S.A., de Jong, R., Han, E.K., Li, T., Stoll, V.S., Powlas, J.A., Oleksijew, A., Mitten, M.J., Shi, Y., Guan, R., McGonigal, T.P., Klinghofer, V., Johnson, E.F., Leverson, J.D., Bouska, J.J., Mamo, M., Smith, R.A., Gramling-Evans, E.E., Zinker, B.A., Mika, A.K., Nguyen, P.T., Oltersdorf, T., Rosenberg, S.H., Li, Q., and Giranda, V.L. 2005. Potent and selective inhibitors of Akt kinases slow the progress of tumors in vivo. Mol Cancer Ther 4(6): 977-986.

Lynes, M.D. and Widmaier, E.P. 2011. Involvement of CD36 and intestinal alkaline phosphatases in fatty acid transport in enterocytes, and the response to a high-fat diet. Life Sci 88(9-10): 384-391.

Lyo, D., Xu, L., and Foster, D.A. 2010. Phospholipase D stabilizes HDM2 through an mTORC2/SGK1 pathway. Biochem Biophys Res Commun 396(2): 562-565.

Ma, L., Chen, Z., Erdjument-Bromage, H., Tempst, P., and Pandolfi, P.P. 2005. Phosphorylation and functional inactivation of TSC2 by Erk implications for tuberous sclerosis and cancer pathogenesis. Cell 121(2): 179-193.

Mabuchi, S., Ohmichi, M., Kimura, A., Hisamoto, K., Hayakawa, J., Nishio, Y., Adachi, K., Takahashi, K., Arimoto-Ishida, E., Nakatsuji, Y., Tasaka, K., and Murata, Y. 2002. Inhibition of phosphorylation of BAD and Raf-1 by Akt sensitizes human ovarian cancer cells to paclitaxel. J Biol Chem 277(36): 33490-33500.

Maier, G., Palmada, M., Rajamanickam, J., Shumilina, E., Bohmer, C., and Lang, F. 2006. Upregulation of HERG channels by the serum and glucocorticoid inducible kinase isoform SGK3. Cell Physiol Biochem 18(4-5): 177-186.

Maiyar, A.C., Huang, A.J., Phu, P.T., Cha, H.H., and Firestone, G.L. 1996. p53 stimulates promoter activity of the sgk. serum/glucocorticoid-inducible serine/threonine protein kinase gene in rodent mammary epithelial cells. J Biol Chem 271(21): 12414-12422.

Maiyar, A.C., Leong, M.L., and Firestone, G.L. 2003. Importin-alpha mediates the regulated nuclear targeting of serum- and glucocorticoid-inducible protein kinase (Sgk) by recognition of a nuclear localization signal in the kinase central domain. Mol Biol Cell 14(3): 1221-1239.

Maiyar, A.C., Phu, P.T., Huang, A.J., and Firestone, G.L. 1997. Repression of glucocorticoid receptor transactivation and DNA binding of a glucocorticoid response element within the serum/glucocorticoid-inducible protein kinase (sgk) gene promoter by the p53 tumor suppressor protein. Mol Endocrinol 11(3): 312-329.

Malumbres, M. and Barbacid, M. 2009. Cell cycle, CDKs and cancer: a changing paradigm. Nat Rev Cancer 9(3): 153-166.

Manning, B.D. and Cantley, L.C. 2007. AKT/PKB signaling: navigating downstream. Cell 129(7): 1261-1274.

Manning, B.D., Tee, A.R., Logsdon, M.N., Blenis, J., and Cantley, L.C. 2002. Identification of the tuberous sclerosis complex-2 tumor suppressor gene product tuberin as a target of the phosphoinositide 3-kinase/akt pathway. Mol Cell 10(1): 151-162.

Markman, B., Atzori, F., Perez-Garcia, J., Tabernero, J., and Baselga, J. 2010a. Status of PI3K inhibition and biomarker development in cancer therapeutics. Ann Oncol 21(4): 683-691.

Markman, B., Dienstmann, R., and Tabernero, J. 2010b. Targeting the PI3K/Akt/mTOR pathway--beyond rapalogs. Oncotarget 1(7): 530-543.

Mauro, T.M., McCormick, J.A., Wang, J., Boini, K.M., Ray, L., Monks, B., Birnbaum, M.J., Lang, F., and Pearce, D. 2009. Akt2 and SGK3 are both determinants of postnatal hair follicle development. Faseb J 23(9): 3193-3202.

Mayer, C. and Grummt, I. 2006. Ribosome biogenesis and cell growth: mTOR coordinates transcription by all three classes of nuclear RNA polymerases. Oncogene 25(48): 6384-6391.

Mayo, L.D. and Donner, D.B. 2001. A phosphatidylinositol 3-kinase/Akt pathway promotes translocation of Mdm2 from the cytoplasm to the nucleus. Proc Natl Acad Sci U S A 98(20): 11598-11603.

McCormick, J.A., Feng, Y., Dawson, K., Behne, M.J., Yu, B., Wang, J., Wyatt, A.W., Henke, G., Grahammer, F., Mauro, T.M., Lang, F., and Pearce, D. 2004. Targeted disruption of the protein kinase SGK3/CISK impairs postnatal hair follicle development. Mol Biol Cell 15(9): 4278-4288.

McDermott, P.J., Rothblum, L.I., Smith, S.D., and Morgan, H.E. 1989. Accelerated rates of ribosomal RNA synthesis during growth of contracting heart cells in culture. J Biol Chem 264(30): 18220-18227.

McGlade, C.J., Ellis, C., Reedijk, M., Anderson, D., Mbamalu, G., Reith, A.D., Panayotou, G., End, P., Bernstein, A., Kazlauskas, A., and et al. 1992. SH2 domains of the p85 alpha subunit of phosphatidylinositol 3-kinase regulate binding to growth factor receptors. Mol Cell Biol 12(3): 991-997.

McGuire, W.P., Hoskins, W.J., Brady, M.F., Kucera, P.R., Partridge, E.E., Look, K.Y., Clarke-Pearson, D.L., and Davidson, M. 1996. Cyclophosphamide and cisplatin versus paclitaxel and cisplatin: a phase III randomized trial in patients with suboptimal stage III/IV ovarian cancer (from the Gynecologic Oncology Group). Semin Oncol 23(5 Suppl 12): 40-47.

Mehta, R.R., Yamada, T., Taylor, B.N., Christov, K., King, M.L., Majumdar, D., Lekmine, F., Tiruppathi, C., Shilkaitis, A., Bratescu, L., Green, A., Beattie, C.W., and Das Gupta, T.K. 2011. A cell penetrating peptide derived from azurin inhibits angiogenesis and tumor growth by inhibiting phosphorylation of VEGFR-2, FAK and Akt. Angiogenesis 14(3): 355-369.

Melhem, A., Yamada, S.D., Fleming, G.F., Delgado, B., Brickley, D.R., Wu, W., Kocherginsky, M., and Conzen, S.D. 2009. Administration of glucocorticoids to ovarian cancer patients is associated with expression of the anti-apoptotic genes SGK1 and MKP1/DUSP1 in ovarian tissues. Clin Cancer Res 15(9): 3196-3204.

Memmott, R.M. and Dennis, P.A. 2009. Akt-dependent and -independent mechanisms of mTOR regulation in cancer. Cell Signal 21(5): 656-664.

Menakongka, A. and Suthiphongchai, T. 2010. Involvement of PI3K and ERK1/2 pathways in hepatocyte growth factor-induced cholangiocarcinoma cell invasion. World J Gastroenterol 16(6): 713-722.

Meng, F., Yamagiwa, Y., Taffetani, S., Han, J., and Patel, T. 2005. IL-6 activates serum and glucocorticoid kinase via p38alpha mitogen-activated protein kinase pathway. Am J Physiol Cell Physiol 289(4): C971-981.

Meyuhas, O. 2000. Synthesis of the translational apparatus is regulated at the translational level. Eur J Biochem 267(21): 6321-6330.

Micalizzi, D.S., Farabaugh, S.M., and Ford, H.L. 2010. Epithelial-mesenchymal transition in cancer: parallels between normal development and tumor progression. J Mammary Gland Biol Neoplasia 15(2): 117-134.

Mikosz, C.A., Brickley, D.R., Sharkey, M.S., Moran, T.W., and Conzen, S.D. 2001. Glucocorticoid receptor-mediated protection from apoptosis is associated with induction of the serine/threonine survival kinase gene, sgk-1. J Biol Chem 276(20): 16649-16654.

Mills, G.B., Lu, Y., Fang, X., Wang, H., Eder, A., Mao, M., Swaby, R., Cheng, K.W.,

Stokoe, D., Siminovitch, K., Jaffe, R., and Gray, J. 2001. The role of genetic abnormalities of PTEN and the phosphatidylinositol 3-kinase pathway in breast and ovarian tumorigenesis, prognosis, and therapy. Semin Oncol 28(5 Suppl 16): 125-141.

Mizuno, H. and Nishida, E. 2001. The ERK MAP kinase pathway mediates induction of SGK (serum- and glucocorticoid-inducible kinase) by growth factors. Genes Cells 6(3): 261-268.

Mo, J.S., Ann, E.J., Yoon, J.H., Jung, J., Choi, Y.H., Kim, H.Y., Ahn, J.S., Kim, S.M., Kim, M.Y., Hong, J.A., Seo, M.S., Lang, F., Choi, E.J., and Park, H.S. 2011. Serum- and glucocorticoid-inducible kinase 1 (SGK1) controls Notch1 signaling by downregulation of protein stability through Fbw7 ubiquitin ligase. J Cell Sci 124(Pt 1): 100-112.

Montagne, J., Stewart, M.J., Stocker, H., Hafen, E., Kozma, S.C., and Thomas, G. 1999. Drosophila S6 kinase: a regulator of cell size. Science 285(5436): 2126-2129.

Montanaro, L., Mazzini, G., Barbieri, S., Vici, M., Nardi-Pantoli, A., Govoni, M., Donati, G., Trere, D., and Derenzini, M. 2007. Different effects of ribosome biogenesis inhibition on cell proliferation in retinoblastoma protein- and p53-deficient and proficient human osteosarcoma cell lines. Cell Prolif 40(4): 532-549.

Moolenaar, W.H. and Perrakis, A. 2011. Insights into autotaxin: how to produce and present a lipid mediator. Nat Rev Mol Cell Biol 12(10): 674-679.

Mootha, V.K., Lindgren, C.M., Eriksson, K.F., Subramanian, A., Sihag, S., Lehar, J., Puigserver, P., Carlsson, E., Ridderstrale, M., Laurila, E., Houstis, N., Daly, M.J., Patterson, N., Mesirov, J.P., Golub, T.R., Tamayo, P., Spiegelman, B., Lander, E.S., Hirschhorn, J.N., Altshuler, D., and Groop, L.C. 2003. PGC-1alpha-responsive genes involved in oxidative phosphorylation are coordinately downregulated in human diabetes. Nat Genet 34(3): 267-273.

Mora, A., Komander, D., van Aalten, D.M., and Alessi, D.R. 2004. PDK1, the master regulator of AGC kinase signal transduction. Semin Cell Dev Biol 15(2): 161-170.

Morgan, H.E. and Beinlich, C.J. 1997. Contributions of increased efficiency and capacity of protein synthesis to rapid cardiac growth. Mol Cell Biochem 176(1-2): 145-151.

Moss, T., Langlois, F., Gagnon-Kugler, T., and Stefanovsky, V. 2007. A housekeeper with power of attorney: the rRNA genes in ribosome biogenesis. Cell Mol Life Sci 64(1): 29-49.

Muller, A., Homey, B., Soto, H., Ge, N., Catron, D., Buchanan, M.E., McClanahan, T., Murphy, E., Yuan, W., Wagner, S.N., Barrera, J.L., Mohar, A., Verastegui, E., and Zlotnik, A. 2001. Involvement of chemokine receptors in breast cancer metastasis. Nature 410(6824): 50-56.

Muller, A.J., Young, J.C., Pendergast, A.M., Pondel, M., Landau, N.R., Littman, D.R., and Witte, O.N. 1991. BCR first exon sequences specifically activate the BCR/ABL tyrosine kinase oncogene of Philadelphia chromosome-positive human leukemias. Mol Cell Biol 11(4): 1785-1792.

Murakami, M., Ichisaka, T., Maeda, M., Oshiro, N., Hara, K., Edenhofer, F., Kiyama, H., Yonezawa, K., and Yamanaka, S. 2004. mTOR is essential for growth and proliferation in early mouse embryos and embryonic stem cells. Mol Cell Biol 24(15): 6710-6718.

Murano, K., Okuwaki, M., Hisaoka, M., and Nagata, K. 2008. Transcription regulation of the rRNA gene by a multifunctional nucleolar protein, B23/nucleophosmin, through its histone chaperone activity. Mol Cell Biol 28(10): 3114-3126.

Myers, M.P., Pass, I., Batty, I.H., Van der Kaay, J., Stolarov, J.P., Hemmings, B.A., Wigler, M.H., Downes, C.P., and Tonks, N.K. 1998. The lipid phosphatase activity of PTEN is critical for its tumor supressor function. Proc Natl Acad Sci U S A 95(23): 13513-13518.

Naishiro, Y., Yamada, T., Idogawa, M., Honda, K., Takada, M., Kondo, T., Imai, K., and Hirohashi, S. 2005. Morphological and transcriptional responses of untransformed intestinal epithelial cells to an oncogenic beta-catenin protein. Oncogene 24(19): 3141-3153.

Nam, E.J. and Kim, Y.T. 2008. Alteration of cell-cycle regulation in epithelial ovarian cancer. Int J Gynecol Cancer 18(6): 1169-1182.

Naray-Fejes-Toth, A., Canessa, C., Cleaveland, E.S., Aldrich, G., and Fejes-Toth, G. 1999. sgk is an aldosterone-induced kinase in the renal collecting duct. Effects on epithelial na+ channels. J Biol Chem 274(24): 16973-16978.

Nasir, O., Wang, K., Foller, M., Gu, S., Bhandaru, M., Ackermann, T.F., Boini, K.M., Mack, A., Klingel, K., Amato, R., Perrotti, N., Kuhl, D., Behrens, J., Stournaras, C., and Lang, F. 2009. Relative resistance of SGK1 knockout mice against chemical carcinogenesis. IUBMB Life 61(7): 768-776.

Nazarewicz, R.R., Salazar, G., Patrushev, N., San Martin, A., Hilenski, L., Xiong, S., and Alexander, R.W. 2011. Early endosomal antigen 1 (EEA1) is an obligate scaffold for angiotensin II-induced, PKC-alpha-dependent Akt activation in endosomes. J Biol Chem 286(4): 2886-2895.

Neshat, M.S., Mellinghoff, I.K., Tran, C., Stiles, B., Thomas, G., Petersen, R., Frost, P., Gibbons, J.J., Wu, H., and Sawyers, C.L. 2001. Enhanced sensitivity of PTEN-deficient tumors to inhibition of FRAP/mTOR. Proc Natl Acad Sci U S A 98(18): 10314-10319.

Neufeld, T.P. and Edgar, B.A. 1998. Connections between growth and the cell cycle. Curr Opin Cell Biol 10(6): 784-790.

Nishida, Y., Nagata, T., Takahashi, Y., Sugahara-Kobayashi, M., Murata, A., and Asai, S. 2004. Alteration of serum/glucocorticoid regulated kinase-1 (sgk-1) gene

expression in rat hippocampus after transient global ischemia. Brain Res Mol Brain Res 123(1-2): 121-125.

Nobukuni, T., Joaquin, M., Roccio, M., Dann, S.G., Kim, S.Y., Gulati, P., Byfield, M.P., Backer, J.M., Natt, F., Bos, J.L., Zwartkruis, F.J., and Thomas, G. 2005. Amino acids mediate mTOR/raptor signaling through activation of class 3 phosphatidylinositol 3OH-kinase. Proc Natl Acad Sci U S A 102(40): 14238-14243.

Nuber, U.A., Kriaucionis, S., Roloff, T.C., Guy, J., Selfridge, J., Steinhoff, C., Schulz, R., Lipkowitz, B., Ropers, H.H., Holmes, M.C., and Bird, A. 2005. Up-regulation of glucocorticoid-regulated genes in a mouse model of Rett syndrome. Hum Mol Genet 14(15): 2247-2256.

Okada, T., Ishii, Y., Masujin, K., Yasoshima, A., Matsuda, J., Ogura, A., Nakayama, H., Kunieda, T., and Doi, K. 2006. The critical roles of serum/glucocorticoid-regulated kinase 3 (SGK3) in the hair follicle morphogenesis and homeostasis: the allelic difference provides novel insights into hair follicle biology. Am J Pathol 168(4): 1119-1133.

Onishi, I., Lin, P.J., Numata, Y., Austin, P., Cipollone, J., Roberge, M., Roskelley, C.D., and Numata, M. 2012. Organellar (Na+, K+)/H+ exchanger NHE7 regulates cell adhesion, invasion cells. Oncol Rep 27(2): 311-317.

Ozols, R.F. 2000. Optimum chemotherapy for ovarian cancer. Int J Gynecol Cancer 10(S1): 33-37.

Palmada, M., Boehmer, C., Akel, A., Rajamanickam, J., Jeyaraj, S., Keller, K., and Lang, F. 2006. SGK1 kinase upregulates GLUT1 activity and plasma membrane expression. Diabetes 55(2): 421-427.

Palmada, M., Dieter, M., Boehmer, C., Waldegger, S., and Lang, F. 2004a. Serum and glucocorticoid inducible kinases functionally regulate ClC-2 channels. Biochem Biophys Res Commun 321(4): 1001-1006.

Palmada, M., Dieter, M., Speil, A., Bohmer, C., Mack, A.F., Wagner, H.J., Klingel, K., Kandolf, R., Murer, H., Biber, J., Closs, E.I., and Lang, F. 2004b. Regulation of intestinal phosphate cotransporter NaPi IIb by ubiquitin ligase Nedd4-2 and by serum- and glucocorticoid-dependent kinase 1. Am J Physiol Gastrointest Liver Physiol 287(1): G143-150.

Palmada, M., Speil, A., Jeyaraj, S., Bohmer, C., and Lang, F. 2005. The serine/threonine kinases SGK1, 3 and PKB stimulate the amino acid transporter ASCT2. Biochem Biophys Res Commun 331(1): 272-277.

Pao, A.C., McCormick, J.A., Li, H., Siu, J., Govaerts, C., Bhalla, V., Soundararajan, R., and Pearce, D. 2007. NH2 terminus of serum and glucocorticoid-regulated kinase 1 binds to phosphoinositides and is essential for isoform-specific physiological functions. Am J Physiol Renal Physiol 292(6): F1741-1750.

Park, J., Leong, M.L., Buse, P., Maiyar, A.C., Firestone, G.L., and Hemmings, B.A.

1999. Serum and glucocorticoid-inducible kinase (SGK) is a target of the PI 3-kinase-stimulated signaling pathway. Embo J 18(11): 3024-3033.

Parrott, J.A. and Skinner, M.K. 2000. Expression and action of hepatocyte growth factor in human and bovine normal ovarian surface epithelium and ovarian cancer. Biol Reprod 62(3): 491-500.

Pende, M., Um, S.H., Mieulet, V., Sticker, M., Goss, V.L., Mestan, J., Mueller, M., Fumagalli, S., Kozma, S.C., and Thomas, G. 2004. S6K1(-/-)/S6K2(-/-) mice exhibit perinatal lethality and rapamycin-sensitive 5'-terminal oligopyrimidine mRNA translation and reveal a mitogen-activated protein kinase-dependent S6 kinase pathway. Mol Cell Biol 24(8): 3112-3124.

Peng, D.J., Wang, J., Zhou, J.Y., and Wu, G.S. 2010. Role of the Akt/mTOR survival pathway in cisplatin resistance in ovarian cancer cells. Biochem Biophys Res Commun 394(3): 600-605.

Perrotti, N., He, R.A., Phillips, S.A., Haft, C.R., and Taylor, S.I. 2001. Activation of serum- and glucocorticoid-induced protein kinase (Sgk) by cyclic AMP and insulin. J Biol Chem 276(12): 9406-9412.

Peyssonnaux, C., Provot, S., Felder-Schmittbuhl, M.P., Calothy, G., and Eychene, A. 2000. Induction of postmitotic neuroretina cell proliferation by distinct Ras downstream signaling pathways. Mol Cell Biol 20(19): 7068-7079.

Pfau, A., Grossmann, C., Freudinger, R., Mildenberger, S., Benesic, A., and Gekle, M. 2007. Ca2+ but not H2O2 modulates GRE-element activation by the human mineralocorticoid receptor in HEK cells. Mol Cell Endocrinol 264(1-2): 35-43.

Philp, A.J., Campbell, I.G., Leet, C., Vincan, E., Rockman, S.P., Whitehead, R.H., Thomas, R.J., and Phillips, W.A. 2001. The phosphatidylinositol 3'-kinase p85alpha gene is an oncogene in human ovarian and colon tumors. Cancer Res 61(20): 7426-7429.

Poortinga, G., Hannan, K.M., Snelling, H., Walkley, C.R., Jenkins, A., Sharkey, K., Wall, M., Brandenburger, Y., Palatsides, M., Pearson, R.B., McArthur, G.A., and Hannan, R.D. 2004. MAD1 and c-MYC regulate UBF and rDNA transcription during granulocyte differentiation. Embo J 23(16): 3325-3335.

Potter, C.J., Pedraza, L.G., and Xu, T. 2002. Akt regulates growth by directly phosphorylating Tsc2. Nat Cell Biol 4(9): 658-665.

Powers, T. and Walter, P. 1999. Regulation of ribosome biogenesis by the rapamycin-sensitive TOR-signaling pathway in Saccharomyces cerevisiae. Mol Biol Cell 10(4): 987-1000.

Prediger, E.A. 2001. Detection and quantitation of mRNAs using ribonuclease protection assays. Methods Mol Biol 160: 495-505.

Raikwar, N.S., Snyder, P.M., and Thomas, C.P. 2008. An evolutionarily conserved N-terminal Sgk1 variant with enhanced stability and improved function. Am J

Physiol Renal Physiol 295(5): F1440-1448.

Rangone, H., Poizat, G., Troncoso, J., Ross, C.A., MacDonald, M.E., Saudou, F., and Humbert, S. 2004. The serum- and glucocorticoid-induced kinase SGK inhibits mutant huntingtin-induced toxicity by phosphorylating serine 421 of huntingtin. Eur J Neurosci 19(2): 273-279.

Raska, I., Koberna, K., Malinsky, J., Fidlerova, H., and Masata, M. 2004. The nucleolus and transcription of ribosomal genes. Biol Cell 96(8): 579-594.

Rauhala, H.E., Porkka, K.P., Tolonen, T.T., Martikainen, P.M., Tammela, T.L., and Visakorpi, T. 2005. Dual-specificity phosphatase 1 and serum/glucocorticoid-regulated kinase are downregulated in prostate cancer. Int J Cancer 117(5): 738-745.

Real, S., Meo-Evoli, N., Espada, L., and Tauler, A. 2011. E2F1 regulates cellular growth by mTORC1 signaling. PLoS One 6(1): e16163.

Reid, J.M., Walden, C.A., Qin, R., Ziegler, K.L., Haslam, J.L., Rajewski, R.A., Warndahl, R., Fitting, C.L., Boring, D., Szabo, E., Crowell, J., Perloff, M., Jong, L., Bauer, B.A., Mandrekar, S.J., Ames, M.M., and Limburg, P.J. 2011. Phase 0 clinical chemoprevention trial of the Akt inhibitor SR13668. Cancer Prev Res (Phila) 4(3): 347-353.

Reiling, J.H. and Hafen, E. 2004. The hypoxia-induced paralogs Scylla and Charybdis inhibit growth by down-regulating S6K activity upstream of TSC in Drosophila. Genes Dev 18(23): 2879-2892.

Richards, J.S., Fitzpatrick, S.L., Clemens, J.W., Morris, J.K., Alliston, T., and Sirois, J. 1995. Ovarian cell differentiation: a cascade of multiple hormones, cellular signals, and regulated genes. Recent Prog Horm Res 50: 223-254.

Richards, J.S., Sharma, S.C., Falender, A.E., and Lo, Y.H. 2002. Expression of FKHR, FKHRL1, and AFX genes in the rodent ovary: evidence for regulation by IGF-I, estrogen, and the gonadotropins. Mol Endocrinol 16(3): 580-599.

Rodriguez-Antona, C. 2010. Pharmacogenomics of paclitaxel. Pharmacogenomics 11(5): 621-623.

Rosner, M. and Hengstschlager, M. 2012. Detection of cytoplasmic and nuclear functions of mTOR by fractionation. Methods Mol Biol 821: 105-124.

Rotin, D. and Schild, L. 2008. ENaC and its regulatory proteins as drug targets for blood pressure control. Curr Drug Targets 9(8): 709-716.

Royal, I., Lamarche-Vane, N., Lamorte, L., Kaibuchi, K., and Park, M. 2000. Activation of cdc42, rac, PAK, and rho-kinase in response to hepatocyte growth factor differentially regulates epithelial cell colony spreading and dissociation. Mol Biol Cell 11(5): 1709-1725.

Ruggero, D. and Sonenberg, N. 2005. The Akt of translational control. Oncogene 24(50): 7426-7434.

Sahoo, S., Brickley, D.R., Kocherginsky, M., and Conzen, S.D. 2005. Coordinate expression of the PI3-kinase downstream effectors serum and glucocorticoid-induced kinase (SGK-1) and Akt-1 in human breast cancer. Eur J Cancer 41(17): 2754-2759.

Sakoda, H., Gotoh, Y., Katagiri, H., Kurokawa, M., Ono, H., Onishi, Y., Anai, M., Ogihara, T., Fujishiro, M., Fukushima, Y., Abe, M., Shojima, N., Kikuchi, M., Oka, Y., Hirai, H., and Asano, T. 2003. Differing roles of Akt and serum- and glucocorticoid-regulated kinase in glucose metabolism, DNA synthesis, and oncogenic activity. J Biol Chem 278(28): 25802-25807.

Salker, M.S., Christian, M., Steel, J.H., Nautiyal, J., Lavery, S., Trew, G., Webster, Z., Al-Sabbagh, M., Puchchakayala, G., Foller, M., Landles, C., Sharkey, A.M., Quenby, S., Aplin, J.D., Regan, L., Lang, F., and Brosens, J.J. 2011. Deregulation of the serum- and glucocorticoid-inducible kinase SGK1 in the endometrium causes reproductive failure. Nat Med 17(11): 1509-1513.

Samuels, Y., Diaz, L.A., Jr., Schmidt-Kittler, O., Cummins, J.M., Delong, L., Cheong, I., Rago, C., Huso, D.L., Lengauer, C., Kinzler, K.W., Vogelstein, B., and Velculescu, V.E. 2005. Mutant PIK3CA promotes cell growth and invasion of human cancer cells. Cancer Cell 7(6): 561-573.

Samuels, Y. and Ericson, K. 2006. Oncogenic PI3K and its role in cancer. Curr Opin Oncol 18(1): 77-82.

Samuels, Y. and Velculescu, V.E. 2004. Oncogenic mutations of PIK3CA in human cancers. Cell Cycle 3(10): 1221-1224.

Samuels, Y., Wang, Z., Bardelli, A., Silliman, N., Ptak, J., Szabo, S., Yan, H., Gazdar, A., Powell, S.M., Riggins, G.J., Willson, J.K., Markowitz, S., Kinzler, K.W., Vogelstein, B., and Velculescu, V.E. 2004. High frequency of mutations of the PIK3CA gene in human cancers. Science 304(5670): 554.

Sancak, Y., Thoreen, C.C., Peterson, T.R., Lindquist, R.A., Kang, S.A., Spooner, E., Carr, S.A., and Sabatini, D.M. 2007. PRAS40 is an insulin-regulated inhibitor of the mTORC1 protein kinase. Mol Cell 25(6): 903-915.

Sander, E.E., van Delft, S., ten Klooster, J.P., Reid, T., van der Kammen, R.A., Michiels, F., and Collard, J.G. 1998. Matrix-dependent Tiam1/Rac signaling in epithelial cells promotes either cell-cell adhesion or cell migration and is regulated by phosphatidylinositol 3-kinase. J Cell Biol 143(5): 1385-1398.

Sarbassov, D.D., Guertin, D.A., Ali, S.M., and Sabatini, D.M. 2005. Phosphorylation and regulation of Akt/PKB by the rictor-mTOR complex. Science 307(5712): 1098-1101.

Schmelzle, T. and Hall, M.N. 2000. TOR, a central controller of cell growth. Cell 103(2): 253-262.

Schniepp, R., Kohler, K., Ladewig, T., Guenther, E., Henke, G., Palmada, M., Boehmer, C., Rothstein, J.D., Broer, S., and Lang, F. 2004. Retinal colocalization and in vitro interaction of the glutamate transporter EAAT3 and the serum- and glucocorticoid-inducible kinase SGK1 [correction]. Invest Ophthalmol Vis Sci 45(5): 1442-1449.

Schoenebeck, B., Bader, V., Zhu, X.R., Schmitz, B., Lubbert, H., and Stichel, C.C. 2005. Sgk1, a cell survival response in neurodegenerative diseases. Mol Cell Neurosci 30(2): 249-264.

Schwab, M., Lupescu, A., Mota, M., Mota, E., Frey, A., Simon, P., Mertens, P.R., Floege, J., Luft, F., Asante-Poku, S., Schaeffeler, E., and Lang, F. 2008. Association of SGK1 gene polymorphisms with type 2 diabetes. Cell Physiol Biochem 21(1-3): 151-160.

Scotton, C.J., Wilson, J.L., Scott, K., Stamp, G., Wilbanks, G.D., Fricker, S., Bridger, G., and Balkwill, F.R. 2002. Multiple actions of the chemokine CXCL12 on epithelial tumor cells in human ovarian cancer. Cancer Res 62(20): 5930-5938.

Seebohm, G., Strutz-Seebohm, N., Baltaev, R., Korniychuk, G., Knirsch, M., Engel, J., and Lang, F. 2005. Regulation of KCNQ4 potassium channel prepulse dependence and current amplitude by SGK1 in Xenopus oocytes. Cell Physiol Biochem 16(4-6): 255-262.

Segditsas, S., Sieber, O., Deheragoda, M., East, P., Rowan, A., Jeffery, R., Nye, E., Clark, S., Spencer-Dene, B., Stamp, G., Poulsom, R., Suraweera, N., Silver, A., Ilyas, M., and Tomlinson, I. 2008. Putative direct and indirect Wnt targets identified through consistent gene expression changes in APC-mutant intestinal adenomas from humans and mice. Hum Mol Genet 17(24): 3864-3875.

Seger, Y.R., Garcia-Cao, M., Piccinin, S., Cunsolo, C.L., Doglioni, C., Blasco, M.A., Hannon, G.J., and Maestro, R. 2002. Transformation of normal human cells in the absence of telomerase activation. Cancer Cell 2(5): 401-413.

Setiawan, I., Henke, G., Feng, Y., Bohmer, C., Vasilets, L.A., Schwarz, W., and Lang, F. 2002. Stimulation of Xenopus oocyte Na(+),K(+)ATPase by the serum and glucocorticoid-dependent kinase sgk1. Pflugers Arch 444(3): 426-431.

Shaw, R.J., Bardeesy, N., Manning, B.D., Lopez, L., Kosmatka, M., DePinho, R.A., and Cantley, L.C. 2004. The LKB1 tumor suppressor negatively regulates mTOR signaling. Cancer Cell 6(1): 91-99.

Shaw, R.J. and Cantley, L.C. 2006. Ras, PI(3)K and mTOR signalling controls tumour cell growth. Nature 441(7092): 424-430.

Shchors, K., Shchors, E., Rostker, F., Lawlor, E.R., Brown-Swigart, L., and Evan, G.I. 2006. The Myc-dependent angiogenic switch in tumors is mediated by interleukin 1beta. Genes Dev 20(18): 2527-2538.

Shekar, S.C., Wu, H., Fu, Z., Yip, S.C., Nagajyothi, Cahill, S.M., Girvin, M.E., and

Backer, J.M. 2005. Mechanism of constitutive phosphoinositide 3-kinase activation by oncogenic mutants of the p85 regulatory subunit. J Biol Chem 280(30): 27850-27855.

Shelly, C. and Herrera, R. 2002. Activation of SGK1 by HGF, Rac1 and integrin-mediated cell adhesion in MDCK cells: PI-3K-dependent and -independent pathways. J Cell Sci 115(Pt 9): 1985-1993.

Sherk, A.B., Frigo, D.E., Schnackenberg, C.G., Bray, J.D., Laping, N.J., Trizna, W., Hammond, M., Patterson, J.R., Thompson, S.K., Kazmin, D., Norris, J.D., and McDonnell, D.P. 2008. Development of a small-molecule serum- and glucocorticoid-regulated kinase-1 antagonist and its evaluation as a prostate cancer therapeutic. Cancer Res 68(18): 7475-7483.

Shibata, S., Nagase, M., Yoshida, S., Kawachi, H., and Fujita, T. 2007. Podocyte as the target for aldosterone: roles of oxidative stress and Sgk1. Hypertension 49(2): 355-364.

Shields, R., Brooks, R.F., Riddle, P.N., Capellaro, D.F., and Delia, D. 1978. Cell size, cell cycle and transition probability in mouse fibroblasts. Cell 15(2): 469-474.

Shojaiefard, M., Christie, D.L., and Lang, F. 2005. Stimulation of the creatine transporter SLC6A8 by the protein kinases SGK1 and SGK3. Biochem Biophys Res Commun 334(3): 742-746.

Simon, P., Schneck, M., Hochstetter, T., Koutsouki, E., Mittelbronn, M., Merseburger, A., Weigert, C., Niess, A., and Lang, F. 2007. Differential regulation of serum- and glucocorticoid-inducible kinase 1 (SGK1) splice variants based on alternative initiation of transcription. Cell Physiol Biochem 20(6): 715-728.

Slagsvold, T., Marchese, A., Brech, A., and Stenmark, H. 2006. CISK attenuates degradation of the chemokine receptor CXCR4 via the ubiquitin ligase AIP4. Embo J 25(16): 3738-3749.

Smyth, G.K. 2005. Limma: linear models for microarray data. In: 'Bioinformatics and Computational Biology Solutions using R and Bioconductor'. Springer, New York.

Snyder, P.M., Olson, D.R., Kabra, R., Zhou, R., and Steines, J.C. 2004. cAMP and serum and glucocorticoid-inducible kinase (SGK) regulate the epithelial Na(+) channel through convergent phosphorylation of Nedd4-2. J Biol Chem 279(44): 45753-45758.

Snyder, P.M., Olson, D.R., and Thomas, B.C. 2002. Serum and glucocorticoid-regulated kinase modulates Nedd4-2-mediated inhibition of the epithelial Na+ channel. J Biol Chem 277(1): 5-8.

Soengas, M.S., Alarcon, R.M., Yoshida, H., Giaccia, A.J., Hakem, R., Mak, T.W., and Lowe, S.W. 1999. Apaf-1 and caspase-9 in p53-dependent apoptosis and tumor inhibition. Science 284(5411): 156-159.

Sofer, A., Lei, K., Johannessen, C.M., and Ellisen, L.W. 2005. Regulation of mTOR and cell growth in response to energy stress by REDD1. Mol Cell Biol 25(14): 5834-5845.

Solomon, B. and Pearson, R.B. 2009. Class IA phosphatidylinositol 3-kinase signaling in non-small cell lung cancer. J Thorac Oncol 4(7): 787-791.

Soukas, A.A., Kane, E.A., Carr, C.E., Melo, J.A., and Ruvkun, G. 2009. Rictor/TORC2 regulates fat metabolism, feeding, growth, and life span in Caenorhabditis elegans. Genes Dev 23(4): 496-511.

Soundararajan, R., Wang, J., Melters, D., and Pearce, D. 2010. Glucocorticoid-induced Leucine zipper 1 stimulates the epithelial sodium channel by regulating serum- and glucocorticoid-induced kinase 1 stability and subcellular localization. J Biol Chem 285(51): 39905-39913.

Staal, S.P. 1987. Molecular cloning of the akt oncogene and its human homologues AKT1 and AKT2: amplification of AKT1 in a primary human gastric adenocarcinoma. Proc Natl Acad Sci U S A 84(14): 5034-5037.

Stahl, J.M., Sharma, A., Cheung, M., Zimmerman, M., Cheng, J.Q., Bosenberg, M.W., Kester, M., Sandirasegarane, L., and Robertson, G.P. 2004. Deregulated Akt3 activity promotes development of malignant melanoma. Cancer Res 64(19): 7002-7010.

Stambolic, V. and Woodgett, J.R. 2006. Functional distinctions of protein kinase B/Akt isoforms defined by their influence on cell migration. Trends Cell Biol 16(9): 461-466.

Stemke-Hale, K., Gonzalez-Angulo, A.M., Lluch, A., Neve, R.M., Kuo, W.L., Davies, M., Carey, M., Hu, Z., Guan, Y., Sahin, A., Symmans, W.F., Pusztai, L., Nolden, L.K., Horlings, H., Berns, K., Hung, M.C., van de Vijver, M.J., Valero, V., Gray, J.W., Bernards, R., Mills, G.B., and Hennessy, B.T. 2008. An integrative genomic and proteomic analysis of PIK3CA, PTEN, and AKT mutations in breast cancer. Cancer Res 68(15): 6084-6091.

Stichel, C.C., Schoenebeck, B., Foguet, M., Siebertz, B., Bader, V., Zhu, X.R., and Lubbert, H. 2005. sgk1, a member of an RNA cluster associated with cell death in a model of Parkinson's disease. Eur J Neurosci 21(2): 301-316.

Strunk, C.J., Platzbecker, U., Thiede, C., Schaich, M., Illmer, T., Kang, Z., Leahy, P., Li, C., Xie, X., Laughlin, M.J., Lazarus, H.M., Gerson, S.L., Bunting, K.D., Ehninger, G., and Tse, W. 2009. Elevated AF1q expression is a poor prognostic marker for adult acute myeloid leukemia patients with normal cytogenetics. Am J Hematol 84(5): 308-309.

Strutz-Seebohm, N., Seebohm, G., Korniychuk, G., Baltaev, R., Ureche, O., Striegel, M., and Lang, F. 2006. Additive regulation of GluR1 by stargazin and serum- and glucocorticoid-inducible kinase isoform SGK3. Pflugers Arch 452(3): 276-282.

Strutz-Seebohm, N., Seebohm, G., Mack, A.F., Wagner, H.J., Just, L., Skutella, T., Lang, U.E., Henke, G., Striegel, M., Hollmann, M., Rouach, N., Nicoll, R.A., McCormick, J.A., Wang, J., Pearce, D., and Lang, F. 2005. Regulation of GluR1 abundance in murine hippocampal neurones by serum- and glucocorticoid-inducible kinase 3. J Physiol 565(Pt 2): 381-390.

Strutz-Seebohm, N., Shojaiefard, M., Christie, D., Tavare, J., Seebohm, G., and Lang, F. 2007. PIKfyve in the SGK1 mediated regulation of the creatine transporter SLC6A8. Cell Physiol Biochem 20(6): 729-734.

Subramanian, A., Tamayo, P., Mootha, V.K., Mukherjee, S., Ebert, B.L., Gillette, M.A., Paulovich, A., Pomeroy, S.L., Golub, T.R., Lander, E.S., and Mesirov, J.P. 2005. Gene set enrichment analysis: a knowledge-based approach for interpreting genome-wide expression profiles. Proc Natl Acad Sci U S A 102(43): 15545-15550.

Sulic, S., Panic, L., Dikic, I., and Volarevic, S. 2005. Deregulation of cell growth and malignant transformation. Croat Med J 46(4): 622-638.

Suzuki, A., de la Pompa, J.L., Stambolic, V., Elia, A.J., Sasaki, T., del Barco Barrantes, I., Ho, A., Wakeham, A., Itie, A., Khoo, W., Fukumoto, M., and Mak, T.W. 1998. High cancer susceptibility and embryonic lethality associated with mutation of the PTEN tumor suppressor gene in mice. Curr Biol 8(21): 1169-1178.

Szebeni, B., Vannay, A., Sziksz, E., Prokai, A., Cseh, A., Veres, G., Dezsofi, A., Gyorffy, H., Szabo, I.R., and Arato, A. 2010. Increased expression of serum- and glucocorticoid-regulated kinase-1 in the duodenal mucosa of children with coeliac disease. J Pediatr Gastroenterol Nutr 50(2): 147-153.

Szmulewitz, R.Z., Chung, E., Al-Ahmadie, H., Daniel, S., Kocherginsky, M., Razmaria, A., Zagaja, G.P., Brendler, C.B., Stadler, W.M., and Conzen, S.D. 2012. Serum/glucocorticoid-regulated kinase 1 expression in primary human prostate cancers. Prostate.

Taddei, M.L., Giannoni, E., Fiaschi, T., and Chiarugi, P. 2012. Anoikis: an emerging hallmark in health and diseases. J Pathol 226(2): 380-393.

Tai, D.J., Su, C.C., Ma, Y.L., and Lee, E.H. 2009. SGK1 phosphorylation of IkappaB Kinase alpha and p300 Up-regulates NF-kappaB activity and increases N-Methyl-D-aspartate receptor NR2A and NR2B expression. J Biol Chem 284(7): 4073-4089.

Tanno, S., Mitsuuchi, Y., Altomare, D.A., Xiao, G.H., and Testa, J.R. 2001. AKT activation up-regulates insulin-like growth factor I receptor expression and promotes invasiveness of human pancreatic cancer cells. Cancer Res 61(2): 589-593.

Team, R.R.D.C. 2011. R: A language and environment for statistical computing. . R Foundation for Statistical Computing, Vienna, Austria.

Tessier, M. and Woodgett, J.R. 2006a. Role of the Phox homology domain and

phosphorylation in activation of serum and glucocorticoid-regulated kinase-3. J Biol Chem 281(33): 23978-23989.

Tessier, M. and Woodgett, J.R. 2006b. Serum and glucocorticoid-regulated protein kinases: variations on a theme. J Cell Biochem 98(6): 1391-1407.

Thoresen, S.B., Pedersen, N.M., Liestol, K., and Stenmark, H. 2010. A phosphatidylinositol 3-kinase class III sub-complex containing VPS15, VPS34, Beclin 1, UVRAG and BIF-1 regulates cytokinesis and degradative endocytic traffic. Exp Cell Res 316(20): 3368-3378.

Thullberg, M., Gad, A., Le Guyader, S., and Stromblad, S. 2007. Oncogenic H-Ras V12 promotes anchorage-independent cytokinesis in human fibroblasts. Proc Natl Acad Sci U S A 104(51): 20338-20343.

Thullberg, M. and Stromblad, S. 2008. Anchorage-independent cytokinesis as part of oncogenic transformation? Cell Cycle 7(8): 984-988.

Tran, H., Brunet, A., Griffith, E.C., and Greenberg, M.E. 2003. The many forks in FOXO's road. Sci STKE 2003(172): RE5.

Trinh-Trang-Tan, M.M., Vilela-Lamego, C., Picot, J., Wautier, M.P., and Cartron, J.P. 2010. Intercellular adhesion molecule-4 and CD36 are implicated in the abnormal adhesiveness of sickle cell SAD mouse erythrocytes to endothelium. Haematologica 95(5): 730-737.

Tsai, K.J., Chen, S.K., Ma, Y.L., Hsu, W.L., and Lee, E.H. 2002. sgk, a primary glucocorticoid-induced gene, facilitates memory consolidation of spatial learning in rats. Proc Natl Acad Sci U S A 99(6): 3990-3995.

Tsao, S.W., Mok, S.C., Fey, E.G., Fletcher, J.A., Wan, T.S., Chew, E.C., Muto, M.G., Knapp, R.C., and Berkowitz, R.S. 1995. Characterization of human ovarian surface epithelial cells immortalized by human papilloma viral oncogenes (HPV-E6E7 ORFs). Exp Cell Res 218(2): 499-507.

Tsurutani, J., West, K.A., Sayyah, J., Gills, J.J., and Dennis, P.A. 2005. Inhibition of the phosphatidylinositol 3-kinase/Akt/mammalian target of rapamycin pathway but not the MEK/ERK pathway attenuates laminin-mediated small cell lung cancer cellular survival and resistance to imatinib mesylate or chemotherapy. Cancer Res 65(18): 8423-8432.

Tulasne, D. and Foveau, B. 2008. The shadow of death on the MET tyrosine kinase receptor. Cell Death Differ 15(3): 427-434.

Ullrich, S., Berchtold, S., Ranta, F., Seebohm, G., Henke, G., Lupescu, A., Mack, A.F., Chao, C.M., Su, J., Nitschke, R., Alexander, D., Friedrich, B., Wulff, P., Kuhl, D., and Lang, F. 2005. Serum- and glucocorticoid-inducible kinase 1 (SGK1) mediates glucocorticoid-induced inhibition of insulin secretion. Diabetes 54(4): 1090-1099.

Umezu-Goto, M., Kishi, Y., Taira, A., Hama, K., Dohmae, N., Takio, K., Yamori, T., Mills,

G.B., Inoue, K., Aoki, J., and Arai, H. 2002. Autotaxin has lysophospholipase D activity leading to tumor cell growth and motility by lysophosphatidic acid production. J Cell Biol 158(2): 227-233.

Vander Haar, E., Lee, S.I., Bandhakavi, S., Griffin, T.J., and Kim, D.H. 2007. Insulin signalling to mTOR mediated by the Akt/PKB substrate PRAS40. Nat Cell Biol 9(3): 316-323.

Vanhaesebroeck, B., Guillermet-Guibert, J., Graupera, M., and Bilanges, B. 2010. The emerging mechanisms of isoform-specific PI3K signalling. Nat Rev Mol Cell Biol 11(5): 329-341.

Vanhaesebroeck, B. and Waterfield, M.D. 1999. Signaling by distinct classes of phosphoinositide 3-kinases. Exp Cell Res 253(1): 239-254.

Vasudevan, K.M., Barbie, D.A., Davies, M.A., Rabinovsky, R., McNear, C.J., Kim, J.J., Hennessy, B.T., Tseng, H., Pochanard, P., Kim, S.Y., Dunn, I.F., Schinzel, A.C., Sandy, P., Hoersch, S., Sheng, Q., Gupta, P.B., Boehm, J.S., Reiling, J.H., Silver, S., Lu, Y., Stemke-Hale, K., Dutta, B., Joy, C., Sahin, A.A., Gonzalez-Angulo, A.M., Lluch, A., Rameh, L.E., Jacks, T., Root, D.E., Lander, E.S., Mills, G.B., Hahn, W.C., Sellers, W.R., and Garraway, L.A. 2009. AKT-independent signaling downstream of oncogenic PIK3CA mutations in human cancer. Cancer Cell 16(1): 21-32.

Viglietto, G., Motti, M.L., Bruni, P., Melillo, R.M., D'Alessio, A., Califano, D., Vinci, F., Chiappetta, G., Tsichlis, P., Bellacosa, A., Fusco, A., and Santoro, M. 2002. Cytoplasmic relocalization and inhibition of the cyclin-dependent kinase inhibitor p27(Kip1) by PKB/Akt-mediated phosphorylation in breast cancer. Nat Med 8(10): 1136-1144.

Villunger, A., Michalak, E.M., Coultas, L., Mullauer, F., Bock, G., Ausserlechner, M.J., Adams, J.M., and Strasser, A. 2003. p53- and drug-induced apoptotic responses mediated by BH3-only proteins puma and noxa. Science 302(5647): 1036-1038.

Virbasius, J.V., Song, X., Pomerleau, D.P., Zhan, Y., Zhou, G.W., and Czech, M.P. 2001. Activation of the Akt-related cytokine-independent survival kinase requires interaction of its phox domain with endosomal phosphatidylinositol 3-phosphate. Proc Natl Acad Sci U S A 98(23): 12908-12913.

Vivanco, I. and Sawyers, C.L. 2002. The phosphatidylinositol 3-Kinase AKT pathway in human cancer. Nat Rev Cancer 2(7): 489-501.

Vogt, P.K., Gymnopoulos, M., and Hart, J.R. 2009. PI 3-kinase and cancer: changing accents. Curr Opin Genet Dev 19(1): 12-17.

Waerntges, S., Klingel, K., Weigert, C., Fillon, S., Buck, M., Schleicher, E., Rodemann, H.P., Knabbe, C., Kandolf, R., and Lang, F. 2002. Excessive transcription of the human serum and glucocorticoid dependent kinase hSGK1 in lung fibrosis. Cell Physiol Biochem 12(2-3): 135-142.

Wagner, C.A., Broer, A., Albers, A., Gamper, N., Lang, F., and Broer, S. 2000. The heterodimeric amino acid transporter 4F2hc/LAT1 is associated in Xenopus oocytes with a non-selective cation channel that is regulated by the serine/threonine kinase sgk-1. J Physiol 526 Pt 1: 35-46.

Waldegger, S., Barth, P., Raber, G., and Lang, F. 1997. Cloning and characterization of a putative human serine/threonine protein kinase transcriptionally modified during anisotonic and isotonic alterations of cell volume. Proc Natl Acad Sci U S A 94(9): 4440-4445.

Waldegger, S., Erdel, M., Nagl, U.O., Barth, P., Raber, G., Steuer, S., Utermann, G., Paulmichl, M., and Lang, F. 1998. Genomic organization and chromosomal localization of the human SGK protein kinase gene. Genomics 51(2): 299-302.

Waldegger, S., Klingel, K., Barth, P., Sauter, M., Rfer, M.L., Kandolf, R., and Lang, F. 1999. h-sgk Serine-Threonine Protein Kinase Gene as Transcriptional Target of Transforming Growth Facto B in Human Intestine. Gastroenterology 116(5): 1081-1088.

Wandzioch, E., Edling, C.E., Palmer, R.H., Carlsson, L., and Hallberg, B. 2004. Activation of the MAP kinase pathway by c-Kit is PI-3 kinase dependent in hematopoietic progenitor/stem cell lines. Blood 104(1): 51-57.

Wang, J., Barbry, P., Maiyar, A.C., Rozansky, D.J., Bhargava, A., Leong, M., Firestone, G.L., and Pearce, D. 2001. SGK integrates insulin and mineralocorticoid regulation of epithelial sodium transport. Am J Physiol Renal Physiol 280(2): F303-313.

Wang, K., Gu, S., Nasir, O., Foller, M., Ackermann, T.F., Klingel, K., Kandolf, R., Kuhl, D., Stournaras, C., and Lang, F. 2010a. SGK1-dependent intestinal tumor growth in APC-deficient mice. Cell Physiol Biochem 25(2-3): 271-278.

Wang, L., Zhou, C., Zhu, Q., Luo, J., Xu, Y., Huang, Y., Zhang, X., and Wang, X. 2010b. Up-regulation of serum- and glucocorticoid-induced protein kinase 1 in the brain tissue of human and experimental epilepsy. Neurochem Int 57(8): 899-905.

Wang, Q., Zhang, A., Li, R., Liu, J., Xie, J., Deng, A., Feng, Y., and Zhu, Z. 2008. High glucose promotes the CTGF expression in human mesangial cells via serum and glucocorticoid-induced kinase 1 pathway. J Huazhong Univ Sci Technolog Med Sci 28(5): 508-512.

Wang, T.H., Wang, H.S., and Soong, Y.K. 2000. Paclitaxel-induced cell death: where the cell cycle and apoptosis come together. Cancer 88(11): 2619-2628.

Wang, X. and Proud, C.G. 2006. The mTOR pathway in the control of protein synthesis. Physiology (Bethesda) 21: 362-369.

Wang, X. and Proud, C.G. 2009. Nutrient control of TORC1, a cell-cycle regulator. Trends Cell Biol 19(6): 260-267.

Wang, X. and Proud, C.G. 2011. mTORC1 signaling: what we still don't know. J Mol Cell Biol 3(4): 206-220.

Wang, Y., Pennock, S., Chen, X., and Wang, Z. 2002. Endosomal signaling of epidermal growth factor receptor stimulates signal transduction pathways leading to cell survival. Mol Cell Biol 22(20): 7279-7290.

Wang, Y., Zhou, D., Phung, S., Masri, S., Smith, D., and Chen, S. 2011. SGK3 is an estrogen-inducible kinase promoting estrogen-mediated survival of breast cancer cells. Mol Endocrinol 25(1): 72-82.

Wang, Z., Gerstein, M., and Snyder, M. 2009. RNA-Seq: a revolutionary tool for transcriptomics. Nat Rev Genet 10(1): 57-63.

Warntges, S., Friedrich, B., Henke, G., Duranton, C., Lang, P.A., Waldegger, S., Meyermann, R., Kuhl, D., Speckmann, E.J., Obermuller, N., Witzgall, R., Mack, A.F., Wagner, H.J., Wagner, A., Broer, S., and Lang, F. 2002. Cerebral localization and regulation of the cell volume-sensitive serum- and glucocorticoid-dependent kinase SGK1. Pflugers Arch 443(4): 617-624.

Webster, M.K., Goya, L., and Firestone, G.L. 1993a. Immediate-early transcriptional regulation and rapid mRNA turnover of a putative serine/threonine protein kinase. J Biol Chem 268(16): 11482-11485.

Webster, M.K., Goya, L., Ge, Y., Maiyar, A.C., and Firestone, G.L. 1993b. Characterization of sgk, a novel member of the serine/threonine protein kinase gene family which is transcriptionally induced by glucocorticoids and serum. Mol Cell Biol 13(4): 2031-2040.

Weigmann, K., Cohen, S.M., and Lehner, C.F. 1997. Cell cycle progression, growth and patterning in imaginal discs despite inhibition of cell division after inactivation of Drosophila Cdc2 kinase. Development 124(18): 3555-3563.

Wendel, H.G., De Stanchina, E., Fridman, J.S., Malina, A., Ray, S., Kogan, S., Cordon-Cardo, C., Pelletier, J., and Lowe, S.W. 2004. Survival signalling by Akt and eIF4E in oncogenesis and cancer therapy. Nature 428(6980): 332-337.

West, K.A., Castillo, S.S., and Dennis, P.A. 2002. Activation of the PI3K/Akt pathway and chemotherapeutic resistance. Drug Resist Updat 5(6): 234-248.

Wilson, F.H., Disse-Nicodeme, S., Choate, K.A., Ishikawa, K., Nelson-Williams, C., Desitter, I., Gunel, M., Milford, D.V., Lipkin, G.W., Achard, J.M., Feely, M.P., Dussol, B., Berland, Y., Unwin, R.J., Mayan, H., Simon, D.B., Farfel, Z., Jeunemaitre, X., and Lifton, R.P. 2001. Human hypertension caused by mutations in WNK kinases. Science 293(5532): 1107-1112.

Wolf, S.C., Schultze, M., Risler, T., Rieg, T., Lang, F., Schulze-Osthoff, K., and Brehm, B.R. 2006. Stimulation of serum- and glucocorticoid-regulated kinase-1 gene expression by endothelin-1. Biochem Pharmacol 71(8): 1175-1183.

Won, M., Park, K.A., Byun, H.S., Kim, Y.R., Choi, B.L., Hong, J.H., Park, J., Seok,

J.H., Lee, Y.H., Cho, C.H., Song, I.S., Kim, Y.K., Shen, H.M., and Hur, G.M. 2009. Protein kinase SGK1 enhances MEK/ERK complex formation through the phosphorylation of ERK2: implication for the positive regulatory role of SGK1 on the ERK function during liver regeneration. J Hepatol 51(1): 67-76.

Wong, A.S., Pelech, S.L., Woo, M.M., Yim, G., Rosen, B., Ehlen, T., Leung, P.C., and Auersperg, N. 2001. Coexpression of hepatocyte growth factor-Met: an early step in ovarian carcinogenesis? Oncogene 20(11): 1318-1328.

Wong, K.K., Engelman, J.A., and Cantley, L.C. 2010. Targeting the PI3K signaling pathway in cancer. Curr Opin Genet Dev 20(1): 87-90.

Wu, R., Hendrix-Lucas, N., Kuick, R., Zhai, Y., Schwartz, D.R., Akyol, A., Hanash, S., Misek, D.E., Katabuchi, H., Williams, B.O., Fearon, E.R., and Cho, K.R. 2007. Mouse model of human ovarian endometrioid adenocarcinoma based on somatic defects in the Wnt/beta-catenin and PI3K/Pten signaling pathways. Cancer Cell 11(4): 321-333.

Wu, W., Chaudhuri, S., Brickley, D.R., Pang, D., Karrison, T., and Conzen, S.D. 2004. Microarray analysis reveals glucocorticoid-regulated survival genes that are associated with inhibition of apoptosis in breast epithelial cells. Cancer Res 64(5): 1757-1764.

Wu, W., Zou, M., Brickley, D.R., Pew, T., and Conzen, S.D. 2006. Glucocorticoid receptor activation signals through forkhead transcription factor 3a in breast cancer cells. Mol Endocrinol 20(10): 2304-2314.

Wulff, P., Vallon, V., Huang, D.Y., Volkl, H., Yu, F., Richter, K., Jansen, M., Schlunz, M., Klingel, K., Loffing, J., Kauselmann, G., Bosl, M.R., Lang, F., and Kuhl, D. 2002. Impaired renal Na(+) retention in the sgk1-knockout mouse. J Clin Invest 110(9): 1263-1268.

Wullschleger, S., Loewith, R., and Hall, M.N. 2006. TOR signaling in growth and metabolism. Cell 124(3): 471-484.

Wyatt, A.W., Hussain, A., Amann, K., Klingel, K., Kandolf, R., Artunc, F., Grahammer, F., Huang, D.Y., Vallon, V., Kuhl, D., and Lang, F. 2006. DOCA-induced phosphorylation of glycogen synthase kinase 3beta. Cell Physiol Biochem 17(3-4): 137-144.

Xing, Y., Liu, D., Zhang, R., Joachimiak, A., Songyang, Z., and Xu, W. 2004. Structural basis of membrane targeting by the Phox homology domain of cytokine-independent survival kinase (CISK-PX). J Biol Chem 279(29): 30662-30669.

Xu, B.E., Stippec, S., Chu, P.Y., Lazrak, A., Li, X.J., Lee, B.H., English, J.M., Ortega, B., Huang, C.L., and Cobb, M.H. 2005a. WNK1 activates SGK1 to regulate the epithelial sodium channel. Proc Natl Acad Sci U S A 102(29): 10315-10320.

Xu, B.E., Stippec, S., Lazrak, A., Huang, C.L., and Cobb, M.H. 2005b. WNK1 activates SGK1 by a phosphatidylinositol 3-kinase-dependent and non-catalytic mechanism. J Biol Chem 280(40): 34218-34223.

Xu, J., Liao, L., Qin, J., Liu, D., and Songyang, Z. 2009. Identification of Flightless-I as a Substrate of the Cytokine-independent Survival Kinase CISK. J Biol Chem 284(21): 14377-14385.

Xu, J., Liu, D., Gill, G., and Songyang, Z. 2001. Regulation of cytokine-independent survival kinase (CISK) by the Phox homology domain and phosphoinositides. J Cell Biol 154(4): 699-705.

Yadav, V. and Denning, M.F. 2011. Fyn is induced by Ras/PI3K/Akt signaling and is required for enhanced invasion/migration. Mol Carcinog.

Yan, Y. and Backer, J.M. 2007. Regulation of class III (Vps34) PI3Ks. Biochem Soc Trans 35(Pt 2): 239-241.

Yan, Y., Flinn, R.J., Wu, H., Schnur, R.S., and Backer, J.M. 2009. hVps15, but not Ca2+/CaM, is required for the activity and regulation of hVps34 in mammalian cells. Biochem J 417(3): 747-755.

Yang, X., Yang, C., Farberman, A., Rideout, T.C., de Lange, C.F., France, J., and Fan, M.Z. 2008. The mammalian target of rapamycin-signaling pathway in regulating metabolism and growth. J Anim Sci 86(14 Suppl): E36-50.

Yao, L.J., McCormick, J.A., Wang, J., Yang, K.Y., Kidwai, A., Luca Colussi, G., Boini, K.M., Birnbaum, M.J., Lang, F., German, M.S., and Pearce, D. 2011. Novel Role for SGK3 in Glucose Homeostasis Revealed in SGK3/Akt2 Double-Null Mice. Mol Endocrinol.

Yap, T.A., Yan, L., Patnaik, A., Fearen, I., Olmos, D., Papadopoulos, K., Baird, R.D., Delgado, L., Taylor, A., Lupinacci, L., Riisnaes, R., Pope, L.L., Heaton, S.P., Thomas, G., Garrett, M.D., Sullivan, D.M., de Bono, J.S., and Tolcher, A.W. 2011. First-in-man clinical trial of the oral pan-AKT inhibitor MK-2206 in patients with advanced solid tumors. J Clin Oncol 29(35): 4688-4695.

Yoo, D., Kim, B.Y., Campo, C., Nance, L., King, A., Maouyo, D., and Welling, P.A. 2003. Cell surface expression of the ROMK (Kir 1.1) channel is regulated by the aldosterone-induced kinase, SGK-1, and protein kinase A. J Biol Chem 278(25): 23066-23075.

Yu, S., Murph, M.M., Lu, Y., Liu, S., Hall, H.S., Liu, J., Stephens, C., Fang, X., and Mills, G.B. 2008. Lysophosphatidic acid receptors determine tumorigenicity and aggressiveness of ovarian cancer cells. J Natl Cancer Inst 100(22): 1630-1642.

Yuan, T.L. and Cantley, L.C. 2008. PI3K pathway alterations in cancer: variations on a theme. Oncogene 27(41): 5497-5510.

Yuan, Z.Q., Sun, M., Feldman, R.I., Wang, G., Ma, X., Jiang, C., Coppola, D., Nicosia, S.V., and Cheng, J.Q. 2000. Frequent activation of AKT2 and induction of apoptosis by inhibition of phosphoinositide-3-OH kinase/Akt pathway in human ovarian cancer. Oncogene 19(19): 2324-2330.

Yun, C.C., Palmada, M., Embark, H.M., Fedorenko, O., Feng, Y., Henke, G., Setiawan, I., Boehmer, C., Weinman, E.J., Sandrasagra, S., Korbmacher, C., Cohen, P., Pearce, D., and Lang, F. 2002. The serum and glucocorticoid-inducible kinase SGK1 and the Na+/H+ exchange regulating factor NHERF2 synergize to stimulate the renal outer medullary K+ channel ROMK1. J Am Soc Nephrol 13(12): 2823-2830.

Zambrowicz, B.P., Abuin, A., Ramirez-Solis, R., Richter, L.J., Piggott, J., BeltrandelRio, H., Buxton, E.C., Edwards, J., Finch, R.A., Friddle, C.J., Gupta, A., Hansen, G., Hu, Y., Huang, W., Jaing, C., Key, B.W., Jr., Kipp, P., Kohlhauff, B., Ma, Z.Q., Markesich, D., Payne, R., Potter, D.G., Qian, N., Shaw, J., Schrick, J., Shi, Z.Z., Sparks, M.J., Van Sligtenhorst, I., Vogel, P., Walke, W., Xu, N., Zhu, Q., Person, C., and Sands, A.T. 2003. Wnk1 kinase deficiency lowers blood pressure in mice: a gene-trap screen to identify potential targets for therapeutic intervention. Proc Natl Acad Sci U S A 100(24): 14109-14114.

Zhang, B.H., Tang, E.D., Zhu, T., Greenberg, M.E., Vojtek, A.B., and Guan, K.L. 2001. Serum- and glucocorticoid-inducible kinase SGK phosphorylates and negatively regulates B-Raf. J Biol Chem 276(34): 31620-31626.

Zhang, H., Stallock, J.P., Ng, J.C., Reinhard, C., and Neufeld, T.P. 2000. Regulation of cellular growth by the Drosophila target of rapamycin dTOR. Genes Dev 14(21): 2712-2724.

Zhang, L., Cui, R., Cheng, X., and Du, J. 2005. Antiapoptotic effect of serum and glucocorticoid-inducible protein kinase is mediated by novel mechanism activating I{kappa}B kinase. Cancer Res 65(2): 457-464.

Zhao, J.J., Cheng, H., Jia, S., Wang, L., Gjoerup, O.V., Mikami, A., and Roberts, T.M. 2006. The p110alpha isoform of PI3K is essential for proper growth factor signaling and oncogenic transformation. Proc Natl Acad Sci U S A 103(44): 16296-16300.

Zhao, J.J., Gjoerup, O.V., Subramanian, R.R., Cheng, Y., Chen, W., Roberts, T.M., and Hahn, W.C. 2003. Human mammary epithelial cell transformation through the activation of phosphatidylinositol 3-kinase. Cancer Cell 3(5): 483-495.

Zhao, J.J., Liu, Z., Wang, L., Shin, E., Loda, M.F., and Roberts, T.M. 2005. The oncogenic properties of mutant p110alpha and p110beta phosphatidylinositol 3-kinases in human mammary epithelial cells. Proc Natl Acad Sci U S A 102(51): 18443-18448.

Zhao, J.J., Roberts, T.M., and Hahn, W.C. 2004. Functional genetics and experimental models of human cancer. Trends Mol Med 10(7): 344-350.

Zhou, Q., Wang, Y., Yang, L., Chen, P., Dong, X., and Xie, L. 2008. Histone deacetylase inhibitors blocked activation and caused senescence of corneal stromal cells. Mol Vis 14: 2556-2565.

Zhou, R. and Snyder, P.M. 2005. Nedd4-2 phosphorylation induces serum and glucocorticoid-regulated kinase (SGK) ubiquitination and degradation. J Biol

Chem 280(6): 4518-4523.

Zhu, G., Decker, S.J., and Saltiel, A.R. 1992. Direct analysis of the binding of Src-homology 2 domains of phospholipase C to the activated epidermal growth factor receptor. Proc Natl Acad Sci U S A 89(20): 9559-9563.